EFFECT OF INCLINATION, WATER CUT, BETA RATIO AND VISCOSITY ON VENTURI PRESSURE DROP MEASUREMENTS FOR OIL-WATER FLOW EXPERIMENTS

BY

MUJAHID ELOBEID

A Thesis Presented to the

DEANSHIP OF GRADUATE STUDIES

KING FAHD UNIVERSITY OF PETROLEUM & MINERALS

DHAHRAN, SAUDI ARABIA

In Partial Fulfillment of the
Requirements for the Degree of

MASTER OF SCIENCE

In

MECHANICAL ENGINEERING

December, 2016

KING FAHD UNIVERSITY OF PETROLEUM & MINERALS

DHAHRAN- 31261, SAUDI ARABIA

DEANSHIP OF GRADUATE STUDIES

This thesis, written by **MUJAHID OMER SEED AHMED ELOBEID** under the direction his thesis advisor and approved by his thesis committee, has been presented and accepted by the Dean of Graduate Studies, in partial fulfillment of the requirements for the degree of **MASTER OF SCIENCE IN MECHANICAL ENGINEERING.**

Dr. Luai M. Alhems

(Advisor)

Dr. Abdelsalam M. Al-Sarkhi

(Member)

Dr. Haitham M. Bahaidarah

(Member)

Dr. Zuhair M. Gasem

Department Chairman

Dr. Salam A. Zummo

Dean of Graduate Studies

15/1/17

Date

This thesis is dedicated to my dearest parents, brothers, my beloved fiancée and my friends

ACKNOWLEDGMENTS

Starting in the name of Allah, the most beneficent, the Most Merciful. All the praises glory and thanks are due to Almighty Allah for bestowing me with the blessings, health, knowledge, opportunity, courage, guidance and patience to accomplish this work. Thereafter, acknowledgements are due to King Fahd University of Petroleum and Minerals (KFUPM) for the support given to pursue my graduate studies.

During this work, my parents were a constant and important source of motivation and support. My Mother: a strong and gentle soul who taught me to trust in Allah, believe in hard work and that so much could be done with little. My Father: for earning an honest living for us and for supporting and encouraging me to believe in myself. Second, special thanks to my beloved fiancée, words cannot describe how lucky I am to have her in my life and I look forward to our lifelong journey. Also acknowledges are due to my grandmother and my aunts for their sacrifice and their financial and moral support for me and my brothers throughout of our educational journeys.

This work would not have been complete without the support of many people. I would like to thank my thesis advisor and the director of the Center for Engineering Research Dr. Luai M. Alhems, for his supervision; his patience, help and support; and for introducing me to the world of risk assessment. The members of my thesis committee, Dr. Abdelsalam M. Al-Sarkhi and Dr. Haitham M. Bahaidarah, have generously given their time and expertise to better my work. I thank them for their contribution and their good-natured support. Furthermore, many thanks and appreciation to professor Dr. AbdelSalaam M. Al-Sarkhi

for persevering with me as my advisor through out the time it took me to complete this research and write the thesis.

I gratefully wish to acknowledge the support provided by Saudi Aramco, Dhahran, Saudi Arabia, for funding this work through project No. CER02386. Also the Center of Engineering Research (CER) at the Research Institute of King Fahd University of Petroleum and Minerals, Dhahran, Saudi Arabia is acknowledged, for their technical supporting to complete this research work.

My thanks must go also to my teamwork members, Mr. Aftab Ahmad, Mr. Syed M. Shaahid, Mr. Mehaboob Basha and Mr. Mansoor Alam for their continuous technical support and help received in the experimental work. Especially, I need to express my gratitude and deep appreciation to Mr. Aftab Ahmad for his continuous and generous help and support since the beginning of this work. Also for good-natured support and for his time while persevering with me as his son.

Lastly, but not the least, sincere thanks to my best and dearest of friends Abubakar Mahjoub and Mohamed Kamal Eldin. Every challenging work needs self-efforts as well as encouragement, support and guidance of friends especially those who are very close to our heart. Their example kept me working when I wanted to give up. Abubakar and Mohamed facilitated my research by assisting my family in my home country when they were in need of any kind of help. They gave me a new appreciation for the meaning and importance of friendship. They have consistently helped me keep perspective on what is important in life and shown me how to deal with reality. The greatest gift I have received in this life is their unconditional friendship. A friendship, I deeply appreciate, honor and forever proud of.

TABLE OF CONTENTS

LIST OF TABLES

LIST OF FIGURES

LIST OF ABBREVIATIONS

k	Modified venturi discharge coefficient, m2.s/h
β	Venturi beta ratio
A_t	Venturi throat cross sectional area, m^2
A_p	Pipe cross-sectional area, m^2
D or D_h	Hydraulic diameter, m
C_d	Venturi discharge coefficient
Cp_m	Mixture venturi pressure coefficient
$\mathcal{A}$	Water volume fraction or water cut
Q_m	Mixture flow rate, m^3/h
Q_{meas}	Measured fluid mixture flow rate, m^3/h
Q_{cal}	Calculated fluid mixture flow rate, m^3/h
θ	Inclination angle, degrees
V_m	Mixture average velocity at venturi inlet, m/s
Re_m	Mixture Reynolds number

Greek Symbols

ΔP	Venturi pressure drop, Pa
υ_m	Mixture kinematic viscosity, m^2/s
μ_m	Mixture dynamic viscosity, Pa.s
μ_w	Water dynamic viscosity, Pa.s
μ_o	Oil dynamic viscosity, Pa.s
ρ_m	Fluid (or Liquid) mixture density, kg/m^3

Subscripts

o	Oil
w	Water
m	Mixture
t	Venturi throat
p	Pipe

ABSTRACT

Full Name : MUJAHID OMER SEED AHMED ELOBEID

Thesis Title : EFFECT OF INCLINATION, WATER CUT, BETA RATIO AND VISCOSITY ON VENTURI PRESSURE DROP MEASUREMENTS FOR OIL-WATER FLOW EXPERIMENTS

Major Field : MECHANICAL ENGINEERING

Date of Degree : December 2016

The performances of the venturi meters for oil-water flow under real oil well operating conditions were investigated in the present experimental investigation. The pressure drop measurements were studied in Tercom flanged machined venturi meters with a beta ratio (β) = 0.4, 0.5 and 0.6 for oil-water two-phase flow experiments in a 0.0762 m (3-inch) pipe. The experimental data for different fluid mixture flow rates and water cuts was acquired using a two-phase, large-scale inclinable flow loop. Potable water and Exxsol mineral oils (D80 and D130) were used for the single-phase and two-phase oil-water experiments for the three venturi meters. The experiments were conducted for water cuts varying from 0% to 100% in steps of 20%, flow rates ranging from 2,000 barrels per day (bpd) to 12,000 bpd, and for different flow loop inclinations from horizontal to vertical positions (0°, 40º, 60º and 90°). Field flow rates were matched by selecting test liquid flow rates representative of those in real oil wells.

The experimental results showed that the venturi pressure drop varies parabolically with fluid flow rate for given water cut through the venturi meters studied. For given flow rate and water cut, the venturi pressure drop is inversely proportional to the venturi β; however, the venturi pressure drop varies almost linearly with the water cut for a given fluid flow rate. Within the range of test fluid flow rates, the venturi pressure drop measurements were

unaffected by the oils (D80 and D130) viscosities and the inclination of the three venturi meters studied in the flow loop. This is very important from an application standpoint. A new modified venturi coefficient, k, which is a function of pressure losses and geometry, was defined and its value obtained from the oil-water two-phase flow experiments. Furthermore, different empirical correlations were developed to predict the mixture venturi pressure coefficient Cp_m. The correlations showed very high accuracy and low discrepancy in predictions. In this study, attention was focused on the variables affecting the performance of the venturi meter for oil-water flow under real oil wells operating conditions.

ملخص الرسالة

الاسم الكامل: **مجاهد عمر سيد أحمد العبيد**

عنوان الرسالة: تأثير الميلان وحِصة الماء ونسبة بيتا واللزوجة على انخفاضات الضغط في جهاز القياس الفنتوري لتجارب سريان الزيت-الماء

التخصص: الهندسة الميكانيكية

تاريخ الدرجة العلمية: ديسمبر 2016

في هذه الدراسة الحالية تم التحقيق عمليا من أداء مقاييس الفنتوري لسريان الزيت-المياه تحت الظروف التشغيلية كما في أبار النفط. قياسات انخفاض الضغط دُرِست في جهاز فنتوري من النوع (TERCOM) ذو الحافة المشكّلة ذو نسبة بيتا (β= 0.4، 0.5 و0.6) لتجارب سريان الزيت-الماء ثنائية الطور في أنبوب 0.0762 م (3 بوصة). تم الحصول على البيانات التجريبية لمختلف معدلات تدفق خليط السوائل ومختلف حِصص الماء باستخدام حلقة السريان الثنائي الكبيرة ذات النوع القابل للميلان. وقد أستخدمت المياه الصالحة للشرب والزيوت المعدنية من النوع (D80 وD130) Exxsol لإجراء التجارب ذات الطور الواحد لكلٍ من الماء والزيت لأجهزة الفنتوري الثلاث. وأُجريت التجارب لحِصص ماء تتراوح بين 0٪ إلى 100٪ بطول خطوة 20٪، ومعدلات تدفق تتراوح من 2000 برميل يوميا إلى 12،000 برميل يوميا، ولمختلف الميلانات لحلقة السريان من الوضع الأفقي إلى العمودي (0º، 40º، 60º و90°). معدلات تدفق السوائل تم اختيارها لتُطابِق معدلات التدفق الموجودة في آبار النفط الحقيقية.

وأظهرت النتائج التجريبية أن انخفاض ضغط الفنتوري يتغير كقطع مكافئ مع معدل تدفق المائع لكل حِصّة معينة من الماء المارة خلال الفنتوريات الثلاث التي دُرِسْت. لمعدل تدفق معين، وحصة ماء معينة وُجِد أن انخفاض ضغط الفنتوري يتناسب عكسيا مع النسبة بيتا (β) للفنتوري، وبالإضافة إلى ذلك، وُجِد أن انخفاض الفنتوري يتناسب طرديا مع حِصّة الماء لمعدل تدفق المائع المعني. ضِمن مدى معدلات تدفق اختبار المائع، قياسات انخفاض الضغط الفنتوري لم تتأثر باختلاف لزوجة الزيتين (D80 وD130) وكذلك لم تتأثر بانحناءات حلقة السريان لأجهزة الفنتوري الثلاث التي دُرِست. وهذا مهم جدا من وجهة نظر التطبيقية. تم التعرف على معامل معدّل جديد للفنتوري k، وهو عبارة عن دالة في فقودات الضغط وشكل الهندسي للفنتوري، وتم الحصول على قيمته من تجارب الزيت-الماء ذات الطور الثنائي. وعلاوة على ذلك، تم تطوير عدة علاقات رياضية امبراطورية مختلفة للتنبؤ بمعامل ضغط خليط الفنتوري Cpm.

العلاقات الرياضية أظهرت دِقة عالية جدا وتباين منخفض في التنبؤات. في هذه الدراسة، تم التركيز والاهتمام على المتغيرات التي تؤثر على أداء جهاز القياس الفنتوري لتدفق النفط-المياه تحت الظروف التشغيلية لأبار النفط الحقيقية.

.

CHAPTER 1

INTRODUCTION

1.1 Background

The term of multiphase flow is used to refer to flow of any fluid consisting of more than one phase or component with different chemical properties through a pipe or channel simultaneously. Lately Professor Shao Lee Soo of the University of Illinois (1965) coined the term multiphase flow and it comprises of fluid dynamics motion of multiple phases. In fact, this can be defined as the concurrent phase flow of different materials, the numerous phases of the same material or the same material phase, but with varying materials, or particle sizes with different chemical characteristics, Maksimovic (2005) [1]. Multi-phase flow is to be distinguished from multi-species which refer to a “mixture formulation when all components of various materials are mixed at the same molecular level, velocity and temperature" (Maksimovic 2005) [1].

Multi-phase flows are of large practical attention in a huge number of different engineering disciplines, including the mechanical, chemical, nuclear, petroleum and civil fields. Multiphase flows are commonly came across during all the production and processing stages in the oil and gas industry fields. The complex nature of two-phase flow is due to the existence of multiple, deformable and moving interface (s). The main difference between single phase and multiphase flow through pipes exist in the being of

diverse flow configurations or flow patterns, which differ from each other in the spatial distribution of the interface. For a given two-phase flow system the existing of flow pattern depends on the operational parameters (liquid and gas flow rates, temperature and pressure), the geometrical variables (pipe diameter, roughness and inclination angle), and the physical properties of the two phases (gas and liquid densities, viscosities and surface tension).

Liquid-Liquid Two-Phase Flows:

Liquid-liquid flows have many important applications in a diverse range of process industries in the petroleum production particularly, where oil and water are often produced and transported together. Two-phase flow of oil and water is commonly monitored in wellbores, and its behavior under an extensive range of flow conditions and angles of inclination constitutes a pertinent unresolved issue for the petroleum industry. However, despite their importance, such flows have not been explored to the same extent of the gas-liquid flows. The flow oil and water is a limiting case of the more general case of three-phase flow, and is usually associated with wells producing from under saturated reservoirs with water-flooding operations and with active aquifers. As a result, the most common predictive theories for pressure gradient that are used in liquid-liquid flows are developments of models created for gas-liquid flows. A pressure drop in horizontal and inclinable wells will always occur as a necessity for flow. Although the main application of such flows has been in the transport of oil-water mixtures in steel pipelines, most of the experimental work has been carried out in glass or acrylic pipes. These of course have

many advantages of being transparent, allowing the flow to be observed, their wall properties (roughness and wettability) may be very different to those of steel tubes and this may affect the design parameters such as the pressure drop. In the literature evidence found indicates that precise knowledge of the patterns of oil-water flow, their ranges of existence as a function of phases flow rates and inclination angles of the pipe, and values for their associated hydrodynamic parameters (holdup and pressure gradient).

- **Oil-Water Two-Phase Flow:**

Multiphase flow is commonly seen in industrial processes such as pipeline transportation, fluidized beds and power plants. A typical multiphase oil–water two-phase flow is often encountered in petroleum industries, and measuring their process parameters (especially individual flow rate of oil and water) is an important issue in oil exploitation and transportation. The process parameters of the most interests in oil–water two phase flow are the flow rate (by volume or mass) of each individual phase, especially of oil. Accurate and cost-effective means for measuring gas flows is a matter of concern for a wide range of upstream oil and gas measurement applications. While measuring dry gas flow rate is a well-served application for a wide range of gas flow metering technologies, accurate and cost-effective measurement of wet gas flow remains a long-standing multiphase flow measurement challenge for the upstream oil and gas industry. Differential pressure flow meters such as the Venturi, standard concentric orifice plate, V-cone, and wedge are popular for these Compared with other kinds of differential pressure (DP) devices, Venturi has little influence on flow patterns, the smallest pressure loss, and the shortest straight

pipe upstream and downstream. Considering the great technical importance as well as pure scientific interest, the Venturi meter has been widely used in gas–liquid two-phase flow measurement applications.

- **Venturi Flow Meter (VFM):**

A flow meter is an instrument for measuring rate of flow of a fluid. The study of flow meters and their capabilities for measuring mass flow rates for single-phase flows has been the subject of research for the past two hundred years. In response to there being an increased need for accurate flow measurements of viscous fluids through various types of differential pressure flow meters, experimental study was conducted to more accurately define the characteristics of the discharge coefficient, (C_d) at high Reynolds numbers. Accurate flow measurement is one of the greatest concerns among many industries, because uncertainties in product flows can cost companies considerable profits. Differential pressure meters are popular for these applications because they are relatively inexpensive and produce reliable results.

The venturi is a device that allows determination of flow rate by measurement of a pressure differential brought about by a velocity change due to a change in area. Mr. Clemens M. Herschel (1881) used venturi's concept of conical reducing and expanding tubes for measuring water flow rates [2]. The venturi flow meter obtains a pressure differential by constricting the flow area and therefore increasing the velocity at the constriction, which creates a lower pressure according to Bernoulli's Theorem. Venturi

meter measurement has become a key technology in the oilfield development especially in a downhole.

In many difference scientific research and industrial fields, a venturi meter was applied successfully in the single-phase flow as a measurement device. The venturi meter device can easily be considered for measurement of two-phase flow applications, just according to its successful applications in the cases of single-phase flows. Multiphase flow is common occurrence in venture meters specifically in downhole and upstream pipelines. Pressure is the main key parameter for assessing individual phase (oil-water) flow rates in pipelines, which include venturi meters for the pressure measurements.

- **Pressure Drop:**

Pressure drop is the difference in static pressure between two location points of the fluid flow and it called pressure gradient when represents the pressure drop per unit length along the pipe. A pressure drop in horizontal and inclinable wells will always occur as a flow necessity.

Analogously in multiphase flow, probably the key toward understanding the phenomena of pressure drop behavior in oil field industries in order to optimize between the huge costs of production and transportation. There remain many challenges associated with an understanding of multiphase flow pressure drop in production wells and transportation pipelines. Therefore, it is more important to study behavior of pressure drop measurement

response to characterize the flow of two immiscible liquids (oil-water) through venturi meter in upstream and inclined production pipelines.

The total pressure gradient consists of three components. Firstly, the frictional pressure gradient is major one that originates by frictional force due to the fluid flow resistance which affected mostly by velocity and viscosity. Secondly, the gravitational pressure gradient occurs in inclined pipes due to gravity and its magnitude depends on the determination of fluid mixture density. Thirdly, the acceleration pressure gradient presents due to the change in velocity and it consider three terms compressibility, mass transfer and change of area. The total pressure gradient components can be presented as follow:

$$\left[\frac{dP}{dL}\right]_T = \left\{\frac{dP}{dL}\right\}_F + \left\{\frac{dP}{dL}\right\}_G + \left\{\frac{dP}{dL}\right\}_A \quad (1.1)$$

The term dp/dL, based on the definition of a derivative, is negative because the pressure usually drops from one position to another one along the pipe.

In our case of study, we considered the frictional and gravitational components because all experiments have been carried out for different inclinations of flow loop from the horizontal to the vertical positions, so the acceleration component insignificant and can neglected because the experiments conducted for liquid flows only (oil and water).

- **Problem Definition and Study Motivation:**

Multiphase flow is a complex phenomenon involving simultaneous flow of two or more physically immiscible fluids (such as: oil and water) in pipelines. Oil-water two-phase flows are often encountered in petroleum, chemical and petrochemical industries. The physical understanding of two-phase flow characteristics in pipes is of importance since significant savings in pumping power can be derived from the water-lubricated transportation of crude oil. The process parameters of most interest in oil–water two-phase flow is the flow rate (by volume or mass) of each individual phase. Measurement of the process parameters (especially individual flow rate of oil and water) is important in oil exploitation and transportation.

The accurate flow measurement of multi-phase flows is an important task in oil industries. Unlike the measurement of single-phase flows using differential pressure meters, multi-phase flow behavior poses difficulties in accurate measurement. The measurement of phase flow rates is of particular importance for managing oil production, water disposal and/or water reinjection. Also, the widespread occurrence of multiphase flows in pipelines has motivated extensive research in this area. Knowledge of the friction loss (associated with especially individual flow rate of oil and water) in oil-water flows in pipelines is essential in order to specify the size of the pump required to pump the emulsions. Pressure drop is the key parameter for assessing individual phase (oil and water) flow rates in

pipelines. Therefore, it is important to study behavior of pressure drop response to characterize two-phase flow in upstream production pipelines.

Venturi meter measurement has been used successfully in single-phase flows as a measurement device for liquid flow rate. The venturi meter device can also be considered for liquid flow rate measurement of oil-water flow applications with careful attention to the flow pattern and operational conditions. Multiphase flow is a common occurrence in venturi meters specifically in downhole and upstream pipelines. Pressure drop measurements via venturi meter has become a key technology for production and management in the oilfield industry. Several research articles are available in literature on the two-phase flow measurements of oil and water in pipelines.

In light of the research studies in the multiphase flow, there is currently no work available in the literature on pressure drop measurements of oil-water two-phase flow in horizontal and inclined 3-inch flow loop at different flow conditions. Literature also does not address explicitly the impact of venturi pressure drop and venturi coefficients on the flow loop inclination for selected (D80 and D130) oil-water two-phase flow conditions. Also, studies available in literature have not investigated or focused on the variables affecting the performance of the venturi meter for oil-water flow under real oil well operating fluid flow rates. This is the motivation for the present experimental study and it focuses on the effect of flow rates, water-cuts and inclination angle on pressure drop measurements in a venturi using D80 mineral oil-water two-phase flow in a 3-inch inclinable flow loop.

Despite the importance of oil-water flows in oil industries, behavior of such flows has not been explored to an appreciable extent. The current work presents pressure drop

measurements in a Tercom flanged machined venturi meter with beta ratios of 0.4, 0.5 and 0.6. The oils (D80 and D130)-water two-phase flow was run in a 0.0762 m (3-inch) diameter inclinable flow loop for different water cuts and fluid mixture flow rates. The present study considers investigation of effect of four parameters including: (mixture viscosity, venturi beta ratio, inclination and water cut) on the venturi discharge coefficient, C_d. The findings of the study will be helpful in mitigating the pressure drop measurement problems of petroleum industries.

1.2 Thesis Objectives

The main objective of this research is to investigate the multiphase flow of oil and water through venturi meter.

- Oil and water flow in venturi meter were analyzed experimentally to investigate the following parameters:

1. Effect of water fraction (water cut) on the venturi pressure drop measurements.
2. Effect of mixture viscosity on the venturi pressure drop measurements.
3. Effect of venturi beta ratios on the pressure drop measurements.
4. Effect of orientation on the venturi pressure drop measurements.

✓ **To meet the above objectives:**

1. To present the effect of water fraction, a ranging from 0 to 100% in step of 20%, was applied for flow rates varying between 2000 and 12000 bpd with step of 2000 bpd.
2. Two different types of mineral oils were used (D80 and D130) to study the effect of mixture viscosity on the venturi pressure drop measurements and its behavior.
3. Three venturi meters with different beta ratio (β= 0.4, 0.5, and 0.6) were considered to show the effect beta size on the pressure drop measurements.
4. The flow loop was installed with associated electrical induction motor as a prime mover to provide the required inclination form horizontal to vertical situation.

1.3 Outline of the Thesis

The thesis is organized into six chapters. The introductory part and the objectives of present work are given in chapter 1. In addition, it includes background about multiphase flow and information about liquid-liquid two-phase flows, oil-water two-phase flow, venturi flow meter (VFM), pressure drop, and study motivation and problem definition. The descriptions of the remaining five chapters are as follows:

Chapter 2: Review of the research carried out in the field of two-phase flows through venturi meters and researches related to the present work.

Chapter 3: Description of the experimental setup, the instrumentations used and experimental procedure.

Chapter 4: Methodology of pressure calculations and validation results, data analysis and uncertainty analysis.

Chapter 5: Experimental results and discussions.

Chapter 6: Reports the conclusions and provides the recommendations for future research based on the findings of this experimental study.

CHAPTER 2

LITERATURE REVIEW

There remain many challenges associated with an understanding of multiphase flow pressure drop in venturi meters commonly used in production wells and transportation pipelines. With the rapid development of measurement techniques, experimental investigation has become an important and more reliable method to solve practical engineering problems. A substantial number of research articles are available in literature on the two-phase flow measurements of oil and water in pipelines via venturi meters.

In many different scientific research and industrial fields, venturi meters have been applied successfully as measurement devices in single-phase flows. Venturi meters can be easily considered for two-phase flow measurements, due to their successful applications in single-phase flows. Multiphase flows are a common occurrence, specifically in downhole and upstream pipelines. Pressure drop is the key parameter for assessing individual phase (oil-water) flow rates in pipelines, which include venturi meters for the pressure measurements.

If a relatively small volume of liquid is present in a gas, it is generally said to be ‘‘wet’’. In the present age, wet gas measurement is playing an increasingly significant role in the oil and gas industry. Venturi, a classic single-phase flow meter, has proved to be a reliable and accurate wet gas flow meter. In recent years, Venturi has become a hotspot in two-phase flow measurement. This has paved way for considerable/significant research on

Venturi multiphase flow. With the rapidly development of measurements techniques, experimental investigation has become an important and more reliable method to solve practical engineering problems. A substantial amount of research articles are available in literature on the two-phase flow measurements of oil and water in pipelines via venturi meters.

The main objective of this literature review is to understand the exiting work pertaining to the classification of two-phase flow measurement and prediction in oil-water flow measurement with particular focus on the flows through the venturi flow meter (VFM). This literature review was divided into two main parts. The first main part presented the measurement of two-phase (oil-water) flow. Moreover, this section consist of two branches:

1. Two-phase (oil-water) flow through a venturi meter.
2. Alternative measurement techniques of two-phase (oil-water) flow, such as: U-tube, ANN, CRCC and V-cone.

The second main part showed the two-phase (liquid-gas) flow in a Venturi meter. No studies to date have addressed the two-phase (oil-water) flow in a venturi meter in a large size pipes (3 inches) with consideration for the following parameters:

I. The effect of water fraction in the mixture (water cut) on the venturi pressure drop measurements.
II. The effect of mixture viscosity on the venturi pressure drop measurements.
III. The effect of venture beta ratio or on the pressure drop measurements.
IV. The effect of venture orientation on the pressure drop measurements.

2.1 Two phase (Oil-Water) flow

I. Two phase (Oil-Water) flow through venturi meter:

Conventional orifice and venturi meters were used by Pal (1993) to investigate their applicability in monitoring the emulsions of two-phase (oil-water) flow [3]. A single venturi and a single orifice were used to determine the discharge coefficients of different emulsions of oil-in-water (surfactant-stabilized and unstable). Based on the experimental data, empirical correlations of discharge coefficients within ±5% accuracy were developed for the Venturi and orifice meters. The metering results indicated that orifice and venturi meters were feasible flow measuring devices for emulsions.

Zhiyao Huang et al. (2009) conducted an experiment on two phase oil-water measurements [4]. They proposed a new hybrid system to estimate the differential pressure drop of the two phase (oil-water) flow and the total volume flow rate by using an oval gear flow meter and Venturi meter, respectively. The research results showed that the proposed system was effective in measuring oil-water two-phase flow and measurement accuracy was satisfactory. Li et al. (2009) used three horizontal pipes having 15mm, 25mm, and 40mm diameters with a two phase flow loop to investigate experimentally, the performance of a hybrid flow meter system [5]. This system consisted of an oval gear flow meter and venturi meter for two-phase (oil-water) flow measurements. They found that the hybrid flow meter was feasible for measurement of oil-water two-phase flow in terms of total volume flow rate, total mass flow rate, and

density. Also, they found that the measurement results were affected significantly by the chosen venturi meter coefficient and oil fraction.

Si et al. (2012) conducted a study on a two-phase oil-water flow model in a downhole venturi meter by theoretical calculation, numerical simulation and experimental testing [6]. They investigated flow field and pressure characteristics with different flow and oil-water ratios in a venturi tube. Stratified flow was observed as a flow pattern in the venturi tube. Also they found an increase in the pressure gradient with increase in total flow rate. Ding Feng et al. (2012) used venturi meter for the flow measurement of two phase (liquid-liquid) [7]. They developed new measurement method for oil-water two phase using homogeneous model and phase fraction templates. Phase fraction templates data was verified with the Qinhuangdao 32-6-A31 oil field data. Measurement errors remained under ±5%, which assures this method to be a feasible for two phase flow measurement in presence of water and oil.

Brinkhorst et al. (2015) numerically analyzed two different venturi meter nozzles as a liquid flow meter [8]. Herschel venturi meter was found to be more accurate than the ISO 9300 toroid Nozzle due to more stable mass flow with little deviation of only 0.00027%, and the cavitation point was identified geometrically. They showed that oscillating cavity has no influence on the mass flow rate unless cavity length is no less than twice the length of Herschel venture meter cylinder length. In future work they suggested simulations should be compared with the experimental results.

II. Two phase (Oil-Water) flow measurement by U-tube, ANN, CRCC and V-cone:

Han et al. (2008) focused on experimental measurements to confirm the homogeneous pressure drop model in oil-water two-phase flow in horizontal pipe [9]. A V-cone differential pressure meter was used and the adaptive wavelet network was developed to measure the mass flow-rate of the two-phase (oil-water) flow. They found that the measurement error of the total mass flow-rate to be acceptable. The venturi, V-cone, standard concentric orifice plate and wedge flow meters were tested by Hollingshead et al. (2011) to study the performance of discharge coefficients at low Reynolds numbers for viscous fluids and high Reynolds numbers, both of which are associated with pipeline transportation [10]. It was found out that for the venturi, V-cone and wedge flow meters at low Reynolds numbers, the discharge coefficients decreased rapidly with a decreasing Reynolds number. At the same flow conditions, the discharge coefficient of the orifice plate meter increased as the Reynolds number decreased.

A vertical U-tube was used by Zhang et al. (2013) to investigate the performance of metering phase holdup measurement of two phase (oil-water) flow based on the frictional and gravity pressure drop measurements [11]. A U-tube was designed to obtain the same patterns in vertical upward and downward flows (i.e. to obtain the oil holdup based on both gravity and frictional pressure drops measured). The calculation results of the oil holdup showed acceptable predictions with ±10% absolute error.

Modeling of pressure gradients of oil-water flow in pipelines is very crucial. Accurate prediction of pressure gradient leads to better design of energy efficient transportation systems. Al-Wahaibi and Mjalli (2014) developed an artificial neural network (ANN) model with five inputs (oil and water superficial velocities, pipe diameter, pipe roughness, and oil viscosity) to predict the pressure gradient of horizontal oil-water flow based on a

databank of around 765 measurements collected from open literature [12]. Statistical analysis showed that the ANN model has an average error of 0.30%. Hasanvand and Berneti (2015) have also used artificial neural networks (based on 600 data set of Persian Gulf oil) in their study to obtain oil flow rate as an output measurement [13]. The input variables included temperatures and line pressures.

The measurement of individual phase flow rates of oil–water two-phase flow is an important issue in process industries. Tan et al. (2015) used a Conductance Ring Coupled Cone (CRCC) meter for this purpose and compared the obtained results with those from a Conductance Ring Array (CRA) that was installed in front of the Conductance Ring Coupled Cone (CRCC). The CRCC provided multiple outputs for the flow rate and water holdup [14].

2.2 Two Phase (Liquid-Gas) Flow through Venturi Meter

Silvao et al. (1991) conducted experiments of air, water and oil flow in a multiphase flow loop facility consisting of a vertical pipe of a Perspex type having internal diameter of 50 mm and length of 7 m approximately [15]. They used conductance probes to measure the local holdup and found out that the mean liquid holdup before the nozzle and in the throat depended only on the flow quality.

Peixiang and Alimonti (2007) proposed a new method of measuring two-phase mass flowrates in a venturi meter based on the ideas that pressure drop fluctuations are symptomatic of the flow pattern exist, and that the downstream and upstream pressure drops ratio of the throat depend on the air and water individual mass flow rates [16]. They

concluded that it is possible to deduce the individual mass flow rates of air and water in a two-phase mixture from measured pressure drops in a venturi meter with acceptable residual errors ranged from 6 to 13%.

Based on an Eulerian - Eulerian approach for the multi-phase mixture, the Two-Fluid model is used by Paladino Emilio and Maliska Clovis (1999) [17]. Their work focused on the study of dispersed flows. In the designing stage of metering systems, they considered two-dimensional structure knowledge which includes the distribution of gas and liquid. They obtained several results using the proposed model then compared with both the homogeneous model and experimental data. For the calculation of differential pressure, a good agreement has been showed by the two-fluid model than the homogeneous model when compared with practical calculations. Fincke et al (1999) used Murdock's analysis and the experimentally obtained constant M, to compute the gas mass flow rate in a two-phase flow in a venturi meter at different qualities [18]. The results obtained were not satisfactory. Then, they adjust the constant M to fit the data and found that the constant M is not universal.

Steven (2002) [19] compared five correlations based on orifice meter and two correlations based on venturi meter with the data of NEL wet gas loop and came out with his own correlation. Results suggested orifice meter correlations should not be used for venturi meter. De Leeuw (1997) [20] correlation gave best results when tested on Nel wet gas loop data compare to the other venturi meter correlation. As the De Leeuw correlation was calculated on 4" venturi and 0.401 diameter ratio, while the Nel wet gas loop configuration include a venturi meter (0.55 beta ratio) with 6 inch Standard specification and could affect the metering, so he modified this correlation to include the effect of these

parameters. From his correlation gas mass flow rate could be calculated with ±3% accuracy. He recommended his correlation to be tested on other reliable field data.

Hall et al. (2000) investigate the performance of different venturi meters in multiphase flows [21]. The meters were tested using a mixture of stabilized crude oil, magnesium sulfate solution and nitrogen gas with the gas void fraction ranging from 10 to 97.5% and 5 to 100% water cut. The β ratios tested were 0.4, 0.6 and 0.75. Based on the mass flow rate from the reference metering system, the discharge coefficient was evaluated for each test condition. Measurements of differential pressure between the venturi throat and the upstream tapping and of the density from a gamma ray densitometer were made to complete the calculation. The calculated discharge coefficient showed a significant variation with reference gas volume fraction and a smaller effect with reference water cut. A 0.6 β ratio and 21° cone angle Venturi was selected for the final evaluation.

Zhiyao et al. (2005) used a horizontal loop with a 50 mm diameter pipe to conduct experiments on gas–oil two phase flow to measure the flow rate [22]. Furthermore, the electrical capacitance tomography (ECT) was used to determine the cross-sectional void fraction. A venturi meter and void fraction meter were installed by Zhang et al. (2005) to investigate two-phase flow measurement of oil-air flows [23]. They developed a new correlation to measure the flow rate with a consideration for the velocity ratio effect between the gas and liquid phases.

Experiments were conducted by Gysling et al. (2006) to validate the ability of the combination of β = 0.6 venturi dry point (DP) and clamp-on SONAR-based meters to measure liquid and gas flow rates of wet gas using wetness sensitivity coefficients [24].

The experimental results show acceptable measurement accuracy to within ±2% and ±10% of gas and liquid flow rates, respectively.

Arun Kumar et al. (2008) studied the effect of venturi meter in two phase flow [25]. They reported, presence of venturi meter effects the phase distribution mainly in the upstream section. While at lower velocities, pattern transitions were recorded at downstream section. Inverted dispersed flow occurred in the downstream side for the studies flow rates. The mass flow rate can be measured using homogeneous/drift-flux model for oil's having densities closer to water. For heavy/high viscosity oil new calibrations should be performed. The value of CD for two phase flow remained almost equivalent to CD for single phase water flow through the venturi meter. Based on the homogeneous and separated (H-S) flow model, a new metering method for wet gas flow in a venturi tube was presented Lide et al. (2008) [26]. The friction and acceleration venturi pressure drops were considered in a newly developed correlation, and its validity confirmed experimentally.

Three venturi meters with 50 mm pipe diameter and $\beta = 0.40$, 0.55 and 0.70, were mounted horizontally in low-pressure wet gas flow by Lide and Tao (2008) to study their performances systematically [27]. The effects of the following five operational parameters to the venturi tube were analyzed with new independent data under different varied ranges: the pressure (0.15, 0.20 and 0.25) MPa, the densiometric gas Froude number ranges (0.6 to 2.0), the mass flow rate ratio of gas to liquid (0.5 to 0.99) and the modified Lockhart-Maretinelli parameter (0.0022 to 0.06). Finally, they compared the performance of low-pressure wet gas flow with that under high pressure. Their study showed that under high-

pressure the over-reading of a venturi was dependent on the gas Froude number, Lockhart-Martinelli parameter, gas density (or pressure) and the venturi β value.

An experimental work was done by Meng et al. (2010) for air-water two-phase flow using a venturi meter and an Electrical Resistance Tomography (ERT) sensor [28]. The two-phase mixture's mass flow rate was evaluated by Meng based on pressure gradient across the Venturi meter and the mass quality. Seraj et.al. (2010) introduced an application of VFM for wet gas measurement [29]. A tracer injection method was introduced as a tool to measure water and condensate flow rate manually, and radioactive measuring tool as an automated method to measure the gas, water and condensate ratio in the wet gas fluid. Seraj et al. (2010) [29] also elaborated different methods in order to correct over-read values acquired using the Bernoulli equation.

The measurement of fluid flow rates often arises in industrial fields. The most common differential pressure measurement device is the Venturi meter. A vertical universal Venturi tube was used by Hasan et al. (2012) to study the bubbly gas-water two phase flows [30]. The upward bubbly flow of gas-water was assumed homogenous with the same moving velocity for both two phases (i.e. with a unity slip ratio). Differential pressure technique (flow density meter) was used to measure gas volume fraction and mixture flow rate. They concluded that, due to the bubbly-slug transition flow, the homogenous flow model begins to break when the gas volume fraction increased beyond 17.48%.

An experimental analysis was carried out by Gajan et al. (2013) on an annular two phase liquid-gas flow, where the liquid phase contained simultaneous water and oil flow through

a venturi meter [31]. All the experiments were conducted on a downward vertical pipe at low pressure. In a first step, the visual observations enhanced with high-speed video records were used to observe the liquid film structure. Based on the water cut in the liquid phase, the inversion phenomena was observed.

Monni et al. (2014) used a venturi meter to perform the measurement of an annular vertical two-phase flow [32]. The venturi meter (β=0.5) had the following characteristics: throat and inlet diameters of 40 mm and 80 mm, respectively, convergent and divergent angles of 21o. The two-phase mass flow rate and flow quality were estimated. They found that, the accuracy of flow quality, air mass flow rate and water mass flow rate were 5%, 2% and 30%, respectively. A new correlation for wet gas flow rate measurement using VFM on a two-phase mass flow coefficient was proposed by He and Bai (2014) [33]. Comparison between the existing correlations and the newly developed one showed that the developed correlation accurately predicted the flow rate for the following specific conditions: Lockhart-Maartinelli parameter from 0 to 0.3, gas densimetric Froude number from 0.6 to 4.7, the gas-liquid density ratio from 0.01 to 0.081 and the inlet diameter of the VFM from 50 mm to 200 mm. The relative deviation of the gas mass flow rate predicted by the new proposed correlation was from -2% to 3% with a confidence level of 96.7%

Experimental and theoretical investigations were done by Wang et al. (2015) on measurement of two phase (gas-liquid) slug flow through venturi meters [34]. Firstly, techniques of blind source separation were proposed to develop a measurement model. Secondly, a loop facility of two phase (gas-liquid) flow was used to validate the proposed measurement model. They found relative error to be within 10% for the mostly slug flows

obtained from the experimental results. An experimental measurement of wet gas obtained from Colorado Experiment Engineering Station Inc. (CEESI) on a horizontal Venturi meter with (β=0.6) and under high pressure (70 bar), was investigated by Gajan et al. (2015) [35]. They developed a correlation which gave satisfactory accuracy of about 2% when compared with other models. Nevertheless, the inversion point value obtained from their analyses did not correspond to that predicted by the formula of Odozi (2000) [36].

Experiments were conducted by Bertoldi et.al. (2015) on two-phase flashing flows in a venturi tube to study the effect of mass flow rate and concentration of the volatile components present in the liquid phase [37]. The experiments were conducted using R-134a as a volatile component and POE ISO 10 lubricating oil as a nonvolatile component. They concluded that the liquid phase viscosity has a major effect on the pressure difference and recovery in the diverging section. They also concluded that occurrence of two-phase flow in the throat and downstream are sensitive to changes in the operation conditions of the flow. A new correlation was developed by Yuan et.al (2015) to accurately measure the flow of a wet gas flow in a double differential pressure VFM [38]. Data sets were generated using experimental data and dimensionless analysis of several parameters such as differential pressure ratio, gas Froude number, Lockhart-Martinelli parameter and gas-liquid density ratio. The study concluded that the relative deviations of this newly introduced correlation is better than ±1% with a standard deviation of 0.34%.

Currently, no work is available in the literature on pressure drop measurements of mineral oils (D80 and D130)-water two-phase flow in horizontal and inclined 0.0762 m (3-inch) flow loop at different flow conditions for different sizes of venturi meters. Literature also does not address explicitly the impact of venturi meters (with β = 0.4, 0.5 and 0.6) pressure

drop and venturi coefficients on flow loop inclination for selected oils, D80 and D130, water two-phase flow conditions. The variables affecting the performance of different sizes of venturi meters for oil-water flow under real oil well operating fluid flow rates have not been reported in the literature.

In the present work, efforts have been made to present pressure drop measurements in a Tercom flanged machined venturi meters (of $\beta = 0.4$, 0.5 and 0.6) for oil-water two-phase flow in a 0.0762 m (3-inch) diameter inclinable flow loop for different water cuts and fluid mixture flow rates. Oils D80 and D130 and potable water were used for the single-phase and two-phase oil-water experiments. The experiments were conducted for flow rates between 2,000 barrels per day (bpd) to 12,000 bpd, water cuts varying from 0% to 100% in steps of 20%, and two flow loop inclinations: horizontal and vertical positions. The range of liquid flow rates (2,000 bpd to 12,000 bpd) were selected to match the actual flow rates in real oil wells to reflect practical applications. More importantly, the study addresses and examines the effect of venturis ($\beta = 0.4$, 0.5 and 0.6) pressure drop and venturi coefficients on flow loop inclination, for selected D80 and D130-water two-phase flow representative of operating flow conditions in a real oil well. The study will help in solving the pressure drop measurement problems encountered in petroleum industries.

CHAPTER 3

EXPERIMENTAL SETUP AND PROCEDURE

3.1 Experimental Setup

The experiments were conducted to investigate the oil-water two-phase flow through a Tercom flanged machined venturi meter device. The schematic layout of the multi-phase flow loop is shown in Figure 3.1. The flow loop mainly consists of four centrifugal variable speed pumps (water and oil pumps), horizontal oil-water cylindrical gravity separator, fluid mixture catching tank, rectangular channel, and an inclinable flow loop. The two water pumps (WP) and two oil pumps (OP) were used for pumping fluids to the flow loop. Each pump can deliver fluid at a maximum flow rate of 5000 bpd with a delivery pressure of 8 bar gage. The horizontal oil-water separation tank consists of oil and water portions separated by a weir of 0.675 m height. The overall length of the cylindrical separator is 9.55 m and its inner diameter is 1.0 m. The length of the oil portion is 4.102 m, whereas the water section length is 5.448 m. The fluid mixture catch tank is of rectangular cross-section and is used to dump the return fluid mixture to suppress the fluid momentum. A transparent Plexiglas window is provided on the water side of the oil-water separator for visual observation of the multi-phase fluid mixture when it enters from the rectangular channel into the separator tank. The inclinable test section toggles on roller

bearings at the base with inclination,θ, that can be varied from 0 to 90 degree from the horizontal position.

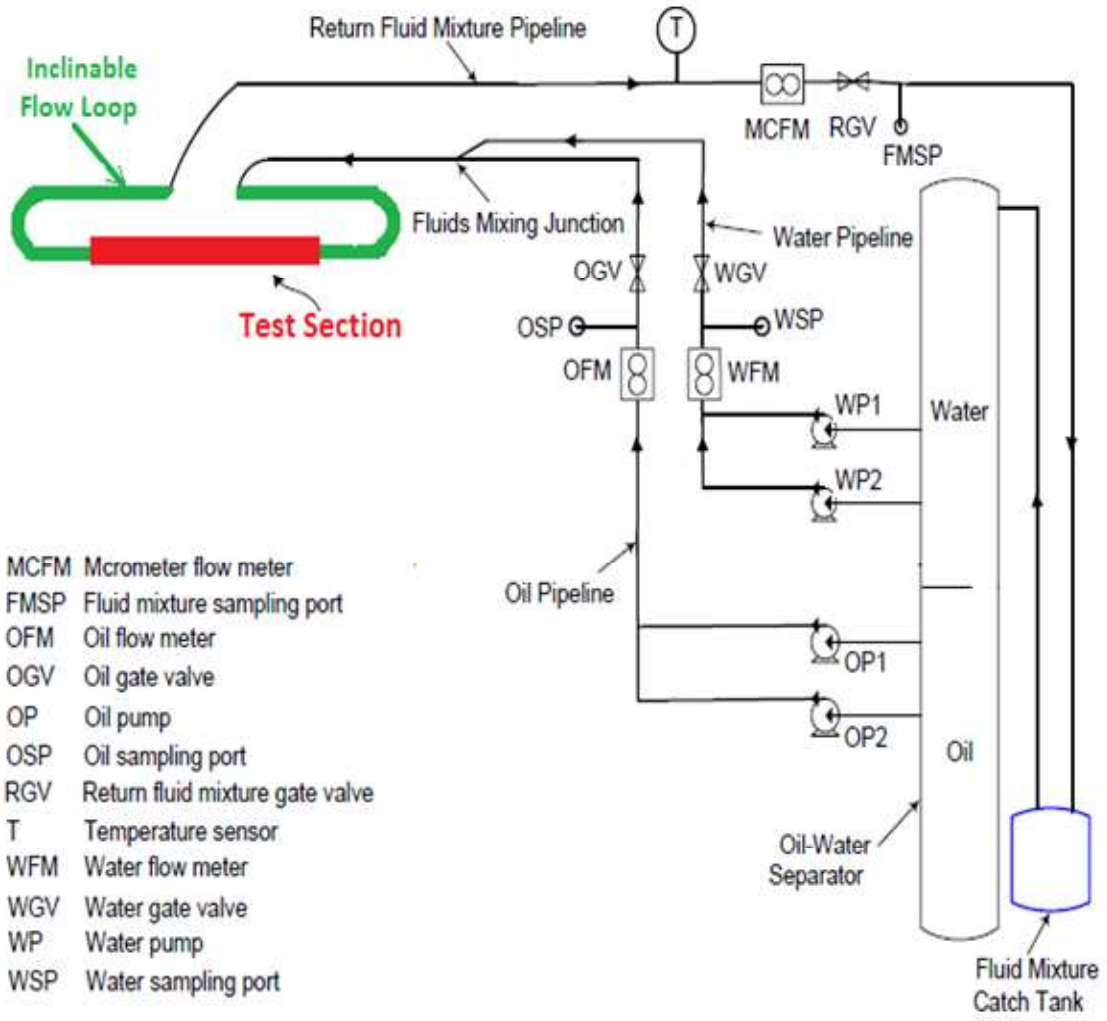

Figure 3.1: Schematic layout diagram of the multi-phase flow loop facility.

The flow loop was instrumented with two OMEGA turbine flow meters (OFM, WFM), and a Mcrometer flow meter (MCFM) for monitoring fluid flow rates. The flow loop had oil, water, and fluid mixture sampling ports (OSP, WSP, and FMSP) to monitor the quality of the fluids in the respective fluid pipelines. The gate valves (OGV, WGV, and RGV)

were provided in the flow loop for controlling line pressure and flow. The return fluid mixture temperature was monitored by the dial gauge type temperature sensor (TS).

➢ Flow - Loop Instrumentations:

The details of the instrumentation used in the experimental work are presented in Table 3.1.

Table 3.1: List of instruments used in the oil-water flow experiments.

Item/Process Parameter	Manufacturer	Model	Capacity/ Range	Accuracy
1. Four Centrifugal Pumps (02 for water & 02 for Oil)	Newar Flow Serve	50-32CPX200	0 - 5000 bpd	---
2. Line Pressure Transmitter (LPT)	Rosemount	Scalable Inline Pressure Transmitter - 3051SITG	0 - 4020 inchH_2O	± 0.025% of FS
3. Differential Pressure Transmitter (DPT)	Rosemount	Scalable Coplanar Pressure Transmitter - 3051S1CD	0 - 1000 inchH_2O	± 0.025% of FS
4. Oil & Water Turbine Flow Meters	Omega	Inline Turbine Meter FTB730	0 - 13714 bpd	± 1.0% of FS
5. Dial Gauge Temperature Sensor	Winters	---	0 - 100 °C	± 0.5 °C
6. Impulse Line	Local Mfr.	½ inch Stainless Steel Pipe w/ NPT Fittings	---	---
7. Venturi Meter	Tercom	Flanged Machined Venturi	Beta ratio = 0.4, 0.5 & 0.6 Inlet diameter = 0.076 m	--

A photographs of schematic layout of the multi-phase flow loop facility are shown in the Figures series from Figure 3.2 to Figure 3.12. As shown in these Figures, the multi-phase flow loop consists of the following installed instrumentations:

Figure 3.2: Oil-water cylindrical gravity separator.

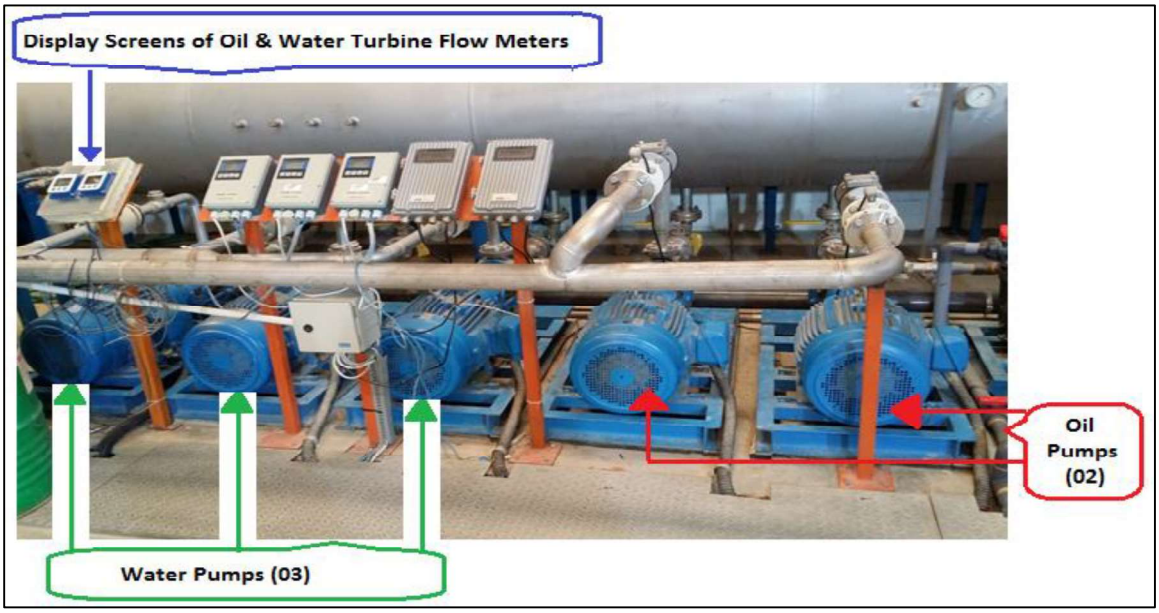

Figure 3.3: Oil and water pumps with induction motors.

Figure 3.4: Close-up view for the catch tank to suppress the fluid momentum.

Figure 3.5: Close-up view for the rectangular channel.

Figure 3.6: Oil and water turbine flow meters (blue colored) used in the experimental work.

Figure 3.7: Mcrometer flow meter (MCFM) for monitoring of the fluids flow rate, and the return gate valve (RGV) to avoid suction at the venturi throat.

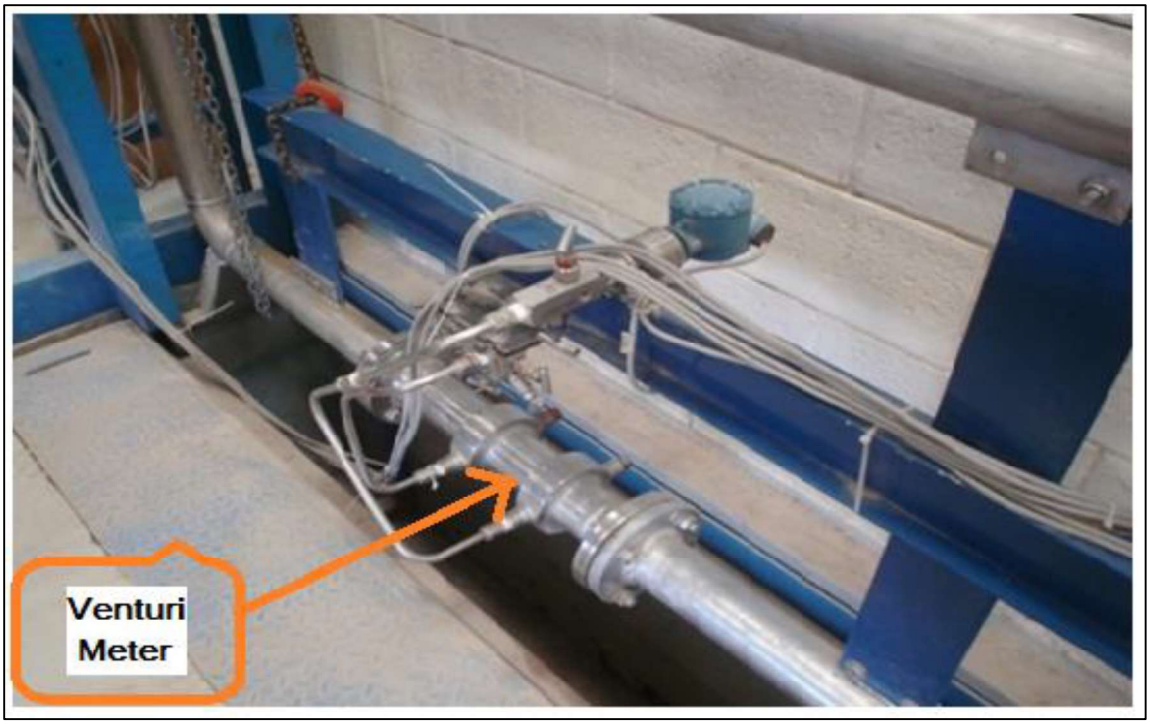

Figure 3.8: Close-up view of the venturi (β= 0.5) at horizontal position.

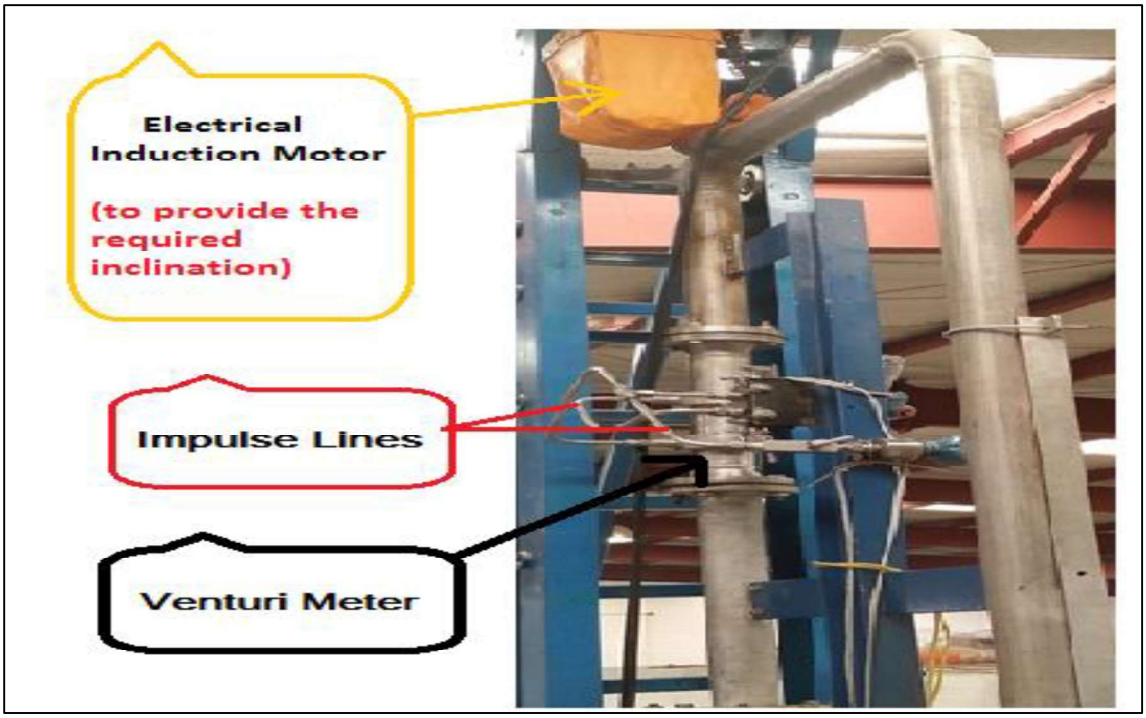

Figure 3.9: Close-up view of the venturi (β= 0.5) at vertical position.

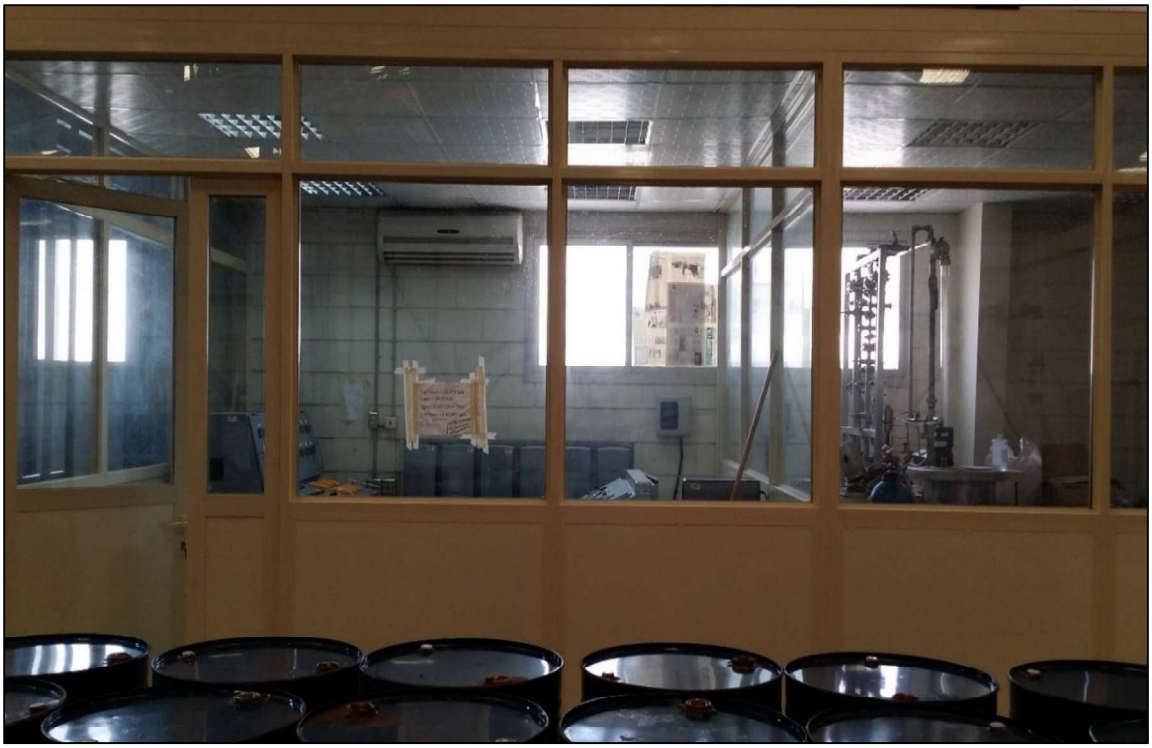

Figure 3.10: Control room of the multiphase flow loop.

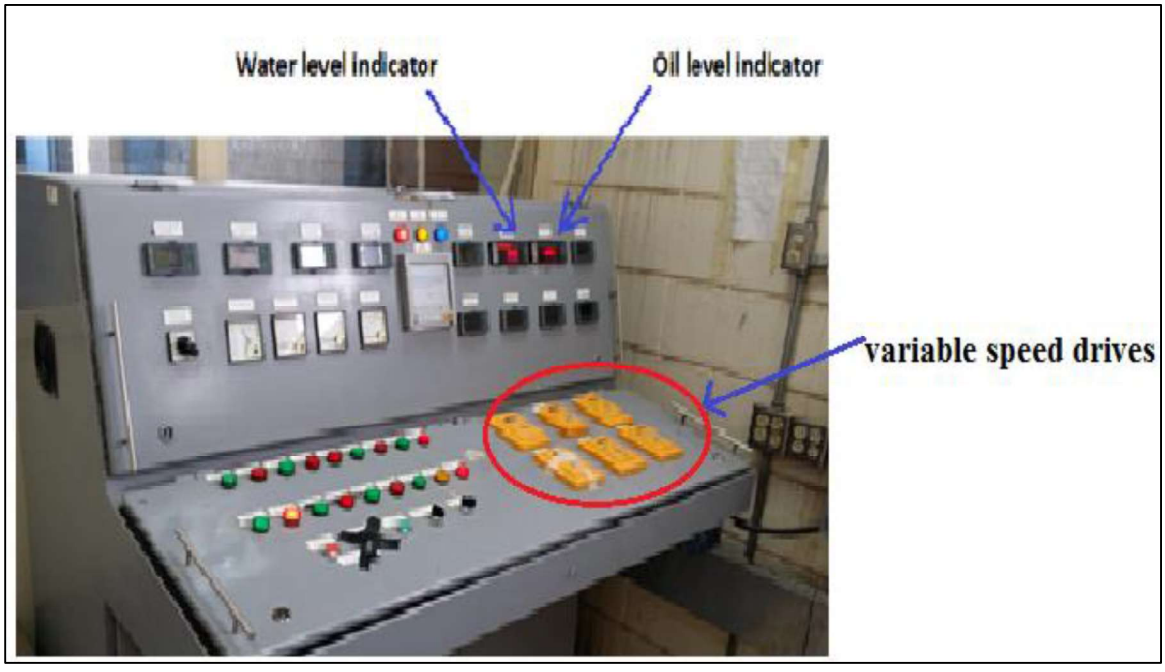

Figure 3.11: Control panel of the multiphase flow loop.

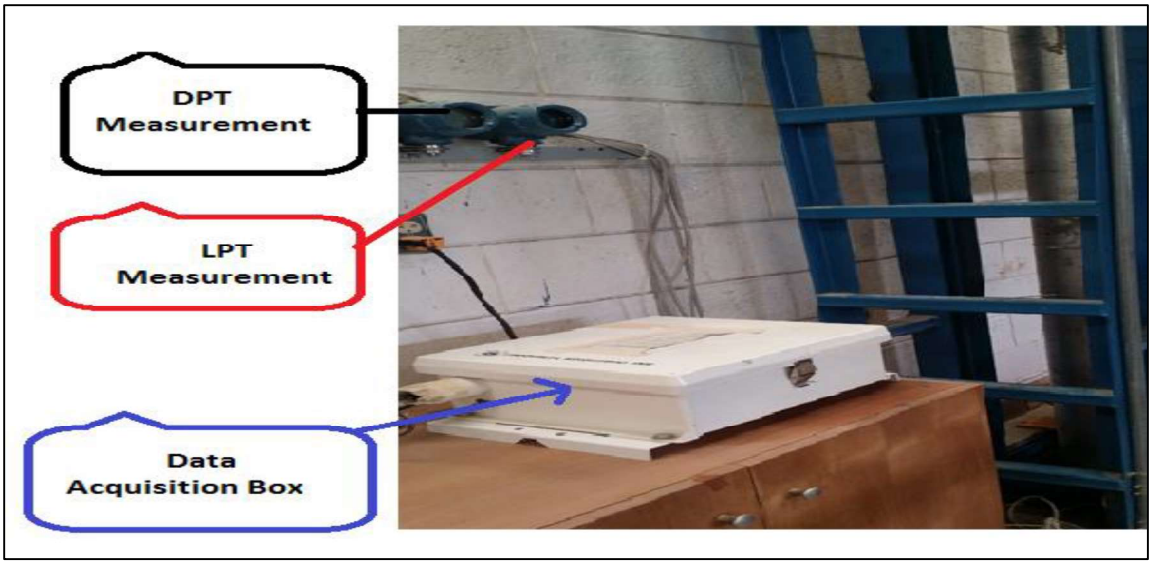

Figure 3.12: Data acquisition system for the oil-water experiments.

- **Details of the Inclinable Flow Loop:**

The detailed drawing of the inclinable flow loop is shown in Figures 3.13 and 3.14. It consists of a static mixer and a venturi. It can be seen from the Figure 3.13 that the static mixer is positioned on the upstream side of the venturi meter for thorough mixing of the multi-phase fluid before it enters into the venturi meter. The detailed physical specifications of the inclinable flow loop test section pipes is shown in Table 3.2.

Table 3.2: Specifications of the inclinable flow loop test section pipe.

Item	Pipe Type	Outside Diameter	Inside Diameter	Pipe Thickness
Specifications	3.5" pipe, Sch J55	0.0889 m	0.0760 m	0.00645 m

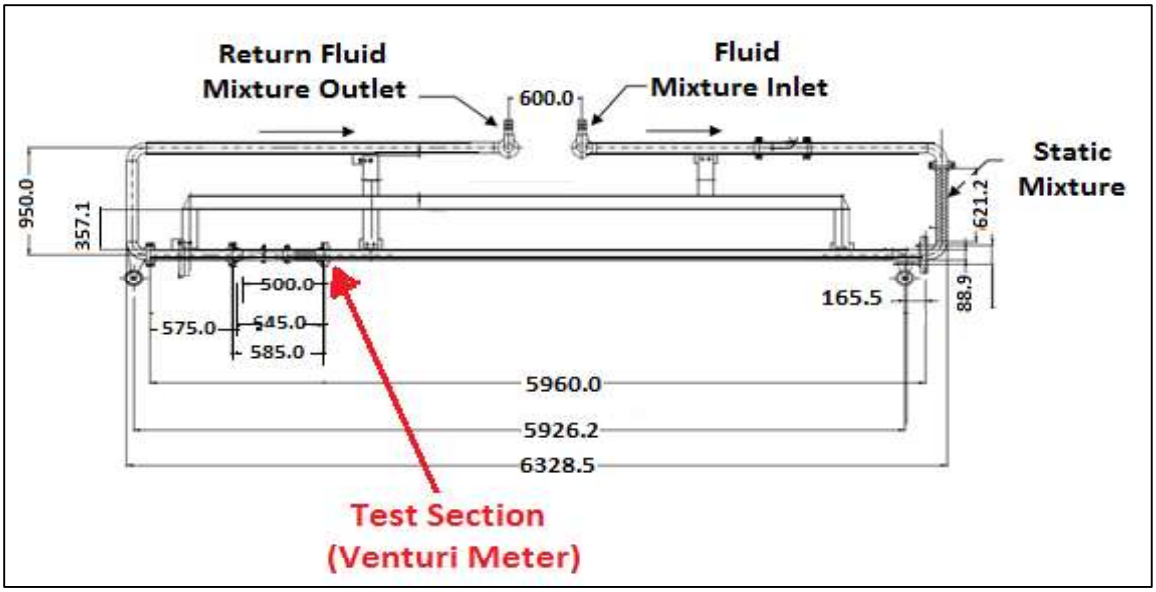

Figure 3.13: Detailed drawing of the inclinable flow loop with a 3.5" steel pipe of Sch J55and a venturi meter.

Figure 3.14: Side - view of the inclinable flow loop with a 3.5" steel pipe of Sch J55and a venturi meter.

The test section of the inclinable flow loop is presented in Figure 3.15. The positions of the installed differential pressure transmitter (DPT) and the line pressure transmitter (LPT) on the venturi meter are shown in Figure 3.15. The DPT was used to measure pressure

drop, ΔP, between inlet and throat of the venturi meter. The LPT was used for gage line pressure measurement at inlet of the venturi meter. The impulse lines (small-bore pipe) are connected to the points at the inlet and throat of the venturi meter to the differential pressure transmitter's ports for measurement of the venturi pressure drop.

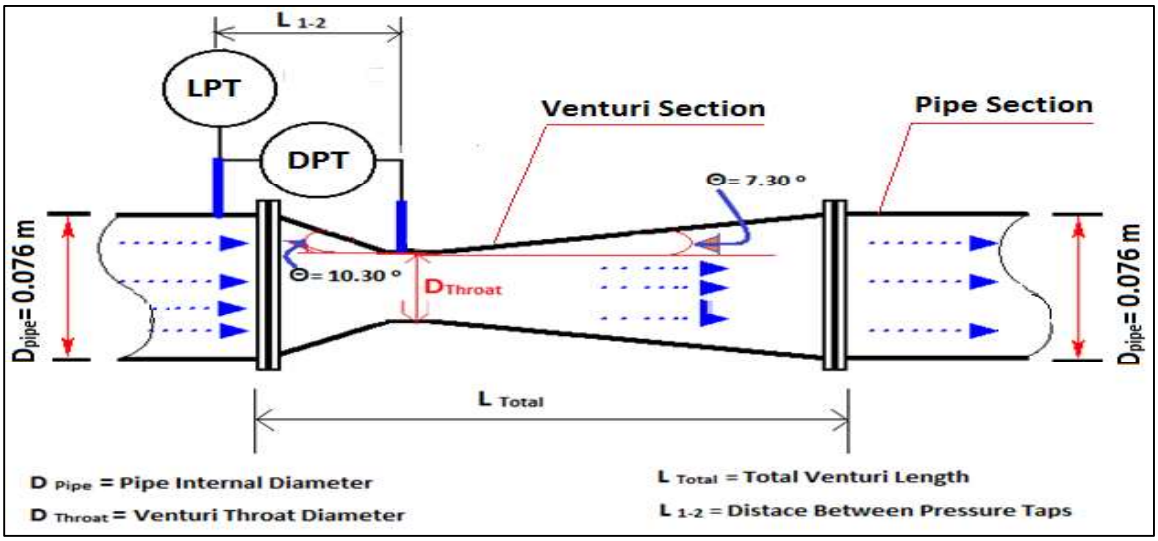

Figure 3.15: Details of the test section showing the venturi meter.

The detailed physical specifications of the three venturi meters are shown in Table 3.3.

Table 3.3: Specifications of Tercom flanged machined venturi meters.

Item	β	Total Venturi Length, L_{Total} (m)	Distance Between Pressure Tappings, L_{1-2} (m)	Venturi Throat Diameter, D_{throat} (m)	Pipe Inside Diameter, D_{pipe} (m)	Flow Rates (bpd)	Venturi and Flange Materials
Venturi Meter 1	0.4	0.585	0.1765	0.0304	0.076	2,000 to 6,000	ASTM A182 Gr. F316
Venturi Meter 2	0.5	0.545	0.1595	0.0380	0.076	2,000 to 10,000	
Venturi Meter 3	0.6	0.500	0.1430	0.0456	0.076	6,000 to 10,000	

- **Physical properties of the Mixture Fluids:**

The physical properties of mineral oils D80 and D130 used in the experimental work are presented in Table 3.4 [21]. The oils Exxsol D80 and Exxsol D130 were procured from ExxonMobil Company. There are dearomatized fluids with low odor, low levels of toxicity, broad evaporation range and narrow boiling range. However, the measurements tests of the physical properties (density and viscosity) for both oils were confirmed again in the laboratories at the Center for Engineering Research (CER) at the Research Institute of King Fahd University of Petroleum and Minerals, Dhahran.

The density test of the potable water was done in the Center of Petroleum and Minerals (CPM) at the Research Institute. Meanwhile its viscosity test was measured at the laboratories of Petroleum Department at King Fahd University of Petroleum and Minerals, Dhahran. The physical properties of used potable water have summarized in Table 3.5.

Table 3.4: Physical properties of the mineral oils D80 and D130 (ExxonMobil chemical 2014) [39].

Properties	**EXXSOL D80**	**EXXSOL D130**	**Units**	**Test Based On**
Initial Boiling Point (IBP)	208	279	°C	N/A
Dry Point (DP)	236	313	°C	N/A
Flash Point (Method A)	82	140	°C	ASTM D93

Aromatic Content	0.2	1	wt%	ExxonMobil Method
Density (15.6 °C)	795	827	kg/m^3	ASTM d4052
Vapor Pressure (20.0 °C)	0.0402	< 0.0402	$inchH_2O$	ExxonMobil Method
Aniline Point (Method E)	77	88	°C	ASTM D611
Kinematic Viscosity (25.0 °C)	$2.18*10^{-6}$	$6.89*10^{-6}$	m^2/s	ASTM D445

Table 3.5: Physical properties of the potable water.

Temperature (°C)	Density (kg/m^3)	Dynamic Viscosity, μ (cP)
20	999	0.849
22	999	0.819
24	998	0.790
26	998	0.756
28	997	0.724
30	996	0.697
32	996	0.667
34	995	0.639
36	994	0.617
38	994	0.590
40	993	0.568
42	992	0.540
44	991	0.510
46	991	0.481
48	990	0.449

3.2 Experimental Procedure

Initially, the experiments were conducted for horizontal position of the flow loop test section for single-phase oils (mineral oil D80 and D130) and water (portable) using a Tercom flanged machined venturi meters with beta ratio, $\beta = 0.4$, 0.5 and 0.6. The fluid flow rates varied from 2000 to 120000 bpd to validate the measurements against available models, and also calibrate the pressure transmitters and flow meters in the loop. The single-phase fluid (water or oils) was pumped in the pipeline using pumps powered by induction motors. The required fluid flow rate was attained by varying the speed of the induction motors through variable speed drives. The Omega inline water and oil turbine flow meters installed downstream of the pumps were used for measuring the single-phase flow rates manually. The pressure drop (ΔP) across the venturi was measured by the differential pressure transmitter, DPT, and the line pressure (LP) by the line pressure gage transmitter, LPT. These pressure transmitters were connected to a Campbell Scientific data acquisition system CR1000. The data acquired from the pressure transmitters were logged automatically every 5 seconds by the data acquisition system and was stored in a predefined file in text format. The collected data was checked for errors and accuracy and then processed further to obtain the required parameters. If the collected data was not satisfactory, the experiment was repeated until high quality data was obtained.

After validation of the single phase oils and water experiments, the multi-phase flow experiments were conducted for fluid mixture flow rates ranging from 2000 to 120000 bpd by using both the oils and water pumps. For a fixed fluid mixture flow rate and inclination of the inclinable flow loop, the experiments were conducted for water cuts

varying from 0 to 100% in steps of 20%. Once the desired water cut was reached, the oil and water flow rate data were recorded manually from the Omega flow meters and data from the pressure transmitters were logged automatically by the data acquisition system. This way experiments were conducted for each mixture fluid flow rates ranging from 2000 to 120000 bpd and for the same inclination but for different water cuts (0 to 100%).

All the experiments as stated above were carried out for different venturi beta size and different inclinations of the flow loop. Also, the return fluid mixture temperature was recorded manually from the dial gauge type temperature sensor during the experiments.

1. Firstly, in the case of venturi 0.4, all the experiments were carried out in horizontal and vertical positions only of the inclinable flow loop and for low flow rates varied from 2000 to 6000 bpd for both oils D80 and D130.
2. Secondly, in the case of venturi 0.5, all the experiments were carried out for different inclinations (0, 40, 60 and 90 degree) of the inclinable flow loop for oil D80, but for horizontal and vertical inclinations only for oil D130 experiments, and for each mixture fluid flow rates ranging from 2000 to 12000 bpd.
3. Thirdly, in the case of venturi 0.6, all the experiments were carried out in horizontal and vertical positions only of the inclinable flow loop but for high flow rates from 8000 to 12000 bpd for both oils D80 and D130.

Also, the return fluid mixture temperature recorded manually from the dial gauge type temperature sensor during the experiments. After completion of the multiphase flow experiments, the collected experimental data were analyzed and presented under the section of results and discussions.

The return gate valve (RGV, see Figures 3.1 and 3.7) of the loop is throttled to set the required pressure at the venturi inlet to avoid suction at the venturi throat. The return fluid mixture coming out of the inclinable flow loop is discharged back into the fluid mixture catch tank. The fluid mixture from the catch tank flows through the rectangular channel of cross-section 0.5 meter wide and 0.45 meter high and length equal to that of the oil-water separator i.e. 9.55 meter. The fluid mixture from the rectangular channel enters into the oil-water separation tank where oil and water separates by gravity. The fluid continuously flows through the loop until the experimental data is obtained satisfactorily. During the multiphase flow experiments, the oil and water samples were collected through the fluid sampling ports (OSP, WSP) to check the quality of oil and water pumped by the respective fluid pumps.

- **Experimental Matrices:**

The experimental work was carried out for oils (D80 and D130) and venturi of beta ratios of (0.4, 0.5, and 0.6) for different water cuts ranging from 0 to 100% in step of 20%, flow rates varying between 2000 to 12000 bpd, a horizontal and vertical inclinations of the inclinable flow loop were considered for all venturi meters, and four different inclination of the inclinable flow loop from horizontal to vertical positions were consider for the venturi meter of beta ratio of 0.5 in case of oil D80 only . The detailed information about the test conditions are mentioned as follows:

I. Experiments for Oil D80:

❖ **Test conditions:**

- **Oil:** Exxsol D80 **Venturi beta ratio:** 0.4, 0.5, and 0.6
- **Flow loop inclination:** 0º and 90º **Water cut**: 0, 20, 40, 60, 80 & 100%.

***Note:** Except for the venturi 0.5, the experiments conducted for four additional inclinations (0, 40, 60 and 90 degrees).

Table 3.6 shows the matrix of multiphase flow experiments conducted for oil D80 for different venturi of beta ratios (0.4, 0.5 and 0.6) and for different inclinations of the flow loop.

Table 3.6: Matrix of multiphase flow experiments conducted for oil D80.

Venturi beta ratio	Flow rate (bpd)	Water cut (%)	Inclination (degrees)			
			0	40	60	90
0.4	2000	0, 20, 40, 60, 80 & 100	√	×		√
	4000		√			√
	6000		√			√
0.5	2000	0, 20, 40, 60, 80 & 100	√	√	√	√
	4000		√	√	√	√
	6000		√	√	√	√
	8000		√	√	√	√
	10000		√	√	√	√
	12000		√	√	√	√
0.6	6000	0, 20, 40, 60, 80 & 100	√	×		√
	8000		√			√
	9000		√			√

II. Experiments for Oil D130:

❖ **Test conditions:**

- **Oil:** Exxsol D130 **Venturi beta ratio:** 0.4, 0.5, and 0.6
- **Flow loop inclination:** 0º and 90º **Water cut**: 0, 20, 40, 60, 80 & 100%.

Table 3.7 shows the matrix of multiphase flow experiments conducted for oil D130 for different venturi of beta ratios (0.4, 0.5 and 0.6) and for different inclinations of the flow loop.

Table 3.7: Matrix of multiphase flow experiments conducted for oil D130.

Venturi beta ratio	Flow rate (bpd)	Water cut (%)	Inclination (degrees)	
			0	90
0.4	2000	0, 20, 40, 60, 80 & 100	√	√
	4000		√	√
	6000		√	√
0.5	2000	0, 20, 40, 60, 80 & 100	√	√
	4000		√	√
	6000		√	√
	8000		√	√
	10000		√	√
	12000		√	√
0.6	8000	0, 20, 40, 60, 80 & 100	√	√
	10000		√	√
	12000		√	√

➢ **Notes:**

- The Total number of clean experiments conducted for all venturi meters for both oils (D80 and D130) are: (360) experiments
- In some cases, when the emulsion is formed. Emulsion is a mixture of two immiscible fluids (oil and eater); one of the fluids is dispersed in the other fluid in form of droplets. In our study we have a dual dispersion: (oil in water) at high water cuts experiments, and (water in oil) in case of low water cuts experiments. In the case of emulsion formation, the experiments were repeated until satisfactory results were obtained.
- Some of photos were captured for emulsions at different temperature as shown in figures 3.16.

Figure 3.16a: Close-up view of the transparent widow when the emulsion of (oil and water) formed.

Figure 3.16b: Close-up view of the gravity separator (Inside of the tank) when the emulsion formed at temperature (T= 24 ºC).

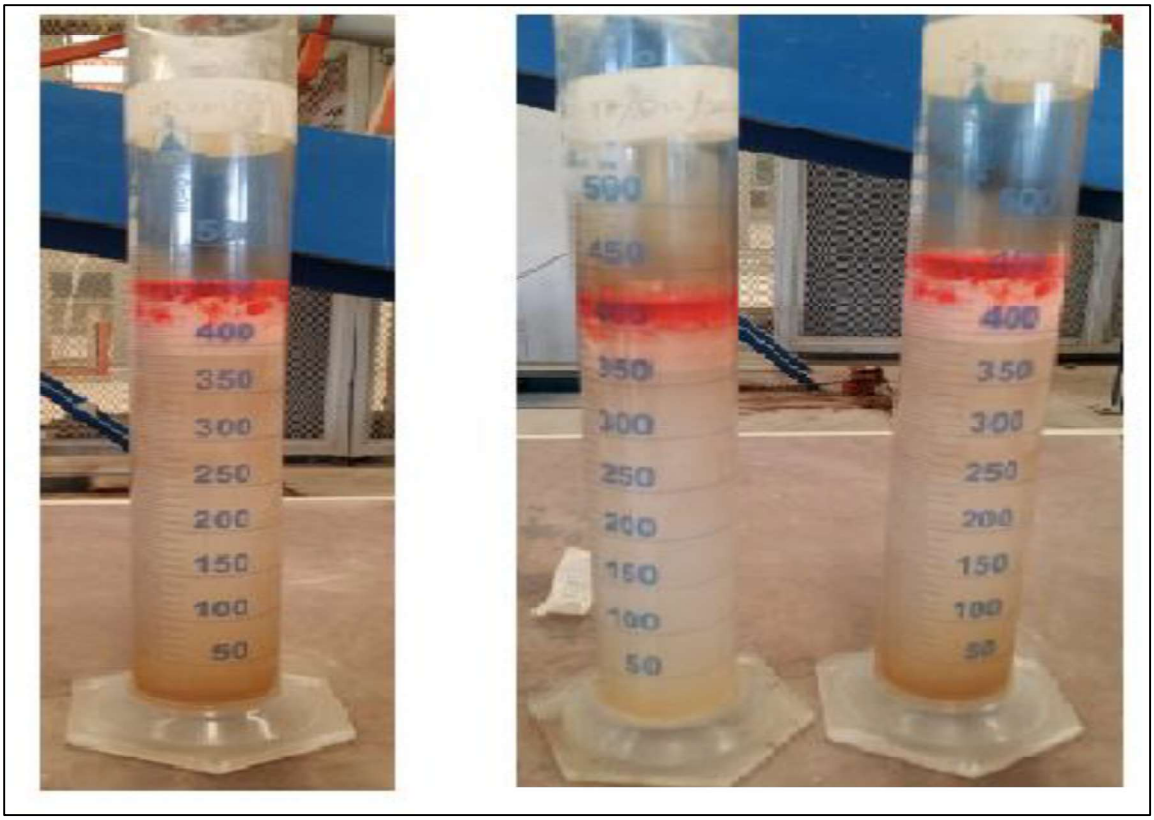

Figure 3.16c: Close-up view of the emulsion samples at glass flasks when formed at temperature (T= 27 ºC).

CHAPTER 4

DATA ANALYSIS AND UNCERTAINTY ANALYSIS

4.1 Validation of the Experimental Results

To validate the single-phase oil and water experiments for the three venturi meters, the calculated and measured venturi pressure drop were plotted in Figures 4.1a to 4.1f. The following equation was used to calculate the venturi pressure drop for single-phase and two-phase flow experiments:

$$\Delta P = \frac{(Q_m / 3600)^2 (1 - \beta^4) \rho_m}{2 C_d{}^2 A_t^2} \tag{4.1}$$

Where,

Qm = Fluid mixture flow rate, m3/h

Cd = Venturi discharge coefficient (Cd = 0.995 from manufacturer)

β = Venturi meter beta ratio (β = 0.4, 0.5 and 0.6)

At = Venturi throat area, m2

ΔP = Calculated venturi pressure drop, Pa

ρm = Fluid mixture density, kg/m3

The oil-water fluid mixture density was calculated based on the homogenous model - homogeneous flow pattern was confirmed at all rates - in terms of the volume fraction of water as following:

$$\rho_m = \rho_w(\lambda) + \rho_o(1-\lambda) \tag{4.2}$$

Where,

λ = Water volume fraction or water cut

ρ_w = Water density, kg/m3

ρ_o = Oil density, kg/m3

Also the oil-water mixture viscosity can be written based on the homogenous model in terms of the volume fraction of water as follows:

$$\mu_m = \mu_w(\lambda) + \mu_o(1-\lambda) \tag{4.3}$$

Where,

$\mu_m =$ Fluid mixture dynamic viscosity, Pa. s

$\mu_w =$ Water dynamic viscosity , Pa. s

$\mu_o =$ Oil dynamic viscosity , Pa. s

$\lambda =$ Water volume fraction

By combining Eqs. 4.1 and 4.2, the relationship between the venturi pressure drop and water cut is given as follows:

$$\Delta P = \frac{(Q_m/3600)^2(1-\beta^4)(\rho_w-\rho_o)}{2C_d{}^2A_t^2}\lambda + \frac{(Q_m/3600)^2(1-\beta^4)\rho_o}{2C_d{}^2A_t^2} \tag{4.4}$$

By considering the actual flow rate (Q_{total}, measured flow rate) from the oil and water flow meters given by the oil and water pumps, and by taking the discharge coefficient (C_d) equal to (0.995) as provided by the Italian manufacture, also the mixture density is known at a certain temperature, in addition to for the venturi meters both the throat diameters and beta ratios are known. Then all these five parameters can be treated as known, finally we plug them in the above equation to obtain the calculated pressed drop, and this calculated pressure drop validated with measured pressure drop from measured from the transmitter (DPT).

Figures 4.1a to 4.2f show the plots for calculated and measured venturi pressure drops for single-phase oils (D80 & D130) and water experiments for the three venturi meters. The results indicate that the measured and the calculated venturi pressure drops for both single-phase oil and single-phase water are in good agreements for all three venturi meters. The experimental results validate the installed pressure transmitter readings.

➢ Validation Results for Oil D80:

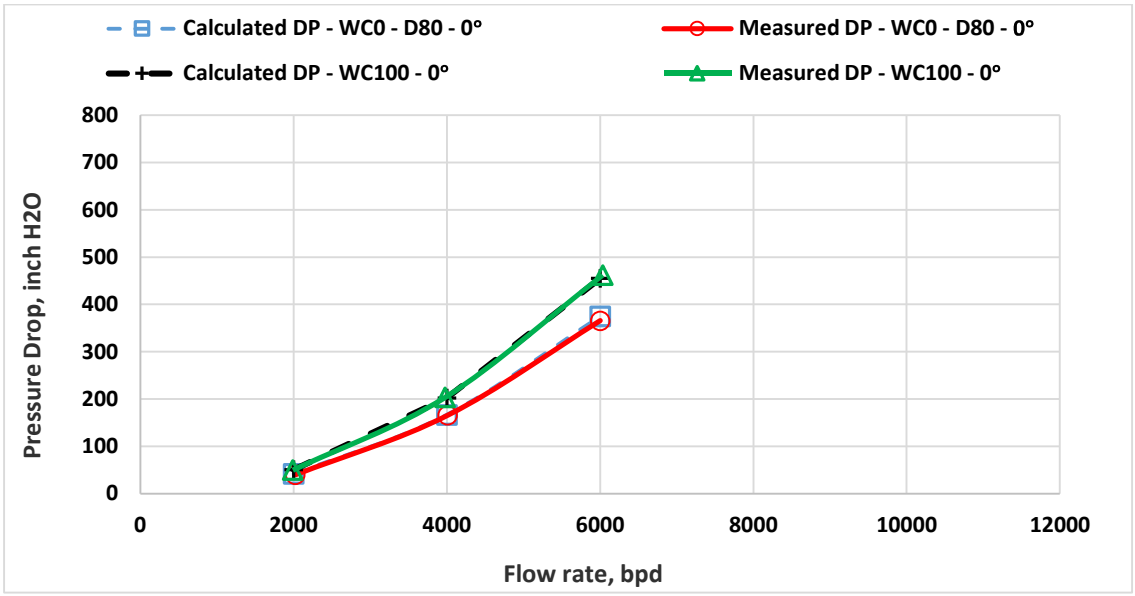

Figure 4.1a: Validation of single phase oil D80 and water experiments for venturi 0.4 for horizontal position of the flow loop.

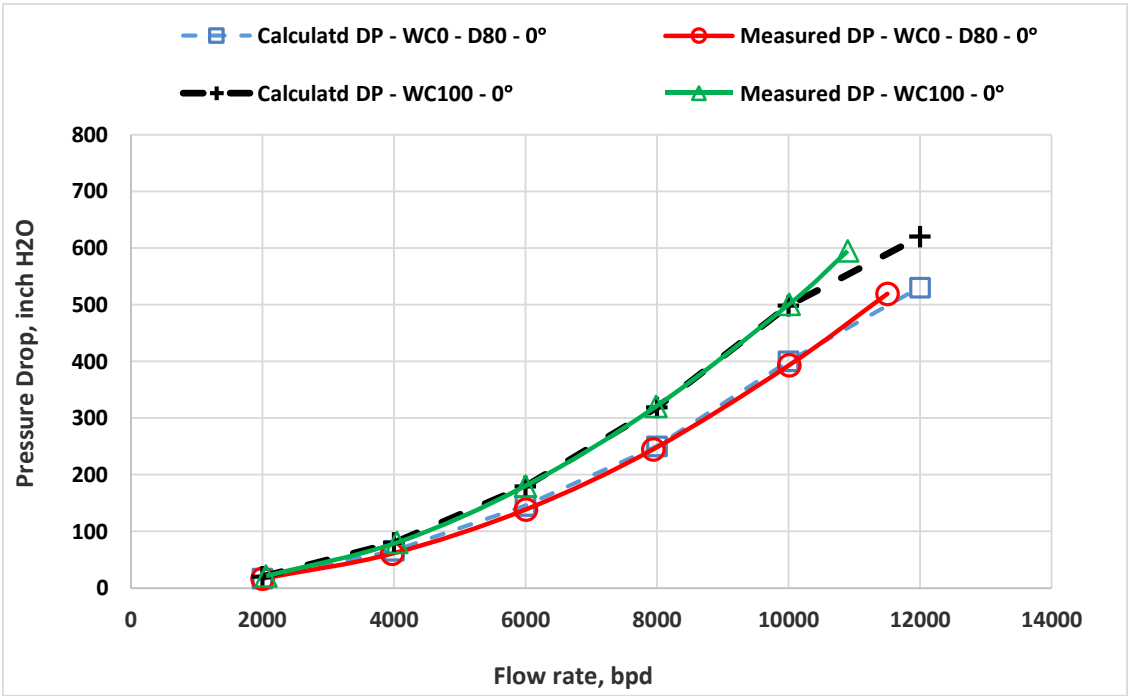

Figure 4.1b: Validation of single phase oil D80 and water experiments for venturi 0.5 for horizontal position of the flow loop.

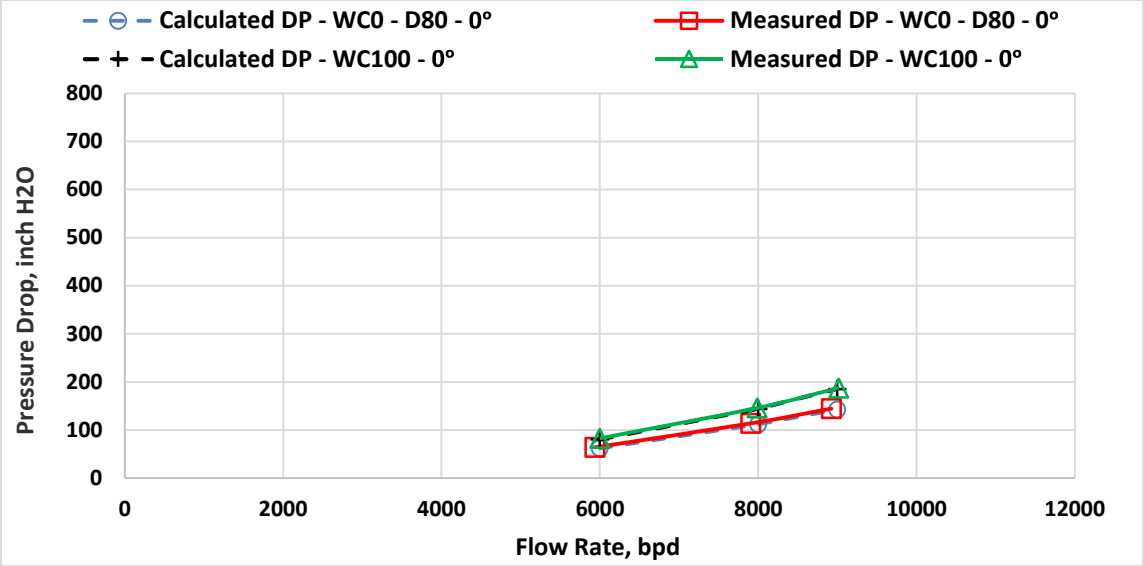

Figure 4.1c: Validation of single phase oil D80 and water experiments for venturi 0.6 for horizontal position of the flow loop.

➢ Validation Results for Oil D130:

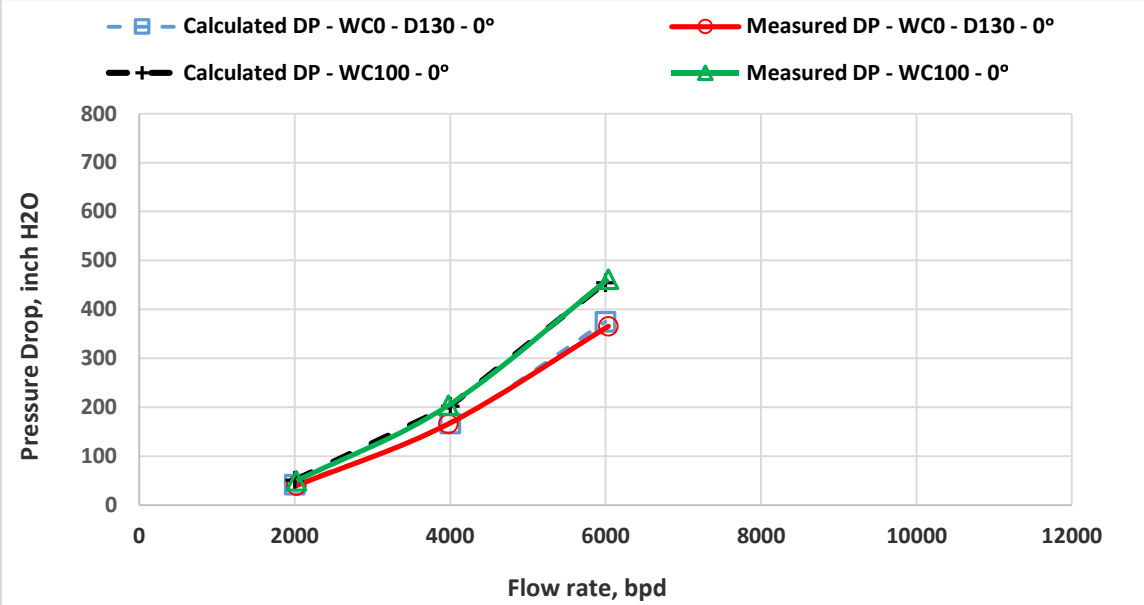

Figure 4.1d: Validation of single phase oil D130 and water experiments for venturi 0.4 for horizontal position of the flow loop.

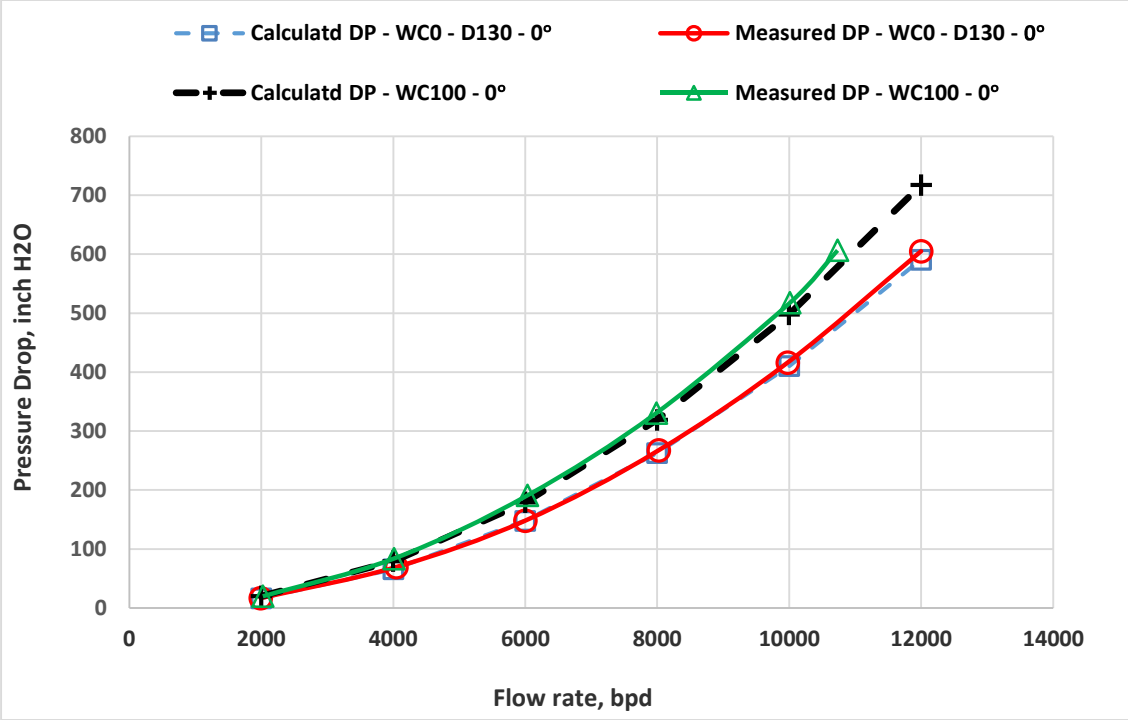

Figure 4.1e: Validation of single phase oil D130 and water experiments for venturi 0.5 for horizontal position of the flow loop.

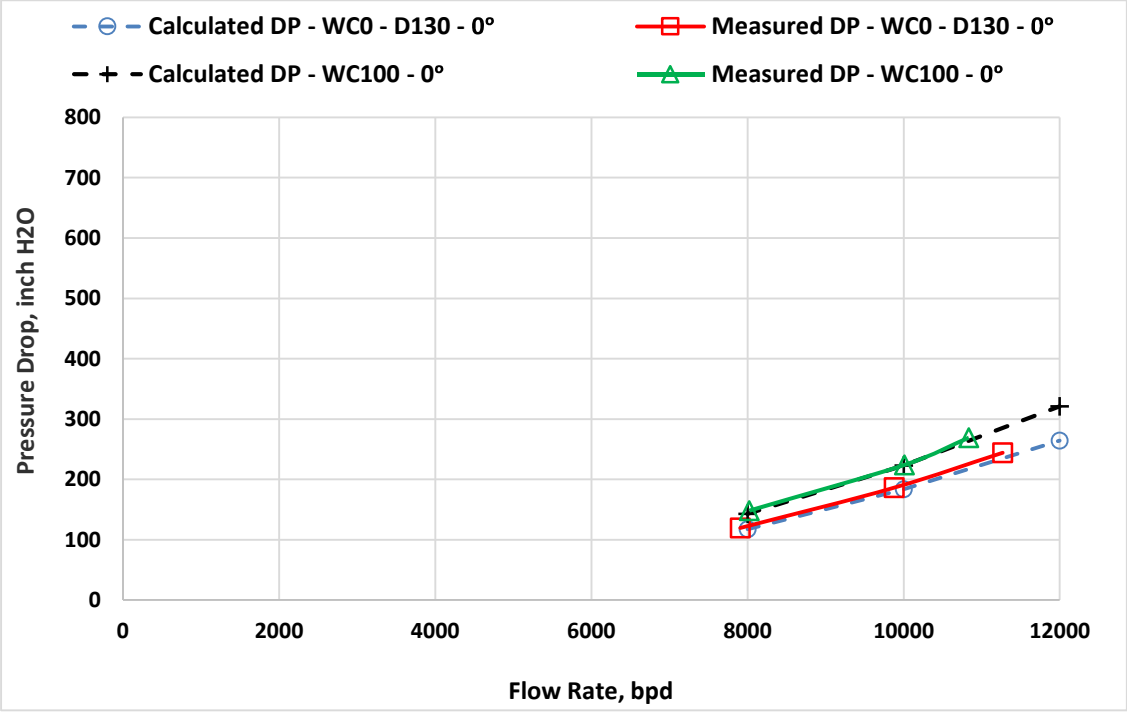

Figure 4.1f: Validation of single phase oil D130 and water experiments for venturi 0.6 for horizontal position of the flow loop.

From the above figures, it can be concluded that the validation results showed a good agreement between the measured and calculated pressure drop measurements. Also from the same figures for both oils and water single phase which corresponding to 0 % and 100% water cut respectively, it can be observe that the maximum flow rate does not reach 12000 bpd due to the using half power of the pumping system in the cases of single phases, because of each single pump can deliver up to 5000 bpd and maximum single-phase flow rated can be obtain is less than 12000 bpd.

4.2 Determination of Modified Venturi Discharge Coefficient, k

For oil-water two-phase flow conditions, the determination of conventional venturi discharge coefficient (C_d) requires the measurement of parameters, such as the fluid mixture flow rate, fluid mixture density, venturi pressure drop, venturi β, and venturi throat area. A modified venturi discharge coefficient, k, which is a function of pressure losses and venturi geometry, is introduced in the present study. The value of k can be obtained by simplifying the venturi governing Eq. 4.1 as:

$$k = Q_m \sqrt{\frac{\rho_m}{\Delta P}} \tag{4.5}$$

Where,

Q_m = Fluid mixture flow rate, m3/h

ΔP = Venturi pressure drop, Pa

ρ_m = Fluid mixture density, kg/m3

k = Modified venturi discharge coefficient, m^2.s/h

The experimental results of the modified venturi discharge coefficient, k, are plotted against the water cut for different fluid mixture flow rates in Figures 5.6a to 5.6l.

- **Determination of Error Percentages, %:**

Based on the average value of k, the percentage error in the total fluid flow rate was calculated for all inclinations of the flow loop and are presented in Figures 5.6b to 5.6l. The percentage error in fluid mixture flow rate is calculated from the following equation:

$$Error, \% = \left|\frac{Q_{meas} - Q_{cal}}{Q_{meas}}\right| \times 100 \quad (4.6)$$

Where,

Q_{meas} = Measured fluid mixture flow rate, m^3/h

Q_{cal} = Calculated fluid mixture flow rate, m^3/h.

The results of percentages of the error are presented graphically 5.6b to 5.6l.

4.3 Determination of Venturi Discharge Coefficient, C_d

The following relation between the coefficient k and C_d can be obtained by combining Eqs. 4.1 and 4.5:

$$C_d = \frac{k}{A_t\sqrt{2}}\sqrt{1-\left(\frac{A_t}{A_p}\right)^2} \tag{4.7}$$

Where,

A_p is the inlet pipe cross-sectional area.

Then, Cd can be written in terms of k and β as shown in Eq. 4.8:

$$C_d = \frac{k}{A_p}\sqrt{\frac{1-\beta^4}{2\beta^4}} \tag{4.8}$$

Eq. 4.8 was used to calculate the Cd using the average k values of each of the three venturi meters, as discussed in the previous section. The obtained C_d is plotted against the water cut for different fluid mixture flow rates and for horizontal inclination of the flow loop for the three venturi meters. The results of Cd are presented graphically in Figures 5.7a to 5.7f.

4.4 Correlations of Venturi Pressure Coefficient, Cp_m

The pressure coefficient is a parameter that describes the ratio of pressure forces to inertial forces. To correlate the results of the oil-water pressure drop in the venturi and in light of the single-phase flow dimensionless parameters, the mixture pressure coefficient seems to be a good candidate. The mixture venturi pressure coefficient can be defined as the ratio of the measured venturi pressure drop to the upstream dynamic pressure as shown in the equation.

$$Cp_m = \frac{\Delta P_m}{\frac{1}{2}\rho_m v_m^2} \tag{4.9}$$

The inlet mixture Reynolds number can be defined as:

$$Re_m = \frac{\rho_m V_m D_h}{\mu_m} \tag{4.10}$$

Where,

ρ_m = Density of the homogeneous mixture

μ_m = Absolute viscosity of the homogeneous mixture

V_m = Mixture velocity at the inlet of the Venturi

D_h = Inlet pipe hydraulic diameter.

Generally, to analyze and plot the experimental data for generating a new formula to correlate the different operational parameters, any curve fitting softwares and regression programs could be used for handling the dependent and independent parameters.

In this study, a new software called DataFit [40] was used to find a relationship for all experimental data. DataFit is an engineering tool can be utilized to simplify the statistical and regression analyses, and data plotting. The images of some screen samples of DataFit program are shown in Figures 4.2a and 4.2b.

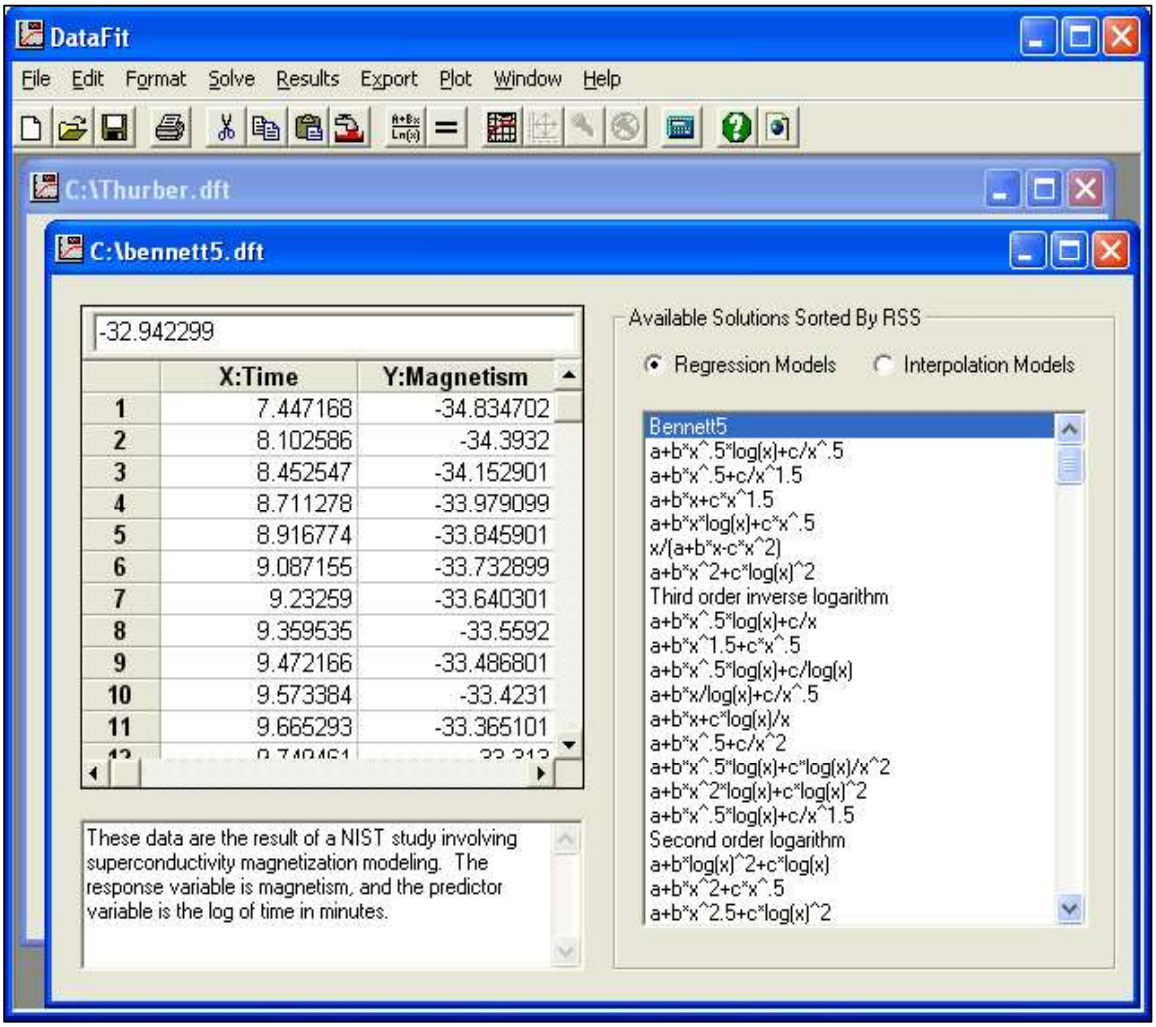

Figure 4.2a: Aphotograph of the main window of the DataFit software.

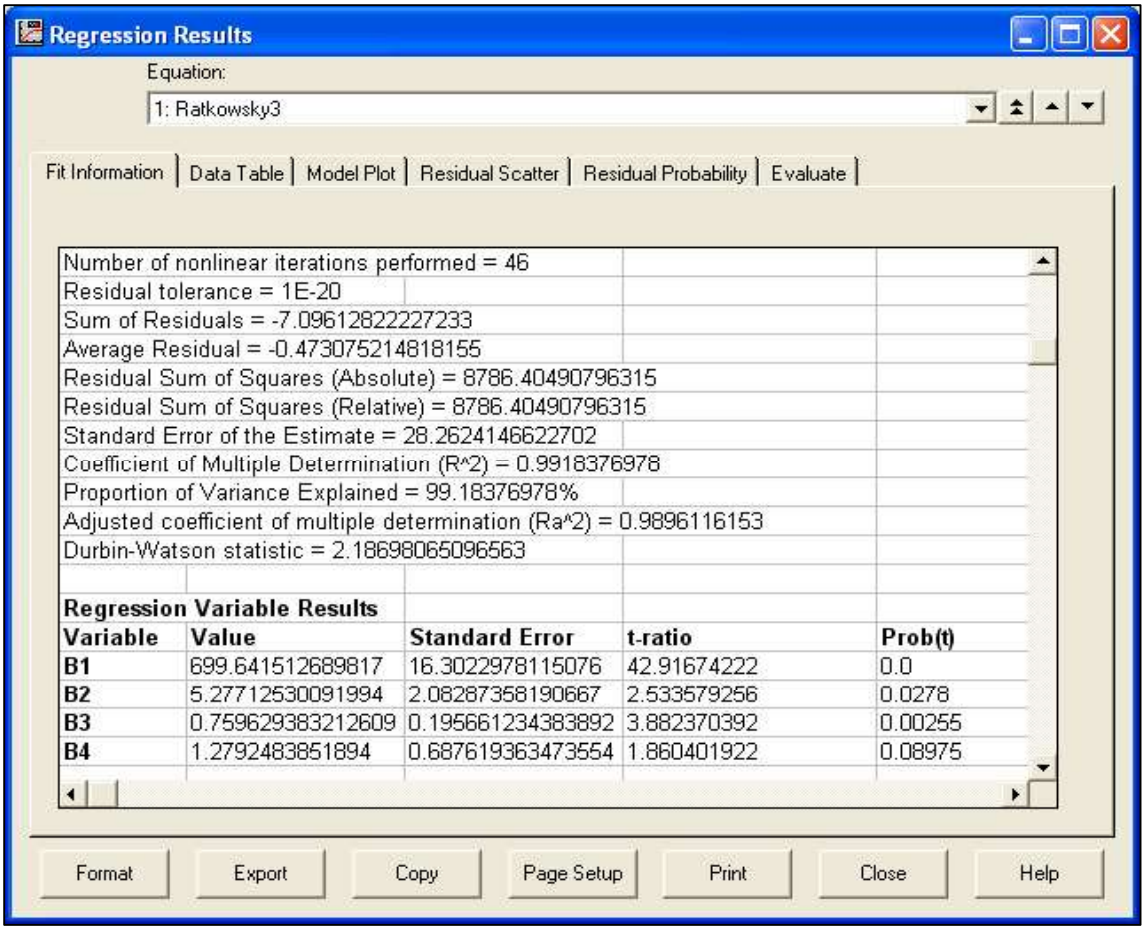

Figure 4.2b: Aphotograph of the window of detailed numerical results of the DataFit software.

To study the effect of the mixture Reynolds numbers on the mixture venturi pressure coefficient, the completely experimental data of each oil have been used to develop several correlations for the mixture pressure coefficient based on the following parameters:

1. Venturi beta ratio.
2. Flow loop inclination.
3. Mixture Reynolds number.
4. Water cut percentage.

Therefore, two exponential empirical correlations have been developed to predict the mixture pressure coefficient for the complete data set of both oils D80 and D130,

individually. In order to study the behavior of the mixture venturi pressure coefficient with the mixture Reynolds numbers, the measured values obtained from Eq. 4.9 and the predicted values are plotted in Figures 5.9a to 5.9f for the three venturi meters and for different operational condition.

- **Reduction of Correlations Input Variables:**

To accomplish which inputs contribute most to output variability, we need to identify relationships between input parameters and the output parameters. When the four in puts parameters were examined by excluding each parameter and to see its effect on the predicted values of venturi pressure coefficient, we end up with: the water cut and inclination have not too much effect and relative contribution on the correlation predictions. Based on the previous assumptions, two input parameters are not correlated which include: water cut and inclination.

Moreover, due to the very small difference between viscosities of oil D80 and oil D130, the complete set of data under the same experimental conditions of both oils was used to develop a new powered correlation for each oil-water ratio.

The generated correlation correlated the mixture Reynolds number and venturi beta ratio as input parameters for each certain water cut. However, the imperial power correlation showed a great potential in predicting of the mixture pressure coefficient when compared with those obtained for each individual oil data when both inclination and water cut were considered.

4.5 Uncertainty Analysis

Uncertainty analysis is a tool utilized to estimate the limits of unknown errors and to describe the reliability of the experimental data.

Generally, according to Morgan and Henrion (1990) [41], Isukapalli (1999) [42], Yen (2002) [43] and U.S. EPA (2003) [44] the uncertainty analysis can be classified as follow:

I. Scenario Uncertainty
II. Parameter Variability
III. Parameter Uncertainty
IV. Model Uncertainty

Firstly, scenario uncertainty is the uncertainty associated with the process of applying a model wherein a petroleum release situation is reduced to a scenario that can be modeled by a numerical model. Some assumptions should be applied in order to introduce and to describe the scenario uncertainty Isukapalli (1999) [42] and U.S. EPA (2003) [44].

Secondly, parameter variability is also mentioned to as natural uncertainty. Regarding to U.S. EPA (1996) [45], numerous of quantities are variable over time, number or space of samples and variability refers to this essential statistical variance.

Thirdly, parameter uncertainty is the uncertainty because of parameters estimations. These comprise what are typically named data uncertainties, which are:

a) Measurement errors
b) Inconsistency and non-homogeneity of data.
c) Data handling and transcription errors.

d) Inadequate representativeness of data sample due to the limitations of time and space.

Finally, model uncertainty is used to describe uncertainties associated with the use of the numerical models in coding processes and is sometimes extended to contain scenario uncertainty.

In this experimental work, the pressure drop observations were measured. Nevertheless, there are errors associated with the pressure drop measurements; therefore, in order to estimate the limits of these errors the Uncertainty analysis (Measurement error) was performed. Uncertainty analysis requires careful planning and implementation to improve the quality measurements and ensure that the study objectives are met.

In this section, the main focusing and concentration were placed on the parameter uncertainty, specifically on measurement errors of the venture pressure drop. Moreover, these measurement uncertainties can be classified into two main types:

1. Random Uncertainty, U_r
2. Systematic Uncertainty, U_s

➢ Random Uncertainty, U_r:

Random (or Type A) uncertainty, U_r, is a statistical determination of error in the experimental measurements, R. H. Dieck (2000) [46]. It is also called the precision error. Based on the standard deviation this type of errors can be expressed mathematically as follow:

Standard deviation, S_x, of N samples is given as:

$$S_x = \sqrt{\frac{\Sigma\left(X - \overline{X}\right)^2}{N-1}} \tag{4.11}$$

Pooled standard deviation is obtained from the following equation:

$$Pooled\ S_x = \sqrt{\frac{S_{x1}{}^2 + S_{x2}{}^2 + S_{x3}{}^2}{3}} \tag{4.12}$$

Where,

S_{x1} , S_{x2} ,and S_{x3} are the standrard deviations of different sets, having the same number of samples, of the same experiment.

Random uncertainty, U_r, which is also called the standard error is as follows:

$$U_r\left(Type\ A\right) = \frac{S_x}{\sqrt{N}} \tag{4.13}$$

Where Ur is the random uncertainty, the coverage factor K (Table 4.1) is used to estimate this error within 95% confidence level.

$$U_r\left(Type\ A\right) = K\frac{S_x}{\sqrt{N}} \tag{4.14}$$

➢ Systematic Uncertainty, U_s:

Systematic (or Type B) uncertainty, U_s, refers to the measurement error associated with the equipment, operator, physical conditions, etc. The systematic uncertainty is given by the following equation:

$$U_s(Type\ B) = \sqrt{\frac{a_1^{\ 2} + a_2^{\ 2} + a_3^{\ 2}}{3}} \tag{4.15}$$

Where,

a1, a2 and a3 are the systematic (or Type B) uncertainties.

Commonly this error occurs due to the experimental conditions and physical conditions. In our experiments systematic errors mainly comes from calibration errors. Due to that, to avoid this kind of uncertainty, all the measuring instrumentations used for the experiments were calibrated. Because of this reason the pressure drop of single phase experiments of oil (WC0%) and water (WC100%) were conducted as shown in Figures 4.1a to 4.1f, and then compared with calculated pressure drop measurements with enhancement of venture discharge coefficient provided by the manufacture to confirm the accuracy of these instrumentations (especially, pressure drop transmitters DPT and LPT).

➢ Expanded Uncertainty, U_e:

The combination of these errors (Random and systematic) is known as expanded uncertainty, it can be given by the following equation, Ue, for a coverage factor of K:

$$U_e = K\sqrt{U_r^{\,2} + U_s^{\,2}} \tag{4.16}$$

Where,

K is a coverage factor. The value of K depends on the confidence level, which is given in the table below:

Table 4.1: Coverage factor versus confidence level (CL)

Coverage Factor, K	**Confidence Level (CL), %**
1	68
2	95
3	99

Generally, the uncertainty in the experimental data is calculated at 95% confidence level, i.e. for a coverage factor of K = 2

Therefore, for coverage factor, K = 2 (CL = 95%), expanded uncertainty is given by the following equation, Ue:

$$U_e = K\sqrt{U_r^{\,2} + \left(\frac{U_s}{2}\right)^2} \tag{4.17}$$

Microsoft excel program was used to run the correlations from 4.11 to 4.17, to calculate the uncertainty analyses calculations which include the random, systematic and expended uncertainties for the all measured data. The measured data of two oils (D80 and D130) for the three venturi meters (β= 0.4, 0.5 and 0.6) and all the flow loop inclinations have been used for the uncertainty analysis. The following figures have been plotted for the random uncertainty of venturi pressure drops for all flow rates.

- **Uncertainty Results for Oil D80 Data:**

For the three venturi metes and all flow loop inclinations for measured experimental data of oil D80, the random uncertainty has been plotted in Figures 4.3a to 4.3h. As can be seen from the Figures, the random uncertainty is less than 0.25% for the measured venturi pressure drops for all: flow rates, water cuts and configurations of the flow loop. In addition, the plots showed that the higher values of the random uncertainty associated with single-phase (WC0% and WC100%) experiments of flow rate (12000 bpd) for the venturi of beta ratio of 0.5. That is because of inability to take exactly the same calculated measurement of the pressure drop at this flow rate (12000 bpd) due to the limitations in the pumping system.

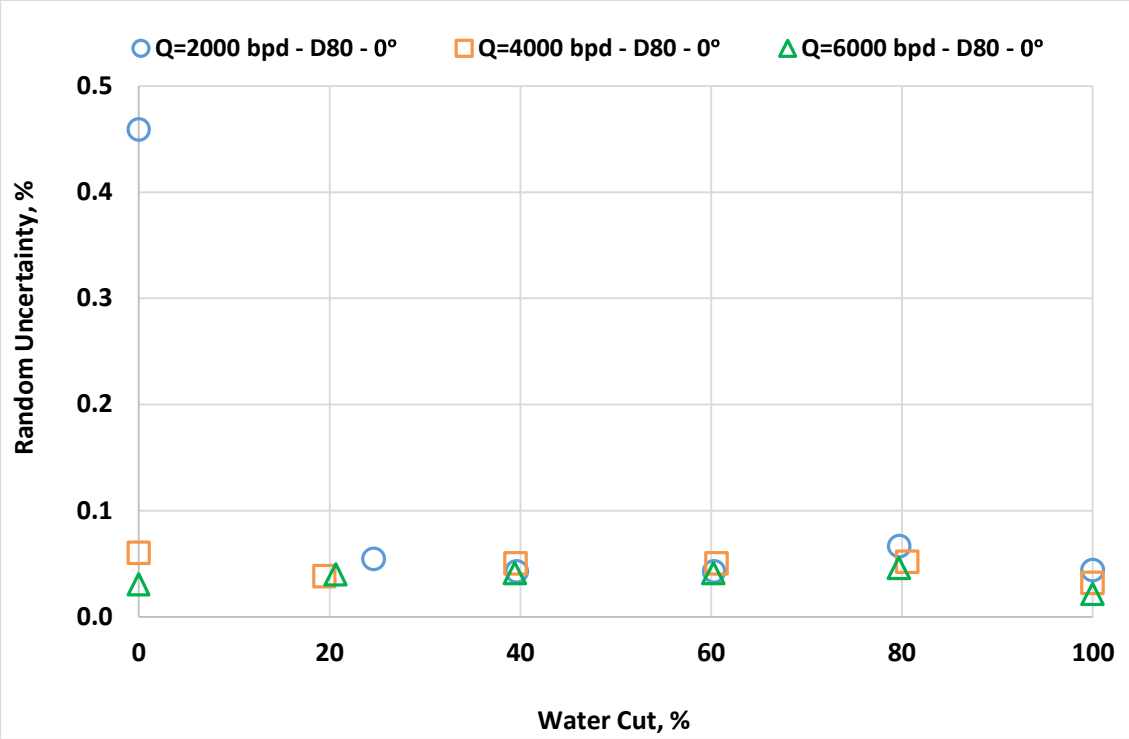

Figure 4.3a: Random uncertainty versus water cut for different fluid mixture flow rates for 0° (β = 0.4, oil D80 and potable water).

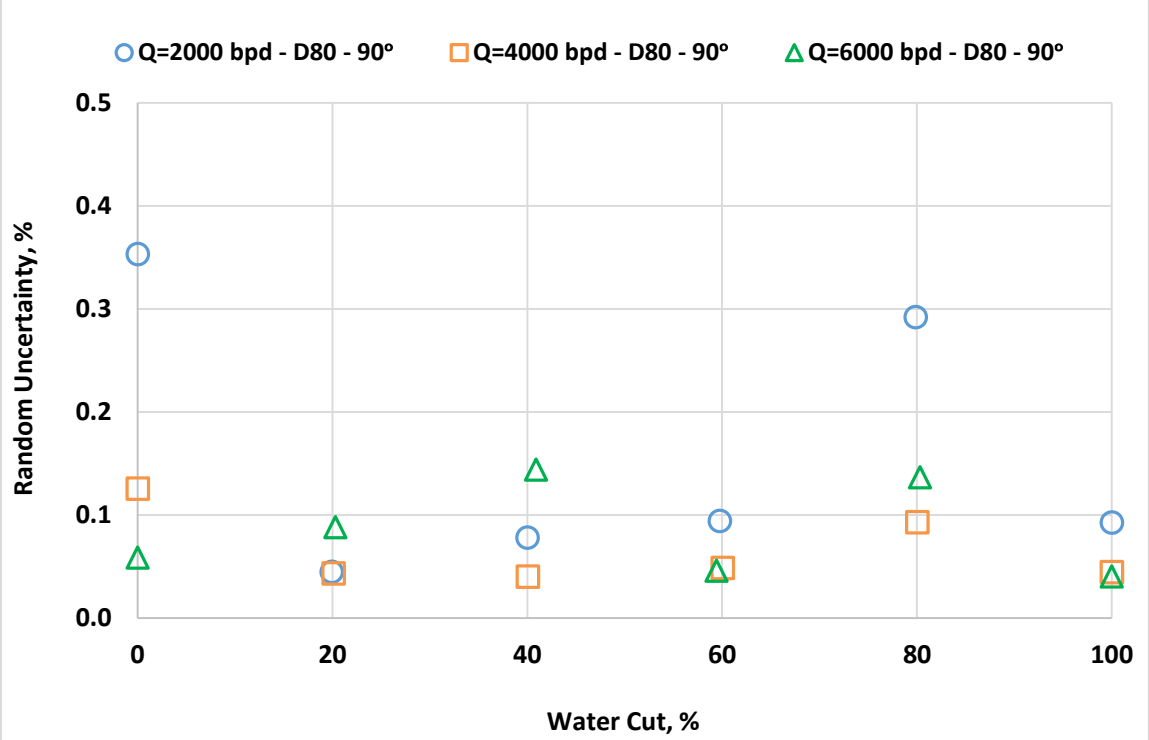

Figure 4.3b: Random uncertainty versus water cut for different fluid mixture flow rates for 90° (β = 0.4, oil D80 and potable water).

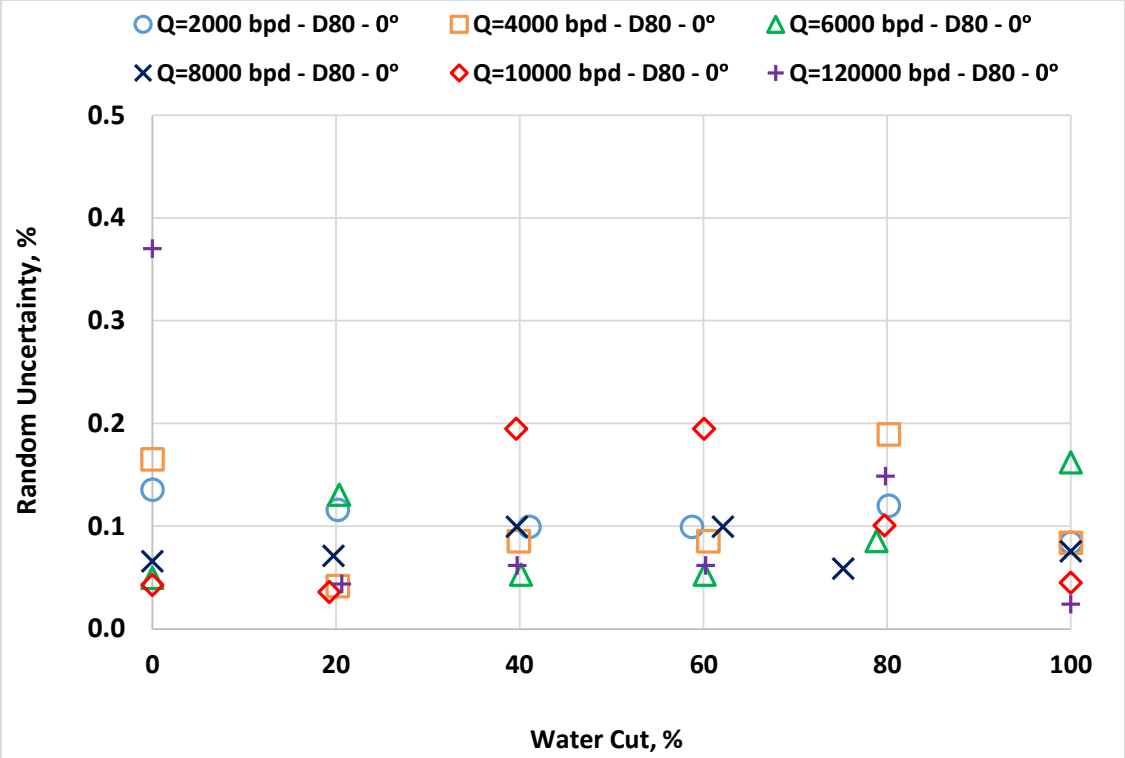

Figure 4.3c: Random uncertainty versus water cut for different fluid mixture flow rates for 0° (β = 0.5, oil D80 and potable water).

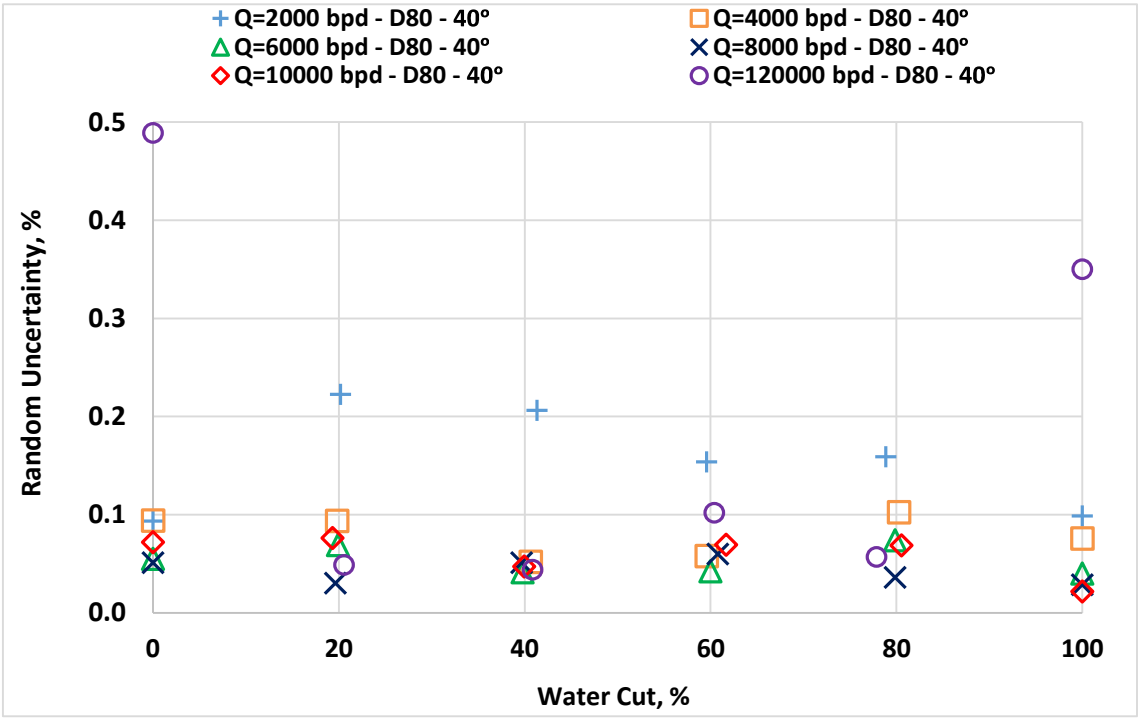

Figure 4.3d: Random uncertainty versus water cut for different fluid mixture flow rates for 40° (β = 0.5, oil D80 and potable water).

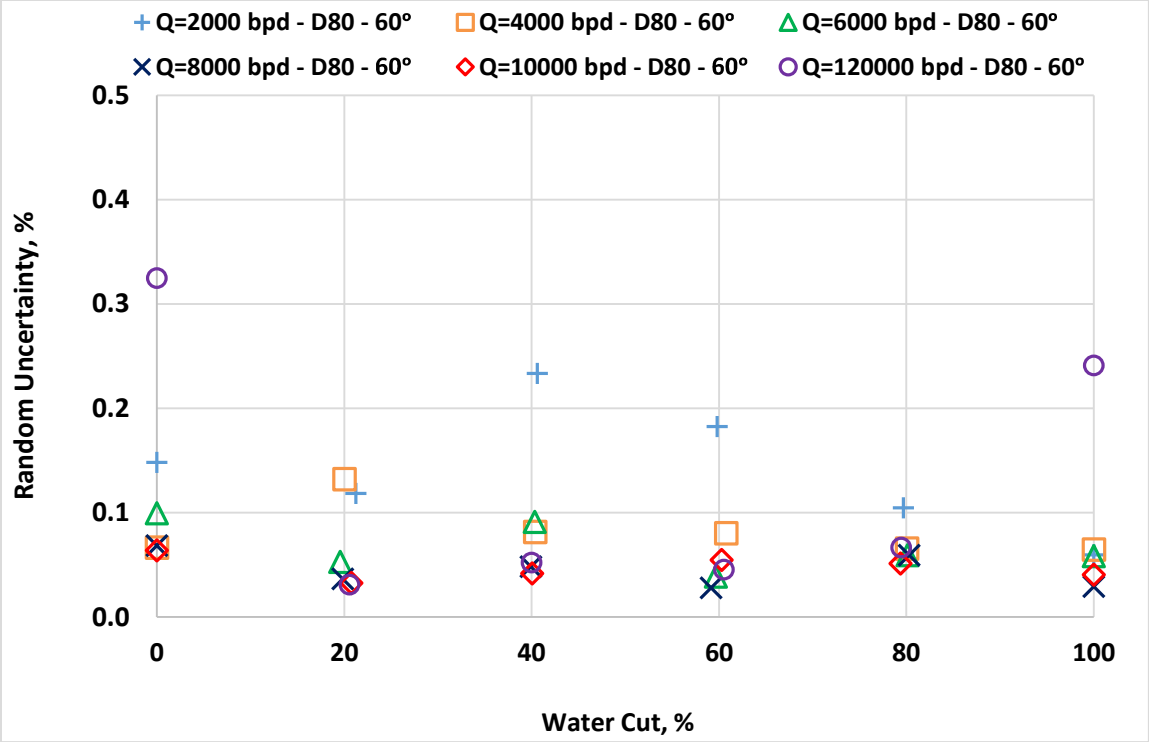

Figure 4.3e: Random uncertainty versus water cut for different fluid mixture flow rates for 60° (β = 0.5, oil D80 and potable water).

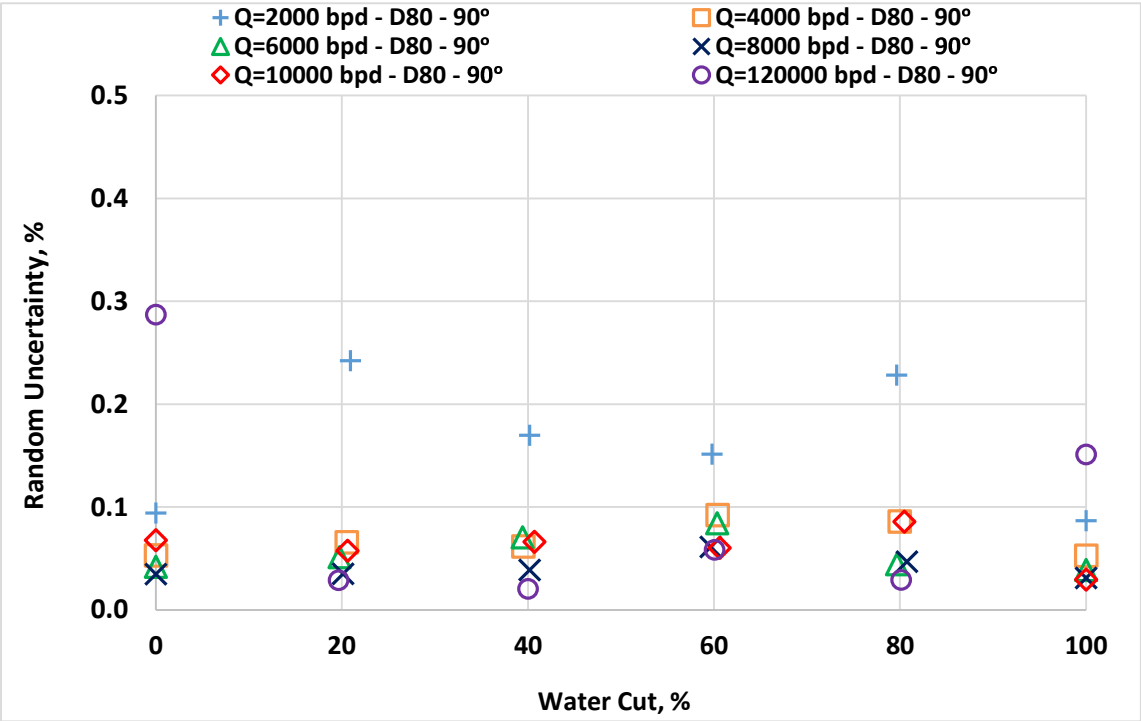

Figure 4.3f: Random uncertainty versus water cut for different fluid mixture flow rates for 90° (β = 0.5, oil D80 and potable water).

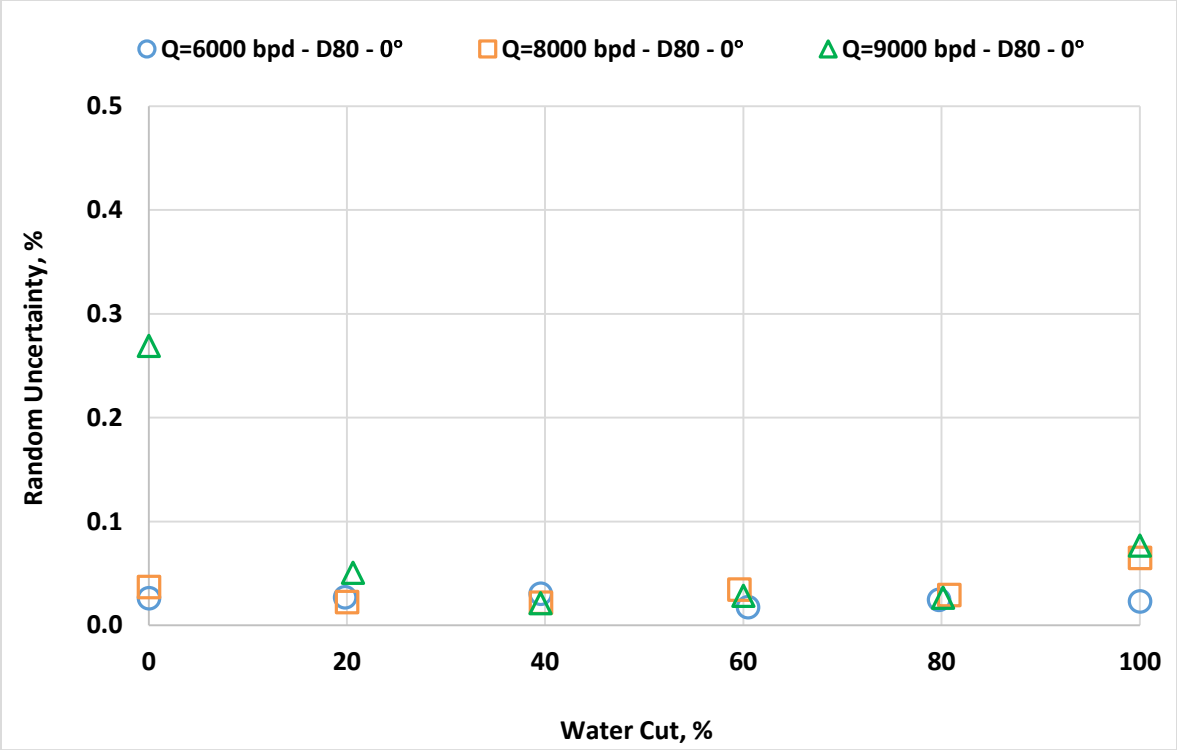

Figure 4.3g: Random uncertainty versus water cut for different fluid mixture flow rates for 0° (β = 0.6, oil D80 and potable water).

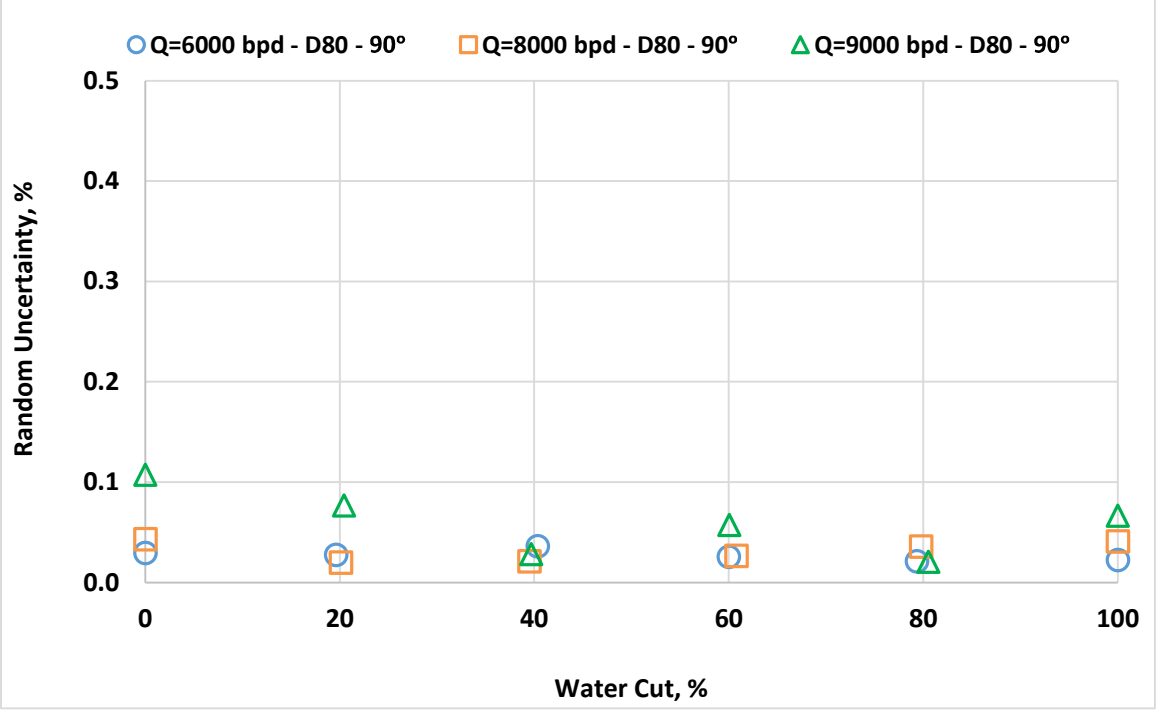

Figure 4.3h: Random uncertainty versus water cut for different fluid mixture flow rates for 90° (β = 0.6, oil D80 and potable water).

➢ Uncertainty Results for Oil D130 Data:

All uncertainty analysis (random, systematic and expanded) of oil D130 data of the three-venturi meters (β= 0.4, 0.5 and 0.6) for all: flow rates, water cuts and flow loop orientations, have been evaluated. The random uncertainty plotted in Figures 4.4a to 4.4f. Similar behavior was observed as shown in the following Figures. Correspondingly, the highest values displayed at single phase experiments of the highest flow rate (12000 bpd) with random uncertainty exceed 0.3%, due to the incapability of the pumping system in the single phase experiments.

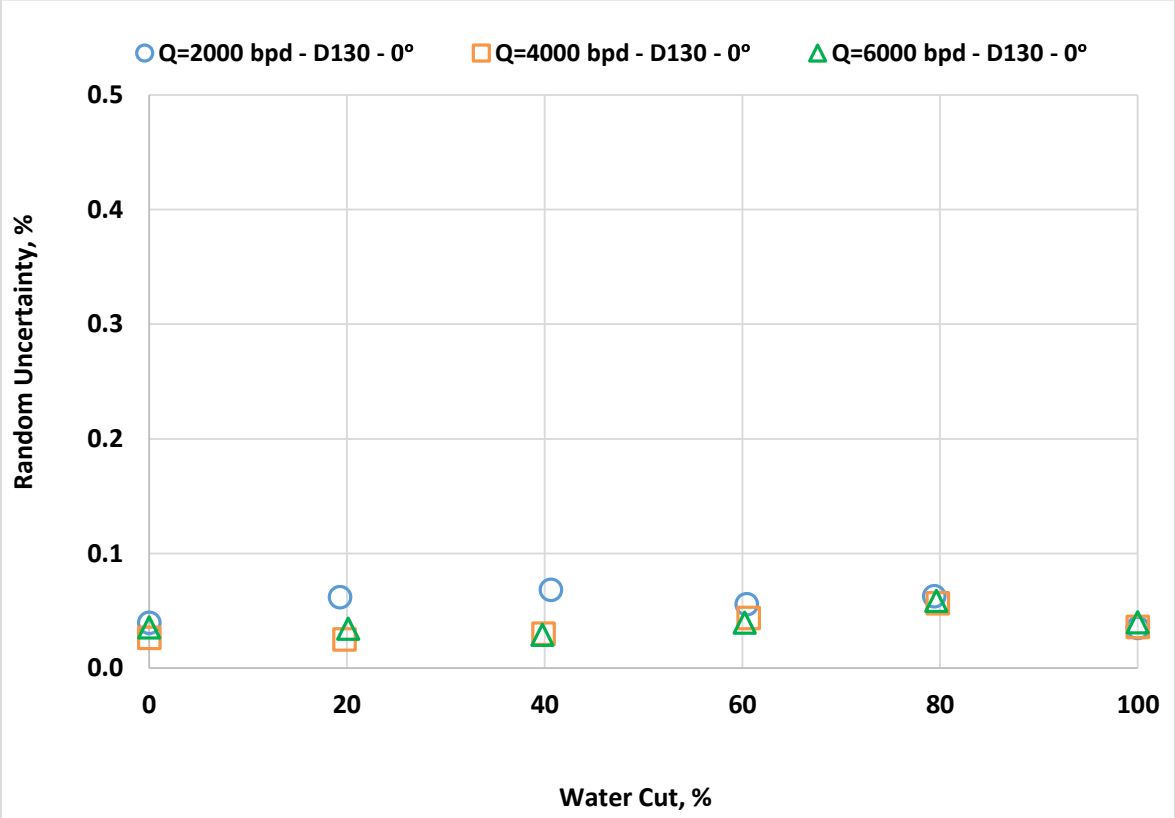

Figure 4.4a: Random uncertainty versus water cut for different fluid mixture flow rates for 0° (β = 0.4, oil D130 and potable water).

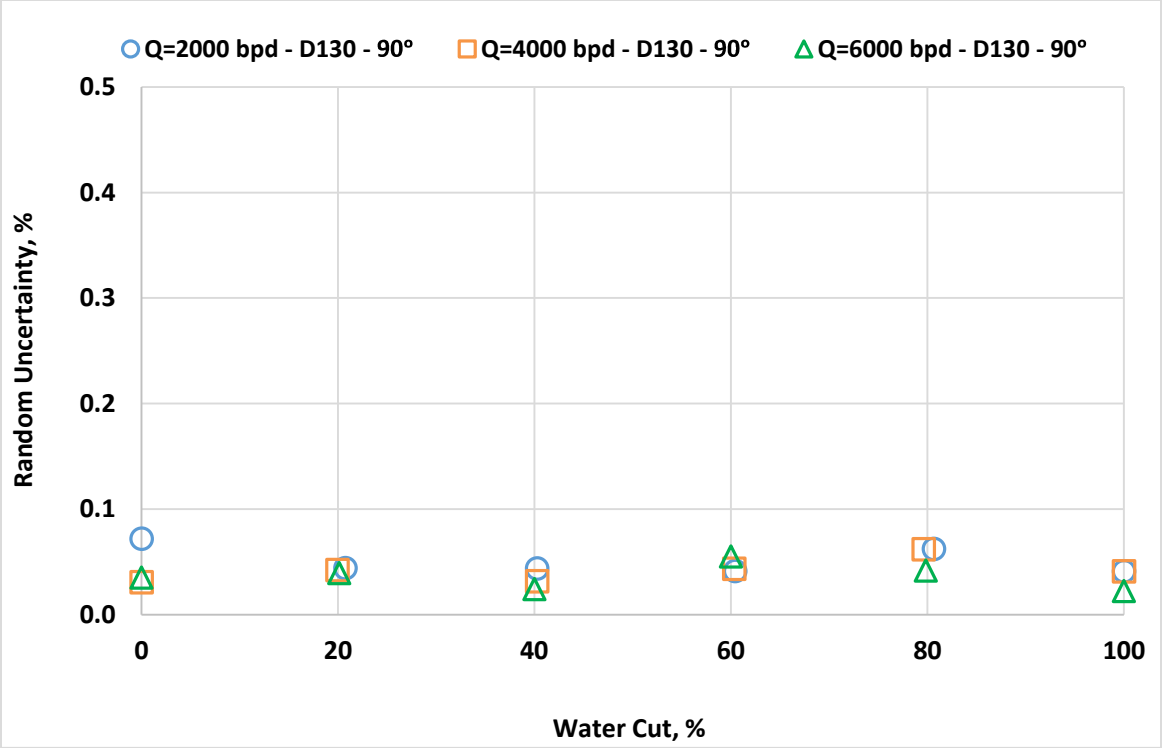

Figure 4.4b: Random uncertainty versus water cut for different fluid mixture flow rates for 90° (β = 0.4, oil D130 and potable water).

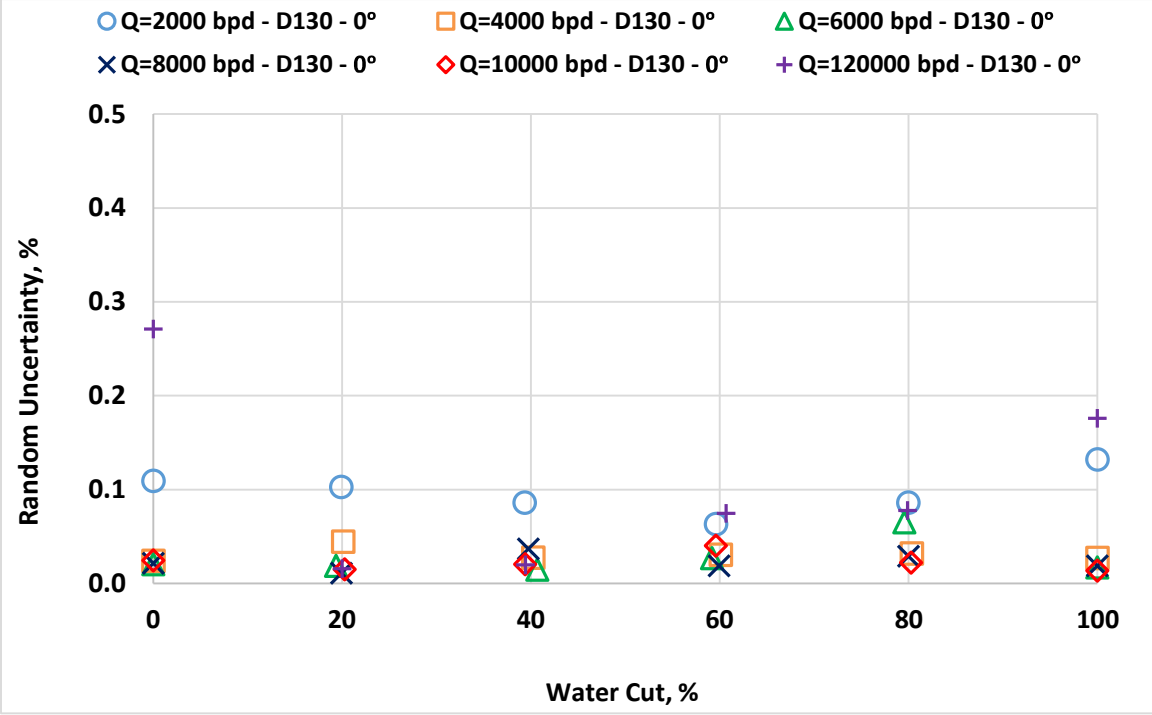

Figure 4.4c: Random uncertainty versus water cut for different fluid mixture flow rates for 0° (β = 0.5, oil D130 and potable water).

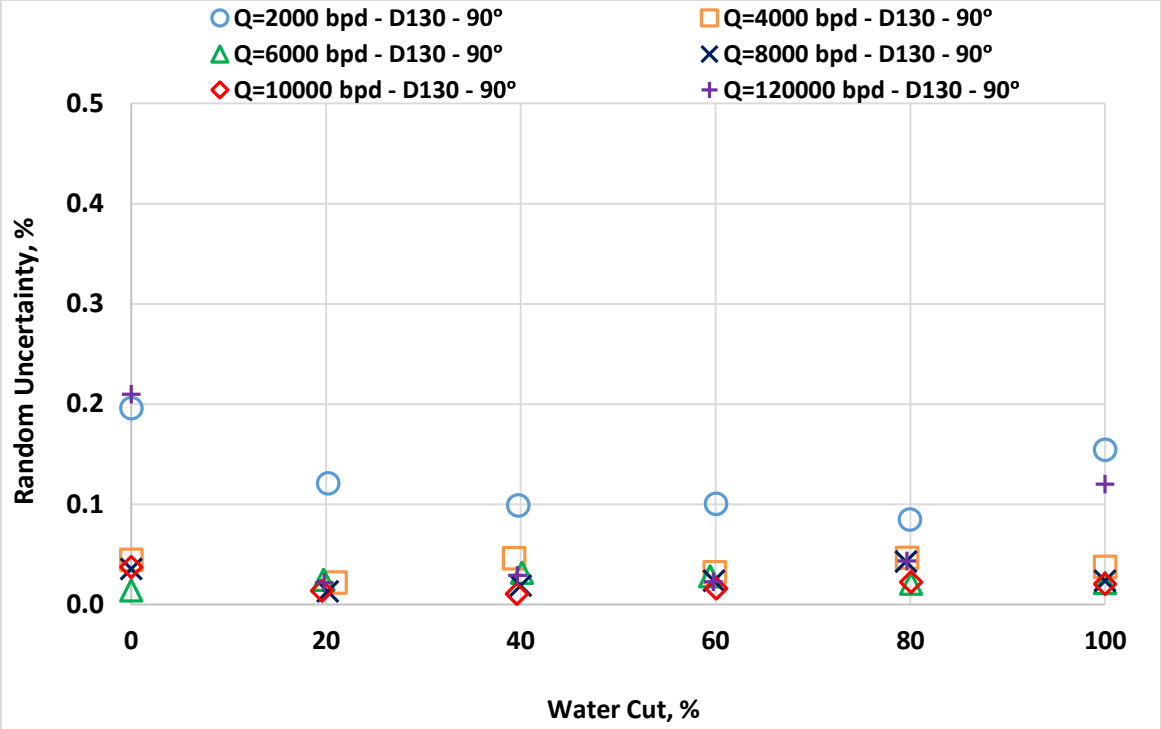

Figure 4.4d: Random uncertainty versus water cut for different fluid mixture flow rates for 90° (β = 0.5, oil D130 and potable water).

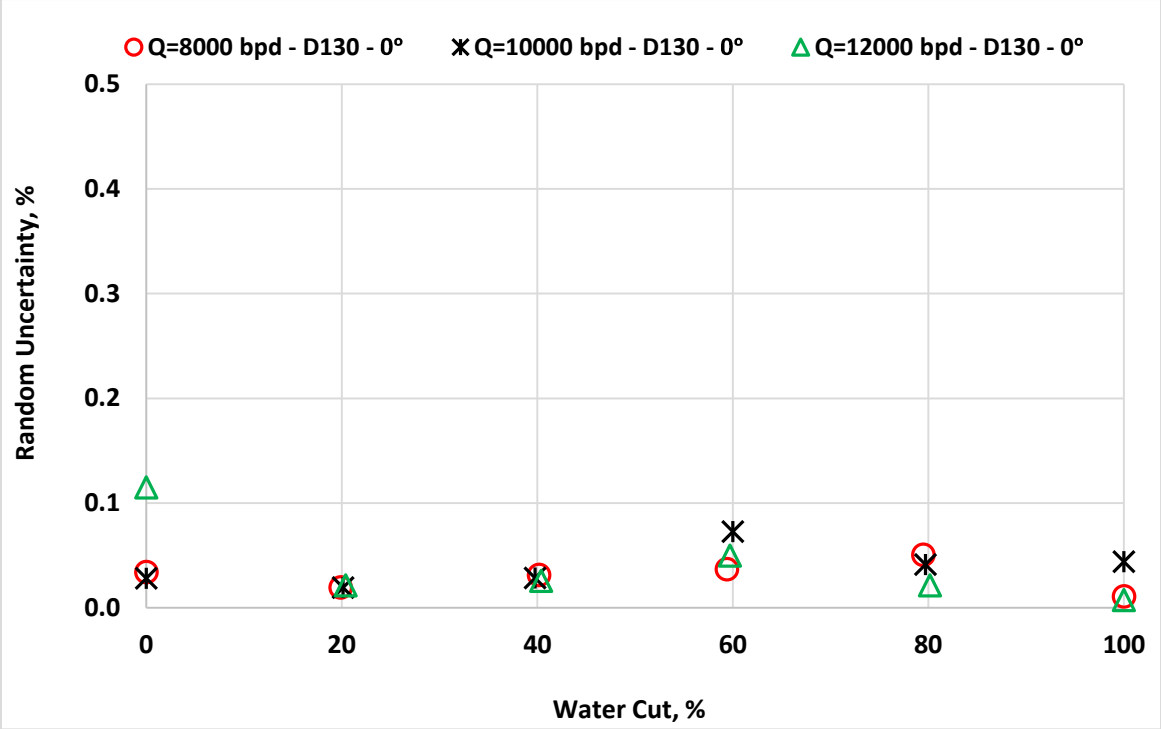

Figure 4.4e: Random uncertainty versus water cut for different fluid mixture flow rates for 0° (β = 0.6, oil D130 and potable water).

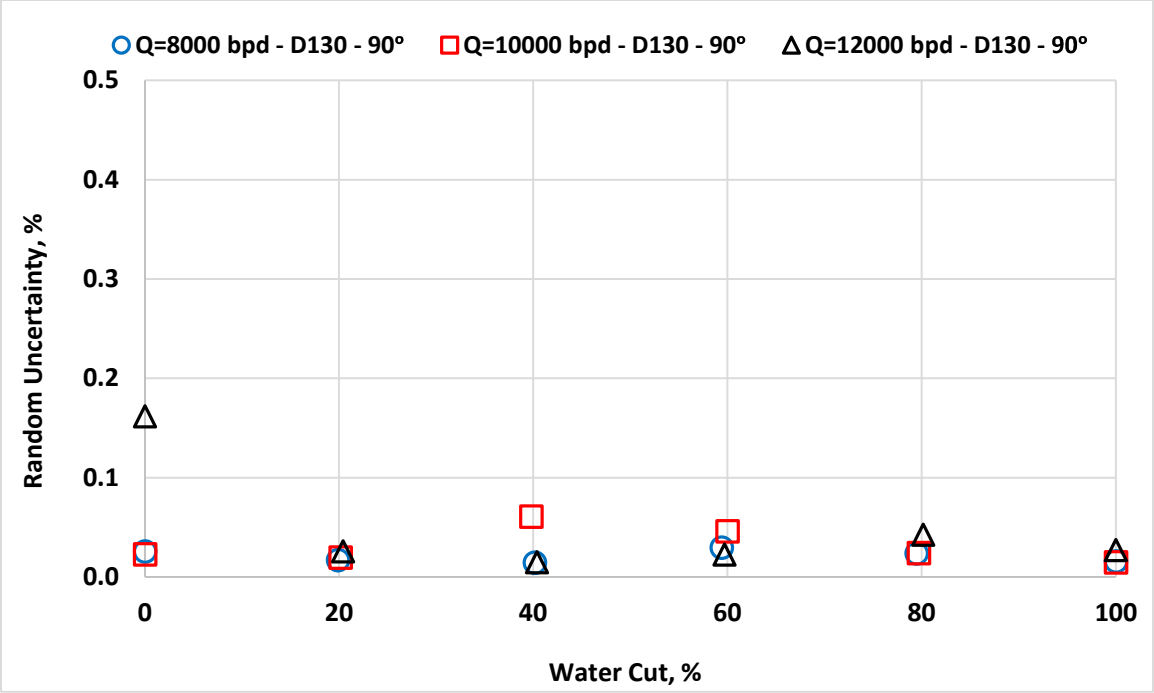

Figure 4.4 f: Random uncertainty versus water cut for different fluid mixture flow rates for 90º (β = 0.6, oil D130 and potable water).

Error analyses were carried out on the venturi pressure drop measurements in the experiments and flow rates from 2,000 bpd to 12,000 bpd. The results yielded standard errors (random errors) between 0.022% to 0.459%, 0.034% to 0.187% and 0.044% to 0.713%, for the β = 0.4, 0.5 and 0.6 venturi pressure, respectively.

The random uncertainty plots do not show any high values which less than 0.5% due to very low standard error. As stated earlier, the highest errors associated with highest flow rate especially at the single phases (WC= 0 and 100%) because of pumps limitations. To avoid the precision limitations measurement of the single-phase experiments, two pumps should be installed one of them in the oil line and the other at the water section.

Further deatails for the random, systematic and expanded uncertainties are presented Appendix A.

Based on the analyses presented in this part it can be concluded that a parametric uncertainty analysis (random, systematic and expanded) of all experimental data of both oils (D80 and 130) can be accurately and efficiently undertaken.

CHAPTER 5

RESULTS AND DISCUSSIONS

At the completion of the all experiments, the experimental investigations for oil D80 and oil D130 were carried out to study the effect of different water cut, venturi beat ratio, fluid mixture flow rate and flow loop inclinations on venturi pressure drop measurements for the three venturi meters (β = 0.4, 0.5 and 0.6) for different water cuts ranging from 0 to 100% in step of 20%, flow rates varying between 2000 to 12000 bpd, and horizontal and vertical of the inclinable flow loop. The experimental results are presented as follow.

5.1 Effect of Fluid Mixture Flow Rate on Venturi Pressure Drop for Different Water Cuts for Oils D80 and D130

The effect of fluid mixture flow rate on venturi pressure drop for different water cuts are presented in Figures 5.1a to 5.1n for horizontal and vertical flow loop inclinations for the three venturi meters (β = 0.4, 0.5 and 0.6), moreover for 40 and 60 degree in case of venturi (β =0.5) for oil D80 experiments. It is evident from the graphical results that the venturi pressure drop varies parabolically with fluid mixture flow rates for a given water cut.

➢ Results for Oil D80:

The experimental results of oil D80 experiments are presented in Figures 5.1a to 5.1h as follow.

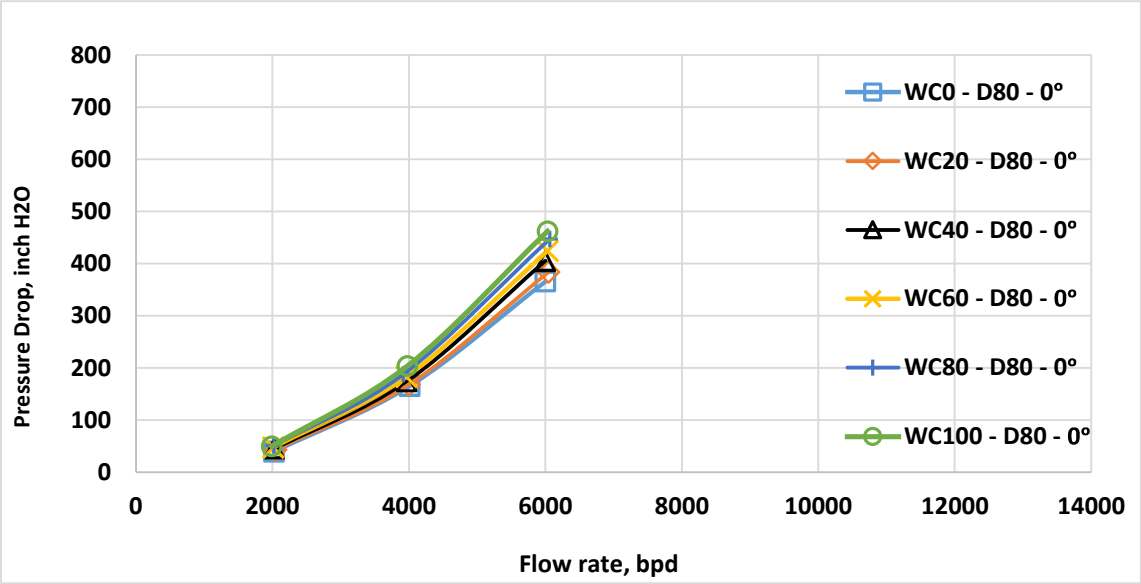

Figure 5.1a: Venturi pressure drop versus fluid mixture flow rate for different water cuts and $\theta = 0^{o}$ ($\beta = 0.4$, oil D80 and potable water).

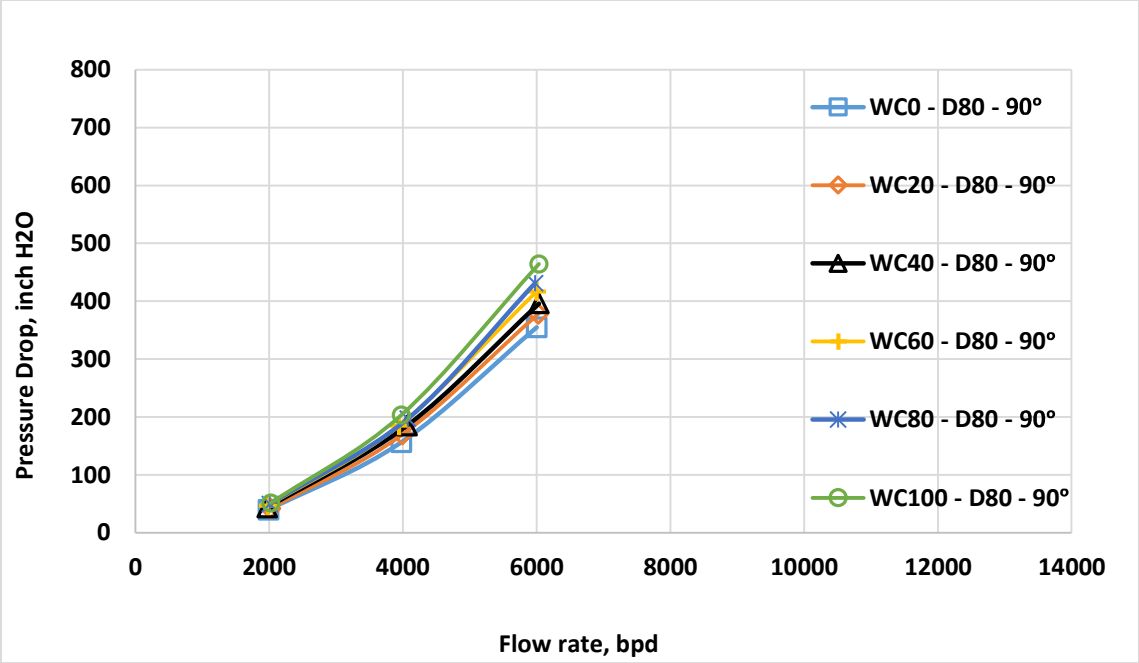

Figure 5.1b: Venturi pressure drop versus fluid mixture flow rate for different water cuts and θ = 90° (β = 0.4, oil D80 and potable water).

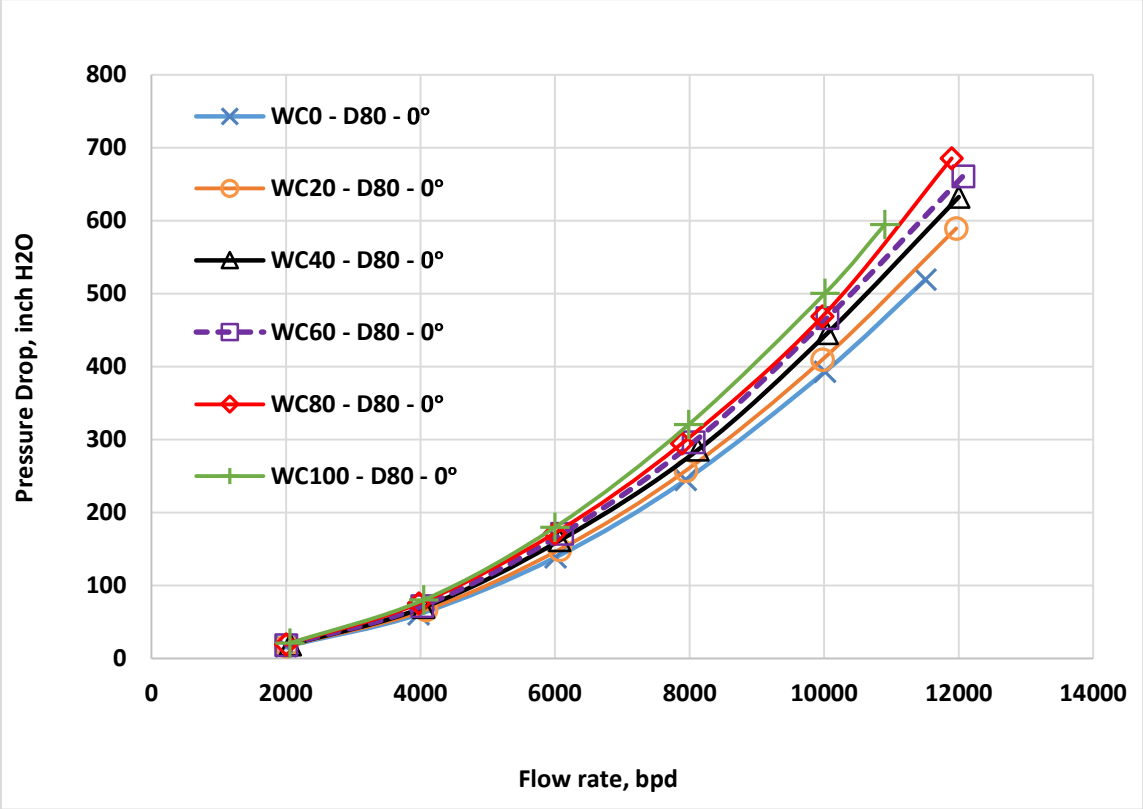

Figure 5.1c: Venturi pressure drop versus fluid mixture flow rate for different water cuts and θ = 0° (β = 0.5, oil D80 and potable water).

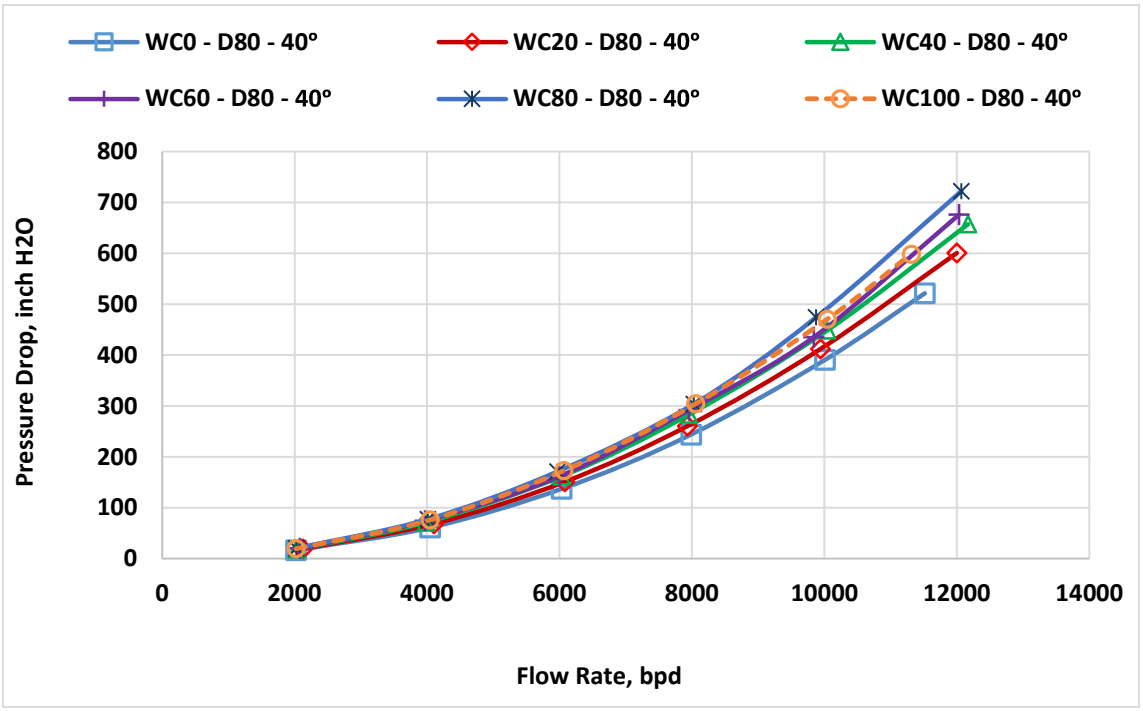

Figure 5.1d: Venturi pressure drop versus fluid mixture flow rate for different water cuts and θ = 40° (β = 0.5, oil D80 and potable water).

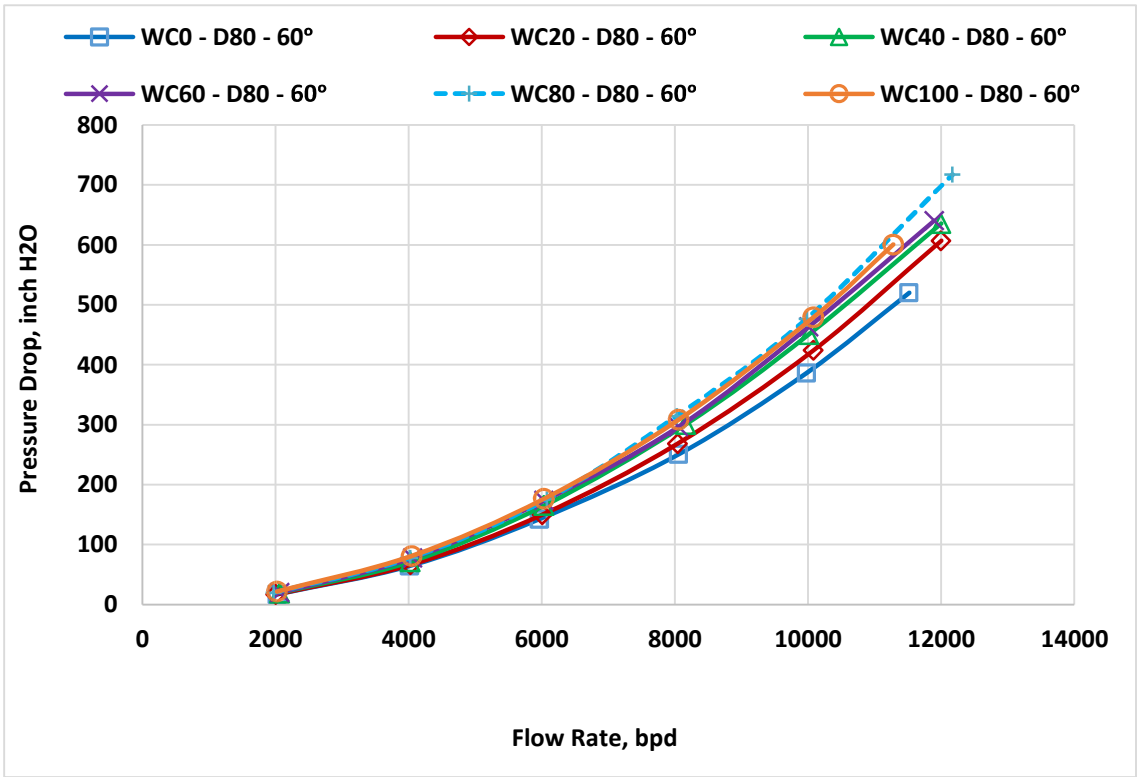

Figure 5.1e: Venturi pressure drop versus fluid mixture flow rate for different water cuts and θ = 60° (β = 0.5, oil D80 and potable water).

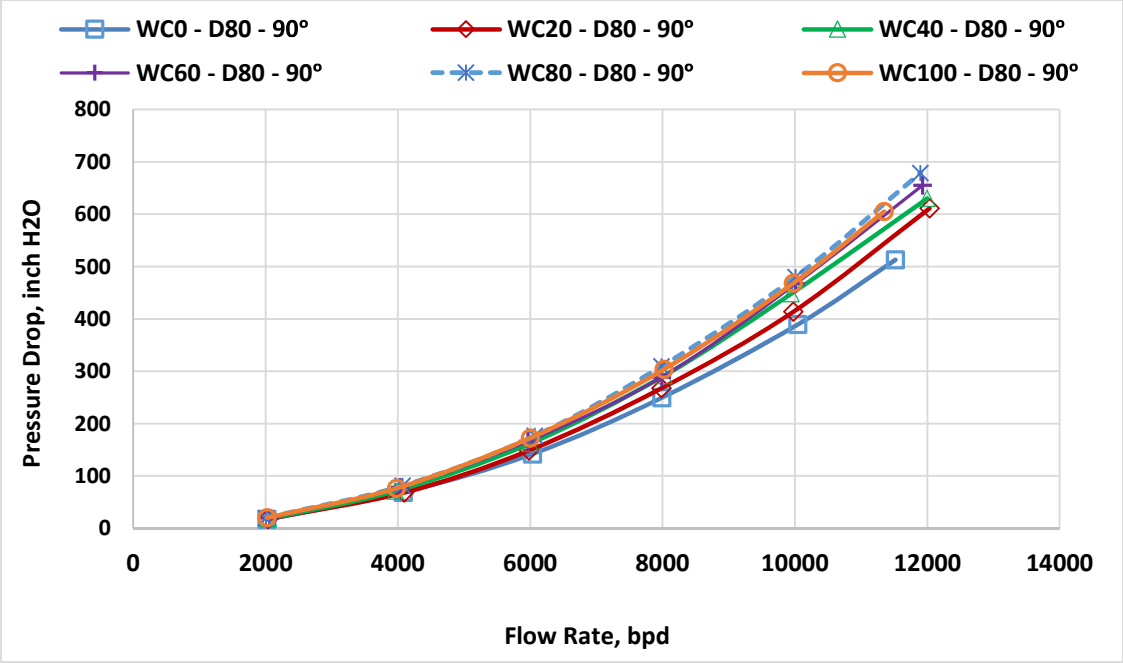

Figure 5.1f: Venturi pressure drop versus fluid mixture flow rate for different water cuts and θ = 90° (β = 0.5, oil D80 and potable water).

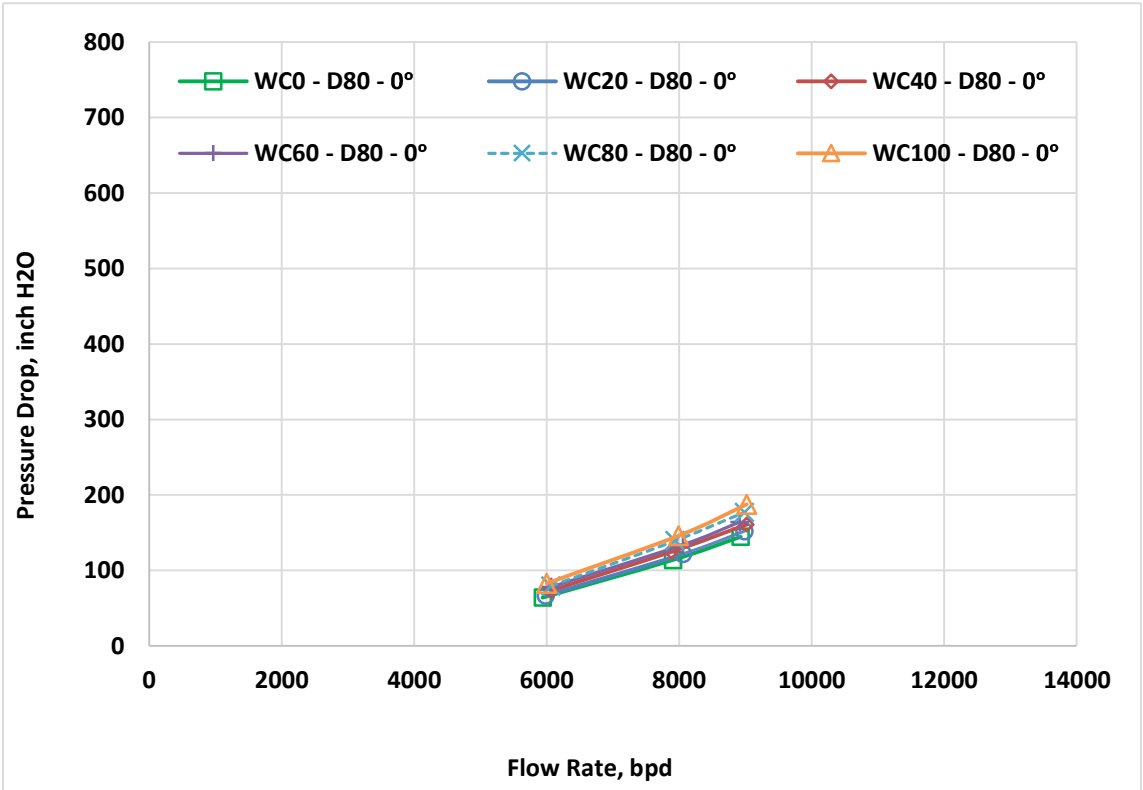

Figure 5.1g: Venturi pressure drop versus fluid mixture flow rate for different water cuts and θ = 0° (β = 0.6, oil D80 and potable water).

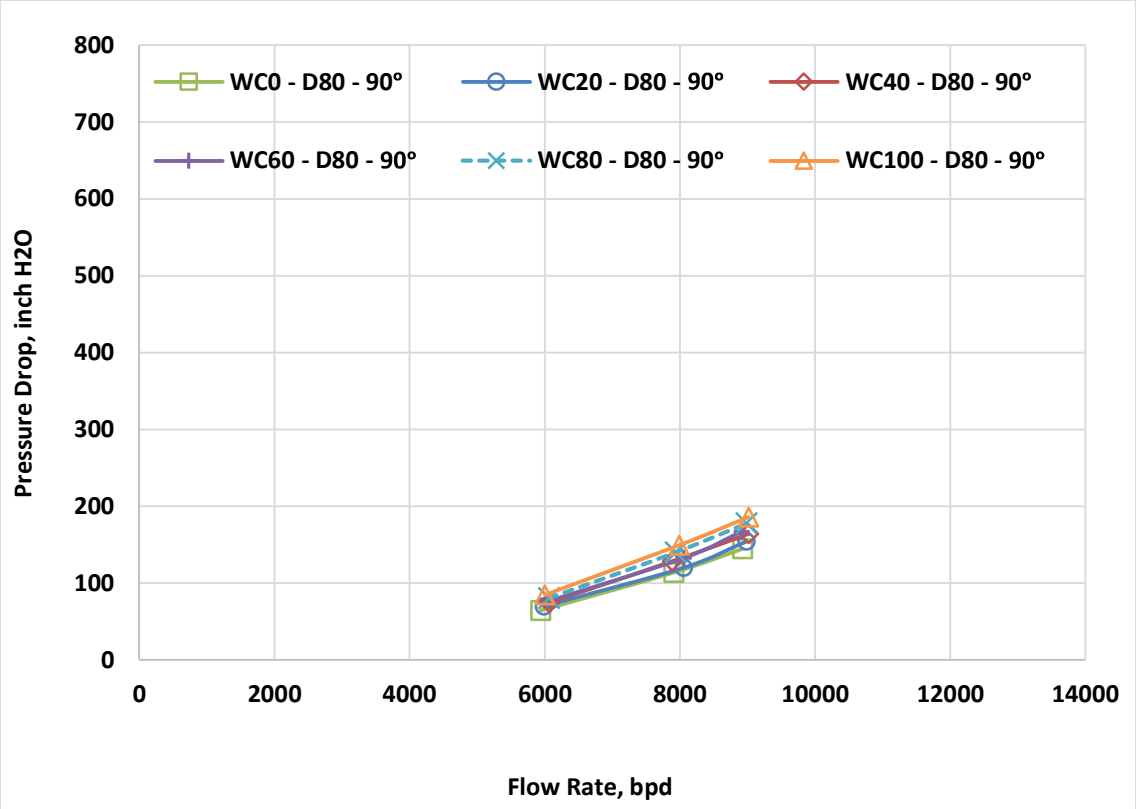

Figure 5.1h: Venturi pressure drop versus fluid mixture flow rate for different water cuts and θ = 90° (β = 0.6, oil D80 and potable water).

➢ Results for Oil D130:

The effect of fluid mixture flow rate on venturi pressure drop for different water cuts for oil D130 are presented in Figures 5.1i to 5.1n for horizontal and vertical inclinations flow loop. Also, it is obviously from the graphical results that the venturi pressure drop varies parabolically with fluid mixture flow rates for given water cut.

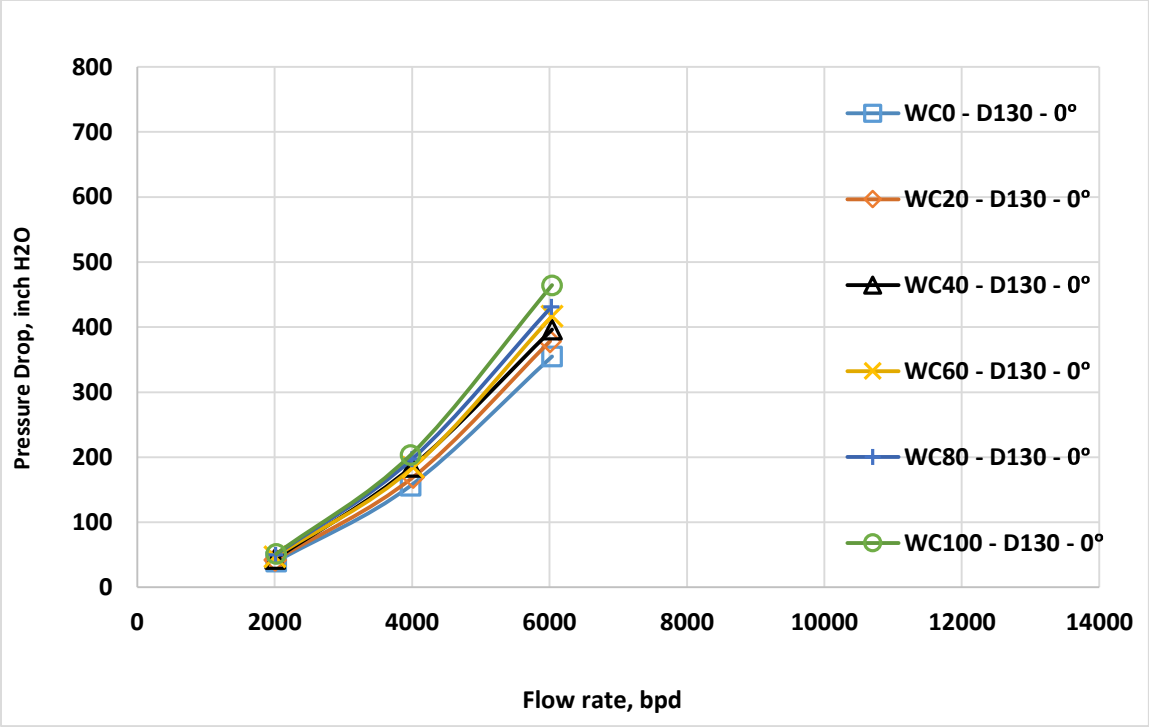

Figure 5.1i: Venturi pressure drop versus fluid mixture flow rate for different water cuts and θ = 0° (β = 0.4, oil D130 and potable water).

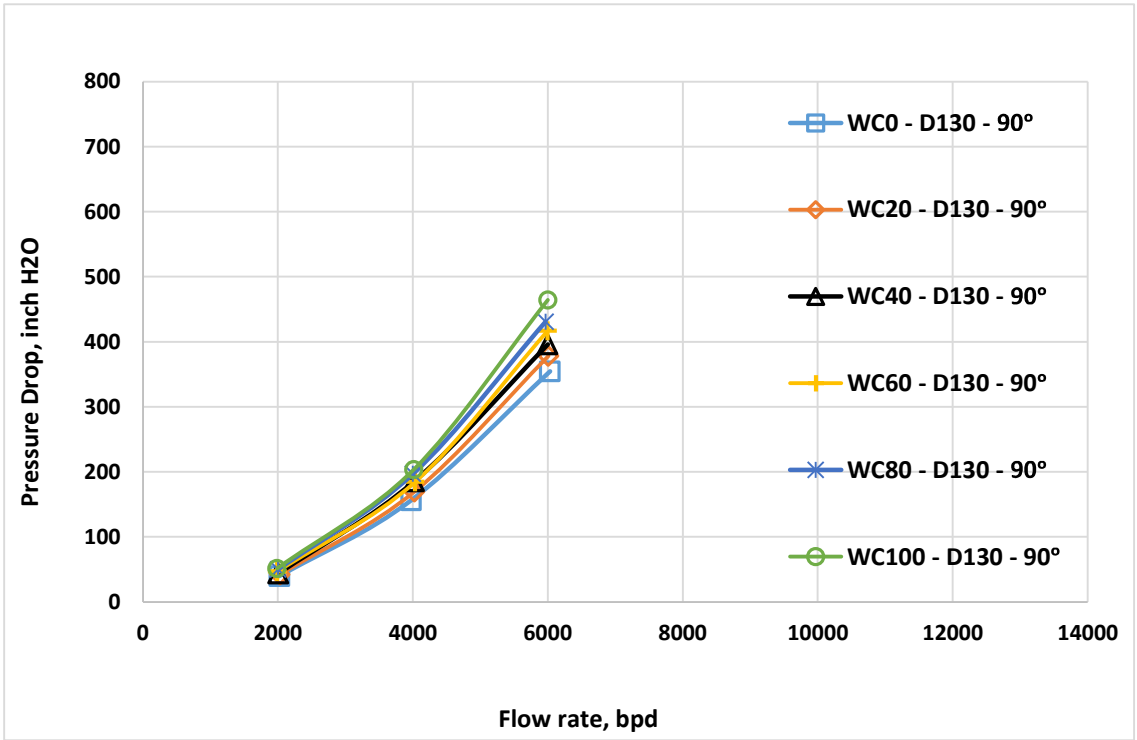

Figure 5.1j: Venturi pressure drop versus fluid mixture flow rate for different water cuts and θ = 90° (β = 0.4, oil D130 and potable water).

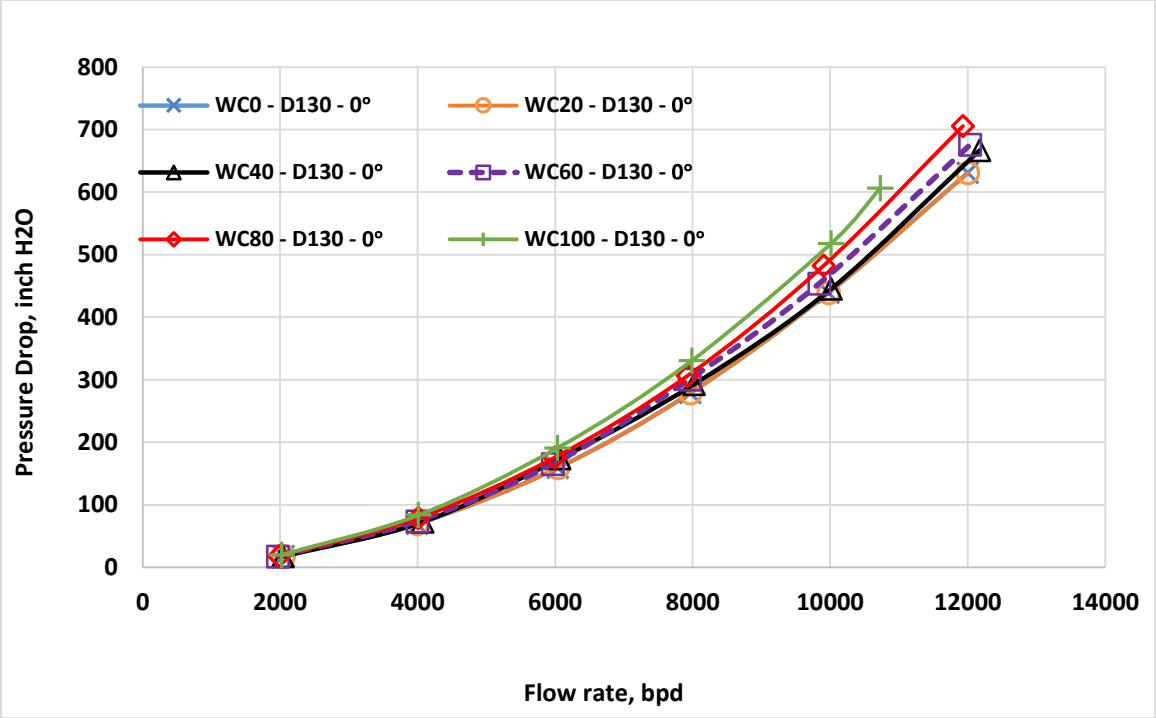

Figure 5.1k: Venturi pressure drop versus fluid mixture flow rate for different water cuts and θ = 0° (β = 0.5, oil D130 and potable water).

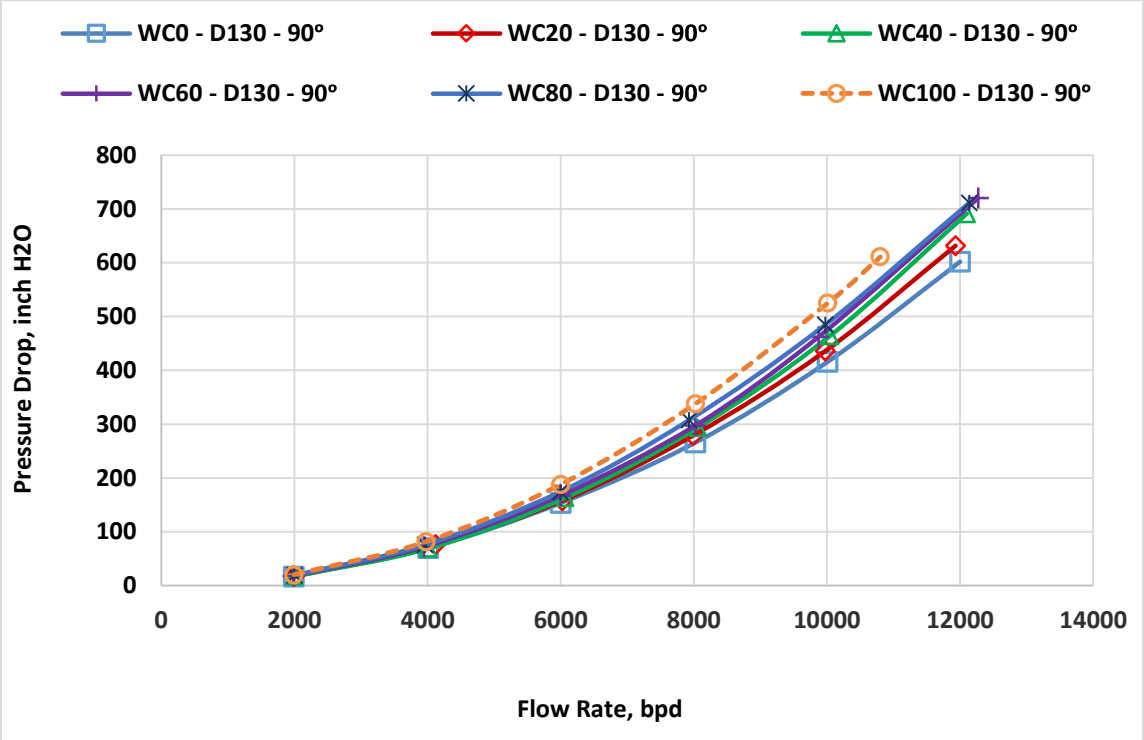

Figure 5.1l: Venturi pressure drop versus fluid mixture flow rate for different water cuts and θ = 90° (β = 0.5, oil D130 and potable water).

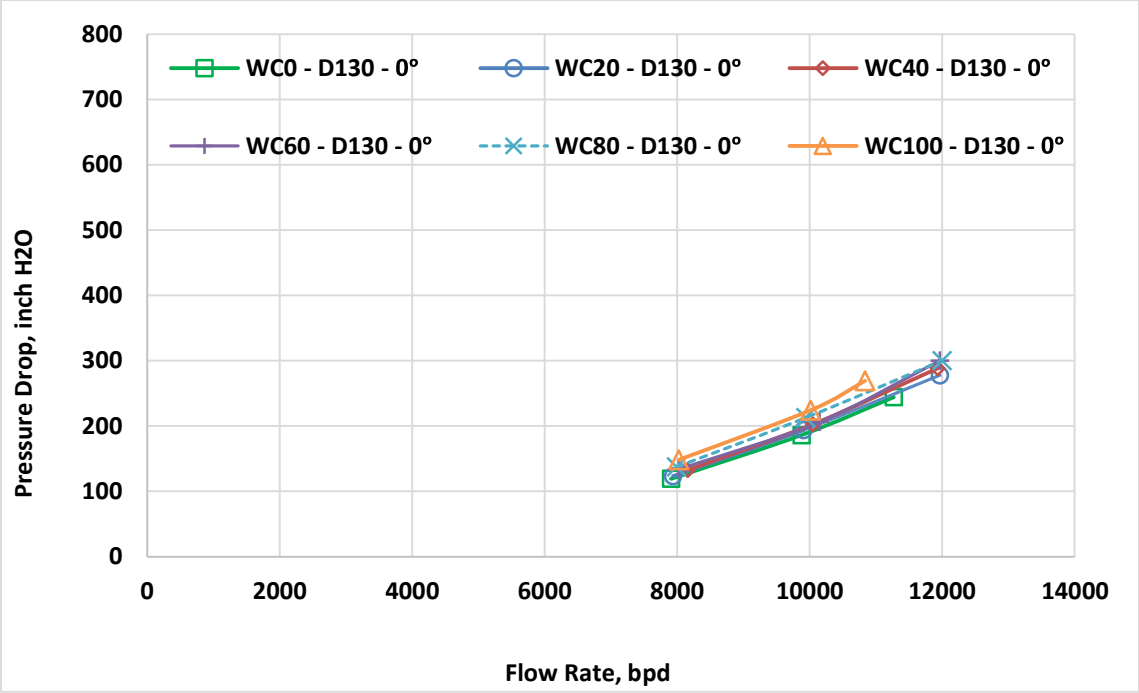

Figure 5.1m: Venturi pressure drop versus fluid mixture flow rate for different water cuts and θ = 0° (β = 0.6, oil D130 and potable water).

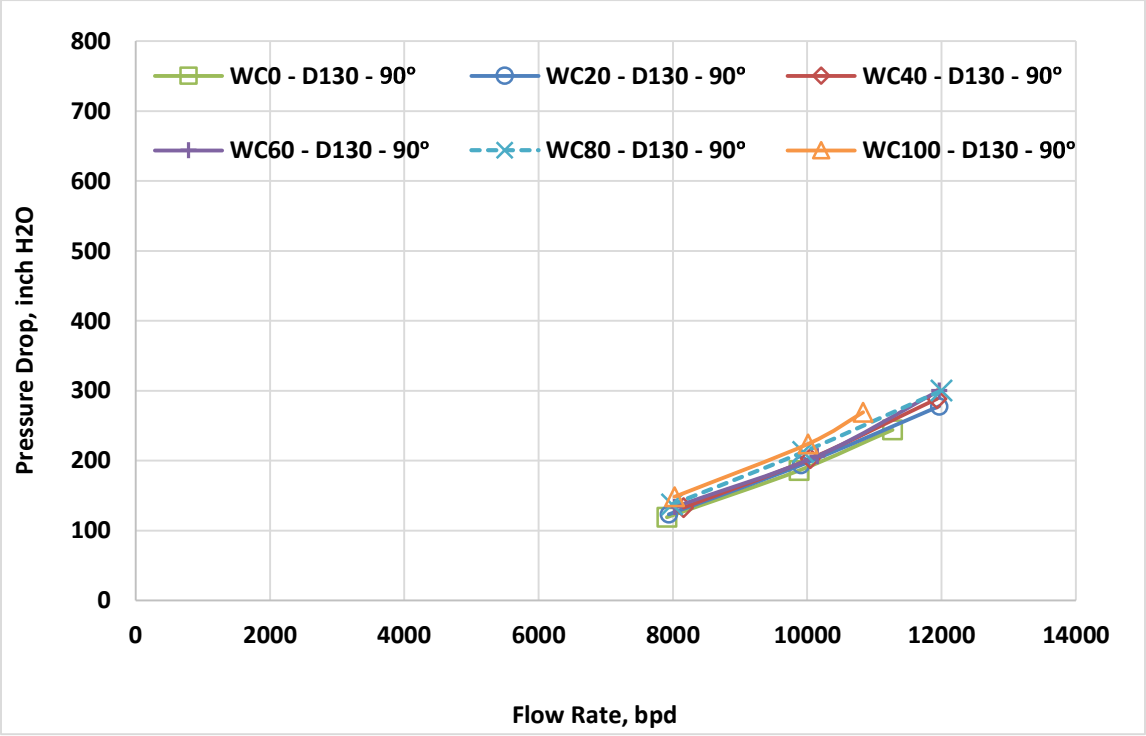

Figure 5.1n: Venturi pressure drop versus fluid mixture flow rate for different water cuts and θ = 90° (β = 0.6, oil D130 and potable water).

In all cases of single phase (WC0% and WC100%), it can be observe that the points of maximum flow rate 12000 bpd were not obtained due to of using half of the pumping system.

In conclusion, the same trend in venturi pressure drop is observed for results of oil D80 and oil D130 in Figures 5.1i to 5.1n for all water cuts ranging from 0% to 100% and for the two inclinations of the flow loop. The experimental results show that the fluid mixture flow rates have a significant effect on venturi pressure drop for the given water cut - or fluid mixture density. For a given flow rate and water cut, the venturi pressure drop is inversely proportional to the β.

5.2 Effect of Water Cut on Venturi Pressure Drop for Different Fluid Mixture Flow Rates for Oils D80 and D130

The effect of water cut on the venturi pressure drop of both oils D80 and D130 on the three venturi meters (β = 0.4, 0.5 and 0.6) for different fluid mixture flow rates are presented in Figures 5.2a to 5.2n for all inclinations of the flow loop.

➢ Results for Oil D80:

For the case of oil D80, the effect of water cut on the venturi pressure drop for different oil-water flow rate varied from 2000 to 12000 bpd, has been showed in Figures 5.2a to 5.2h.

It can be seen from the results that the venturi pressure drop varies linearly with water cut for a given fluid mixture flow rate for all three venturi meters. This concurs with the venturi pressure drop and water cut relationship in Eq. 4.4.

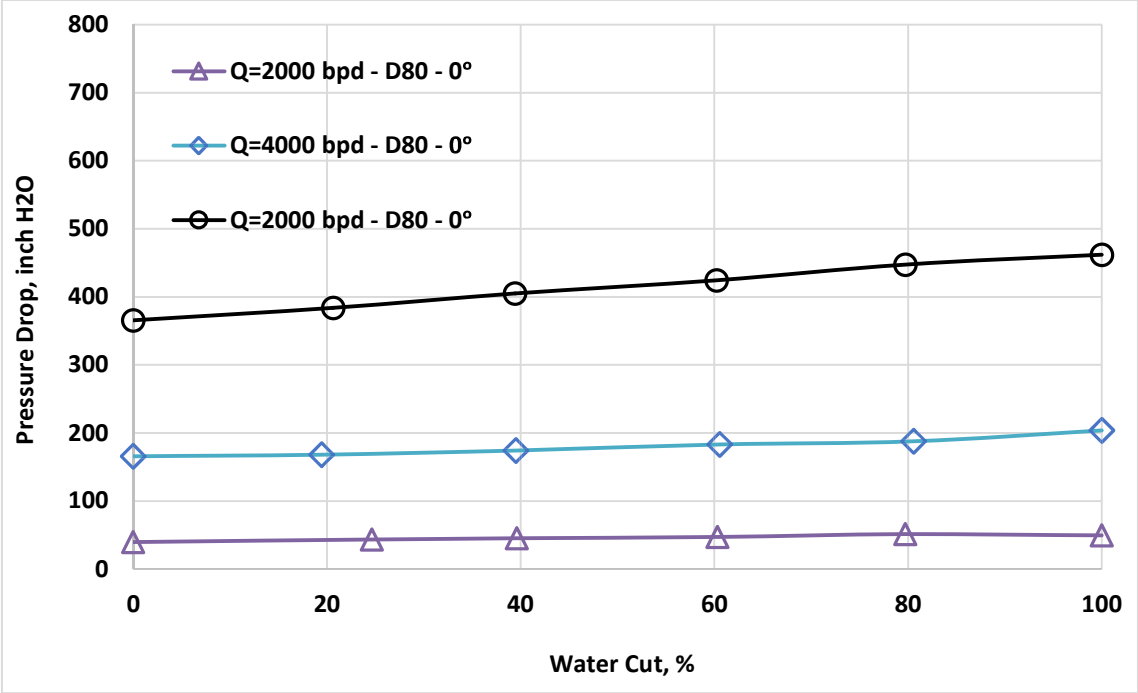

Figure 5.2a: Venturi pressure drop versus water cut for different fluid mixture flow rates and θ = 0° (β = 0.4, oil D80 and potable water).

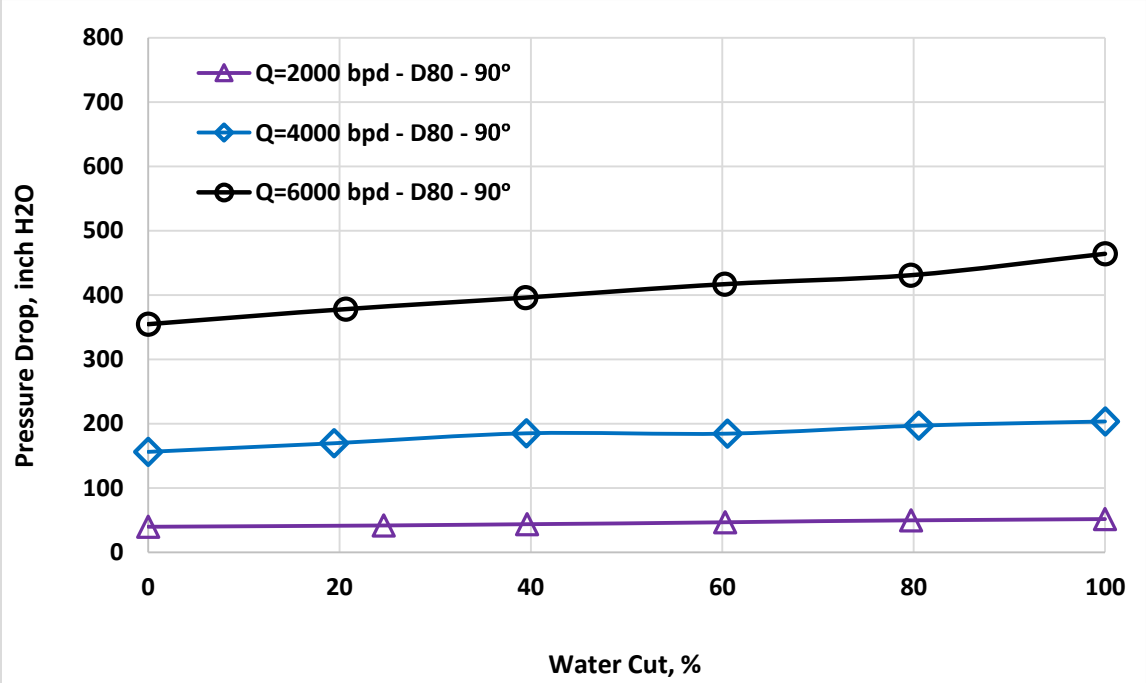

Figure 5.2b: Venturi pressure drop versus water cut for different fluid mixture flow rates and θ = 90° (β = 0.4, oil D80 and potable water).

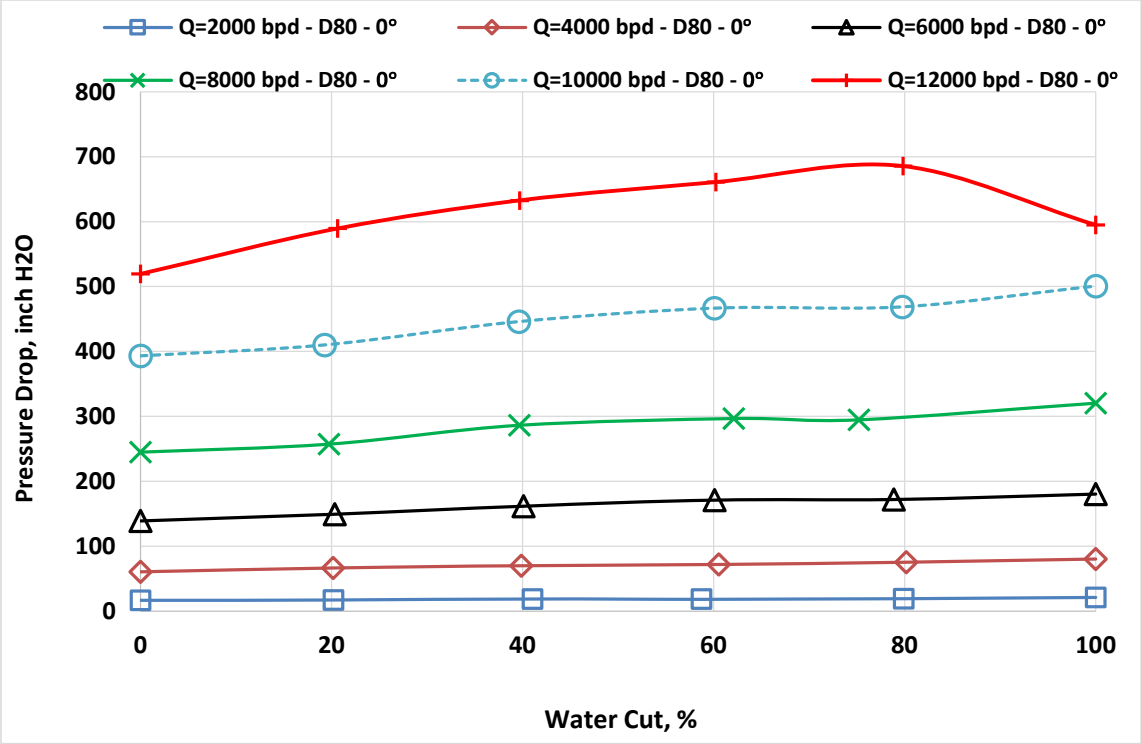

Figure 5.2c: Venturi pressure drop versus water cut for different fluid mixture flow rates and θ = 0° (β = 0.5, oil D80 and potable water).

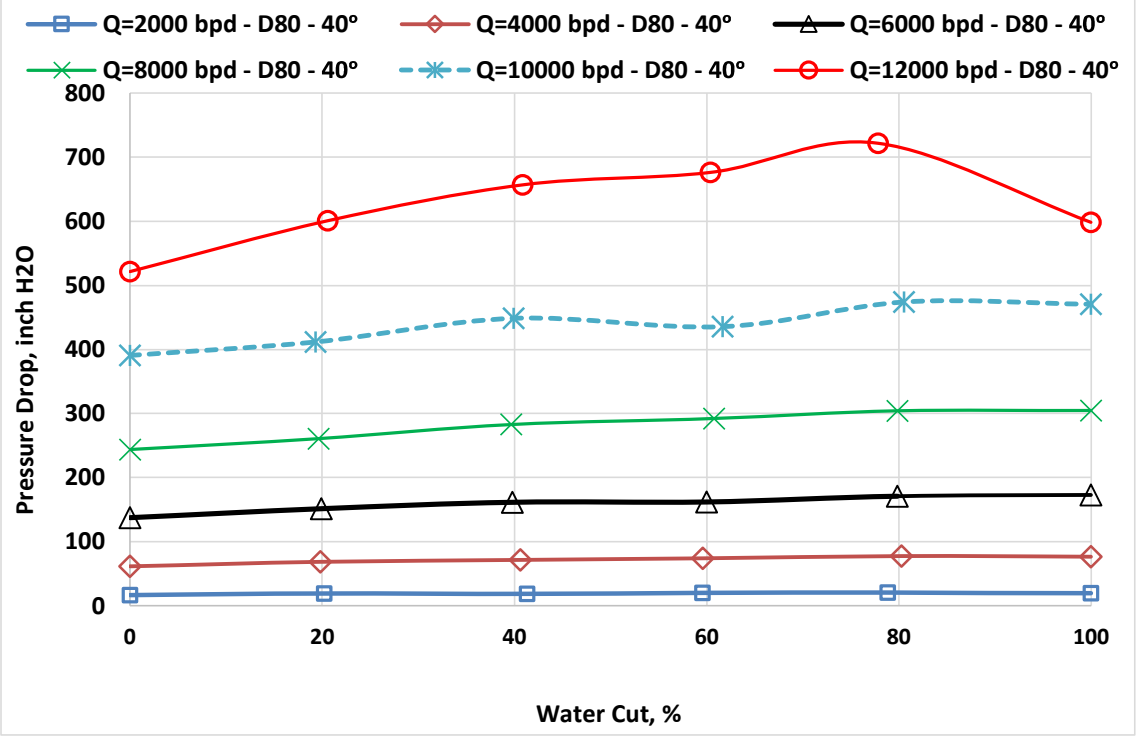

Figure 5.2d: Venturi pressure drop versus water cut for different fluid mixture flow rates and θ = 40° (β = 0.5, oil D80 and potable water).

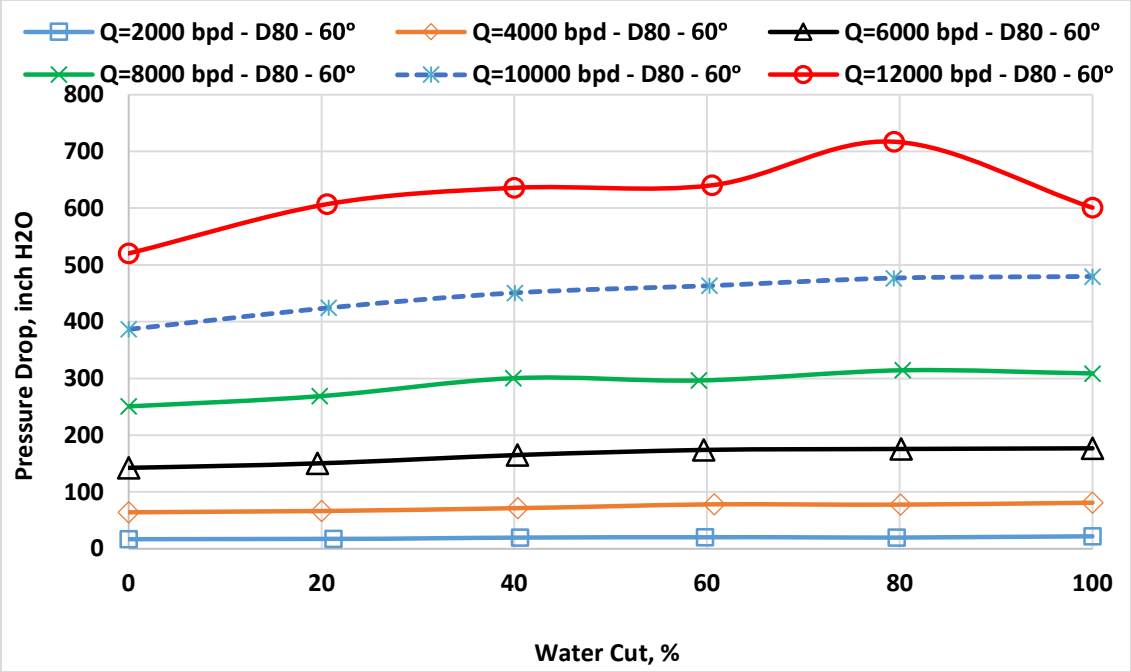

Figure 5.2e: Venturi pressure drop versus water cut for different fluid mixture flow rates and θ = 60° (β = 0.5, oil D80 and potable water).

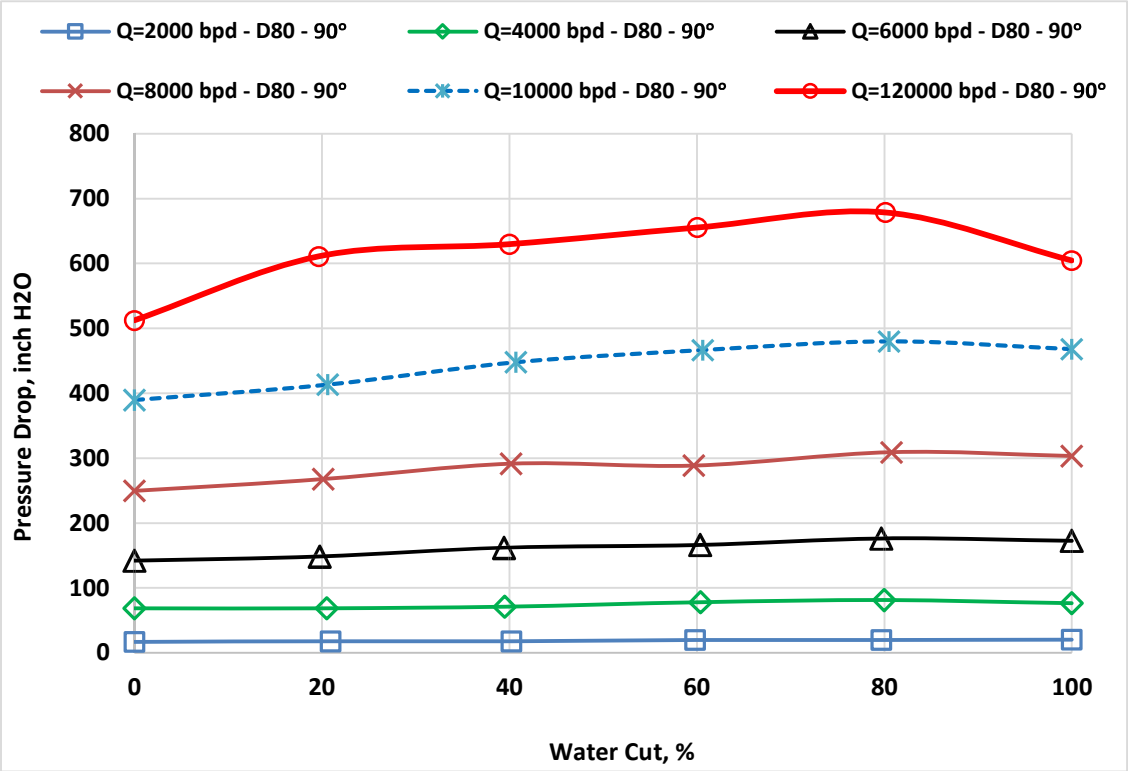

Figure 5.2f: Venturi pressure drop versus water cut for different fluid mixture flow rates and θ = 90° (β = 0.5, oil D80 and potable water).

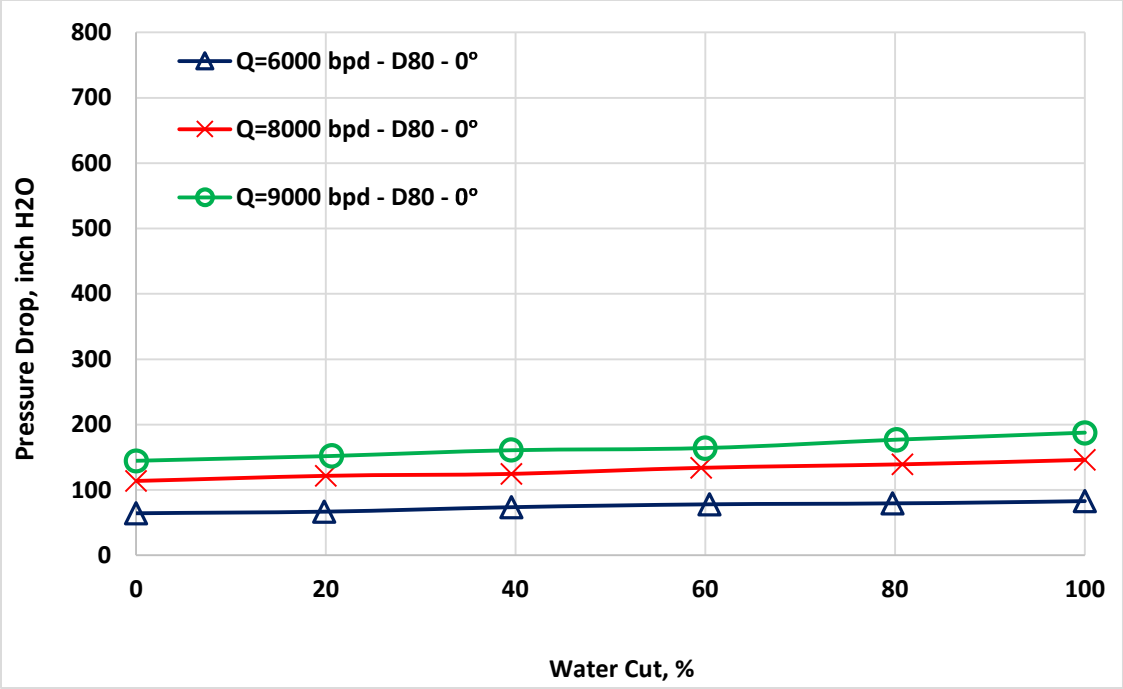

Figure 5.2g: Venturi pressure drop versus water cut for different fluid mixture flow rates and θ = 0° (β = 0.6, oil D80 and potable water).

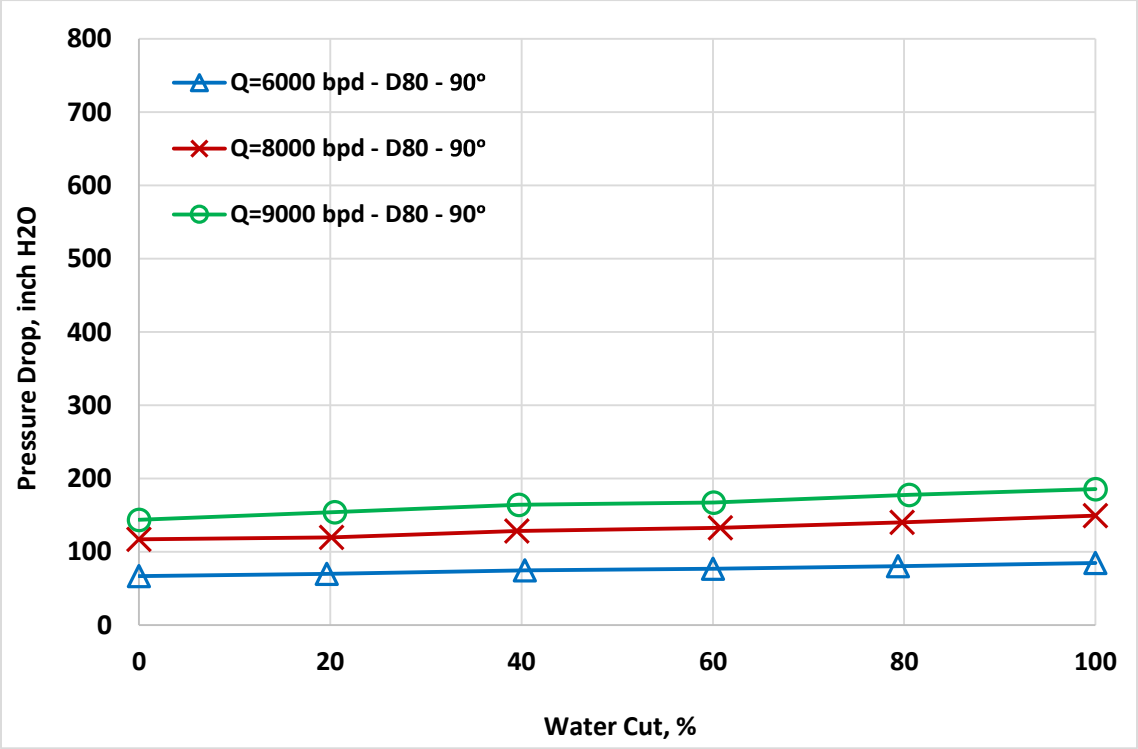

Figure 5.2h: Venturi pressure drop versus water cut for different fluid mixture flow rates and θ = 90° (β = 0.6, oil D80 and potable water).

➢ Results for Oil D130:

For a given oil D130, the effect of water cut for different flow rates on venturi pressure drop is shown in Figures 5.2i to 6.2n. In general, as it can be seen from Figure6.2i to 6.2n, for a given flow rate the pressure drop increases linearly from WC = 20 to WC 80 %. Further increase in WC, venturi pressure drop has been found to increase rapidly. This could be due to phase inversion or change in flow pattern regime. However, for WC = 100%, venturi pressure drop we expect to be higher as compared to venturi pressure drop at WC = 0%. This is due to higher density of water.

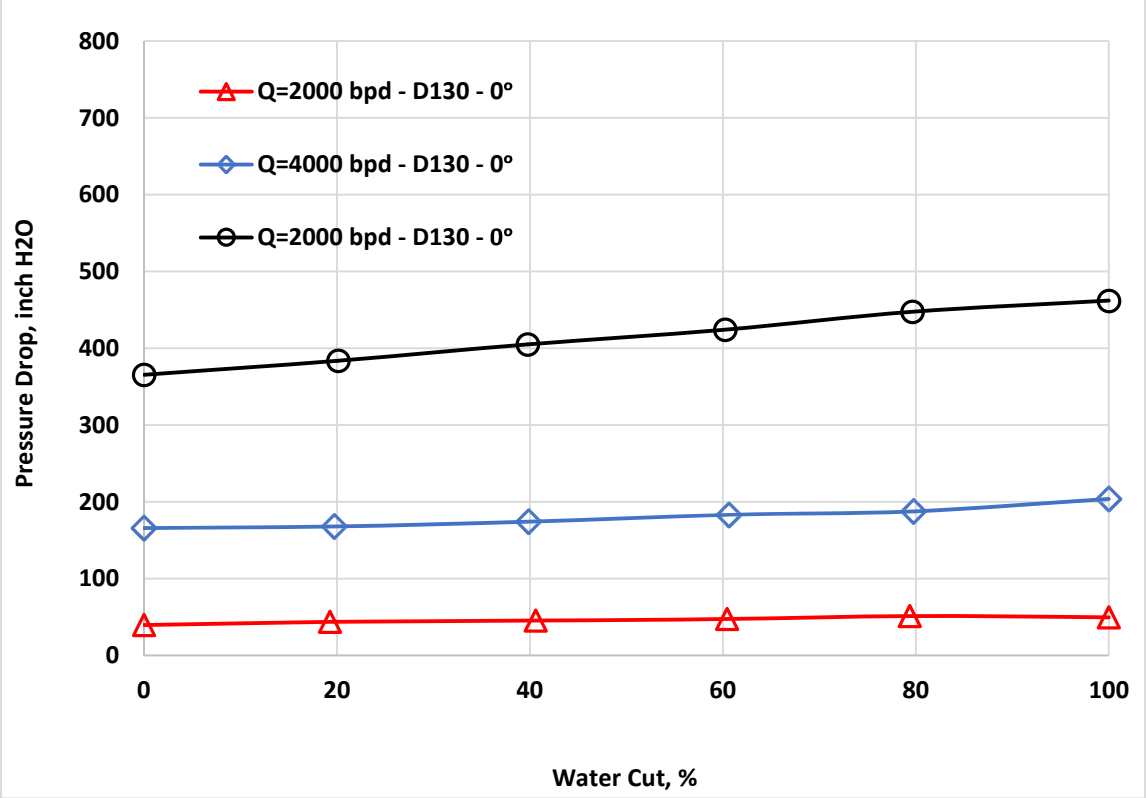

Figure 5.2i: Venturi pressure drop versus water cut for different fluid mixture flow rates and θ = 0° (β = 0.4, oil D130 and potable water).

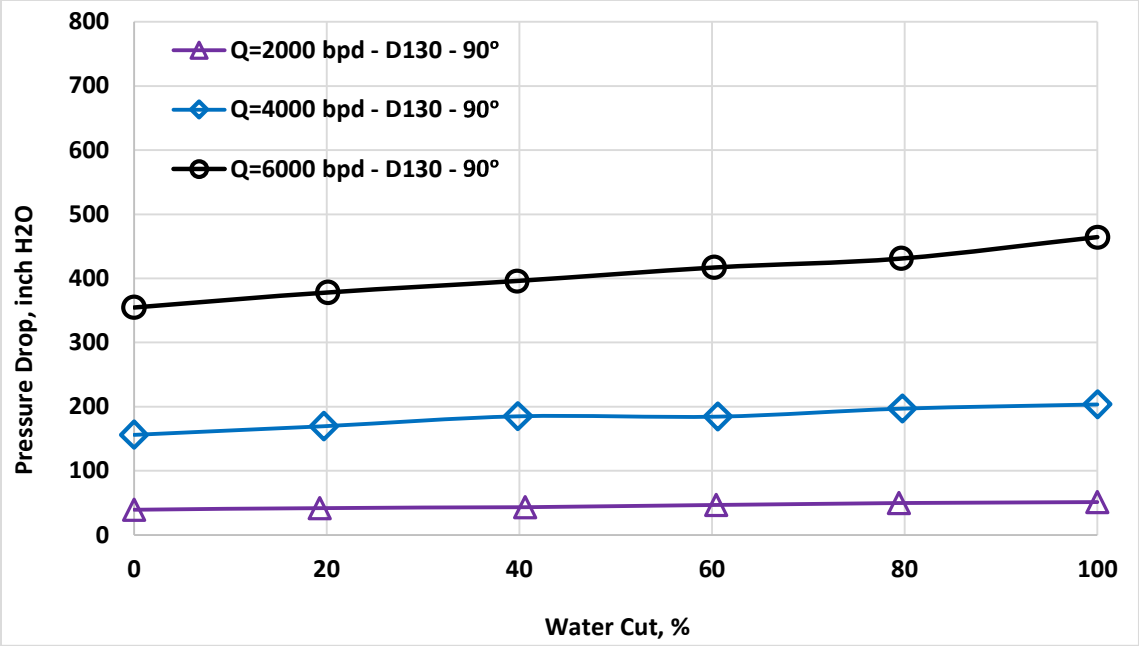

Figure 5.2j: Venturi pressure drop versus water cut for different fluid mixture flow rates and θ = 90° (β = 0.4, oil D130 and potable water).

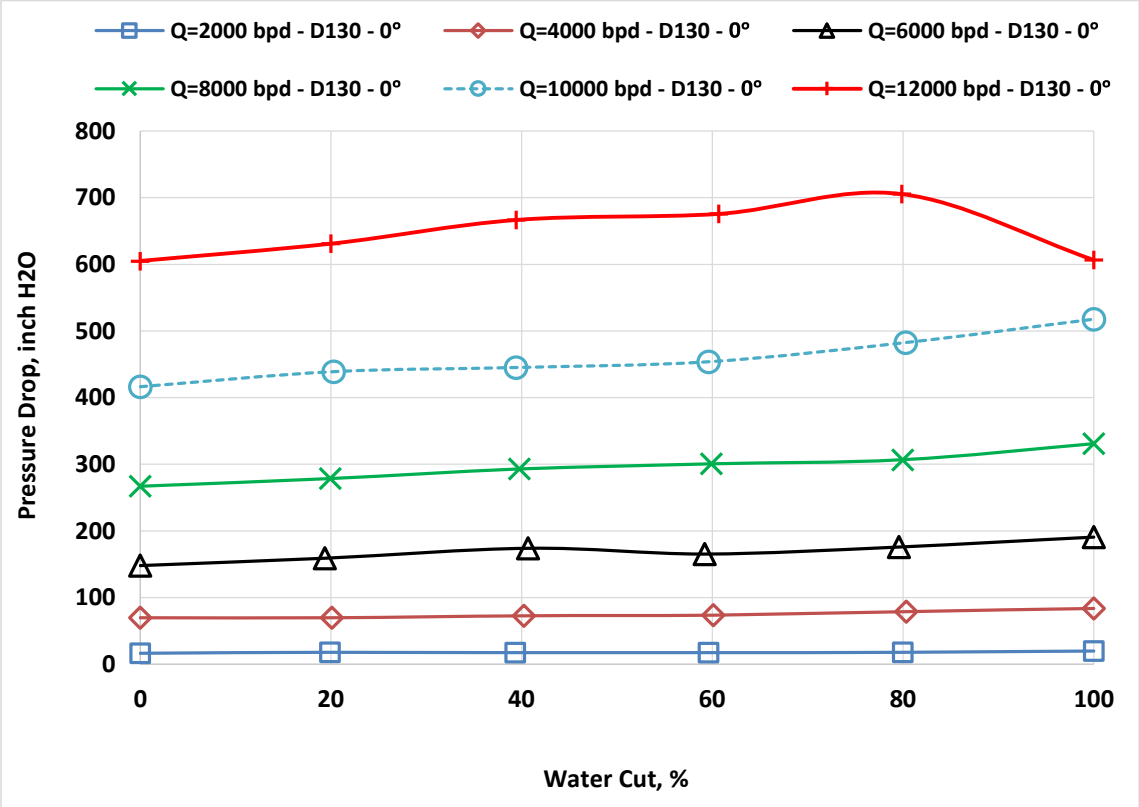

Figure 5.2k: Venturi pressure drop versus water cut for different fluid mixture flow rates and θ = 0° (β = 0.5, oil D130 and potable water).

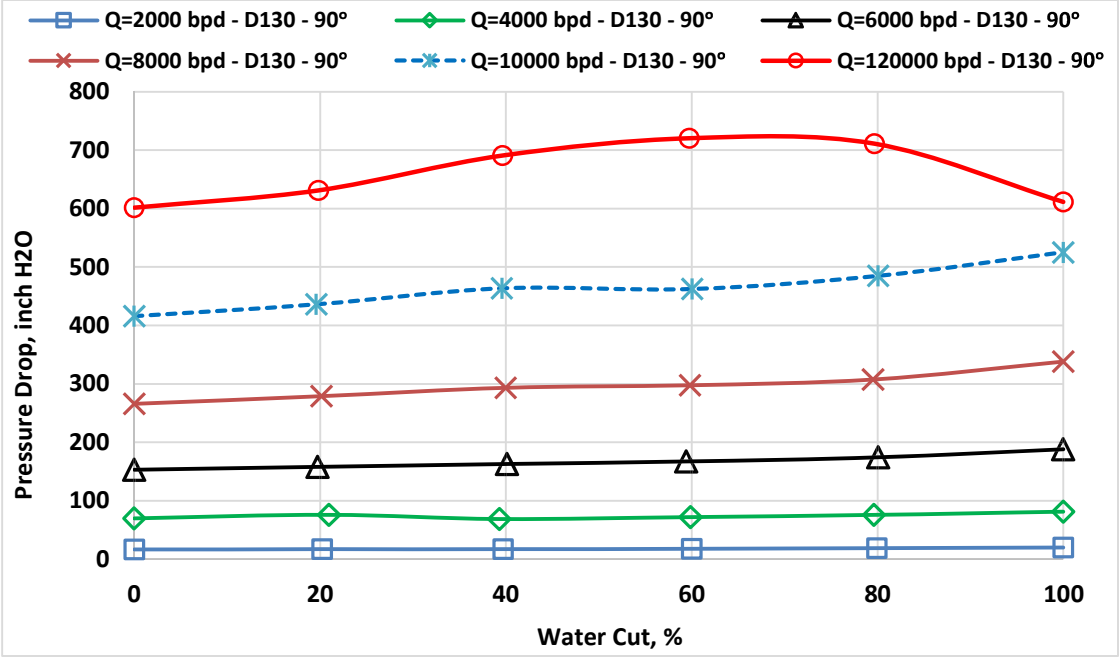

Figure 5.2l: Venturi pressure drop versus water cut for different fluid mixture flow rates and θ = 90° (β = 0.5, oil D130 and potable water).

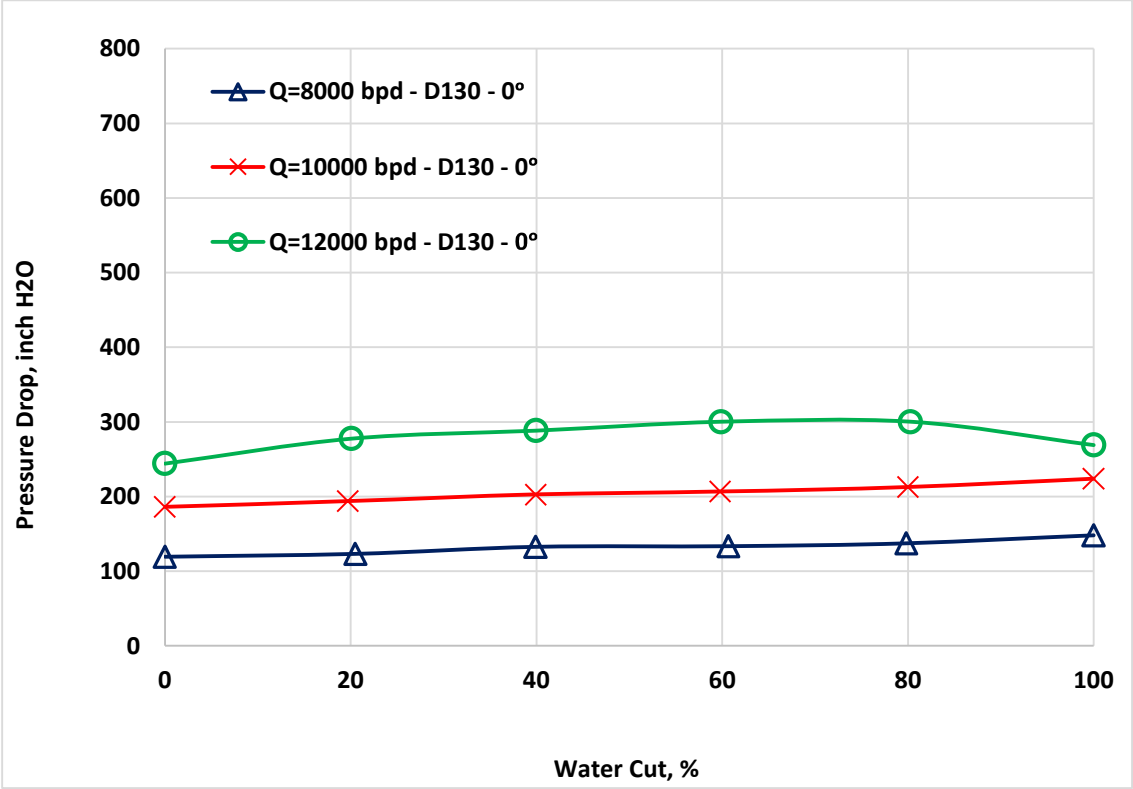

Figure 5.2m: Venturi pressure drop versus water cut for different fluid mixture flow rates and θ = 0° (β = 0.6, oil D130 and potable water).

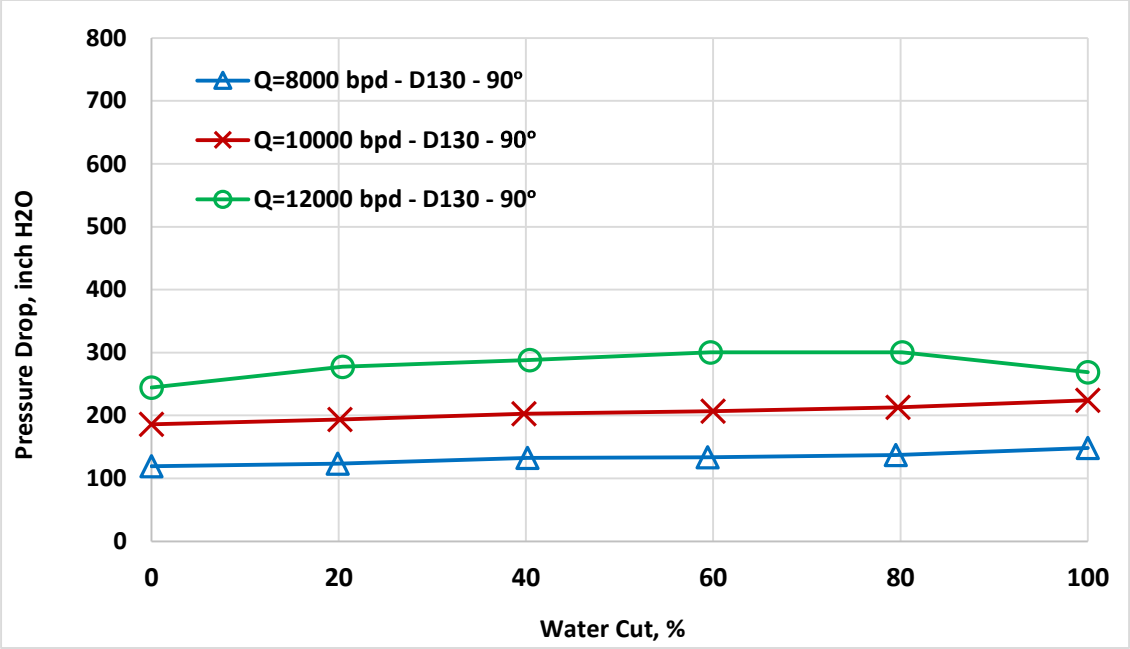

Figure 5.2n: Venturi pressure drop versus water cut for different fluid mixture flow rates and $\theta = 90^{o}$ ($\beta = 0.6$, oil D130 and potable water).

Therefore, it can be seen from all Figures 5.2a to 5.2n, for any given flow rate, the venturi pressure drop increases linearly with increase of water cut for all inclinations of the flow loop, three venturi meters, and all flow rates.

The same trend is observed for all fluid mixture flow rates ranging from 2,000 bpd to 10,000 bpd and for the different inclinations of the flow loop. The exception of this behavior that for maxim flow rate (12000 bpd) at water cuts 0% and 100%, due to the pumps limitation and the actual values of the maximum flow rate were reported: 11500 and 10900 bpd for oil and water single phases respectively.

Also, the pressure drop slope is increasing with the fluid mixture flow rate. This result is very important from a practical standpoint as a check to verify that the mixture flow is in fact in a dispersed homogeneous flow pattern.

5.3 Effect of Flow Loop Inclination on Venturi Pressure Drop for Different Fluid Mixture Flow Rates for Oils D80 and D130

For the sake of brevity, and to show explicitly, the angle effect on pressure drop measurements for different water cuts and different flow rates have been presented.

All multiphase oil-water flow experiments were performed for horizontal and vertical inclinations of flow loop on the venturi pressure drop for different fluid mixture flow rates and water cuts are presented in Figures 5.3a to 5.3k for the three venturi meters (β = 0.4, 0.5 and 0.6).

➢ Results for Oil D80:

For oil D80, the effect of flow loop inclination on venturi pressure drop for different fluid mixture flow rates are presented in Figures 5.3a to 5.3h for all water cuts ranging from 0 to 100%. It is clear from the figures that the venturi pressure drop is almost constant with respect to the flow loop inclinations for a given fluid mixture flow rate.

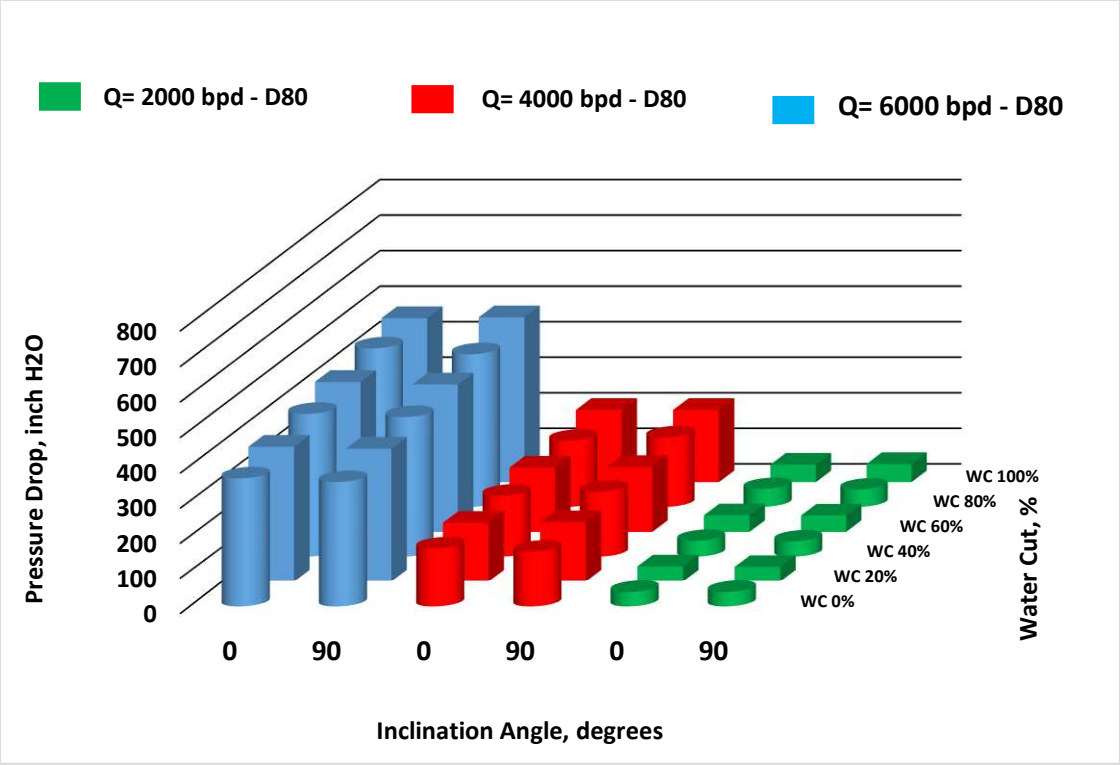

Figure 5.3a: Venturi pressure drop versus flow loop inclination for different fluid mixture flow rates and water cuts (β = 0.4, oil D130 and potable water).

For more verifying and checking, the case of venturi (β = 0.5) and oilD80, has been studied in additional details. All the experiments were conducted for four angles of inclination: (0, 40, 60 and 90) degrees to show as mentioned before the effect of angle of inclination on the venturi pressure drop. Meanwhile, the measurements of venturi pressure drop have been plotted individually for each water cut which varied from 0% to 100% in step of 20%, as shown in the following series of figures, Figures 5.3b to 5.3g.

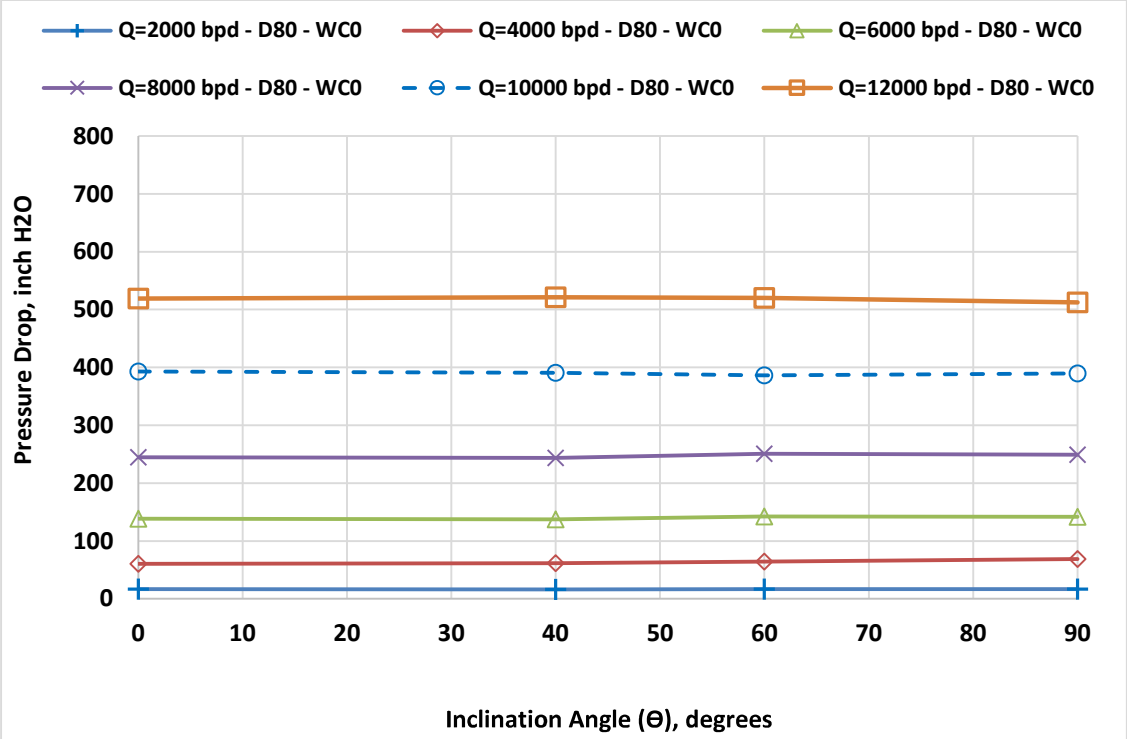

Figure 5.3b: Venturi pressure drop versus flow loop inclination for different fluid mixture flow rates and 0% water cut (β = 0.5, oil D80 and potable water).

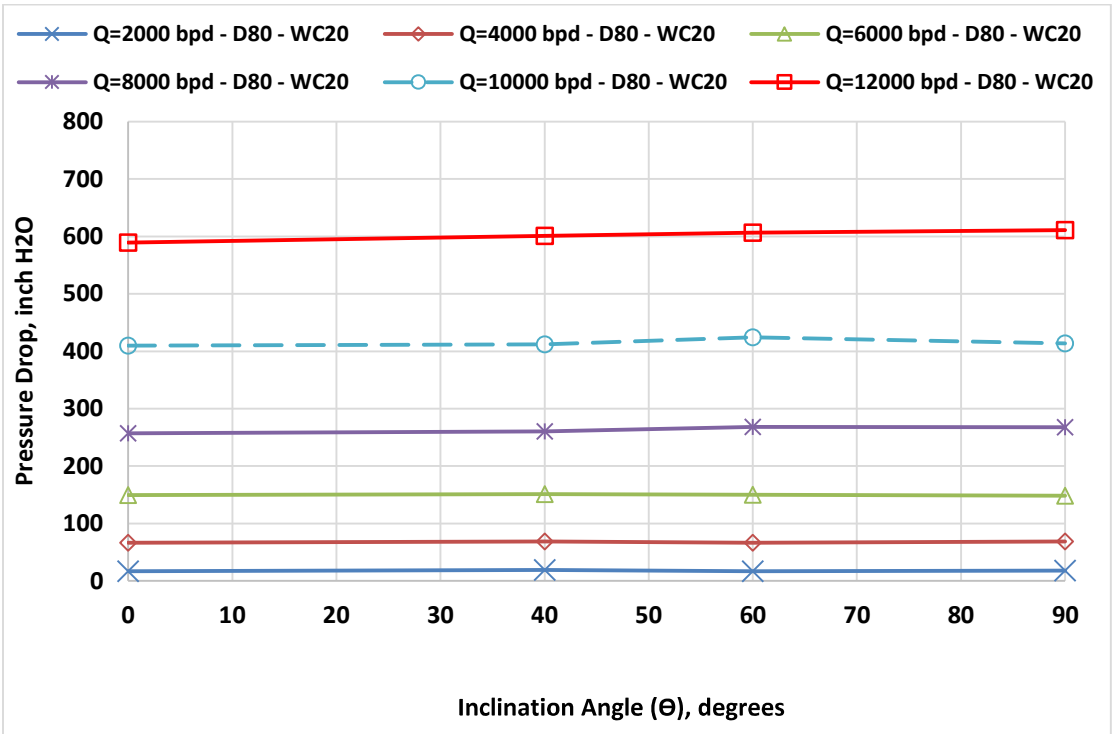

Figure 5.3c: Venturi pressure drop versus flow loop inclination for different fluid mixture flow rates and 20% water cut (β = 0.5, oil D80 and potable water).

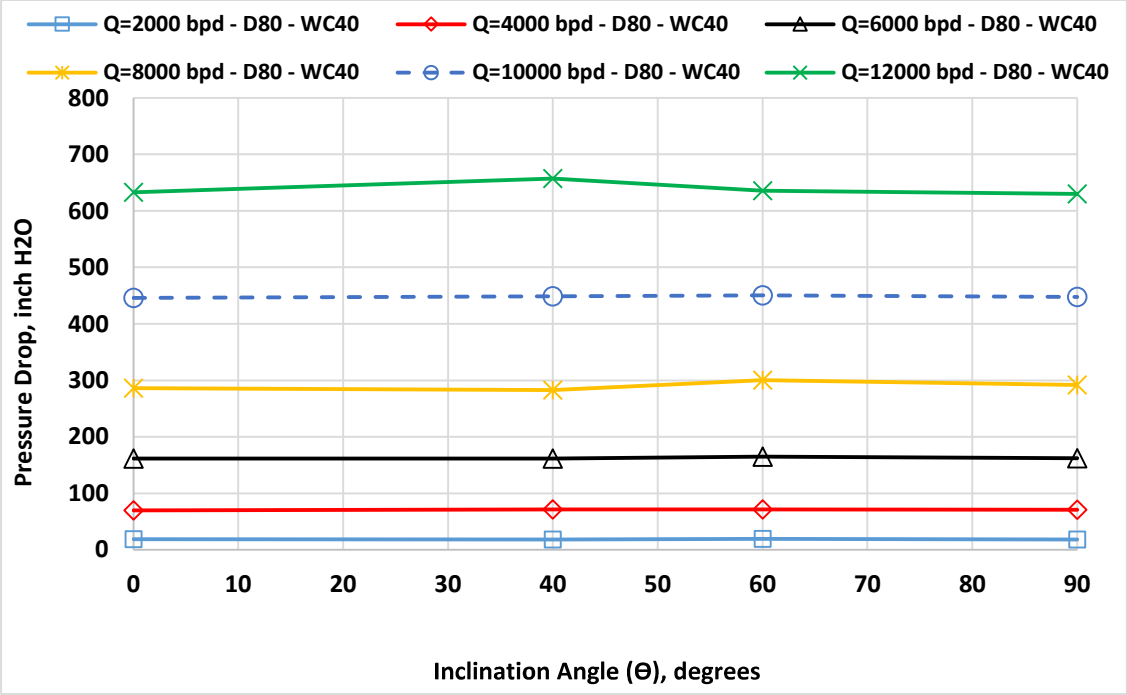

Figure 5.3d: Venturi pressure drop versus flow loop inclination for different fluid mixture flow rates and 40% water cut (β = 0.5, oil D80 and potable water).

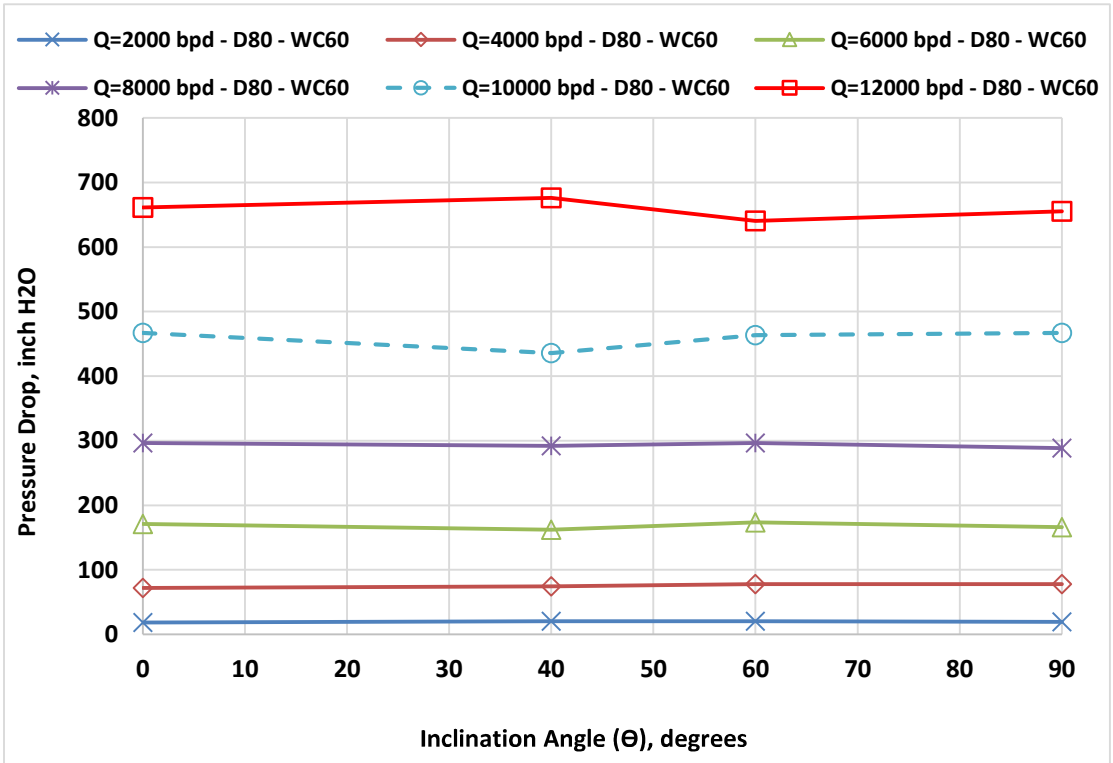

Figure 5.3e: Venturi pressure drop versus flow loop inclination for different fluid mixture flow rates and 60% water cut (β = 0.5, oil D80 and potable water).

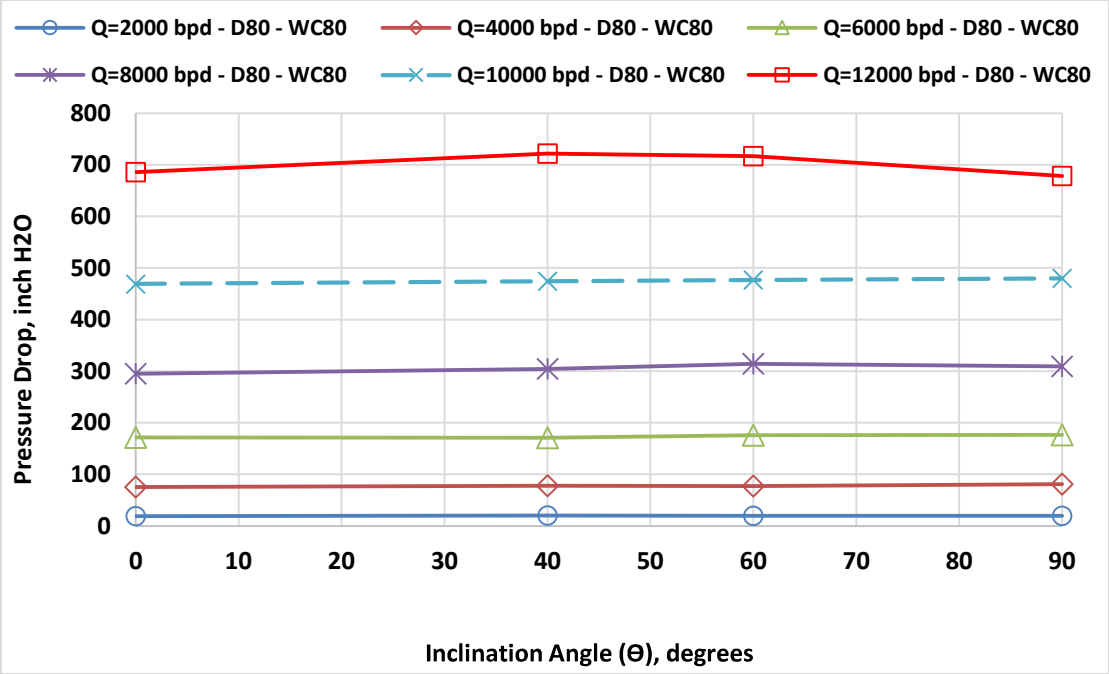

Figure 5.3f: Venturi pressure drop versus flow loop inclination for different fluid mixture flow rates and 80% water cut (β = 0.5, oil D80 and potable water).

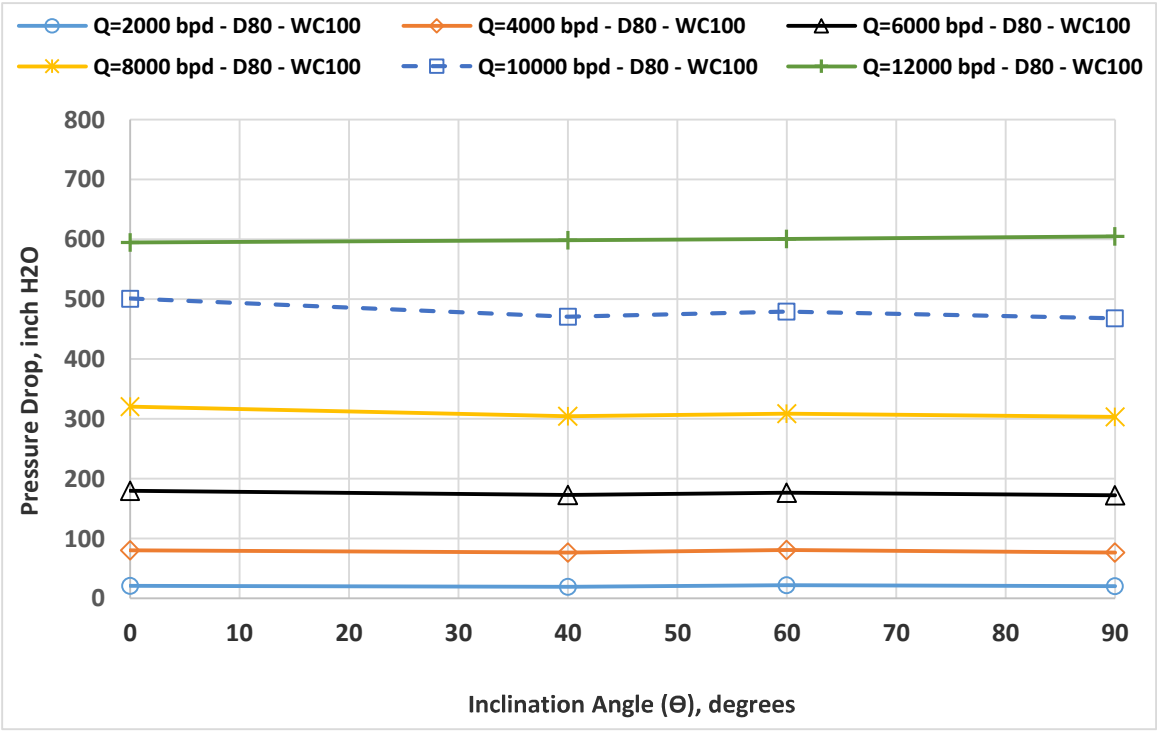

Figure 5.3g: Venturi pressure drop versus flow loop inclination for different fluid mixture flow rates and 100% water cut (β = 0.5, oil D80 and potable water).

For a certain water cut, the effect of inclination for different flow rates on pressure drop is shown in above Figures 5.3b to 5.3g. However for the same oil D80 the experiments were conducted on venturi ((β = 0.6) for horizontal and vertical orientations of the flow loop for high flow rates and different water cut which varied from 0% to 100% in steps of 20%, as shown in the following Figure 5.3h.

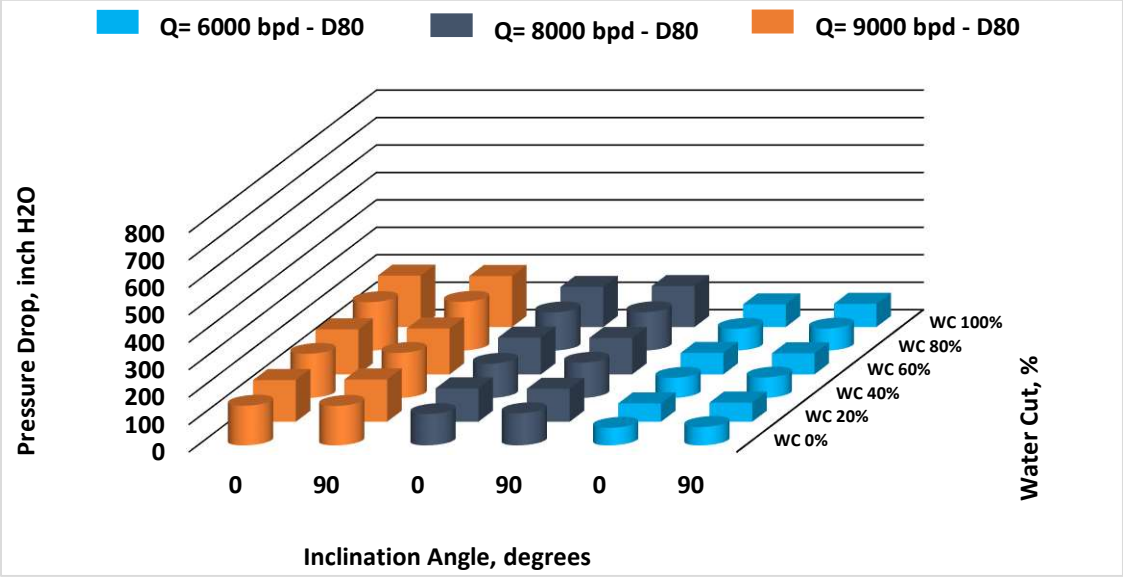

Figure 5.3h: Venturi pressure drop versus flow loop inclination for different fluid mixture flow rates and water cuts (β = 0.6, oil D80 and potable water).

➢ Results for Oil D130:

For a given oil D130, effect of flow loop inclination on the venturi pressure drop for different fluid mixture flow rates and water cuts are presented in Figures 5.3i to 5.3k for the three venturi meters (β = 0.4, 0.5 and 0.6).

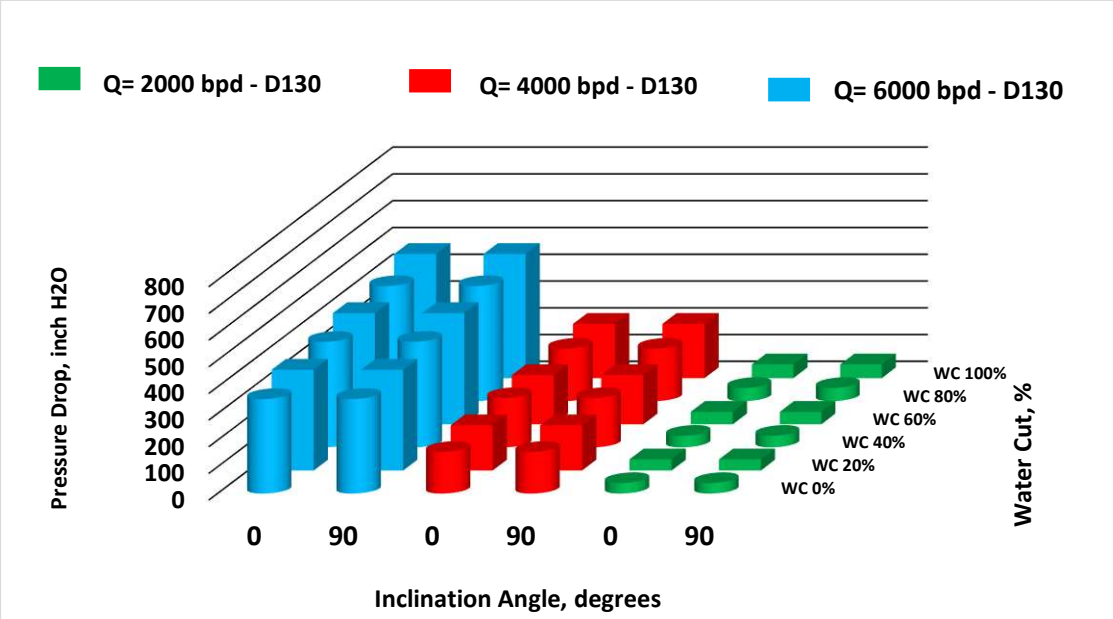

Figure 5.3i: Venturi pressure drop versus flow loop inclination for different fluid mixture flow rates and water cuts (β = 0.4, oil D130 and potable water).

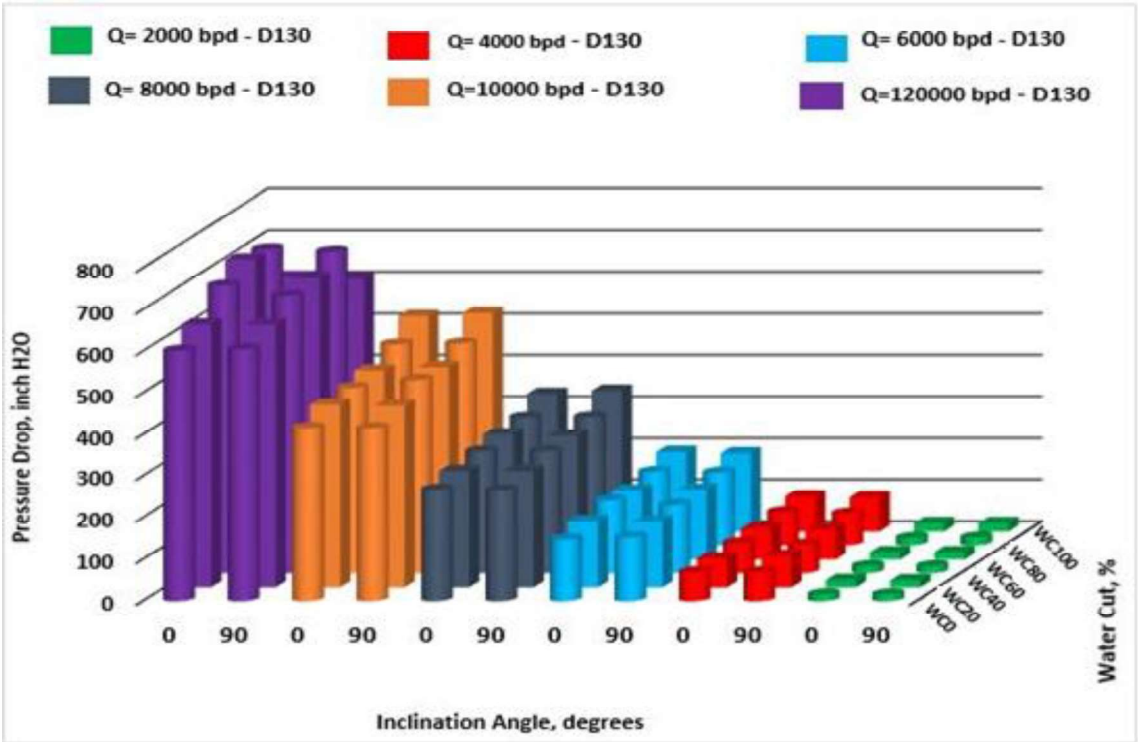

Figure 5.3j: Venturi pressure drop versus flow loop inclination for different fluid mixture flow rates and water cuts (β = 0.5, oil D130 and potable water).

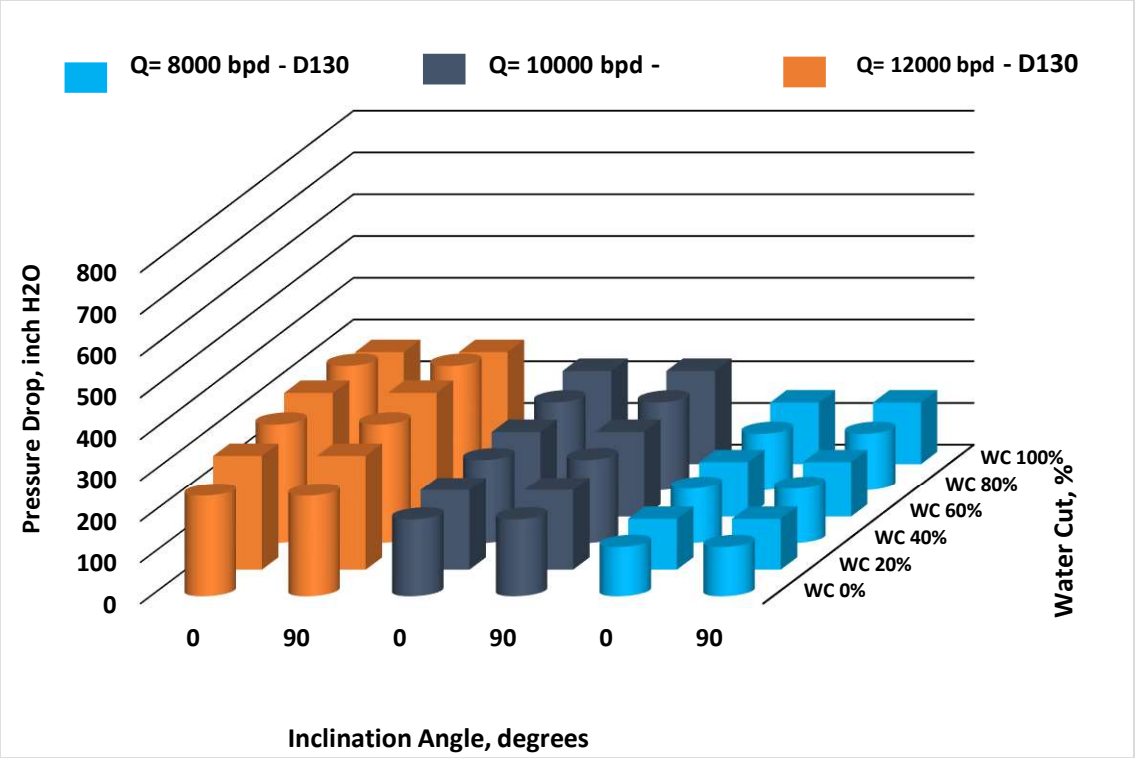

Figure 5.3k: Venturi pressure drop versus flow loop inclination for different fluid mixture flow rates and water cuts (β = 0.6, oil D130 and potable water).

As mentioned earlier, in general, pressure drop increases with flow rate and water cut and the effect of angle is not appreciable. It is very clear from the figures 5.3a to 5.3k that, the venturi pressure drop is almost constant with respect to the flow loop inclinations for given fluid mixture flow rate.

The reason is the venturi equation is derived from Bernoulli's equation. For an inclined pipe, the pressure drop term in the venturi equation is equal to the total pressure drop minus the gravitational pressure drop (which equals to the dynamic pressure gain). In the present case for an inclined flow loop, the differential pressure transmitter measures the differential pressure at the point of connection to the pressure transmitter, the head effect

is neutralized i.e. the measured total pressure drop in fact is the dynamic pressure gain which is independent of the flow loop inclination.

This is a very important conclusion, which expands the applicability of venturi meters to measurement operations of different inclination angles. The same trend in venturi pressure drop is observed for all two-phase oil-water flow rates ranging from 2000 to 12000 bpd and for all water cuts.

5.4 Effect of Venturi β on Pressure Drop for Different Water Cuts for Oils D80 and D130

The effect of β on venturi pressure drop for different water cuts for a fixed fluid flow rate of 6,000 bpd are presented in Figures 5.4a and 5.4b for horizontal and vertical flow loop inclinations. The experiments were performed on oil D80 only to prove that by considering a common flow rate.

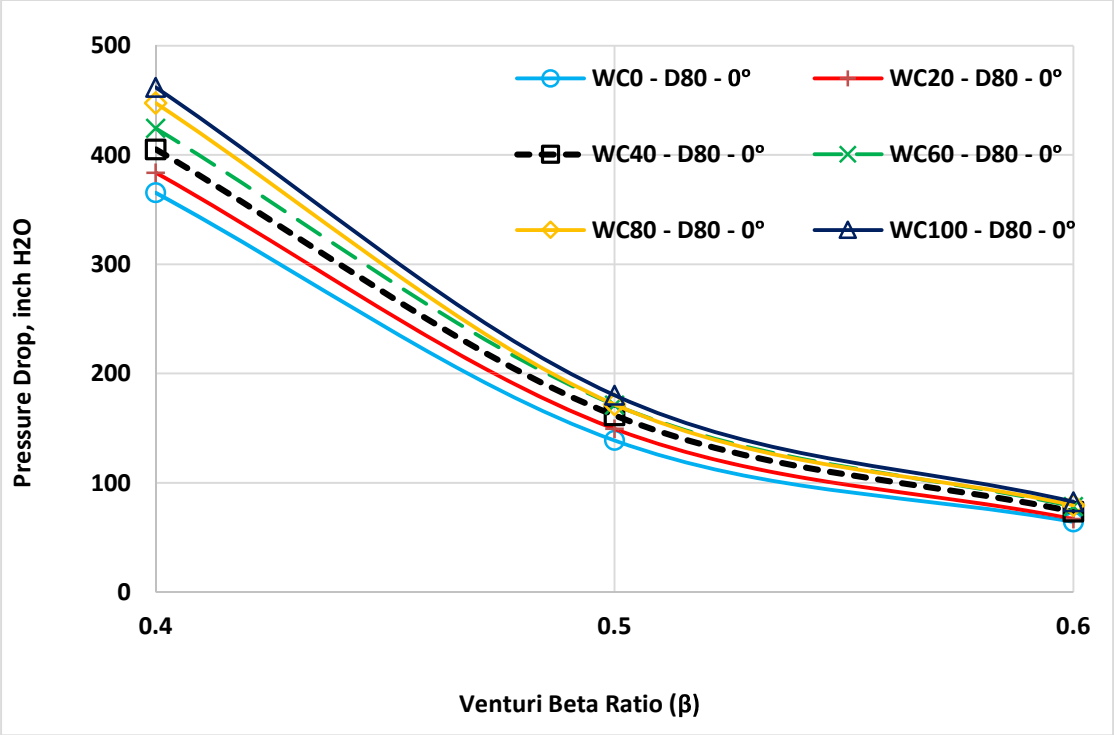

Figure 5.4a: Venturi pressure drop for different beta ratios for a fixed flow rate of 6000 bpd for different water cuts and θ = 0° (Oil D80 and potable water).

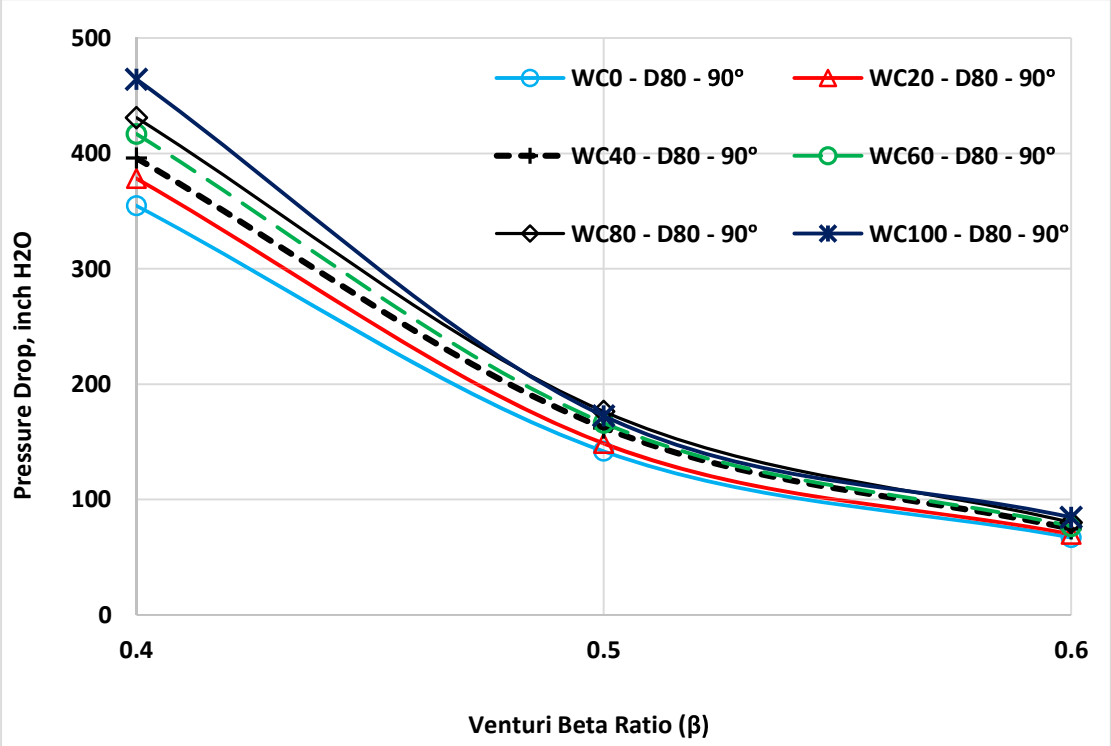

Figure 5.4b: Venturi pressure drop for different beta ratios for a fixed flow rate of 6000 bpd for different water cuts and θ = 90° (Oil D80 and potable water).

It is clear from the figures that the venturi pressure drop decreases nonlinearly with an increase in venturi β. Moreover, the range of venturi pressure drop decreases with the β. Interestingly, the highest pressure drop is for pure water and the lowest is for pure oil, and the effect of water cuts decreases as the β increases.

5.5 Effect of Oil Viscosity on Venturi Pressure Drop Measurements

In order to study the effect of viscosity on the venture pressure drop measurements, two mineral oils (D80 and D130) were consider. The measured kinematic viscosities of them were plotted against the temperature that within the testing ranges as shown in Figure 5.5. It can be seen that the viscosity decreases with the increase of temperature, as a scientific fact the expected behavior was obtained. Because of the high turbulence of the flow and the minor difference between the oils viscosities, the comparison is almost non-existent and the experiments that conducted under the same conditions showed nearly typical measurements for venturi pressure drop

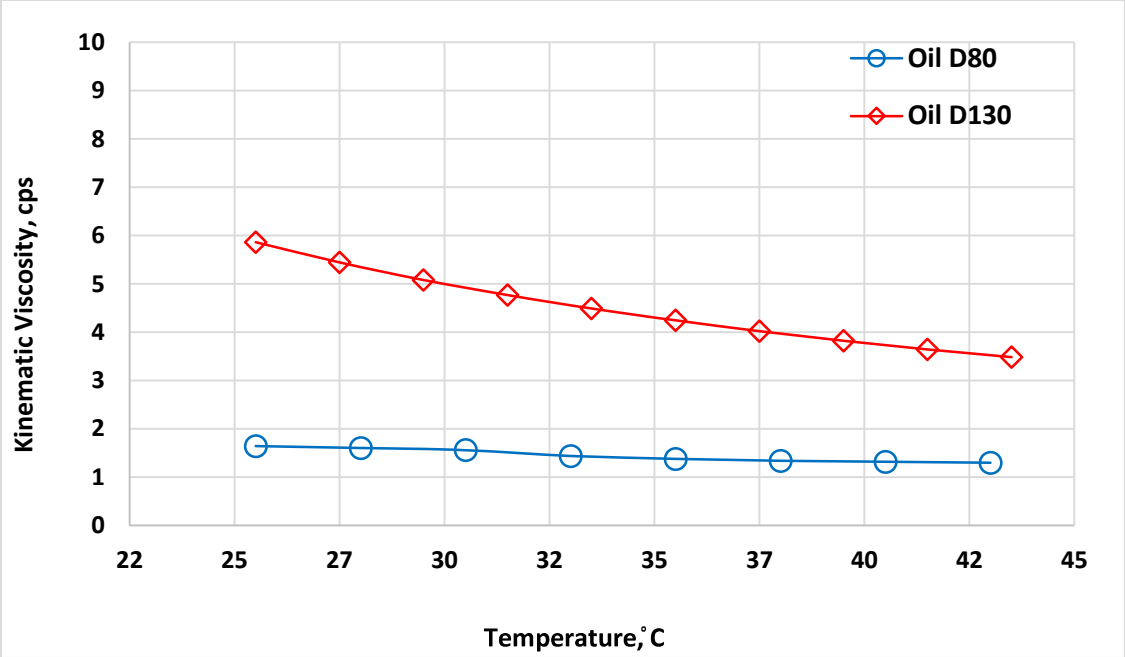

Figure 5.5: Variation of kinematic viscosity for Exxsol (D80 & D130) oils against temperature, [47] (Measurement done at Research Institute, RI in KFUPM).

Finally, the comparison was placed on experimental results of venturi pressure drop between oil D80 and oil D130, and we concluded with that, the effect of viscosity is noticeable at low flow rates only due to the small difference between the kinematic viscosities (T= 25.0 °C) of both oils (oil D80, ν= 2.18*10-6 m²/s) and (D130, ν= $6.89*10^{-6}$ m²/s). This minor difference in viscosity ($4.71*10^{-6}$ m²/s) does not show in remarked variation on pressure drop measurements because all the experiments were carried for a high flow rate similar to that on real oil wells fluid flow which having turbulent flow conditions.

5.6 Calculations of Modified Venturi Discharge Coefficient, *k,* for Oils D80 and D130

A modified venturi discharge coefficient, k, which is a function of pressure losses and venturi geometry, is introduced in the present study. The value of k was obtained from the simplified venturi governing Eq. 4.5.

The k value is determined from the single-phase and oil-water two-phase flow experiments of both oils D80 and D130 for all orientations of the flow loop and for the three venturi meters (β = 0.4, 0.5 and 0.6). The results of the oil-water experiments for different fluid mixture flow rates and water cuts are used to determine the k by using the same Eq. 4.5 for each of the three venturi meters. The obtained experimental values of k are plotted against the water cut for different fluid mixture flow rates as showed in Figures 5.6a to 5.6l, for horizontal cases only.

➢ Modified Venturi Discharge Coefficient k, for Oil 80:

For oil-water two-phase flow conditions of oil D80 experiments, the average values of 3.73 m2.s/h, 5.93 m2.s/h and 8.75 m2.s/h of k for the three venturi meters of β = 0.4, 0.5 and 0.6, respectively.

However, the percentage error in the total flow was calculated based on the average value of (k) for all configurations of the flow loop. As mentioned earlier the angle of inclination is not very much affecting on the venturi results. Due to that, we present the result for the horizontal inclinations only. The following Figures 5.6a to 5.6f show the variation of k

and percentage of error with respect to the water cut for other variables and for the three venturi meters, so the rest of resluts attached in APPENDIX B for other inclinations of the flow loop.

Figure 5.6a: Experimental values of k versus water cuts for different fluid mixture flow rates for θ = 0° (β=0.4, oil D80 and potable water).

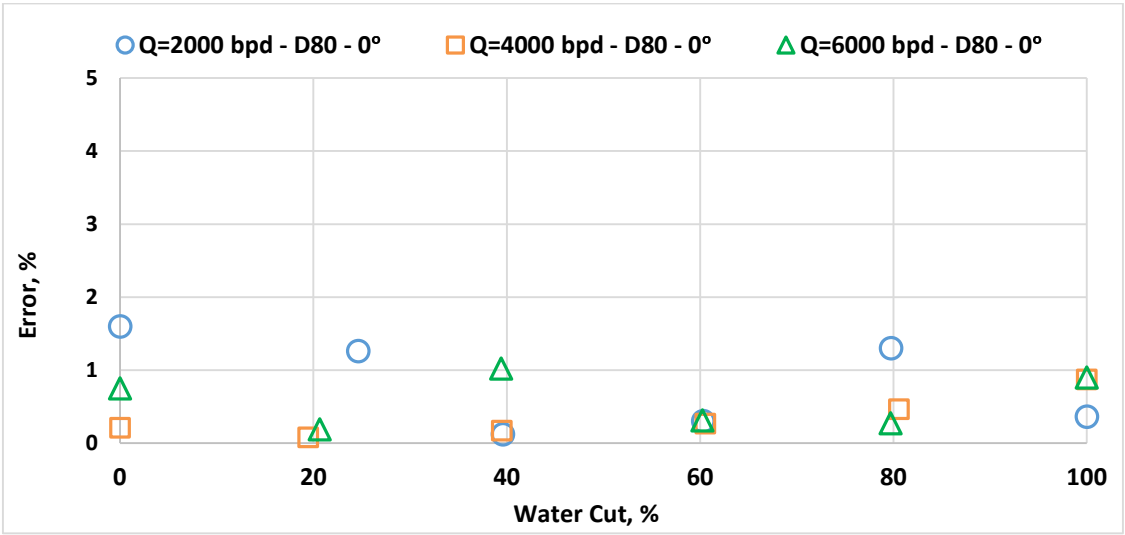

Figure 5.6b: Percentage error in the total flow rate using single value of k = 3.73 m^2.s/h for θ = 0° (β=0.4, oil D80 and potable water).

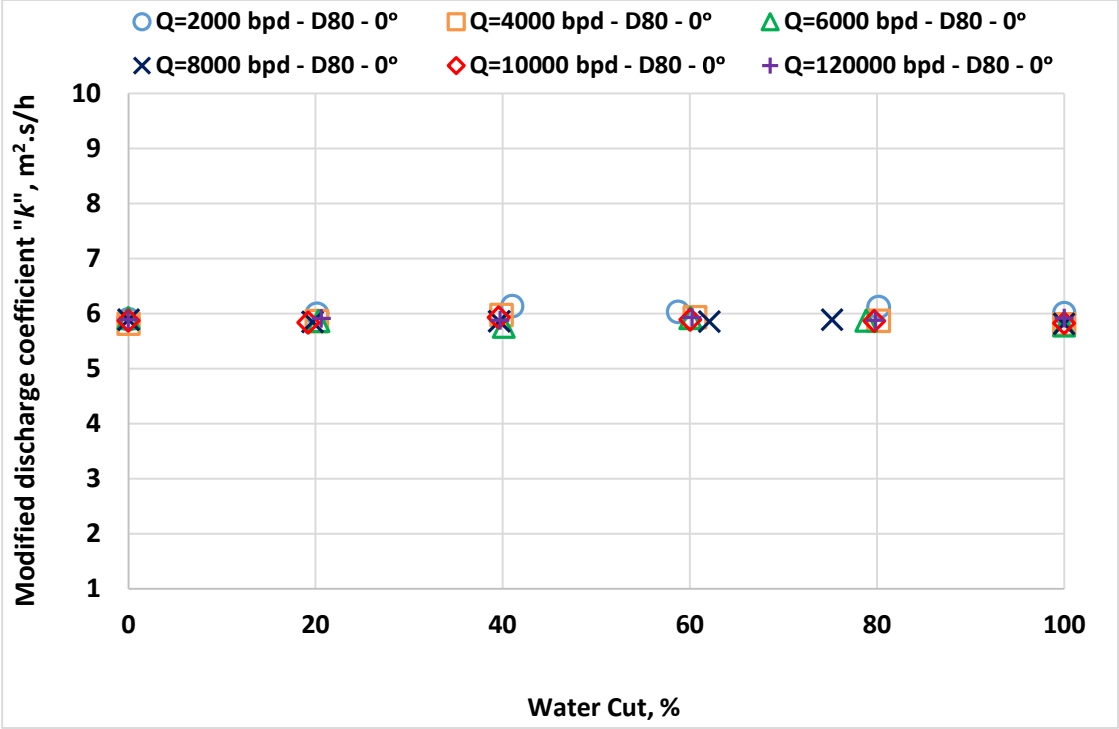

Figure 5.6c: Experimental values of k versus water cuts for different fluid mixture flow rates for θ = 0° (β=0.5, oil D80 and potable water).

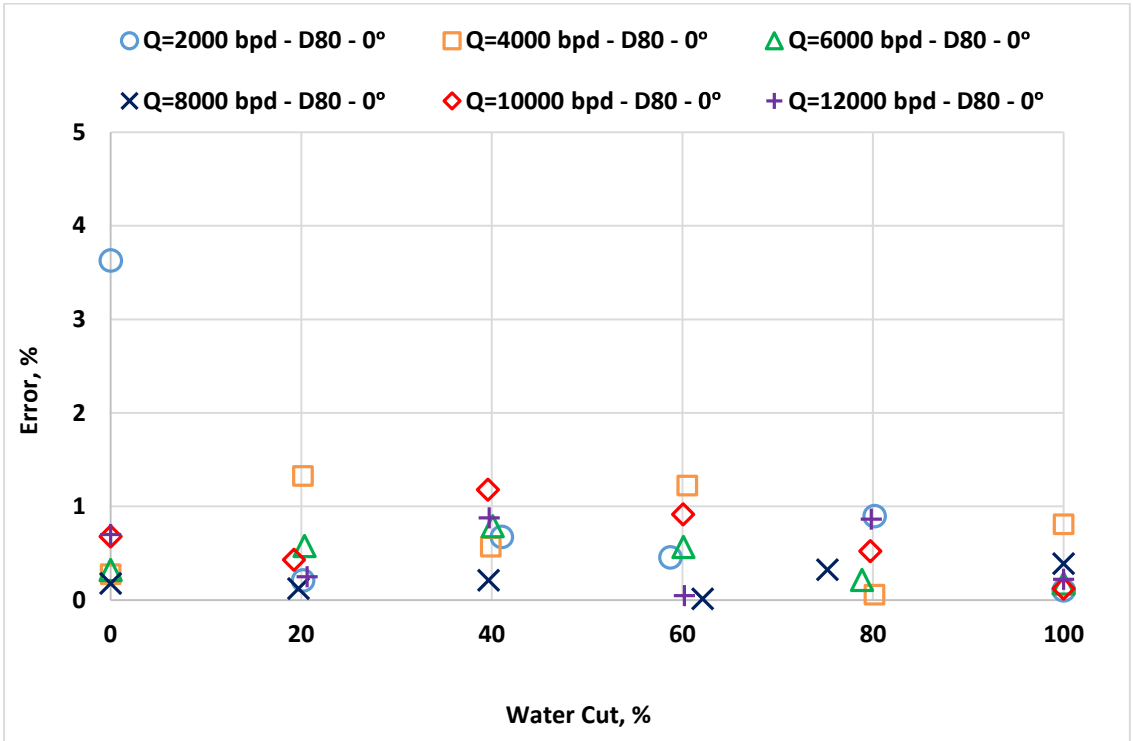

Figure 5.6d: Percentage error in the total flow rate using single value of k = 5.93 m².s/h for θ = 0° (β=0.5, oil D80 and potable water).

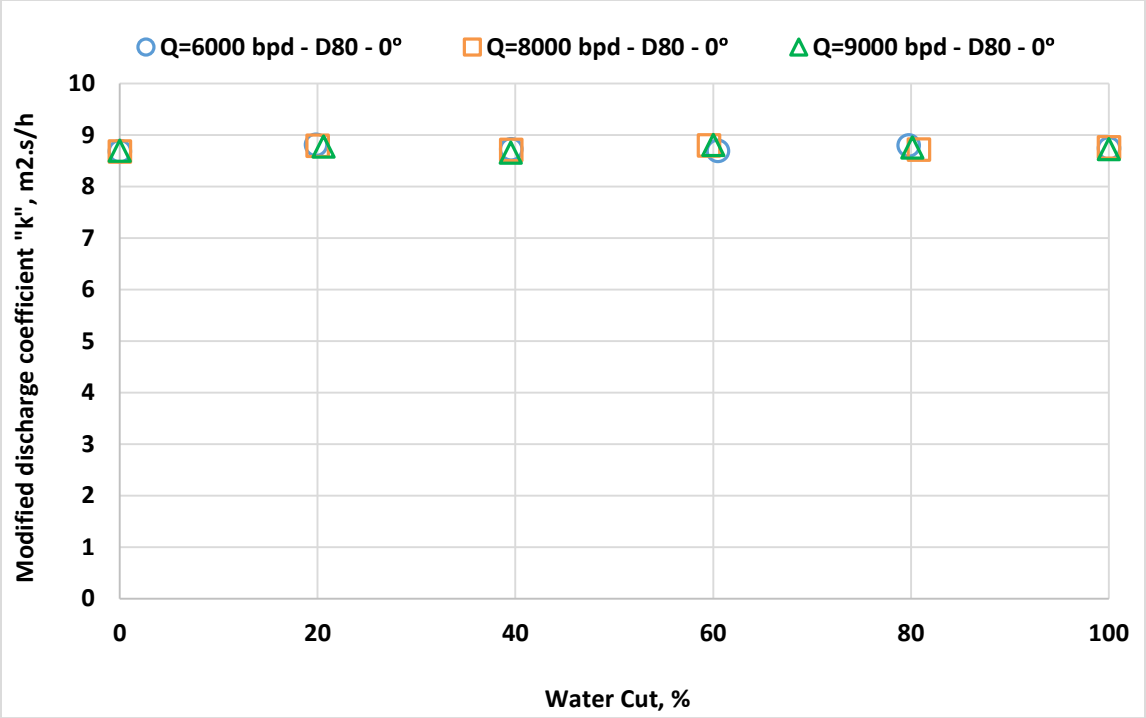

Figure 5.6e: Experimental values of k versus water cuts for different fluid mixture flow rates for θ = 0° (β=0.6, oil D80 and potable water).

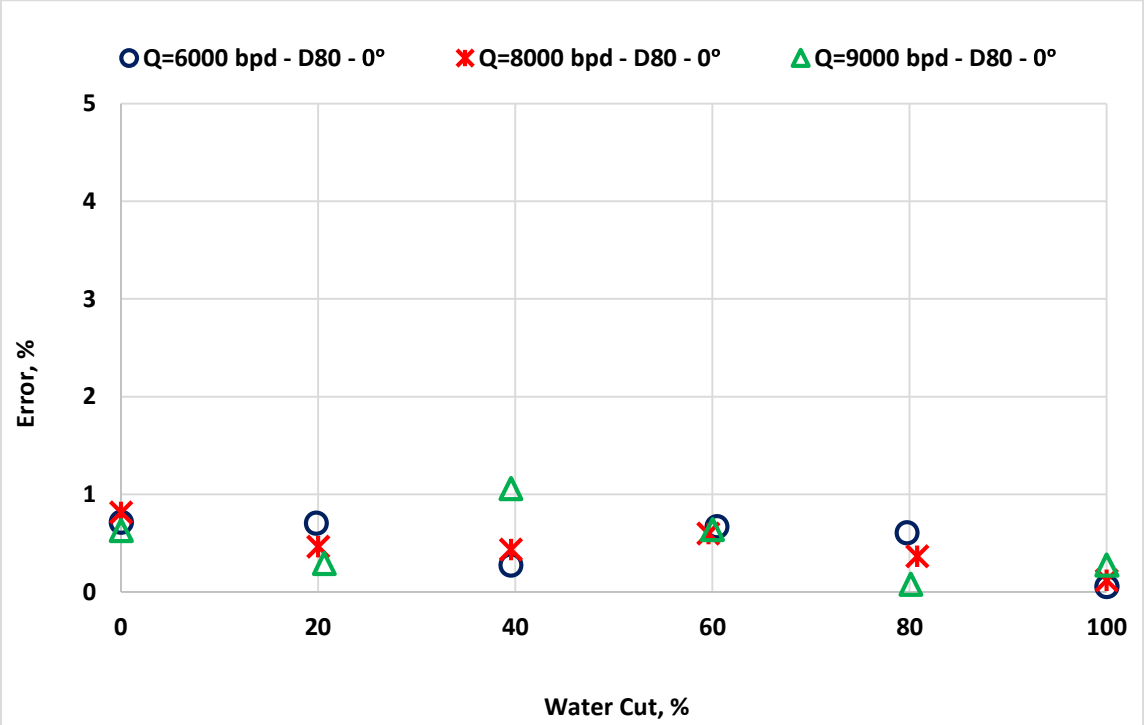

Figure 5.6f: Percentage error in the total flow rate using single value of k = 8.75 m^2.s/h for θ = 0° (β=0.6, oil D80 and potable water).

The average values of modified venturi discharge coefficient k and percentage error are summarized in Table 5.1.

Table 5.1: Average modified discharge coefficient and percentage error in the fluid mixture flow of oil D80 for the three venturi meters.

Venturi β	Modified Discharge Coefficient (k), $m^2.s/h$	Flow Loop Inclination, Angle in Degrees	Average Error in Fluid Mixture Flow Rate (%)
0.4	3.73	0	0.58
		90	0.54
0.5	5.93	0	0.58
		40	1.34
		60	1.30
		90	1.25
0.6	8.75	0	0.49
		90	0.65

It can be seen from Table 5.1 that the average percentage error in the total flow rate is between 1.35% and 0.50%, which is reasonably very good.

➢ Modified Venturi Discharge Coefficient k, for Oil 130:

Correspondingly, in case of oil D130, for the three venturi meters of β = 0.4, 0.5 and 0.6 the average values of k are fluctuating around 3.75 m2.s/h, 5.90 m2.s/h and 8.78 m2.s/h, respectively, which were obtained from the experimental results.

In addition, the variation of k and percentage error have been plotted with respect to the water cut for different flow rates and are presented in Figures 5.6g to 5.6l.

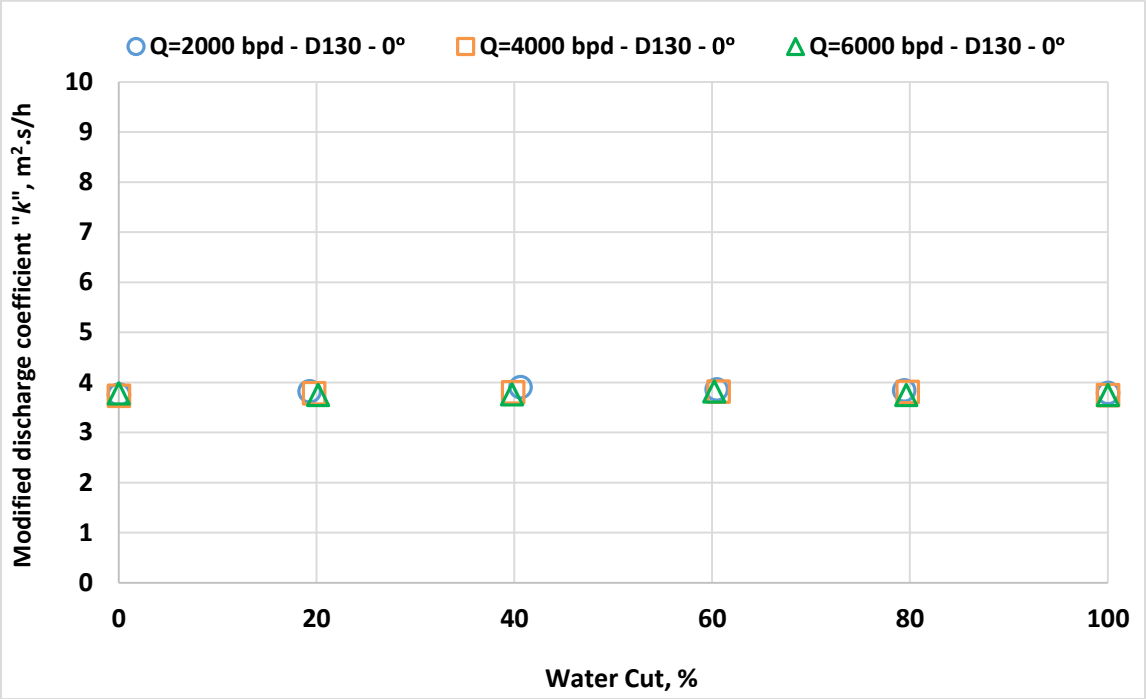

Figure 5.6g: Experimental values of k versus water cuts for different fluid mixture flow rates for θ = 0° (β=0.4, oil D130 and potable water).

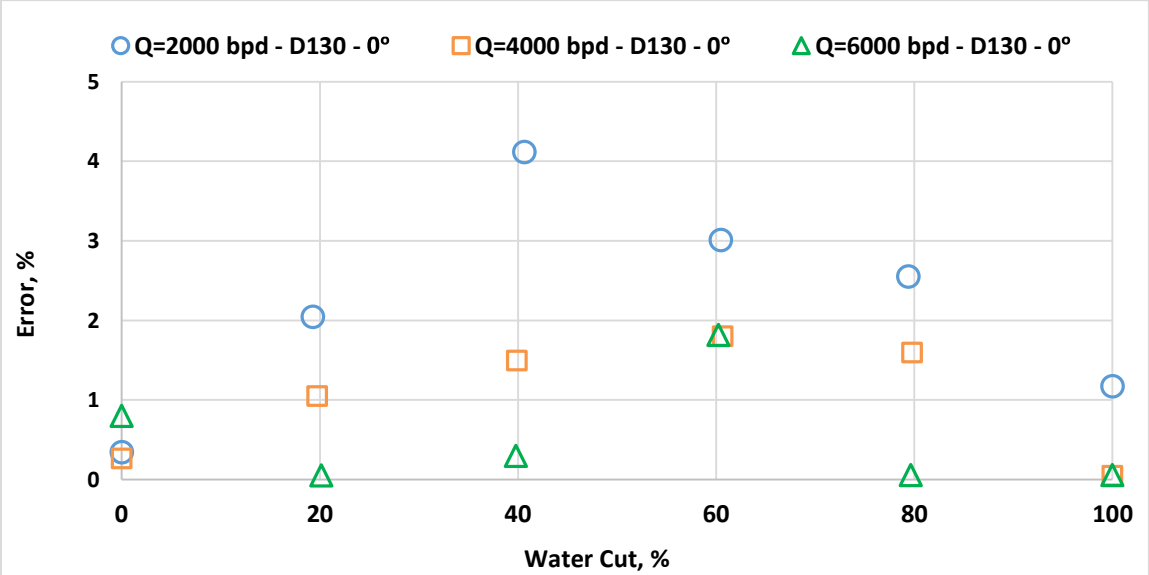

Figure 5.6h: Percentage error in the total flow rate using single value of k = 3.75 m^2.s/h for θ = 0° (β=0.4, oil D130 and potable water).

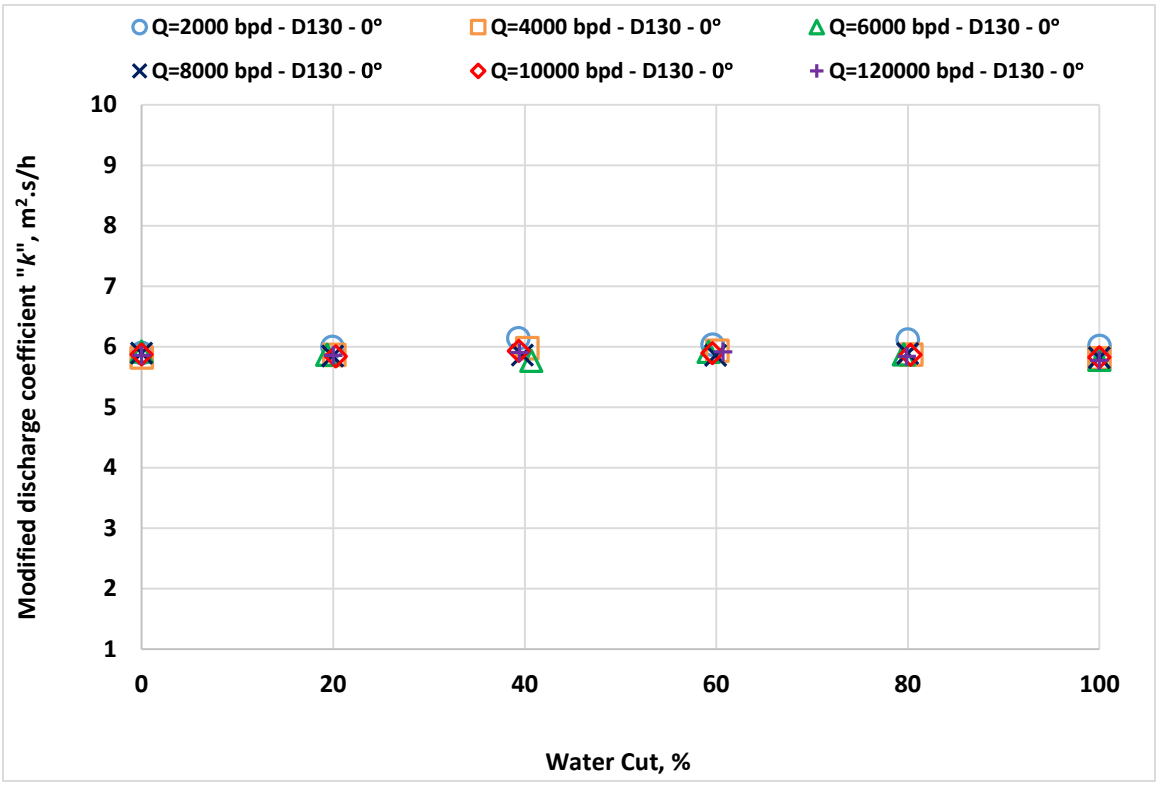

Figure 5.6i: Experimental values of k versus water cuts for different fluid mixture flow rates for θ = 0° (β=0.5, oil D130 and potable water).

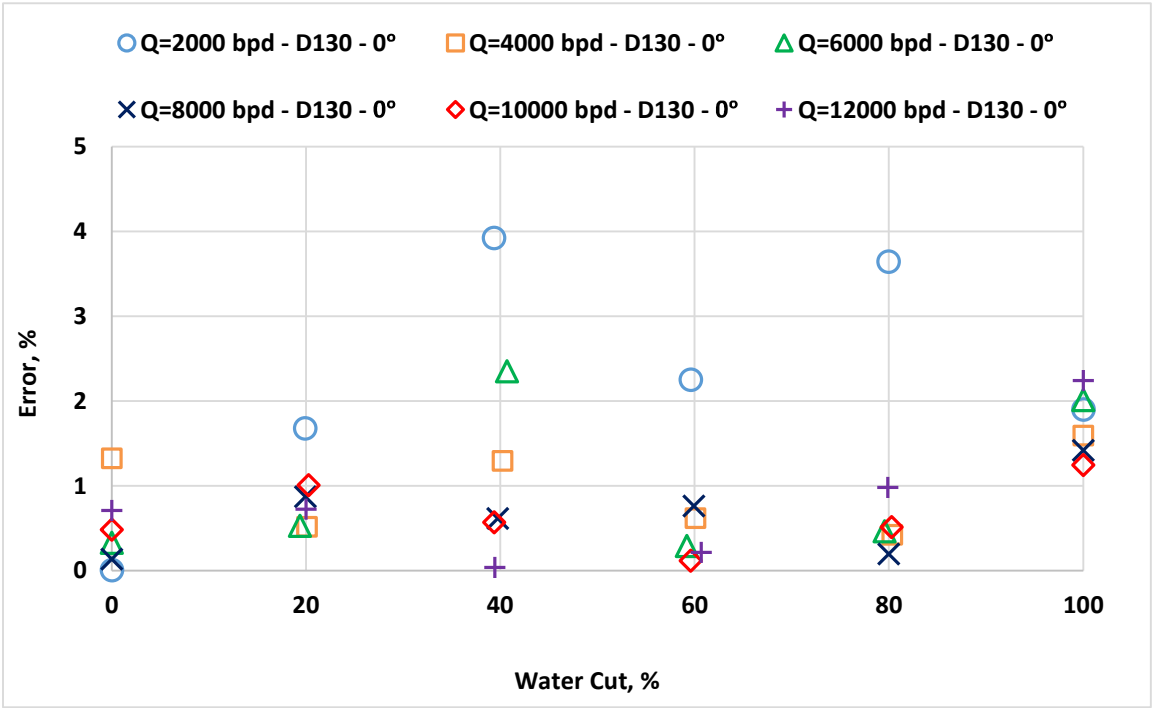

Figure 5.6j: Percentage error in the total flow rate using single value of k = 5.90 m^2.s/h for θ = 0° (β=0.5, oil D130 and potable water).

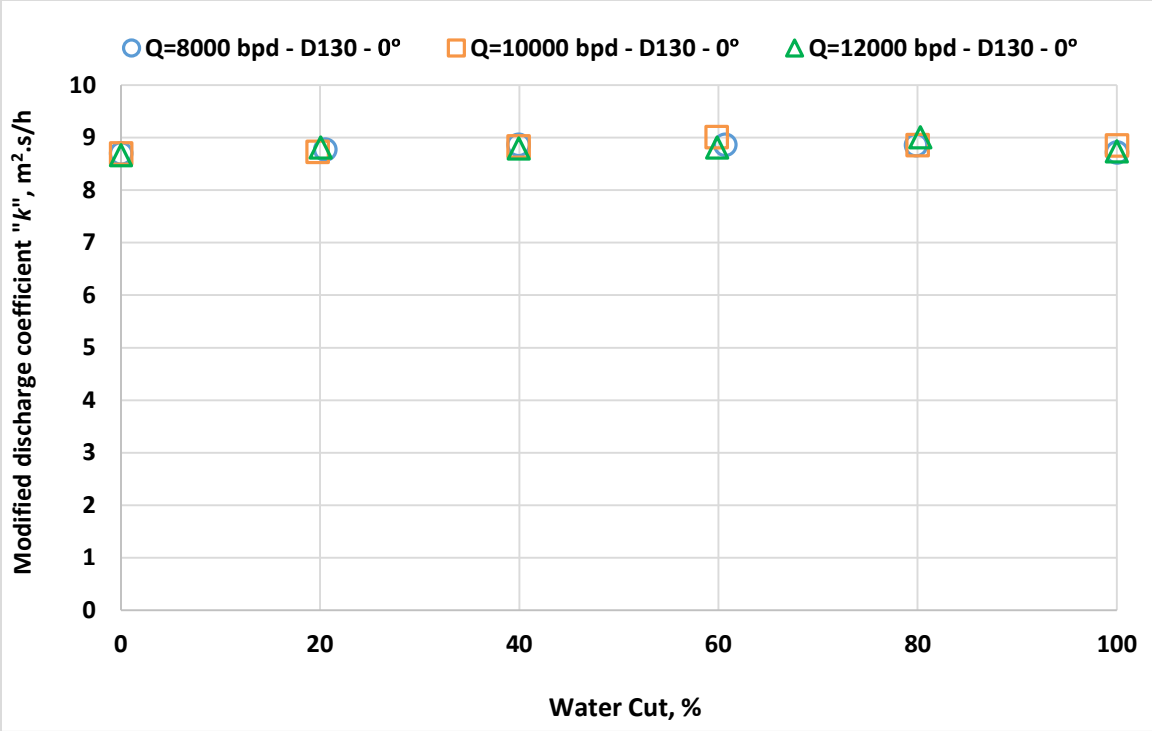

Figure 5.6k: Experimental values of k versus water cuts for different fluid mixture flow rates for θ = 0° (β=0.6, oil D130 and potable water).

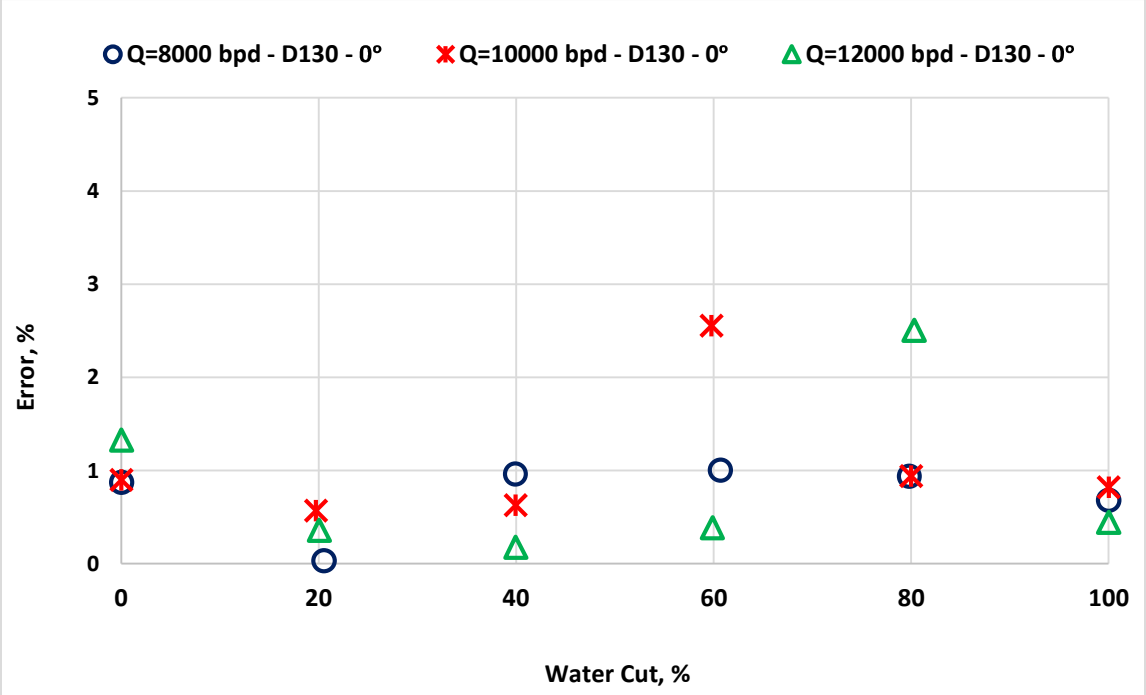

Figure 5.6l: Percentage error in the total flow rate using single value of k = 8.78 m^2.s/h for θ = 0° (β=0.6, oil D130 and potable water).

Table 5.2 can summarize the average values of modified venturi discharge coefficient k and percentage error.

Table 5.2: Average modified discharge coefficient and percentage error in the fluid mixture flow of oil D130 for the three venturi meters.

Venturi β	**Modified Discharge Coefficient (*k*), m^2.s/h**	**Flow Loop Inclination, Angle in Degrees**	**Average Error in Fluid Mixture Flow Rate (%)**
0.4	3.75	0	1.26
		90	1.42
0.5	5.90	0	1.05
		90	1.04
0.6	8.78	0	0.89
		90	0.52

In conclusion, it can be seen clearly a very reasonable accuracy between 0.53% and 1.43%, that was obtained without any impact for the flow loop inclination on the total flow rate calculated by venturi.

5.7 Calculations of Venturi Discharge Coefficient, C_d, for Oils D80 and D130

Venturi discharge coefficient, C_d, was calculate by Eq. 4.8, by considering the average values of the modified venturi discharge coefficient, which were obtained experimentally. The experimental results of C_d that obtained are plotted against the water cut for different

fluid mixture flow rates and for the three venturi meters for the horizontal inclinations of the flow loop, and the results of other inclinations are plotted and presented in APPENDIX C.

➢ Venturi Discharge Coefficient C_d for Oil 80:

For oil D80 experiments and horizontal orientations of the flow loop, the results of C_d are presented graphically in Figures 5.7a to 5.7c.

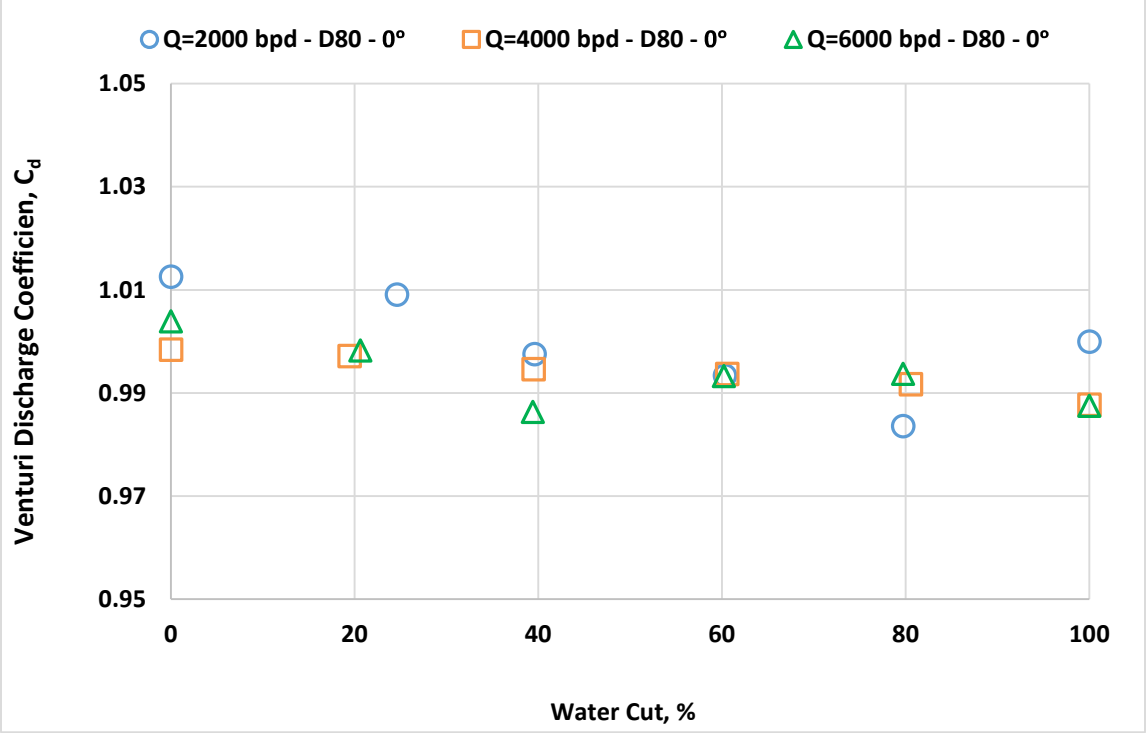

Figure 5.7a: Experimental venturi discharge coefficient, C_d, versus water cut for low fluid mixture flow rates for 0° (β =0.4, oil D80 and potable water).

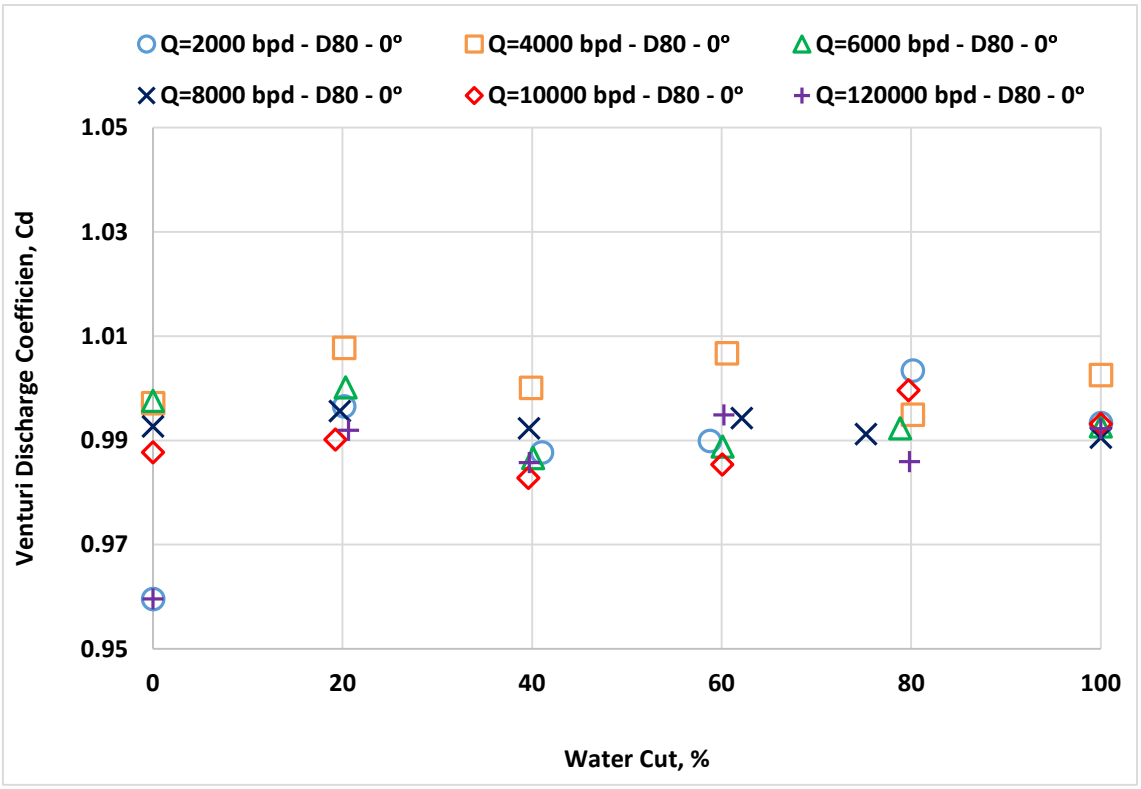

Figure 5.7b: Experimental venturi discharge coefficient, C_d, versus water cut for low fluid mixture flow rates for 0° (β =0.5, oil D80 and potable water).

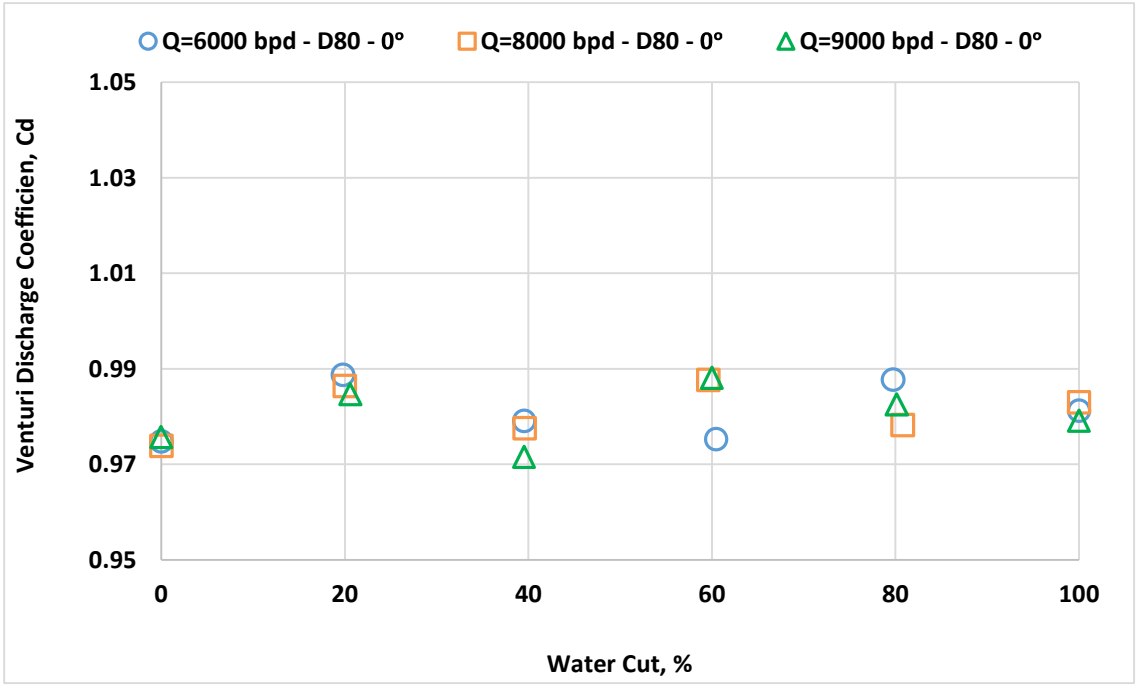

Figure 5.7c: Experimental venturi discharge coefficient, C_d, versus water cut for high fluid mixture flow rates for 0° (β =0.6, oil D80 and potable water).

➢ Venturi Discharge Coefficient C_d for Oil 130:

Also for the same horizontal configuration of the flow loop and oil D130, the experimental results of C_d of three venturi meters are presented graphically in Figures 5.7d to 5.7f.

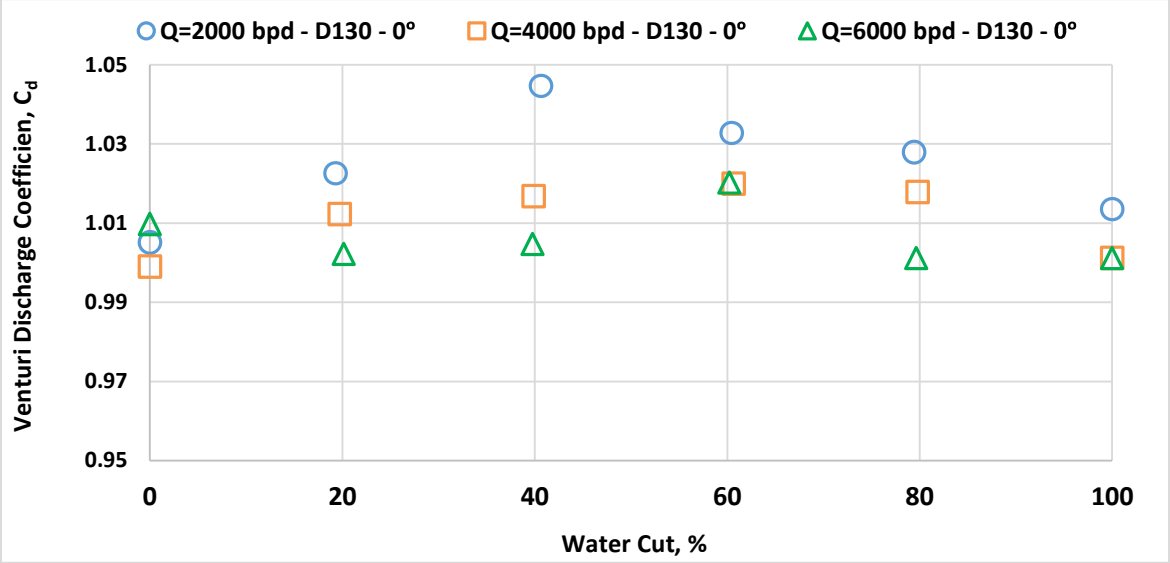

Figure 5.7d: Experimental venturi discharge coefficient, C_d, versus water cut for low fluid mixture flow rates for 0° (β =0.4, oil D130 and potable water).

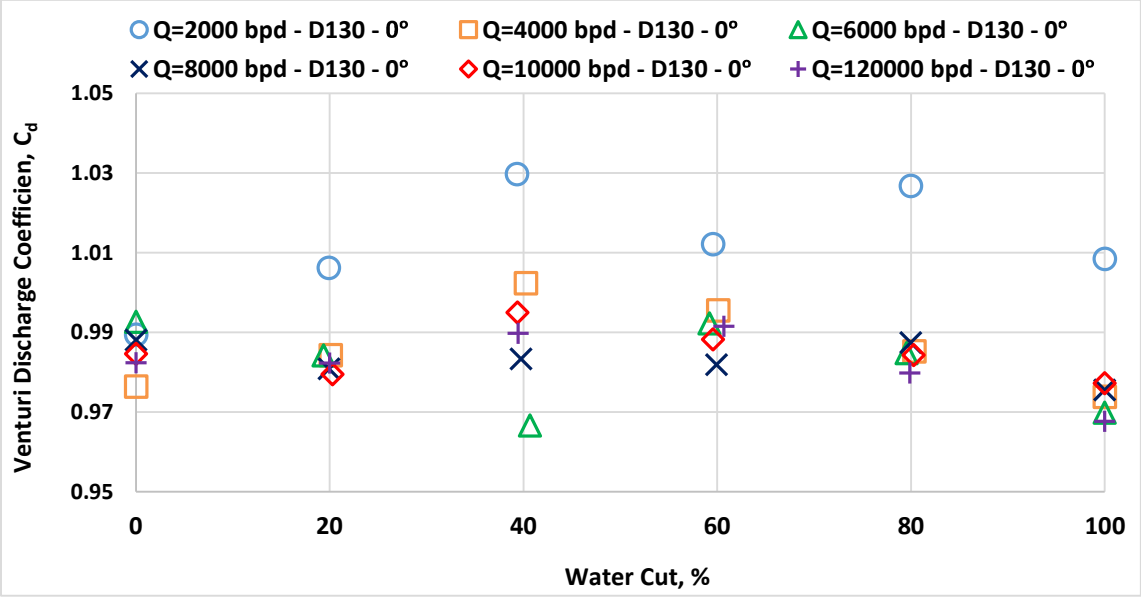

Figure 5.7e: Experimental venturi discharge coefficient, C_d, versus water cut for fluid mixture flow rates for 0° (β =0.5, oil D130 and potable water).

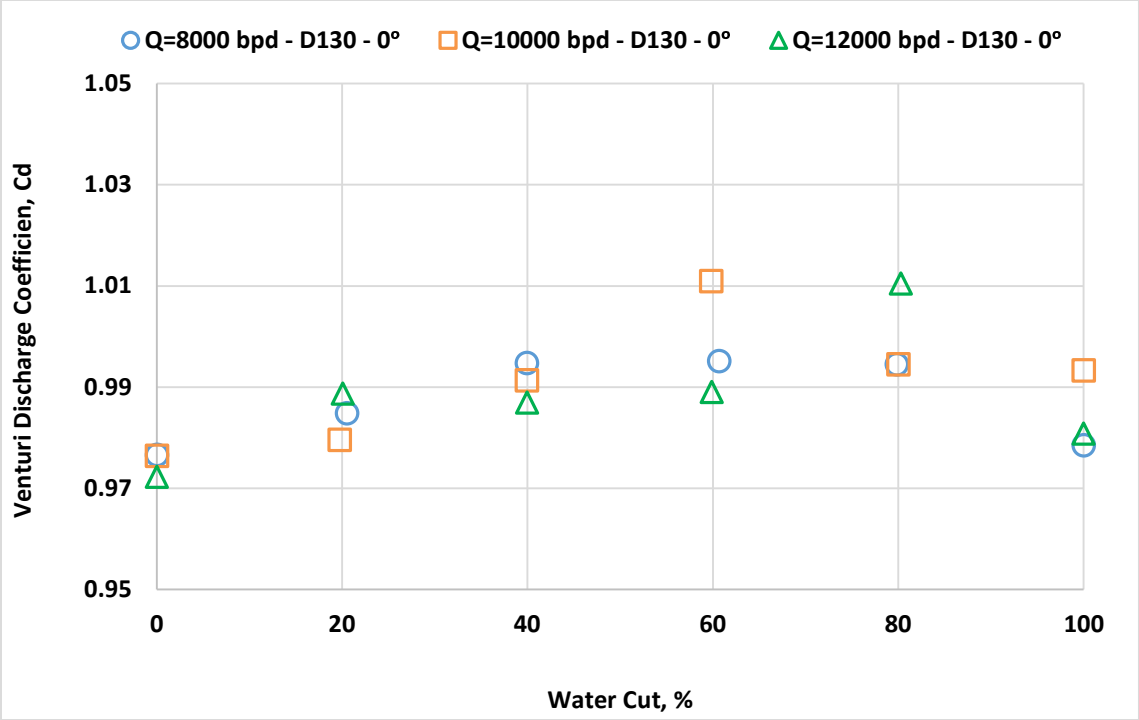

Figure 5.7f: Experimental venturi discharge coefficient, Cd, versus water cut for high fluid mixture flow rates for 0º (β =0.6, oil D130 and potable water).

The scatter plots show that most of the C_d values lie in the range 0.98 to 1.0 except for single phase and WC 40% experiments with values greater than 1.0 and maximum of 1.05. At water cur 40%, this water cut is close to the inversion point at WC 50%, where more energy developed between the two phases of oil and water in the pipe, because of that, the pressured drop measurement was affected.

It can be concluded that the venturi discharge coefficient, C_d, variation at the flow conditions under consideration is minor.

5.8 Correlations for Venturi Pressure Coefficient, Cp_m

Statistical software called DADTFIT [40] was used for performing nonlinear regression and generating new empirical correlations of exponential- form to describe the ratio of the measured venturi pressure drop to the upstream dynamic pressure that can be defined by a parameter knows a mixture venturi pressure coefficient, Cp_m.

Based on the analogous methods those used in two-phase flow, specifically (oil-water) flow, tow correlations were developed for the mixture venturi pressure coefficient, Cp_m, for each oil D80 and D130 under consideration of four main parameters: mixture Reynolds number (Re_m), water cut percentage (WC), flow loop inclination (θ) and venturi meter size (beta ratio, β).Thus, the four parameters were employed throughout in correlating the mixture venturi pressure coefficient, Cp_m as independent variable with the four parameters as dependent variables. The proposed correlations of oil D80 and oil D130 are expressed in Eq. (5.1) and Eq. (5.2), respectively, as follow:

$$Cp_m = \exp[\, 8.2972 * 10^{-3} * WC - 59.7668 * 10^{-8} * Re_m - 8.98215 * \beta + 6.7370 * 10^{-4} * \theta + 7.24194] \quad (5.1)$$

$$Cp_m = \exp[-7.41986 * 10^{-2} * WC + 3.32034 * 10^{-7} * Re_m - 9.05195 * \beta + 1.77209 * 10^{-2} * \theta + 7.255804] \quad (5.2)$$

Where,

β = Venturi beta ratio

WC = Water cut ratio

Rem = Mixture Reynolds number

θ= Flow loop inclination, in radians

Then, the above correlation were tested using different statistical parameters such as, R-squared, variance, average absolute error, and standard deviation. The newly proposed correlations showed a good performance in terms of accuracy as summarized in Table 5.3.

Table 5.3: The statistical analyses for oils (D80 and D130) correlations.

Items	**Oil D80 Correlation**	**Oil D130 Correlation**
Residual Sum of Squares (Absolute & Relative)	58.723	51.029
Standard Error of the Estimate	0.5275	0.6059
Coefficient of Multiple Determination (R^2)	0.9971	0.9973
Adjusted coefficient of multiple determination (Ra^2)	0.9971	0.9972

The testing results of correlation each oil are plotted in Figures 5.8a and 5.8b. Correlations showed high performance in the prediction results of venturi pressure coefficient when compared with the measured values of Cp_m, which were obtained by Eq. (4.9) from the experimental results based on the measured venturi pressure drop.

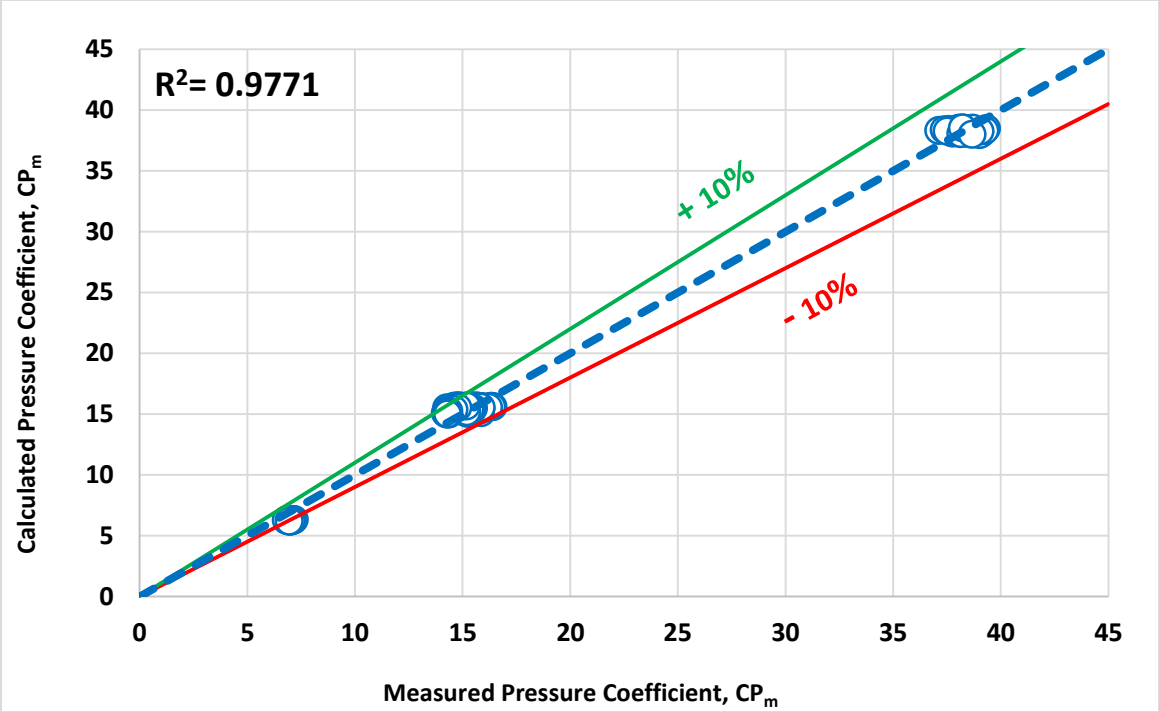

Figure 5.8a: Comparison between measured and calculated mixture venturi pressure coefficient based on correlation of oil D80.

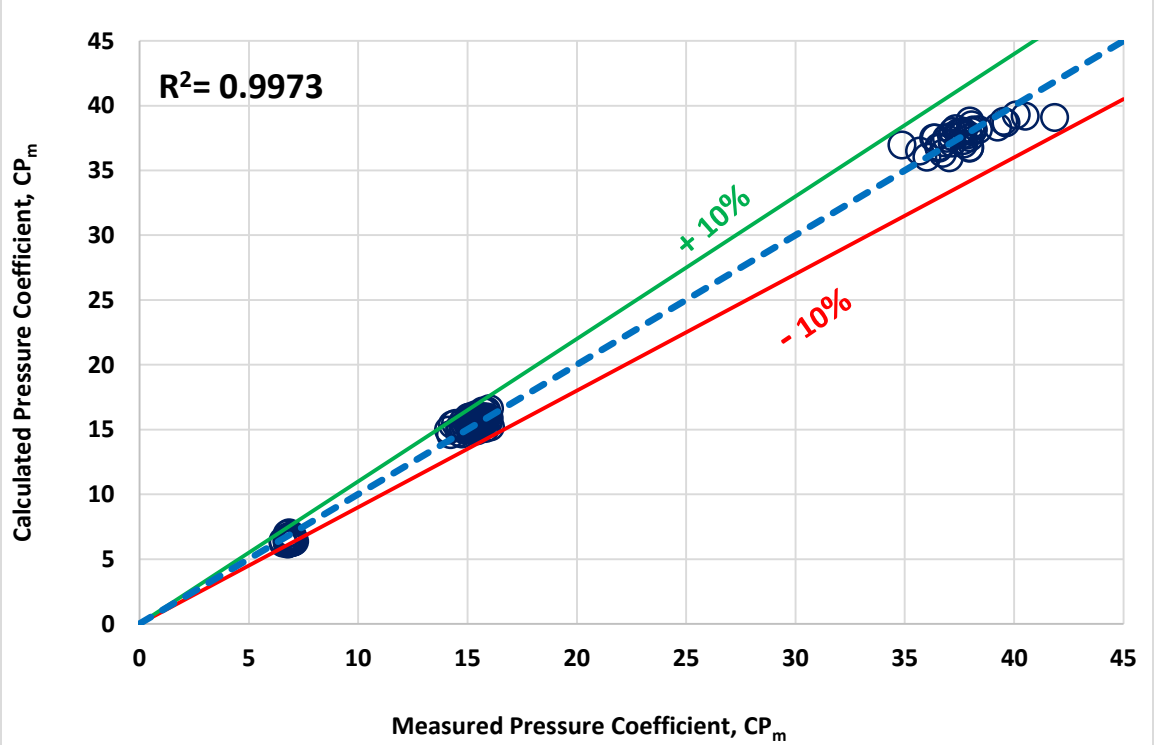

Figure 5.8b: Comparison between measured and calculated mixture venturi pressure coefficient based on correlation of oil D130.

As shown in Figures 5.8a and 5.8b, when the mixture venturi pressure coefficient that have been calculated using the proposed correlations (5.1 &5.2) were plotted against the measured experimental data calculated by Eq. 4.9, they showed a well closed match around the straight line with an angle of 45 degree which indicts the good performance of the new proposed correlations in estimating of the mixture venturi pressure coefficient, Cp_m.

In addition, it can be seen from the Figures 5.8a and 5.8b that mixture venturi pressure coefficient fluctuates around 38.39, 15.55 and 7.00 for the venturi meters with $\beta = 0.4$, 0.5 and 0.6, respectively. The predicted venturi pressure coefficient by the correlations (5.1) and (5.2) were plotted against mixture Reynolds number, and then compared with measured values obtained from Eq. 4.9, for each venturi meter and for each oil individually. The comparison was held as shown in Figures 5.9a to 5.9c and Table 5.3a for oil D80 data, moreover in Figures 5.9d to 5.9f and Table 5.3b for oil D130 experiments data.

1. Results of Venturi Pressure Coefficient, Cp_m for Oil D80:

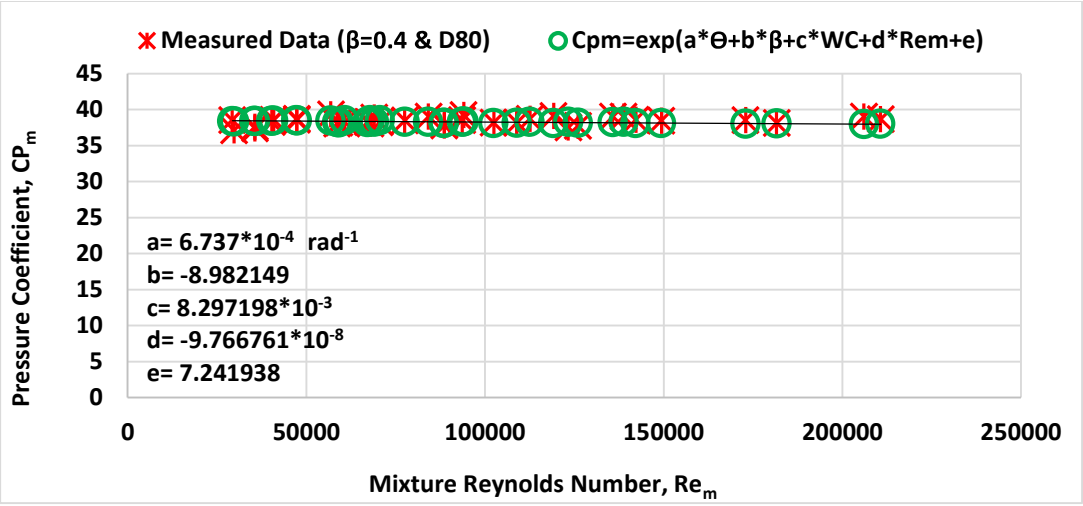

Figure 5.9a: Measured and calculated mixture venturi pressure coefficient versus mixture Reynolds number [Correlation (5.1), β =0.4, D80 oil and potable water].

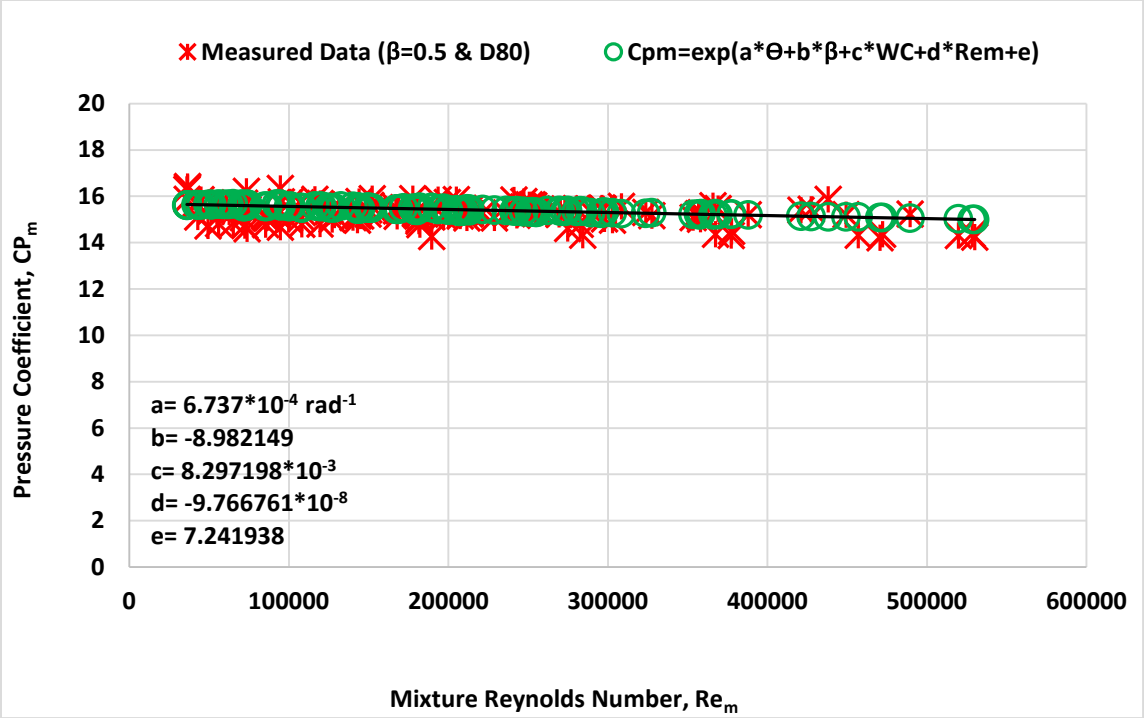

Figure 5.9b: Measured and calculated mixture venturi pressure coefficient versus mixture Reynolds number [Correlation (5.1), β =0.5, D80 oil and potable water].

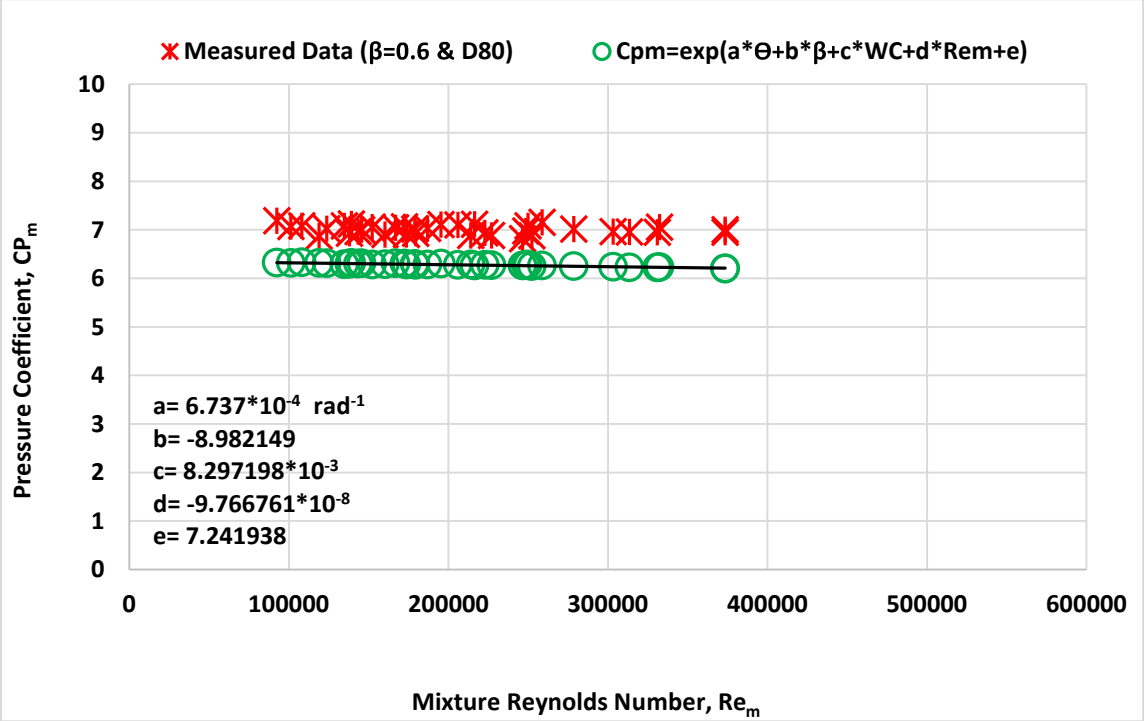

Figure 5.9c: Measured and calculated mixture venturi pressure coefficient versus mixture Reynolds number [Correlation (5.1), β =0.6, D80 oil and potable water].

Table 5.4: Comparison between measured and predicted average values of the mixture venturi pressure coefficient Cpm for homogeneous fluid mixture density of oil D80 data.

Venturi β Size	Flow Loop Inclination	Average of Measured Cp_m by Equation (4.9)	Average of Predicted Cp_m by Correlation (5.1)
0.4	0º	38.40	38.27
	90º	38.38	
0.5	0º	15.22	15.42
	40	15.21	
	60º	15.40	
	90º	15.28	
0.6	0º	6.98	6.28
	90º	7.02	

2. Results of Venturi Pressure Coefficient, Cp_m for Oil D130:

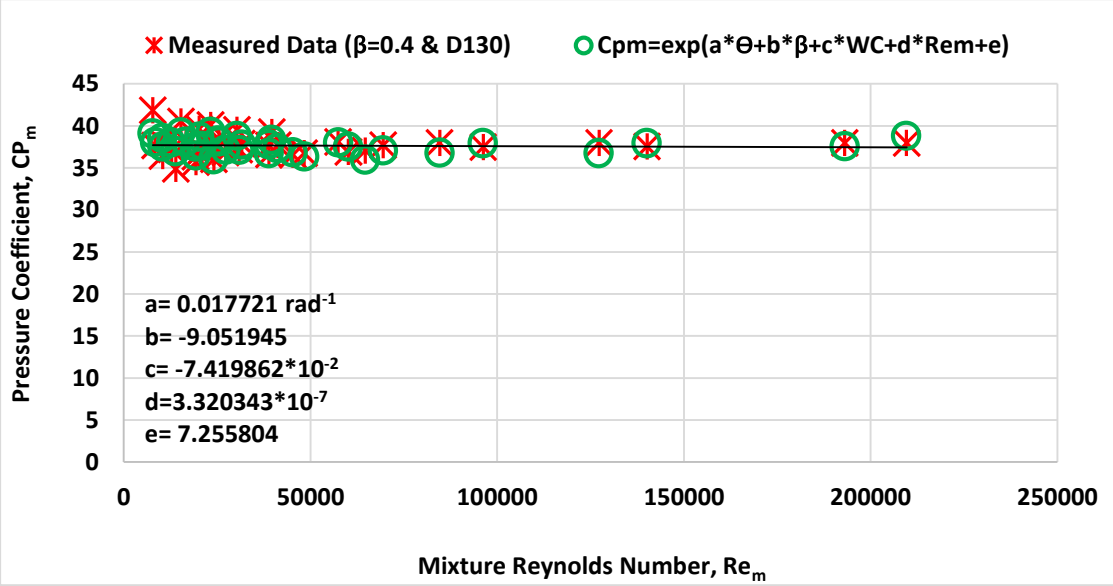

Figure 5.9d: Measured and calculated mixture venturi pressure coefficient versus mixture Reynolds number [Correlation (5.2), β =0.4, D130 oil and potable water].

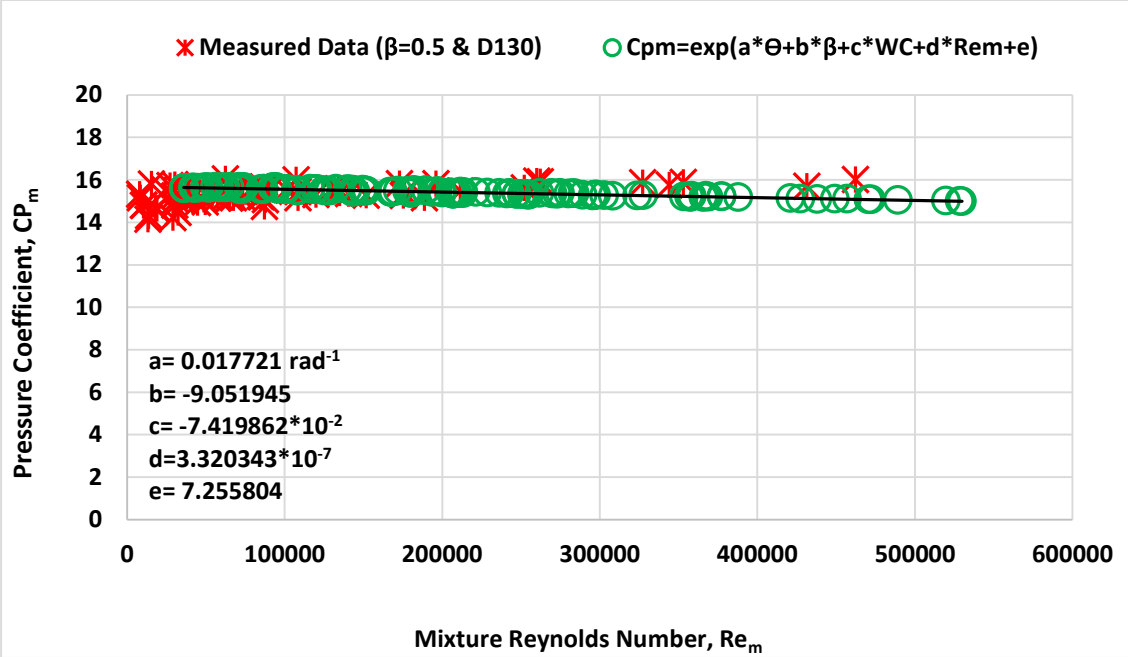

Figure 5.9e: Measured and calculated mixture venturi pressure coefficient versus mixture Reynolds number [Correlation (5.2), β =0.4, D130 oil and potable water].

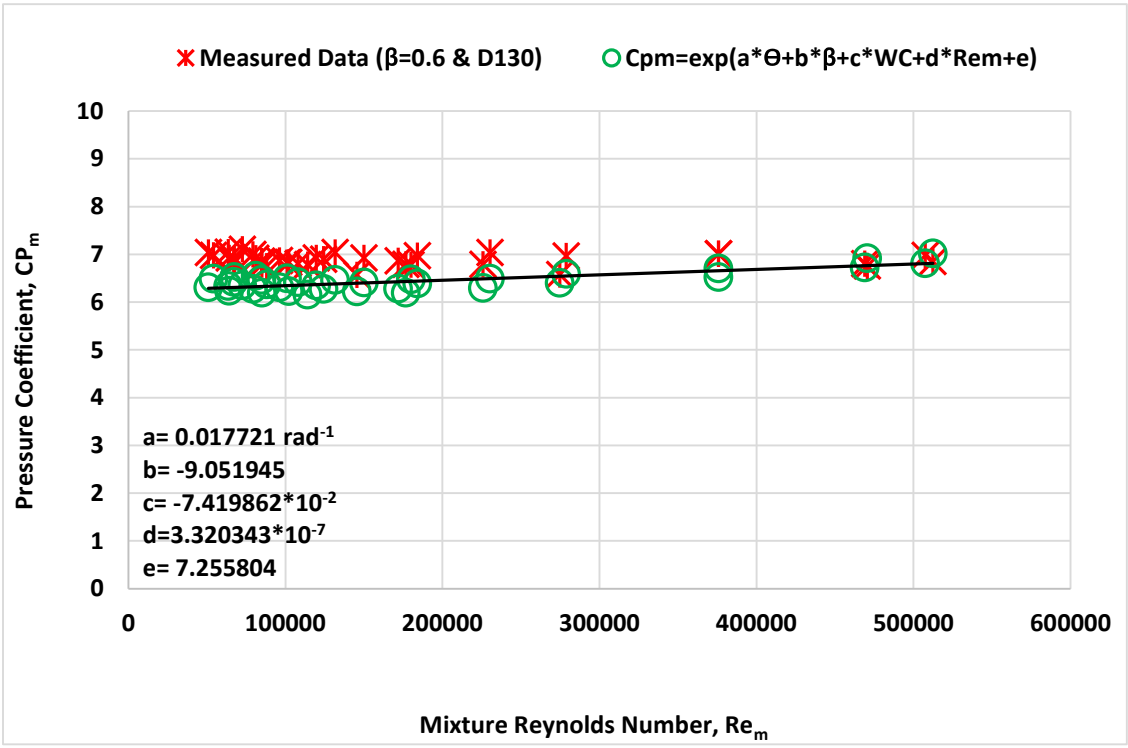

Figure 5.9f: Measured and calculated mixture venturi pressure coefficient versus mixture Reynolds number [Correlation (5.2), β =0.4, D130 oil and potable water].

Table 5.5: Comparison between measured and predicted average values of the mixture venturi pressure coefficient Cpm for homogeneous fluid mixture density of oil D130 data.

Venturi β Size	**Flow Loop Inclination**	**Average of Measured Cp_m by Equation (4.9)**	**Average of Predicted Cp_m by Correlation (5.2)**
0.4	0º	37.03	37.65
	90º	38.41	
0.5	0º	15.36	15.52
	90º	15.31	
0.6	0º	6.87	6.43
	90º	6.90	

In conclusion, it can be clearly seen from Tables (5.4 &5.5) and Figures (5.9a to 5.9f) that the average values of both measure and predicted mixture venturi pressure coefficient fluctuate around 38.39, 15.55 and 7.00 for all orientations of the loop for the venturi meters with $\beta = 0.4$, 0.5 and 0.6, respectively.

In Figures 5.8a and 5.8b, the closeness of between the measured and predicted Cpm plots for the data of oil D80 and oil D130 experiments, implies that the output responses are not sensitive to the inclination and water cut.

Therefore, from the experimental results discussed so far, it can be concluded that the flow loop inclination does not affect the venturi meters result. The behavior of Cpm vs. Rem at high flow rate considered in this work is similar to the behavior of the venturi with a single-phase flow in the venturi regardless of the inclination angles.

5.8.1 Results of Correlations Input Variables Reduction

It is of interest to reduce the number of variables as much as possible to find the variables that contribute most to the mixture venturi pressure coefficient, Cpm. Some of the variables used in the previous regression models of oils (D80 &D130) are closely correlated. As already mentioned, the effect of inclination on pressure drop behavior is not appreciable. So that, for this reason the inclination has no effect on the mixture venturi pressure coefficient, Cpm. Because of that, the effect of inclination (θ) was excluded out of dependent variables.

In addition, variations in oils viscosities were included in this study, but variations between the oils viscosities is very small. Meanwhile, the experimental observations were made at very high-pressure gradients and high flow rates similar to that in real oil field industries, therefore no attempt being made to detect the viscosity variations of the both mineral oils with high-pressure drops and turbulent flows.

It could be pointed out also that since all data were performed on mineral oils only with near closed densities and viscosities, it can only be assumed at present that changes and difference in oils viscosities would produce no fundamental change in the correlation.

Therefore, new powered imperial correlations were built for a certain water cut for the completely sets of data for both oils (D80 &D130). The resultant correlations were fitted using the same regression software DataFit to build good correlations at a certain water cut for the mixture venturi pressure coefficient, Cpm, based on mixture Reynolds number, Rem, and venturi beta ratio, β. The new power empirical correlation can be expressed in the dimensionless form as follows:

$$Cp_m = a(Re_m)^b * (\beta)^c \quad (5.3)$$

Where,

Rem = Mixture Reynolds number

β = Venturi beta ratio

a, b and c = Regression Variables, their values listed in Table 5.6 for each individual water cut.

Table 5.6: The statistical analyses for oils (D80 and D130) correlation, (5.3).

Water Cut	Regression Variables (a, b &c)	Residual Sum of Squares (Absolute & Relative)	Standard Error of the Estimate	Coefficient of Multiple Determination (R^2)	Adjusted coefficient of multiple determination (Ra^2)
WC0%	a= 1.10797 b= -4.066765 c= -0.01706	24.3971	0.6542	0.9964	0.9963
WC20%	a= 0.79260 b= -4.13465 c= 0.00816	12.7777	0.4735	0.9981	0.997
WC40%	a= 0.62 b= -4.17601 c= 0.0271	14.9708	0.5125	0.9977	0.9976
WC60%	a= 0.61325 b= -4.18568 c=0.0 2621	11.6496	0.4521	0.9982	0.9981
WC80%	a= 0.66623 b= -4.16103 c= 0.02005	9.8304	0.4153	0.9985	0.9984
WC100%	a= 0.81171 b= -4.18144 c= 0.00171	19.2013	0.5804	0.9971	0.9970

The correlation was tested for each certain water cut ranged from 0% to 100% in step of 20%, using different statistical parameters such as, residual sum of squares (Absolute & Relative), standard error of the estimate, coefficient of multiple determination (R^2), and Adjusted coefficient of multiple determination (Ra^2). The proposed correlation showed a good agreement between the predicted Cp_m through it and the measured Cp_m obtained from Eq. 4.9, the graphical results of comparison between the predicted and measured of mixture venturi pressure coefficient, Cp_m, are presented in Figures 5.10a to 5.10f as follow for each water cut.

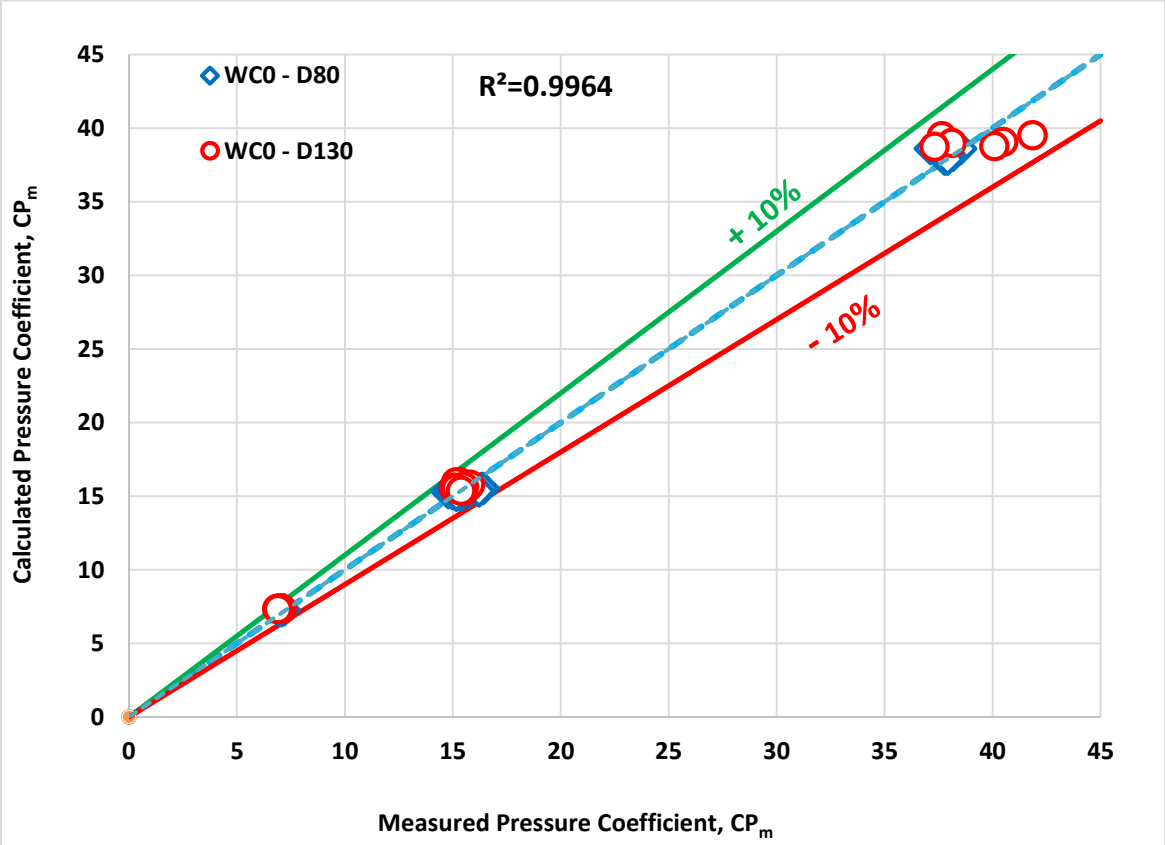

Figure 5.10a: Comparison between measured and calculated mixture venturi pressure coefficient for complete data sets of oils (D80 and D130) for WC0%.

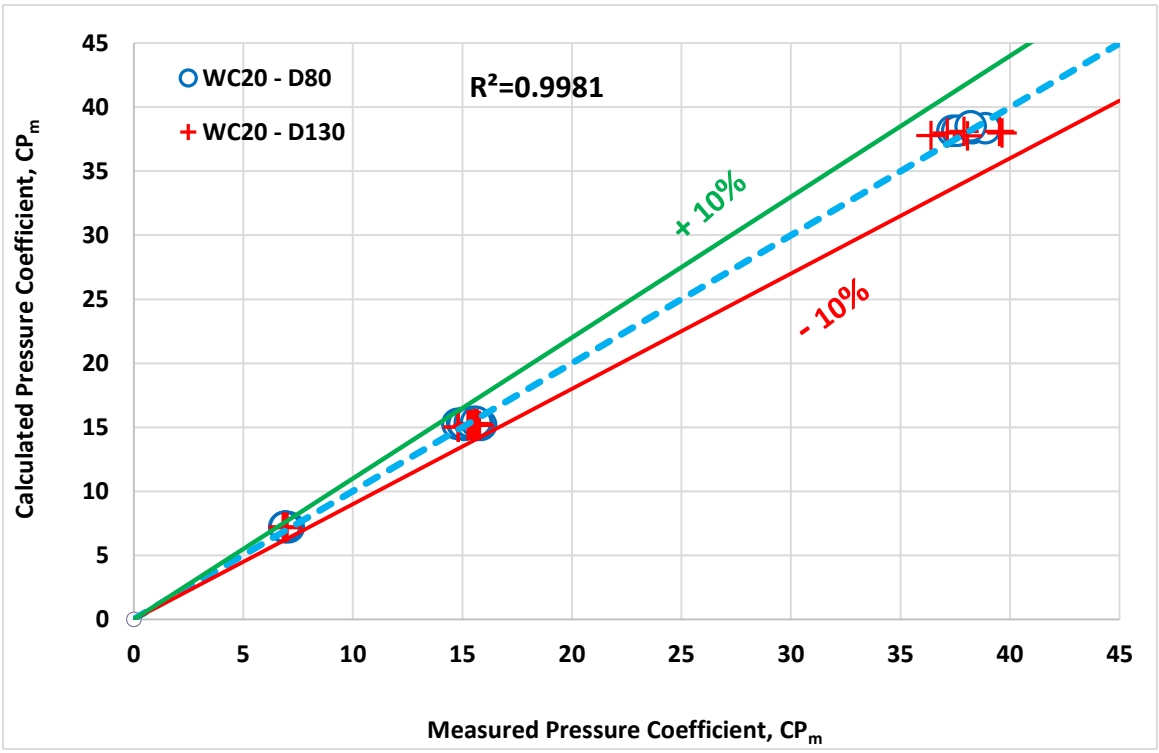

Figure 5.10b: Comparison between measured and calculated mixture venturi pressure coefficient for complete data sets of oils (D80 and D130) for WC20%.

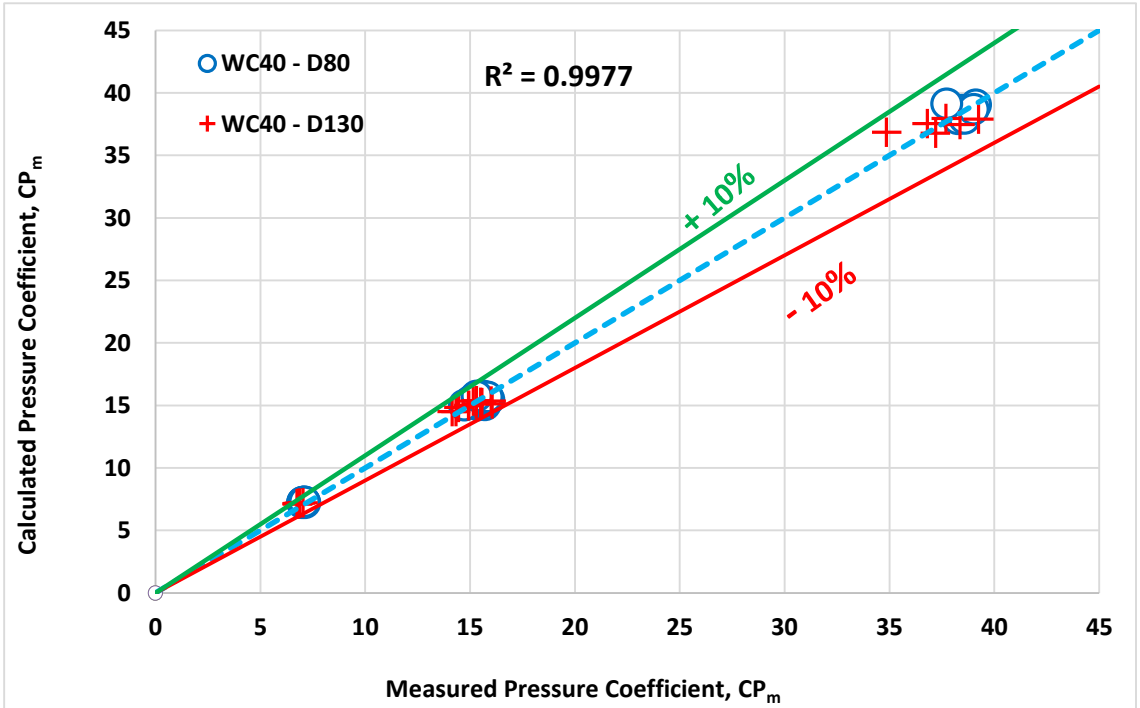

Figure 5.10c: Comparison between measured and calculated mixture venturi pressure coefficient for complete data sets of oils (D80 and D130) for WC40%.

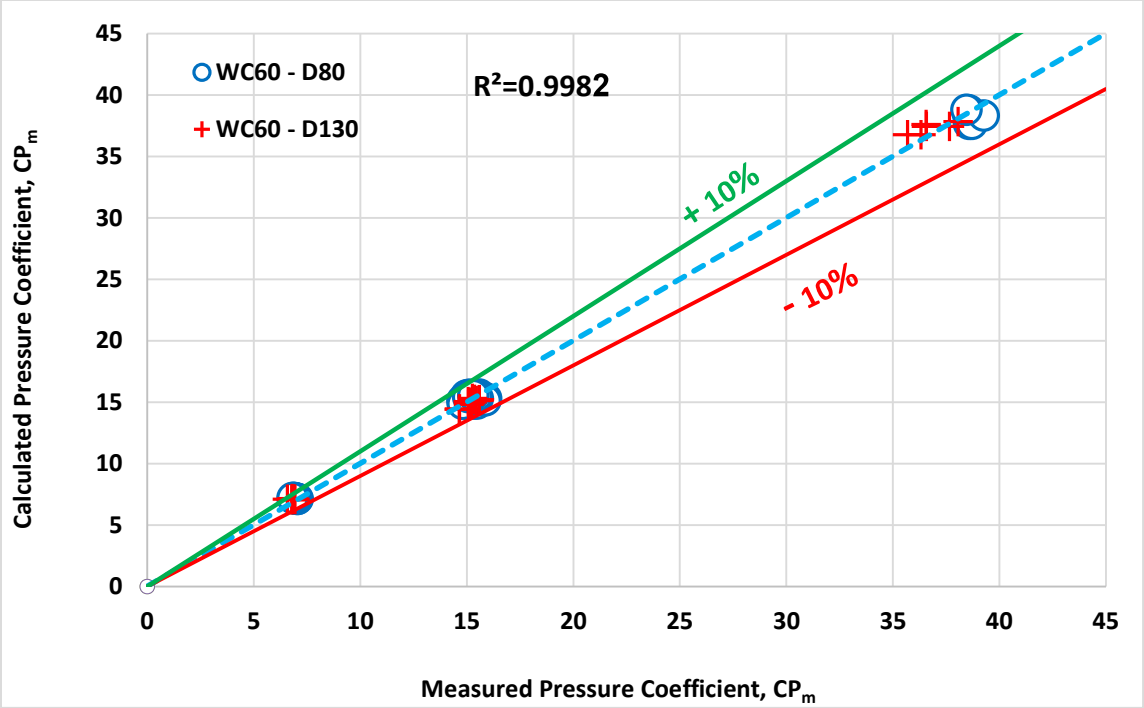

Figure 5.10d: Comparison between measured and calculated mixture venturi pressure coefficient for complete data sets of oils (D80 and D130) for WC60%.

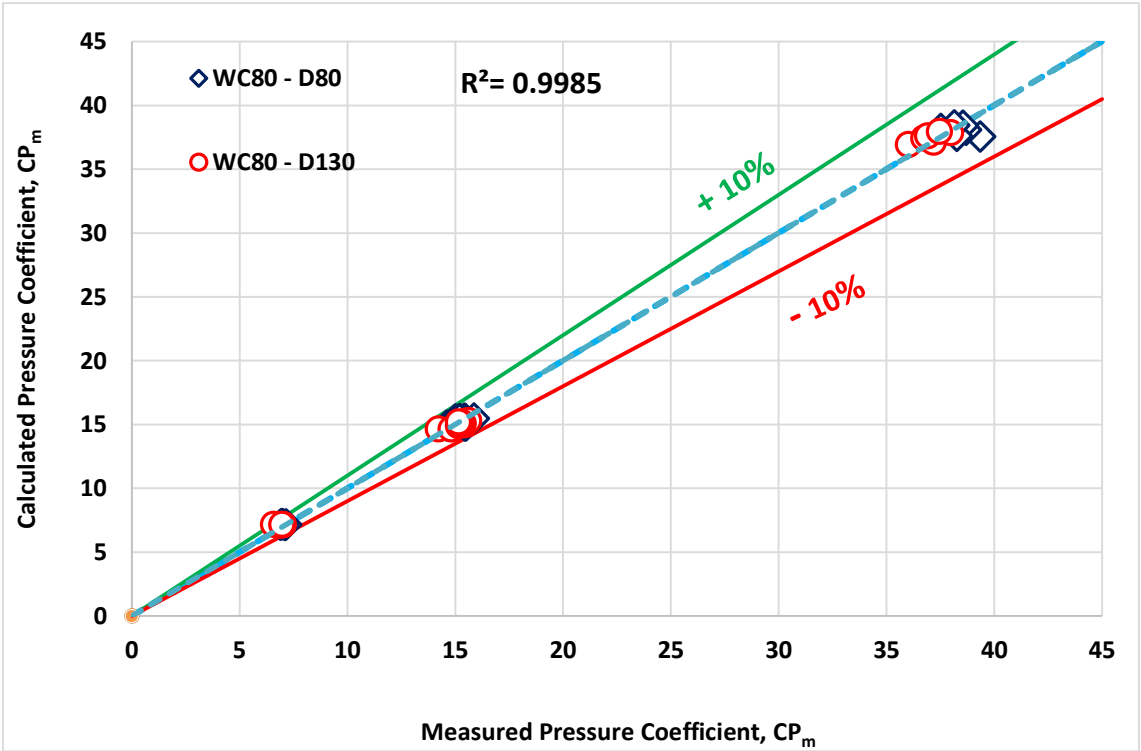

Figure 5.10 e: Comparison between measured and calculated mixture venturi pressure coefficient for complete data sets of oils (D80 and D130) for WC80%.

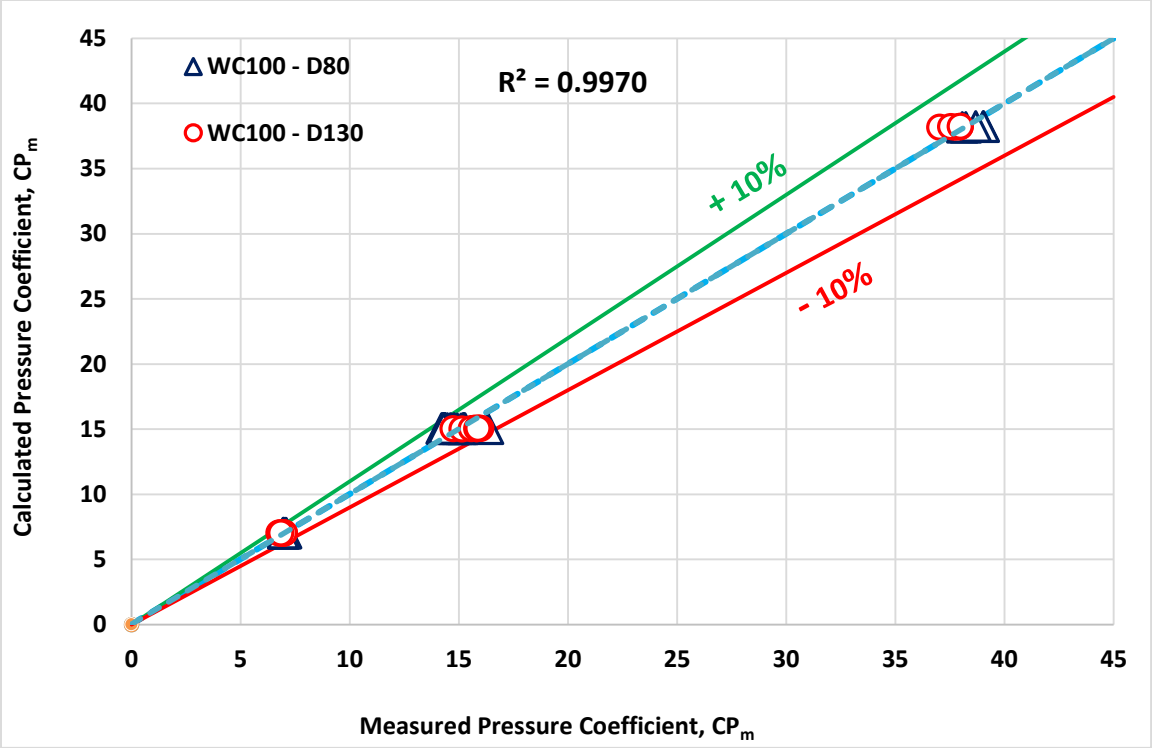

Figure 5.10 f: Comparison between measured and calculated mixture venturi pressure coefficient for complete data sets of oils (D80 and D130) for WC100%.

The statistical analysis presented earlier in Table 5.2a showed that the flow loop (θ) inclination and water cut (WC) parameters are not significantly like mixture Reynolds number (Rem) and venturi beta ratio (β) correlated to venturi pressure coefficient, Cp_m.

The empirical power correlation for the Cp_m, responses were plotted against the corresponding Cp_m obtained from Eq. 4.9.

Figures 5.10a to 5.10f show that the generated Cp_m using the empirical power correlation, match up very closely for all water cuts. The deviation between the Cp_m plots at the higher probabilities are largely negligible and it can be reasonably concluded that the exclusion of, venturi orientation and mixture water cut from the Cp_m correlation does not significantly affect the accuracy of the Correlation predictions. Also due the high turbulent of flow, the

mineral oil type (oil density and viscosity) does not affecting considerably on the predictions of venturi pressure coefficient, Cp_m.

In conclusion, from the score plots, predicted values of mixture venturi pressure coefficient, Cpm, seem to be closely correlated to Cp_m results as measured by the Eq. 4.9 based on the real measured experimental data for both oils (D80& D130) for the three venturi meters (β=0.4, 0.5 and 0.6), and good agreement was found when in the absence of inclination effect.

CHAPTER 6

CONCLUSIONS AND RECOMMENDATIONS

The multiphase flow loop was constructed at King Fahd University of Petroleum and Minerals (KFUPM) in Northern Compound to perform and to characterize experimentally different observations on the multiphase (two and three phases) flow in a large-scale loop for different inclination and flow conditions similar to that one in the real oil and gas field industries.

This chapter was divided into two main sections. Firstly, conclusions section, which presents the main conclusions of this experimental work reported in this thesis. Secondly, recommendations section, which presents the important recommendations and advisements, can be taken into under consideration for the future researches and activities for more improvement and perfection in the quality of research in this area.

6.1 Conclusios

The investigation of pressure drop measurements were studied in Tercom flanged machined venturi meters (β = 0.4, 0.5 and 0.6) for oil-water two-phase flow experiments in a 0.0762 m (3-inch) pipe. The experimental data was acquired using a large-scale, inclinable two-phase flow loop for different fluid mixture flow rates and water cuts. Potable water and two mineral oils (D80 & D130) were used for the single-phase and two-phase oil-water experiments for

the three venturi meters. The experiments were conducted for water cuts varying from 0% to 100% in steps of 20%, flow rates ranging from 2,000 bpd to 12,000 bpd, and for different inclinations of the flow loop, from horizontal to vertical positions.

The experimental results showed that the venturi pressure drop varied parabolically with fluid flow rate for a given water cut for the venturi meters studied. For given flow rate and water cut, the venturi pressure drop was inversely proportional to the venturi β. Subsequently, the venturi pressure drop varied linearly with the water cut for a given fluid flow rate confirming the existence of the homogenous flow pattern. The venturi pressure drop measurements were unaffected by the flow loop inclination for the three venturi meters and test fluid flow rates studied. Also the minor difference between the physical properties (e.g. oils densities and viscosities) of the two mineral oils (D80 &D130) which considered does not affecting on the venturi pressure drop measurements, that is because high flow turbulence.

A modified venturi discharge coefficient, k, which is a function of pressure losses and geometry, was determined separately for the three venturi meters from the oils-water flow experimental data. The average values of (3.73 m2.s/h, 5.93 m2.s/h and 8.75 m2.s/h) of k in oil D80 experiments and (3.75 m2.s/h, 5.90 m2.s/h and 8.78 m2.s/h) in case oil D130, for the three venturi meters of $\beta = 0.4$, 0.5 and 0.6, respectively, were obtained from the experimental results. The experimental and theoretical results of fluid flow rates were compared and were found to be in very good agreement.

The conventional Cd was obtained using the average k values of each of the three venturi meters. The results showed that the Cd values lie mainly in the range of 0.98 to 1.0 with the

exception of 0.96 and 1.03 for a single-phase of oil D80 and D130 experiments for venturi meter(β=0.5), respectively. This exceptional Cd value deviation could be due to the measurement uncertainty.

New empirical correlations were developed to calculate the mixture venturi pressure coefficient, Cp_m. The correlations showed high accuracy in predictions with coefficient of multiple determination (R-squared) ranged between 0.9964 and 0.9985. The developed correlations were further verified using the experimental data obtained from the three venturi meters (β = 0.4, 0.5 and 0.6) using the oils (D80 & D130).

The measured and predicted values of the mixture venturi pressure coefficient fluctuated around 38.00, 15.50 and 7.00 for all orientations of the loop for the venturi meters with β = 0.4, 0.5 and 0.6, respectively. The experimental results show that the venturi pressure drop and the venturi coefficients obtained for the three venturi meters were unaffected by the flow loop inclination for oil-water two phase flow conditions.

Error analysis for the pressure drop measurements for all water cuts and all fluid mixture flow rates was also performed. The results of the error analysis, which shows that the error band of the random uncertainty lies in the range of 0.007% to 0.498% for mineral oils D80 and D130 and for the three venturi meters, and are presented graphically. However, the systematic and expanded uncertainties are implemented accurately. The systematic uncertainty is ± 0.025% of Full Scale, and the expanded uncertainty lies in the range of 0.498% to 0.996%. The highest errors observed at the highest flow rate (12,000 bpd) case and associated with single phase experiments (WC0 & 100%), due to the limitations of the pumping system.

In conclusion, this study focuses on the variables affecting the performance of the venturi meter for oil-water flow under real oil well fluid flow conditions.

6.2 Recommendations

Based on the results presented in this experimental study is an important first step in simulations to that happen for oil wells in real field industries and to fill the existing gaps in two-phase flow in large-scale inclinable loops. The conclusion of this study and the measuring tools developed in this study are important for undertaking further research on pressure drop in venture meters. The following recommendations with respect to further research are made from the experiences gained through this experimental study to improve the quality of the measured data and to extend the scope of the research area:

1. In order to avoid the quick formation of oil-water emulsion, a new big separator tank can be mounted next to this old one. Otherwise two medium separators can be installed individually, one for the oil phase and the other for water phase.
2. The purging process is method of clearing the pressure transmitters from the emulsion droplets. However, this method have several disadvantages such as time consumption, and the risk of falling for the person conducting the experiments especially when performing the inclinable and vertical experiments. It recommend that, a new modern way can be followed by bringing any flexible tools to clean the pressure transmitters or safety tools can be offered like a hydraulic lift.
3. Modifying the multiphase flow loop and adding two more pumps of higher power type to reach high flow rates in the cases of single (oil/water) phase experiment. Then, all

experiments at WC0% and WC100% for high flow rates will be carry out. As a result of that, the probability of measurement errors can be minimized.

4. Because of the high flow rates, many parameters can be investigated in the turbulent regimes such as the performance of polymers in turbulent drag reduction and the performance of nanomaterials.
5. Useful models can be developed based on this rare clear set of data to predict many parameters in multiphase flow in large-scale inclinable pipes for mineral oils at different conditions.
6. As flow loop laboratory already enhanced with air compressor and tow air storage tanks with the controlled pressure capacity of 7.9 bar for each one. Therefore, the gas phase can be injected to the mixture of oil and water to study the behavior of three phases (oil, water and gas) flow in future researches.
7. Visualization techniques (e.g. high-speed camera, transparent pipes and tomographic measurements) can be applied to flow loop in order to characterize more observations (e.g. hold up and flow patterns …etc.).
8. In order to observe the mixture temperature accurately, extra temperature sensor should be mounted on the gravity-settling tank of oil-water mixture.

References

[1] Maksimovic, P. (2005), \multi-phase Flow modeling", Technical report, St John's Conference Center.

[2] C. M. Herschel, "'The Venturi Water Meter: An Instrument Making Use of a New Method of Gauging Water; Applicable to the Cases of Very Large Tubes, and of a Small Value Only, of the Liquid to be Gauged,'" *Am. Soc. Civ. Eng.*, vol. XVII, 1887.

[3] R. Pal, "Flow of oil-in-water emulsions through orifice and venturi meters," *Ind. Eng. Chem. Res.*, vol. 32, no. 6, pp. 1212–1217, 1993.

[4] Zhiyao Huang, Xia Li, Haifeng Ji, Baoliang Wang, and Haiqing Li, "Oil-water two-phase flow measurement based on a hybrid flowmeter and dominant phase identification," *Int. Instrum. Meas. Technol. Conf.*, vol. 2, no. May, pp. 711–714, 2009.

[5] X. Li, Z. Huang, Z. Meng, B. Wang, and H. Li, "Oil-Water Two-Phase Flow Measurement Using a Venturi Meter and an Oval Gear Flow Meter," *Chem. Eng. Commun.*, vol. 197, no. 2, pp. 223–231, 2009.

[6] H. Si, W. Peng, and G. Yuhui, "Theoretical and Experimental Study on Oil-water Two-phase Flow in a Downhole Venturi Meter," vol. 232, pp. 284–287, 2012.

[7] H. Z. Ding Feng, Yu Xie, Zuojie Liao, Jiawei Wang, Ao Xiao, "No Title," in *ICEICE '12 Proceedings of the 2012 Second International Conference on Electric Information and Control Engineering*, 2012, vol. 03, pp. 559–562.

[8] S. Brinkhorst, E. Von Lavante, G. Wendt, and H. Venturi-tube, "Numerical investigation of cavitating Herschel Venturi-Tubes applied to liquid fl ow metering," vol. 43, pp. 23–25, 2015.

[9] J. Han, F. Dong, W. Li, and Y. Xu, "<title>Mass flow-rate measurement of oil-water two-phase flow based on differential pressure and adaptive wavelet network</title>," no. NOVEMBER, pp. 712817–712817–6, 2008.

[10] C. L. Hollingshead, M. C. Johnson, S. L. Barfuss, and R. E. Spall, "Journal of Petroleum Science and Engineering Discharge coef fi cient performance of Venturi , standard concentric ori fi ce plate , V-cone and wedge fl ow meters at low Reynolds numbers," vol. 78, pp. 559–566, 2011.

[11] J. Zhang, J. Y. Xu, Y. X. Wu, D. H. Li, and H. Li, "Experimental validation of the calculation of phase holdup for an oil-water two-phase vertical flow based on the measurement of pressure drops," *Flow Meas. Instrum.*, vol. 31, pp. 96–101, 2013.

[12] T. Al-Wahaibi and F. S. Mjalli, "Prediction of Horizontal Oil-Water Flow Pressure

Gradient Using Artificial Intelligence Techniques," *Chem. Eng. Commun.*, vol. 201, no. 2, pp. 209–224, 2014.

[13] M. Hasanvand and S. M. Berneti, "Predicting Oil Flow Rate due to Multiphase Flow Meter by Using an Artificial Neural Network," *Energy Sources, Part A Recover. Util. Environ. Eff.*, vol. 37, no. 8, pp. 840–845, 2015.

[14] C. Tan, W. Dai, H. Yeung, and F. Dong, "A Kalman estimation based oil–water two-phase flow measurement with CRCC," *Int. J. Multiph. Flow*, vol. 72, pp. 306–317, 2015.

[15] F. S. Silvao, P. Andreussi, and P. Di Marco, "TOTAL MASS FLOWRATE MEASUREMENT IN MULTIPHASE FLOW BY MEANS OF A VENTURI METER," pp. 145–155, 1991.

[16] H. Peixiang and C. Alimonti, "A NEW METHOD OF MEASURING TWO-PHASE MASS FLOW RATES IN A VENTURI," 2007.

[17] E. E. Paladino and C. R. Maliska, "Paper CIT02-0070 MULTI-PHASE FLOW MODELLING IN DIFFERENTIAL PRESSURE FLOW METERS," 1999.

[18] J. K. D. H. J.R. Fincke, C. Ronnenkamp, D. Kruse, "4th International Symposium on Fluid Flow Measurement, Denver," p. 1999, 1999.

[19] R. N. Steven, "Wet gas metering with a horizontally mounted Venturi meter," *Flow Meas. Instrum.*, vol. 12, no. 5–6, pp. 361–372, 2002.

[20] R. de Leeuw, "R. de Leeuw, ' Liquid correction of Venturi meter readings in wet gas flow, ' in: North Sea Flow Measurement Workshop, Norway, Shell Expro, The Netherlands, 1997.," 1997, p. 1997.

[21] M. J. R.-H. and B. C. M. A.R. W. Hall, ",A study of the performance of Venturi meters in multiphase flows, in," *Second North Am. Conf. Multiph. Technol.*, 2000.

[22] Z. Huang, D. Xie, H. Zhang, and H. Li, "Gas–oil two-phase flow measurement using an electrical capacitance tomography system and a Venturi meter," *Flow Meas. Instrum.*, vol. 16, pp. 177–182, 2005.

[23] H. Zhang, W. Yue, and Z. Huang, "Investigation of oil-air two-phase mass flow rate measurement using Venturi and void fraction sensor," *J. Zhejiang Univ. Sci.*, vol. 6A, no. 6, pp. 601–606, 2005.

[24] D. L. Gysling and C. Corporation, "Wet Gas Metering Using Combination of Differential Pressure and SONAR Flow Meters," *24th Int. North Sea Flow Meas. Work.*, no. October, pp. 1–20, 2006.

[25] A. Kumar, G. Das, and P. Kumar, "International Journal of Multiphase Flow The hydrodynamics of liquid – liquid upflow through a venturimeter," *Int. J. Multiph. Flow*, vol. 34, no. 12, pp. 1119–1129, 2008.

[26] F. Lide, Z. Tao, and X. Ying, “Venturi Wet Gas Flow Modeling Based on Homogeneous and Separated Flow Theory,” vol. 2008, 2008.

[27] F. L. and Z. Tao, “Performance of a Horizontally Mounted Venturi in Low pressure Wet Gas Flow,” *Chinese J. Chem. Eng.*, vol. 16, no. 2, pp. 320–324, 2008.

[28] Z. Meng, Z. Huang, B. Wang, H. Ji, H. Li, and Y. Yan, “Air-water two-phase flow measurement using a Venturi meter and an electrical resistance tomography sensor,” *Flow Meas. Instrum.*, vol. 21, no. 3, pp. 268–276, 2010.

[29] H. Seraj, M. Khaled, R. Yusof, and M. F. Rahmat, “Review of wet gas flow measurement using venturi tubes and radio active materials,” *Int. J. Smart Sens. Intell. Syst.*, vol. 3, no. 4, pp. 672–689, 2010.

[30] A.-W. Y. Abbas H. A. M. Hasan1, A. Hadawey1 and and K. F. A.-R. Waleed Abdul-Karem1, “Theoretical and Experimental Study of Bubbly Gas- water Two Phase Flows through a Universal Venturi Tube (UVT),” vol. 2, no. 1, pp. 43–58, 2012.

[31] P. Gajan, G. Salque, J. P. Couput, and J. Berthiaud, “Experimental analysis of the behaviour of a Venturi meter submitted to an upstream air/oil annular liquid film,” *Flow Meas. Instrum.*, vol. 33, pp. 160–167, 2013.

[32] G. Monni, M. De Salve, and B. Panella, “Two-phase flow measurements at high void fraction by a Venturi meter,” *Prog. Nucl. Energy*, vol. 77, pp. 167–175, 2014.

[33] D. He and B. Bai, “A new correlation for wet gas flow rate measurement with Venturi meter based on two-phase mass flow coefficient,” *Measurement*, vol. 58, pp. 61–67, 2014.

[34] W. Wang, X. Liang, and M. Zhang, “Measurment of gas-liquid two-phase slug flow with a Venturi meter based on blind source separation,” *Chinese J. Chem. Eng.*, vol. 23, no. 9, pp. 1447–1452, 2015.

[35] P. Gajan, Q. Decaudin, and J. P. Couput, “Analysis of high pressure tests on wet gas flow metering with a Venturi meter,” *Flow Meas. Instrum.*, vol. 44, pp. 126–131, 2015.

[36] Odozi UA, “Three -phase gas-liquid-liquid slug flow [Ph.D. thesis],” *UK Univ. London*, vol. 0, no. 0, 2000.

[37] D. Bertoldi, C. C. S. Dallalba, and J. R. Barbosa, “Experimental investigation of two-phase flashing flows of a binary mixf infinite relative volatility in a Venturi tube,” *Exp. Therm. Fluid Sci.*, vol. 64, pp. 152–163, 2015.

[38] C. Yuan, Y. Xu, T. Zhang, J. Li, and H. Wang, “Experimental investigation of wet gas over reading in Venturi,” *Exp. Therm. Fluid Sci.*, vol. 66, pp. 63–71, 2015.

[39] “ExxonMobil Company, 2014. Typical Values of Dearomatized Fluid from www.exxonmobilchemical.com”. Visited website in May 2014

[40] “DataFit Software, 2016. from http://www.oakdaleengr.com”. Visited website in October 2016.

[41] Morgan, M.G., and M. Henrion. 1990. Uncertainty: A Guide to Dealing with Uncertainty in Quantitative Risk and Policy Analysis, Cambridge University Press. 332 pp.

[42] Isukapalli, S. S. 1999. Uncertainty Analysis of Transport-Transformation Models. Ph.D. Thesis, The State University of New Jersey.

[43] Yen, B. C. 2002. System and Component Uncertainties in Water Resources.In Risk, Reliability, Uncertainty and Robustness o f Water Resources Systems (Bogardi, Janos J.,Kundzewicz, Zbigniew W., eds), Cambridge University Press, Cambridge, pp. 133-142.

[44] U.S. EPA. 2003. Multimedia, Multipathway, and Multireceptor Risk Assessment

(3MRA) Modeling System. Volume IV: Evaluating Uncertainty and Sensitivity. EPA 530-D-03-001d. July 2003.

[45] U.S. EPA. 1996. Summary report for the Workshop on Monte Carlo Analysis, Superfund Today, September. EPA 630-R-96-010, 1-1.

[46] “Ronald H. Dieck. ‘Measurement Accuracy.’ Copyright 2000 CRC Press LLC. <http://www.engnetbase.com>.,” 2000.

[47] Measurements of kinematic viscosity for Exxsol D80 and Exxsol D130 oils were done on May 2014 and July 2015, Respectivelly at “Research Institute (RI) in King Fahd University of Petroleum and Minerals (KFUPM)”.

APPENDICES

APPENDIX A
UNCERTAINTY ANALYSIS

1. Uncertainty Analysis for Oil D80 Data

Table 1: Uncertainty Analysis Results of Oil D80 Experiments for Venturi (β = 0.4) and Flow Loop Inclination (0º).

Water Cut, %	Flow Rate, bpd	Number of Samples	Standard Error, inch H_2O	Random Uncertainty (U_r), %	Systematic Uncertainty (U_s), %	Expanded Uncertainty (U_e), %
0	2000	46	0.181	0.459	± 0.025% of Full Scale	0.919
	4000	23	0.097	0.060		0.123
	6000	143	0.109	0.031		0.066
20	2000	11	0.038	0.088	± 0.025% of Full Scale	0.178
	4000	21	0.133	0.079		0.160
	6000	26	0.187	0.049		0.101
40	2000	132	0.025	0.055	± 0.025% of Full Scale	0.112
	4000	26	0.067	0.039		0.081
	6000	50	0.163	0.040		0.084
60	2000	164	0.020	0.043	± 0.025% of Full Scale	0.090
	4000	72	0.093	0.051		0.104
	6000	22	0.175	0.041		0.086
80	2000	39	0.034	0.067	± 0.025% of Full Scale	0.136
	4000	46	0.098	0.052		0.107
	6000	57	0.207	0.046		0.096
100	2000	52	0.022	0.044	± 0.025% of Full Scale	0.092
	4000	84	0.066	0.032		0.069
	6000	119	0.101	0.022		0.050

Table 2: Uncertainty Analysis Results of Oil D80 Experiments for Venturi (β = 0.4) and Flow Loop Inclination (90º).

Water Cut, %	Flow Rate, bpd	Number of Samples	Standard Error, inch H_2O	Random Uncertainty (U_r), %	Systematic Uncertainty (U_s), %	Expanded Uncertainty (U_e), %
0	2000	125	0.139	0.353	± 0.025% of Full Scale	0.707
	4000	117	0.196	0.126		0.252
	6000	52	0.208	0.059		0.120
20	2000	110	0.019	0.045	± 0.025% of Full Scale	0.093
	4000	54	0.074	0.043		0.090
	6000	11	0.333	0.088		0.178
40	2000	52	0.034	0.078	± 0.025% of Full Scale	0.159
	4000	40	0.052	0.028		0.062
	6000	10	0.570	0.144		0.289
60	2000	43	0.044	0.094	± 0.025% of Full Scale	0.190
	4000	61	0.090	0.049		0.101
	6000	34	0.192	0.046		0.095
80	2000	12	0.145	0.292	± 0.025% of Full Scale	0.585
	4000	14	0.184	0.093		0.188
	6000	5	0.589	0.137		0.274
100	2000	29	0.048	0.093	± 0.025% of Full Scale	0.187
	4000	62	0.091	0.045		0.093
	6000	50	0.187	0.040		0.084

Table 3: Uncertainty Analysis Results of Oil D80 Experiments for Venturi (β = 0.5) and Flow Loop Inclination (0º).

Water Cut, %	Flow Rate, bpd	Number of Samples	Standard Error, inch H_2O	Random Uncertainty (U_r), %	Systematic Uncertainty (U_s), %	Expanded Uncertainty (U_e), %
0	2000	32	0.023	0.136	± 0.025% of Full Scale	0.273
	4000	39	0.026	0.043		0.090
	6000	22	0.063	0.046		0.095
	8000	35	0.070	0.029		0.062
	10000	33	0.406	0.103		0.208
	12000	34	1.549	0.337		0.424
20	2000	25	0.012	0.070	± 0.025% of Full Scale	0.143
	4000	30	0.110	0.165		0.331
	6000	39	0.074	0.050		0.102
	8000	40	0.169	0.066		0.134
	10000	25	0.175	0.043		0.089
	12000	30	0.219	0.037		0.079
40	2000	41	0.022	0.116	± 0.025% of Full Scale	0.233
	4000	53	0.029	0.042		0.087
	6000	29	0.211	0.131		0.263
	8000	72	0.204	0.071		0.144
	10000	23	0.161	0.036		0.076
	12000	21	0.277	0.044		0.091

Cont-Table 3: Uncertainty Analysis Results of Oil D80 Experiments for Venturi ($\beta = 0.5$) and Flow Loop Inclination (0^o).

Water Cut, %	**Flow Rate, bpd**	**Number of Samples**	**Standard Error, inch H_2O**	**Random Uncertainty (U_r), %**	**Systematic Uncertainty (U_s), %**	**Expanded Uncertainty (U_s), %**
60	2000	51	0.018	0.100	± 0.025% of Full Scale	0.201
	4000	28	0.061	0.085		0.173
	6000	21	0.090	0.053		0.109
	8000	14	0.295	0.100		0.201
	10000	12	0.910	0.195		0.391
	12000	14	0.409	0.062		0.126
80	2000	43	0.018	0.094	± 0.025% of Full Scale	0.190
	4000	21	0.143	0.189		0.380
	6000	22	0.147	0.086		0.173
	8000	17	0.173	0.059		0.120
	10000	11	0.473	0.101		0.203
	12000	10	1.019	0.149		0.298
100	2000	45	0.018	0.084	± 0.025% of Full Scale	0.170
	4000	17	0.130	0.162		0.325
	6000	22	0.136	0.075		0.153
	8000	12	0.145	0.045		0.094
	10000	24	0.169	0.034		0.072
	12000	21	0.141	0.024		0.053

Table 4: Uncertainty Analysis Results of Oil D80 Experiments for Venturi (β = 0.5) and Flow Loop Inclination (40º).

Water Cut, %	Flow Rate, bpd	Number of Samples	Standard Error, inch H_2O	Random Uncertainty (U_r), %	Systematic Uncertainty (U_s), %	Expanded Uncertainty (U_e), %
0	2000	16	0.015	0.094	± 0.025% of Full Scale	0.189
	4000	23	0.058	0.094		0.190
	6000	18	0.076	0.055		0.113
	8000	18	0.124	0.051		0.105
	10000	14	0.281	0.072		0.146
	12000	10	3.43	0.498		0.996
20	2000	16	0.043	0.222	± 0.025% of Full Scale	0.446
	4000	17	0.064	0.094		0.189
	6000	21	0.104	0.069		0.140
	8000	34	0.078	0.030		0.065
	10000	13	0.314	0.076		0.154
	12000	15	0.293	0.049		0.101
40	2000	23	0.038	0.206	± 0.025% of Full Scale	0.413
	4000	32	0.037	0.052		0.107
	6000	26	0.067	0.041		0.086
	8000	20	0.144	0.051		0.105
	10000	11	0.212	0.047		0.098
	12000	8	0.288	0.044		0.091

Cont-Table 4: Uncertainty Analysis Results of Oil D80 Experiments for Venturi (β = 0.5) and Flow Loop Inclination (40º).

Water Cut, %	Flow Rate, bpd	Number of Samples	Standard Error, inch H_2O	Random Uncertainty (U_r), %	Systematic Uncertainty (U_s), %	Expanded Uncertainty (U_e), %
60	2000	22	0.031	0.154	± 0.025% of Full Scale	0.308
	4000	24	0.043	0.058		0.119
	6000	10	0.068	0.042		0.088
	8000	10	0.175	0.060		0.122
	10000	13	0.301	0.069		0.141
	12000	10	0.688	0.102		0.205
80	2000	28	0.033	0.159	± 0.025% of Full Scale	0.319
	4000	26	0.080	0.102		0.206
	6000	16	0.126	0.074		0.150
	8000	8	0.110	0.036		0.076
	10000	7	0.325	0.069		0.139
	12000	5	0.412	0.057		0.117
100	2000	17	0.019	0.099	± 0.025% of Full Scale	0.199
	4000	30	0.058	0.076		0.154
	6000	22	0.069	0.040		0.083
	8000	22	0.087	0.029		0.062
	10000	46	0.102	0.022		0.050
	12000	8	2.530	0.348		0.718

Table 5: Uncertainty Analysis Results of Oil D80 Experiments for Venturi (β = 0.5) and Flow Loop Inclination (60º).

Water Cut, %	Flow Rate, bpd	Number of Samples	Standard Error, inch H_2O	Random Uncertainty (U_r), %	Systematic Uncertainty (U_s), %	Expanded Uncertainty (U_e), %
0	2000	15	0.025	0.148	± 0.025% of Full Scale	0.298
	4000	17	0.043	0.067		0.135
	6000	11	0.142	0.099		0.201
	8000	15	0.171	0.068		0.139
	10000	16	0.247	0.064		0.130
	12000	16	0.676	0.325		0.702
20	2000	27	0.020	0.118	± 0.025% of Full Scale	0.238
	4000	31	0.088	0.132		0.266
	6000	14	0.079	0.053		0.109
	8000	28	0.098	0.037		0.077
	10000	19	0.139	0.033		0.070
	12000	9	0.188	0.031		0.067
40	2000	71	0.045	0.233	± 0.025% of Full Scale	0.467
	4000	27	0.058	0.082		0.165
	6000	21	0.150	0.091		0.184
	8000	24	0.145	0.048		0.100
	10000	18	0.188	0.042		0.087
	12000	15	0.333	0.052		0.108

Cont-Table 5: Uncertainty Analysis Results of Oil D80 Experiments for Venturi (β = 0.5) and Flow Loop Inclination (60º).

Water Cut, %	Flow Rate, bpd	Number of Samples	Standard Error, inch H_2O	Random Uncertainty (U_r), %	Systematic Uncertainty (U_s), %	Expanded Uncertainty (U_e), %
60	2000	22	0.037	0.182	± 0.025% of Full Scale	0.366
	4000	22	0.063	0.081		0.163
	6000	25	0.067	0.039		0.081
	8000	14	0.083	0.028		0.062
	10000	12	0.254	0.055		0.112
	12000	9	0.291	0.046		0.094
80	2000	25	0.021	0.105	± 0.025% of Full Scale	0.211
	4000	18	0.051	0.066		0.134
	6000	7	0.104	0.059		0.121
	8000	9	0.186	0.059		0.121
	10000	12	0.245	0.051		0.106
	12000	8	0.478	0.067		0.136
100	2000	24	0.013	0.059	± 0.025% of Full Scale	0.122
	4000	19	0.053	0.065		0.132
	6000	17	0.103	0.058		0.119
	8000	26	0.090	0.029		0.063
	10000	32	0.195	0.041		0.085
	12000	45	1.719	0.241		0.489

Table 6: Uncertainty Analysis Results of Oil D80 Experiments for Venturi (β = 0.5) and Flow Loop Inclination (90º).

Water Cut, %	Flow Rate, bpd	Number of Samples	Standard Error, inch H_2O	Random Uncertainty (U_r), %	Systematic Uncertainty (U_s), %	Expanded Uncertainty (U_e), %
0	2000	19	0.016	0.094	± 0.025% of Full Scale	0.190
	4000	22	0.036	0.053		0.109
	6000	15	0.060	0.042		0.087
	8000	12	0.0869	0.035		0.074
	10000	11	0.264	0.068		0.138
	12000	19	1.720	0.287		0.623
20	2000	19	0.043	0.242	± 0.025% of Full Scale	0.485
	4000	26	0.045	0.066		0.134
	6000	18	0.076	0.051		0.106
	8000	7	0.094	0.035		0.074
	10000	9	0.237	0.057		0.117
	12000	10	0.176	0.029		0.063
40	2000	40	0.031	0.170	± 0.025% of Full Scale	0.340
	4000	20	0.044	0.062		0.126
	6000	18	0.114	0.070		0.143
	8000	13	0.113	0.039		0.082
	10000	7	0.297	0.066		0.135
	12000	9	0.129	0.020		0.048

Cont-Table 6: Uncertainty Analysis Results of Oil D80 Experiments for Venturi ($\beta = 0.5$) and Flow Loop Inclination (90^o).

Water Cut, %	**Flow Rate, bpd**	**Number of Samples**	**Standard Error, inch H_2O**	**Random Uncertainty (U_r), %**	**Systematic Uncertainty (U_s), %**	**Expanded Uncertainty (U_e), %**
60	2000	37	0.030	0.151	± 0.025% of Full Scale	0.304
	4000	18	0.072	0.092		0.186
	6000	16	0.140	0.084		0.170
	8000	8	0.176	0.061		0.125
	10000	7	0.281	0.060		0.123
	12000	13	0.383	0.058		0.120
80	2000	25	0.045	0.228	± 0.025% of Full Scale	0.457
	4000	15	0.070	0.086		0.174
	6000	12	0.078	0.044		0.092
	8000	9	0.145	0.047		0.097
	10000	9	0.412	0.086		0.173
	12000	7	0.197	0.029		0.063
100	2000	9	0.018	0.087	± 0.025% of Full Scale	0.175
	4000	31	0.040	0.053		0.108
	6000	30	0.067	0.039		0.082
	8000	25	0.094	0.031		0.067
	10000	16	0.138	0.029		0.064
	12000	12	1.026	0.151		0.227

Table 7: Uncertainty Analysis Results of Oil D80 Experiments for Venturi (β = 0.6) and Flow Loop Inclination (0º).

Water Cut, %	Flow Rate, bpd	Number of Samples	Standard Error, inch H_2O	Random Uncertainty (U_r), %	Systematic Uncertainty (U_s), %	Expanded Uncertainty (U_e), %
0	6000	35	0.017	0.026	± 0.025% of Full Scale	0.058
	8000	63	0.042	0.037		0.078
	9000	44	0.388	0.269		0.538
20	6000	75	0.018	0.027	± 0.025% of Full Scale	0.060
	8000	73	0.027	0.022		0.051
	9000	32	0.077	0.050		0.104
40	6000	35	0.022	0.030	± 0.025% of Full Scale	0.066
	8000	52	0.027	0.022		0.050
	9000	54	0.035	0.021		0.050
60	6000	57	0.014	0.017	± 0.025% of Full Scale	0.043
	8000	25	0.046	0.035		0.073
	9000	25	0.047	0.028		0.062
80	6000	53	0.020	0.025	± 0.025% of Full Scale	0.055
	8000	27	0.041	0.029		0.064
	9000	31	0.047	0.027		0.059
100	6000	66	0.019	0.023	± 0.025% of Full Scale	0.052
	8000	12	0.095	0.065		0.132
	9000	5	0.144	0.077		0.155

Table 8: Uncertainty Analysis Results of Oil D80 Experiments for Venturi (β = 0.6) and Flow Loop Inclination (90º).

Water Cut, %	Flow Rate, bpd	Number of Samples	Standard Error, inch H_2O	Random Uncertainty (U_r), %	Systematic Uncertainty (U_s), %	Expanded Uncertainty (U_e), %
0	6000	78	0.020	0.030	± 0.025% of Full Scale	0.064
	8000	43	0.051	0.043		0.090
	9000	64	0.154	0.107		0.216
20	6000	61	0.019	0.028	± 0.025% of Full Scale	0.060
	8000	66	0.024	0.020		0.047
	9000	26	0.118	0.077		0.156
40	6000	30	0.027	0.036	± 0.025% of Full Scale	0.077
	8000	58	0.027	0.021		0.049
	9000	54	0.047	0.028		0.062
60	6000	45	0.020	0.026	± 0.025% of Full Scale	0.057
	8000	33	0.035	0.027		0.059
	9000	12	0.096	0.057		0.117
80	6000	73	0.017	0.021	± 0.025% of Full Scale	0.049
	8000	25	0.050	0.036		0.076
	9000	35	0.037	0.021		0.048
100	6000	73	0.019	0.023	± 0.025% of Full Scale	0.052
	8000	36	0.061	0.041		0.086
	9000	19	0.124	0.067		0.135

2. Uncertainty Analysis for Oil D130 Data

Table 9: Uncertainty Analysis Results of Oil D130 Experiments for Venturi (β = 0.4) and Flow Loop Inclination (0º).

Water Cut, %	Flow Rate, bpd	Number of Samples	Standard Error, inch H_2O	Random Uncertainty (Ur), %	Systematic Uncertainty (U_s), %	Expanded Uncertainty (U_e), %
0	2000	38	0.017	0.040	± 0.025% of Full Scale	0.083
	4000	32	0.044	0.026		0.058
	6000	21	0.132	0.036		0.075
20	2000	57	0.026	0.062	± 0.025% of Full Scale	0.127
	4000	56	0.043	0.025		0.056
	6000	37	0.134	0.034		0.073
40	2000	54	0.029	0.068	± 0.025% of Full Scale	0.139
	4000	18	0.053	0.030		0.065
	6000	39	0.119	0.029		0.063
60	2000	30	0.025	0.056	± 0.025% of Full Scale	0.114
	4000	25	0.080	0.044		0.091
	6000	40	0.162	0.040		0.083
80	2000	75	0.029	0.063	± 0.025% of Full Scale	0.128
	4000	26	0.106	0.057		0.116
	6000	40	0.257	0.059		0.120
100	2000	51	0.018	0.035	± 0.025% of Full Scale	0.075
	4000	33	0.072	0.036		0.076
	6000	19	0.183	0.040		0.084

Table 10: Uncertainty Analysis Results of Oil D130 Experiments for Venturi (β = 0.4) and Flow Loop Inclination (90º).

Water Cut, %	Flow Rate, bpd	Number of Samples	Standard Error, inch H_2O	Random Uncertainty (U_r), %	Systematic Uncertainty (U_s), %	Expanded Uncertainty (U_e), %
0	2000	36	0.032	0.072	± 0.025% of Full Scale	0.146
	4000	55	0.051	0.031		0.067
	6000	34	0.133	0.035		0.074
20	2000	54	0.019	0.044	± 0.025% of Full Scale	0.092
	4000	41	0.075	0.042		0.088
	6000	35	0.153	0.039		0.083
40	2000	55	0.019	0.044	± 0.025% of Full Scale	0.091
	4000	43	0.057	0.032		0.069
	6000	48	0.098	0.024		0.054
60	2000	59	0.018	0.041	± 0.025% of Full Scale	0.087
	4000	25	0.081	0.043		0.090
	6000	27	0.227	0.055		0.113
80	2000	51	0.030	0.063	± 0.025% of Full Scale	0.128
	4000	41	0.116	0.062		0.127
	6000	72	0.176	0.042		0.087
100	2000	112	0.020	0.041	± 0.025% of Full Scale	0.086
	4000	56	0.082	0.041		0.086
	6000	97	0.101	0.022		0.051

Table 11: Uncertainty Analysis Results of Oil D130 Experiments for Venturi (β = 0.5) and Flow Loop Inclination (0º).

Water Cut, %	Flow Rate, bpd	Number of Samples	Standard Error, inch H_2O	Random Uncertainty (U_r), %	Systematic Uncertainty (U_s), %	Expanded Uncertainty (U_e), %
0	2000	21	0.018	0.109	± 0.025% of Full Scale	0.220
	4000	36	0.017	0.024		0.055
	6000	57	0.030	0.020		0.048
	8000	30	0.057	0.021		0.050
	10000	34	0.102	0.025		0.055
	12000	16	1.660	0.271		0.678
20	2000	30	0.018	0.103	± 0.025% of Full Scale	0.208
	4000	32	0.031	0.044		0.092
	6000	33	0.030	0.019		0.045
	8000	105	0.031	0.011		0.033
	10000	65	0.066	0.015		0.039
	12000	35	0.098	0.016		0.040
40	2000	62	0.015	0.086	± 0.025% of Full Scale	0.174
	4000	76	0.020	0.028		0.061
	6000	56	0.026	0.015		0.039
	8000	36	0.108	0.037		0.078
	10000	11	0.090	0.020		0.048
	12000	33	0.132	0.020		0.047

Cont-Table 11: Uncertainty Analysis Results of Oil D130 Experiments for Venturi ($\beta = 0.5$) and Flow Loop Inclination (0^o).

Water Cut, %	Flow Rate, bpd	Number of Samples	Standard Error, inch H_2O	Random Uncertainty (U_r), %	Systematic Uncertainty (U_s), %	Expanded Uncertainty (U_e), %
60	2000	41	0.011	0.064	± 0.025% of Full Scale	0.129
	4000	39	0.023	0.031		0.066
	6000	43	0.044	0.027		0.059
	8000	52	0.056	0.019		0.045
	10000	29	0.183	0.040		0.084
	12000	7	0.504	0.075		0.151
80	2000	21	0.015	0.086	± 0.025% of Full Scale	0.174
	4000	72	0.025	0.032		0.069
	6000	37	0.115	0.065		0.133
	8000	36	0.088	0.029		0.063
	10000	53	0.107	0.022		0.051
	12000	14	0.548	0.078		0.157
100	2000	40	0.026	0.132	± 0.025% of Full Scale	0.265
	4000	59	0.023	0.027		0.060
	6000	72	0.032	0.017		0.042
	8000	46	0.061	0.019		0.045
	10000	54	0.069	0.013		0.037
	12000	16	1.237	0.176		0.194

Table 12: Uncertainty Analysis Results of Oil D130 Experiments for Venturi (β = 0.5) and Flow Loop Inclination (90º).

Water Cut, %	Flow Rate, bpd	Number of Samples	Standard Error, inch H_2O	Random Uncertainty (U_r), %	Systematic Uncertainty (U_s), %	Expanded Uncertainty (U_e), %
0	2000	24	0.032	0.196	± 0.025% of Full Scale	0.393
	4000	27	0.031	0.045		0.093
	6000	62	0.022	0.014		0.038
	8000	20	0.094	0.035		0.075
	10000	13	0.156	0.037		0.079
	12000	12	1.283	0.206		0.468
20	2000	111	0.021	0.121	± 0.025% of Full Scale	0.243
	4000	92	0.017	0.022		0.051
	6000	31	0.039	0.025		0.055
	8000	56	0.037	0.013		0.036
	10000	54	0.060	0.014		0.037
	12000	44	0.137	0.022		0.050
40	2000	149	0.017	0.099	± 0.025% of Full Scale	0.200
	4000	64	0.032	0.046		0.096
	6000	71	0.052	0.032		0.068
	8000	54	0.056	0.019		0.045
	10000	71	0.049	0.011		0.033
	12000	43	0.202	0.029		0.064

Cont-Table 12: Uncertainty Analysis Results of Oil D130 Experiments for Venturi ($\beta = 0.5$) and Flow Loop Inclination (90º).

Water Cut, %	**Flow Rate, bpd**	**Number of Samples**	**Standard Error, inch H_2O**	**Random Uncertainty (U_r), %**	**Systematic Uncertainty (U_s), %**	**Expanded Uncertainty (U_e), %**
60	2000	116	0.018	0.101	± 0.025% of Full Scale	0.203
	4000	117	0.024	0.032		0.070
	6000	119	0.047	0.028		0.062
	8000	55	0.071	0.024		0.054
	10000	36	0.075	0.016		0.041
	12000	31	0.164	0.023		0.052
80	2000	127	0.017	0.085	± 0.025% of Full Scale	0.172
	4000	29	0.036	0.047		0.097
	6000	60	0.037	0.021		0.049
	8000	16	0.132	0.043		0.089
	10000	21	0.109	0.022		0.051
	12000	10	0.309	0.043		0.090
100	2000	43	0.030	0.155	± 0.025% of Full Scale	0.310
	4000	23	0.031	0.038		0.079
	6000	52	0.040	0.021		0.050
	8000	24	0.081	0.024		0.054
	10000	30	0.108	0.021		0.048
	12000	11	0.266	0.120		0.251

Table 13: Uncertainty Analysis Results of Oil D130 Experiments for Venturi (β = 0.6) and Flow Loop Inclination (0º).

Water Cut, %	Flow Rate, bpd	Number of Samples	Standard Error, inch H_2O	Random Uncertainty (U_r), %	Systematic Uncertainty (U_s), %	Expanded Uncertainty (U_e), %
0	8000	57	0.041	0.034	± 0.025% of Full Scale	0.073
	10000	53	0.053	0.028		0.062
	12000	24	0.281	0.115		0.231
20	8000	54	0.024	0.020	± 0.025% of Full Scale	0.046
	10000	49	0.037	0.019		0.046
	12000	51	0.060	0.022		0.050
40	8000	25	0.042	0.032	± 0.025% of Full Scale	0.068
	10000	21	0.058	0.029		0.062
	12000	35	0.074	0.026		0.057
60	8000	22	0.049	0.037	± 0.025% of Full Scale	0.078
	10000	9	0.150	0.073		0.147
	12000	10	0.150	0.050		0.103
80	8000	13	0.070	0.051	± 0.025% of Full Scale	0.105
	10000	20	0.088	0.041		0.086
	12000	38	0.064	0.021		0.050
100	8000	125	0.016	0.011	± 0.025% of Full Scale	0.033
	10000	15	0.099	0.044		0.092
	12000	155	0.020	0.007		0.029

Table 13: Uncertainty Analysis Results of Oil D130 Experiments for Venturi (β = 0.6) and Flow Loop Inclination (90º).

Water Cut, %	Flow Rate, bpd	Number of Samples	Standard Error, inch H_2O	Random Uncertainty (U_r), %	Systematic Uncertainty (U_s), %	Expanded Uncertainty (U_e), %
0	8000	47	0.031	0.026	± 0.025% of Full Scale	0.057
	10000	64	0.043	0.023		0.052
	12000	22	0.440	0.162		0.324
20	8000	39	0.021	0.017	± 0.025% of Full Scale	0.042
	10000	55	0.039	0.020		0.047
	12000	37	0.071	0.026		0.057
40	8000	53	0.019	0.014	± 0.025% of Full Scale	0.038
	10000	18	0.120	0.061		0.124
	12000	41	0.044	0.015		0.039
60	8000	37	0.040	0.030	± 0.025% of Full Scale	0.064
	10000	12	0.096	0.046		0.095
	12000	51	0.068	0.023		0.052
80	8000	49	0.034	0.024	± 0.025% of Full Scale	0.054
	10000	6	0.168	0.077		0.156
	12000	16	0.133	0.043		0.089
100	8000	124	0.02	0.016	± 0.025% of Full Scale	0.040
	10000	30	0.01	0.015		0.039
	12000	25	0.03	0.027		0.060

APPENDIX B

RESULTS OF THE MODIFIED VENTURI DISCHARGE COEFFICIENT, k

1. Results of the Modified Venturi Discharge Coefficient, k for Oil D80 Data for inclinations of (40º, 60º and 90º)

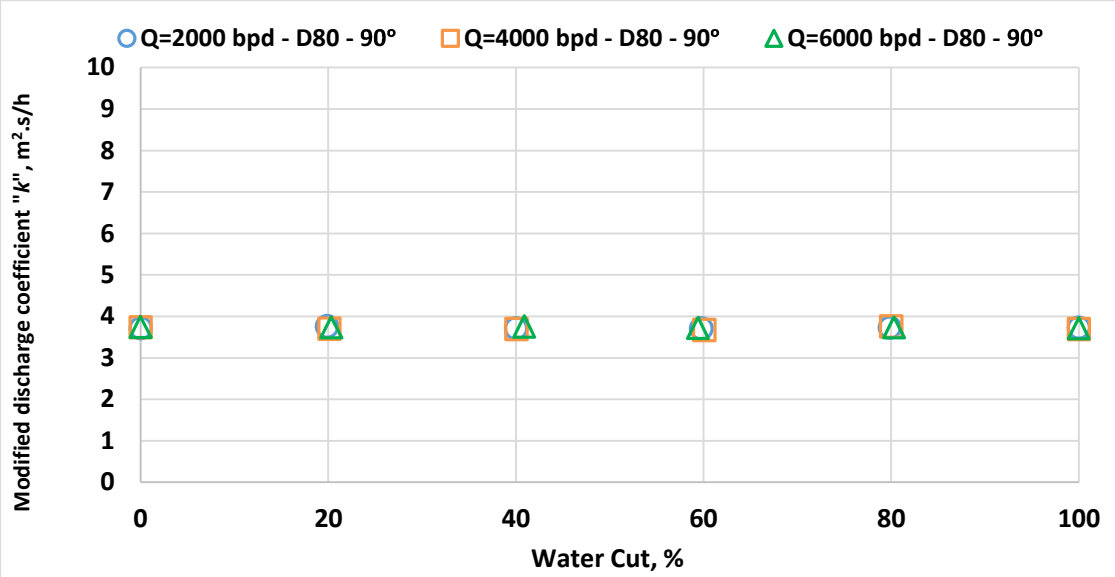

Figure 1.a: Experimental values of k versus water cuts for different fluid mixture flow rates for θ = 90° (β=0.4, oil D80 and potable water).

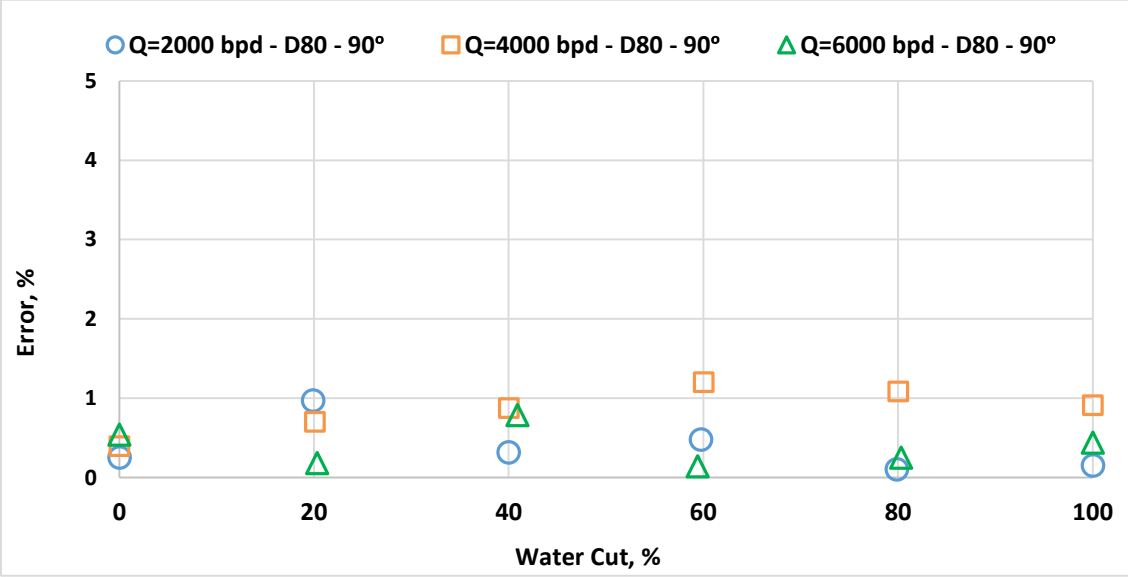

Figure 1.b: Percentage error in the total flow rate using single value of k = 3.73 m^2.s/h for θ = 90° (β=0.4, oil D80 and potable water).

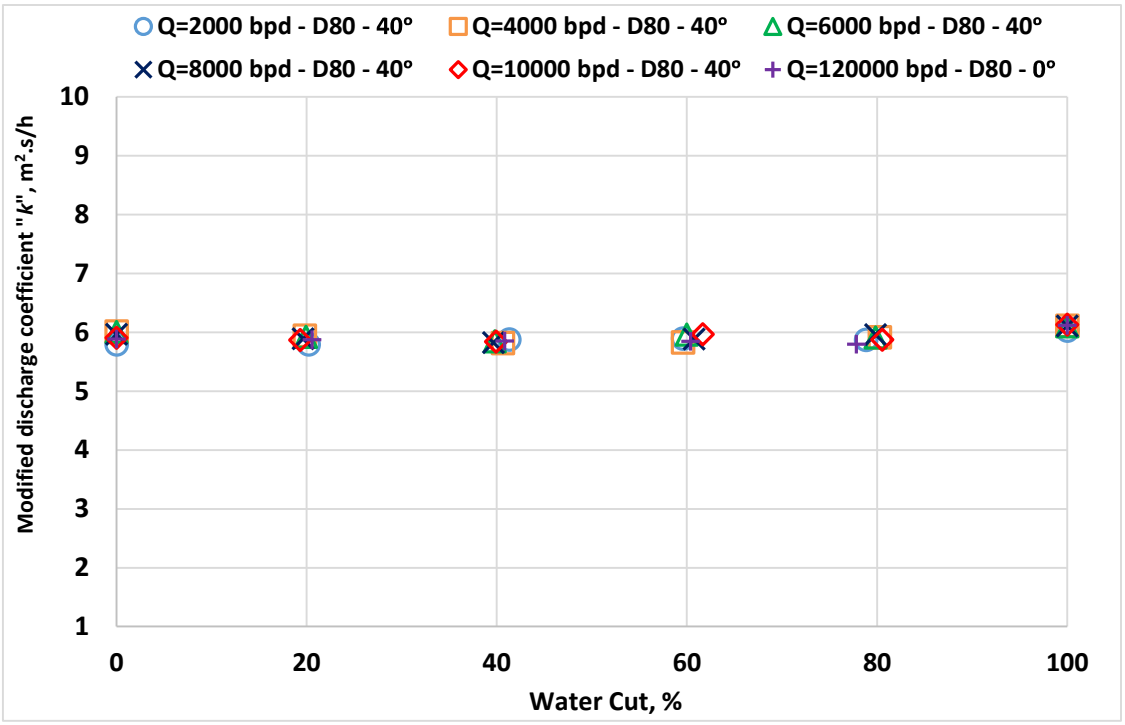

Figure 2.a: Experimental values of k versus water cuts for different fluid mixture flow rates for θ = 40° (β=0.5, oil D80 and potable water).

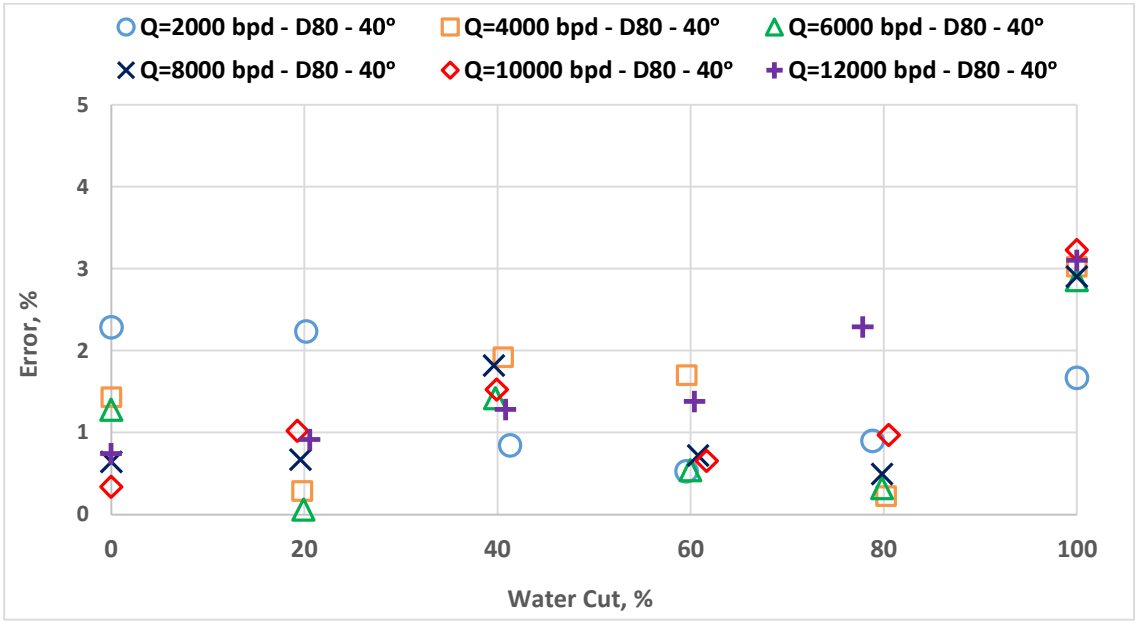

Figure 2.b: Percentage error in the total flow rate using single value of k = 5.93 m^2.s/h for θ = 40° (β=0.5, oil D80 and potable water).

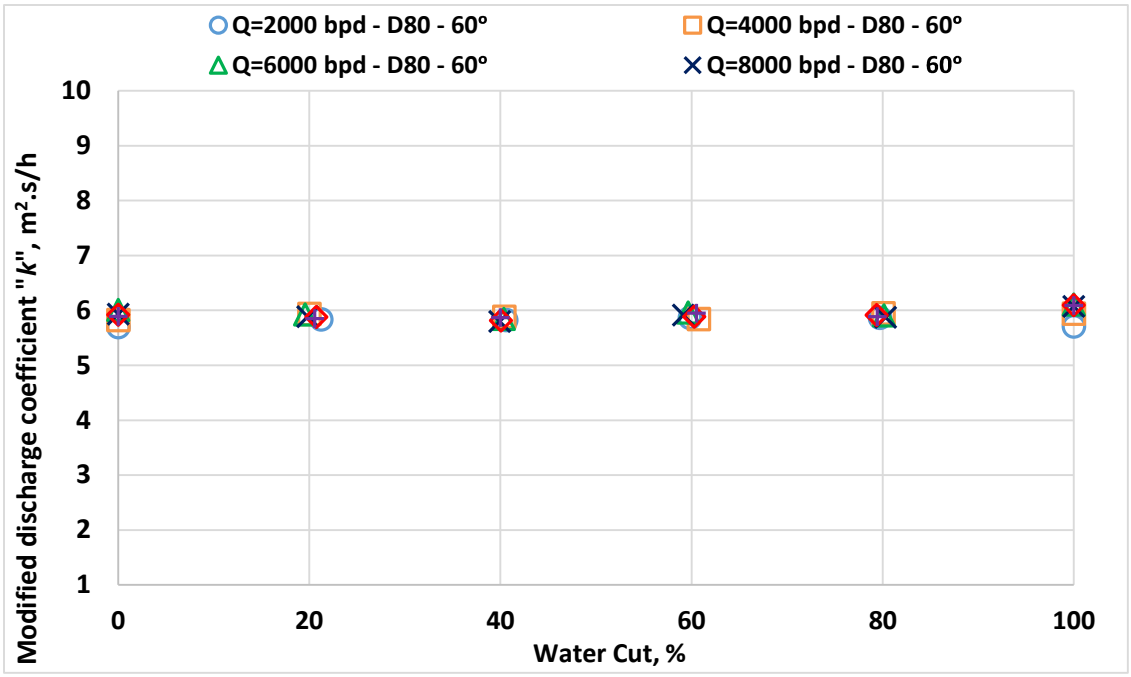

Figure 3.a: Experimental values of k versus water cuts for different fluid mixture flow rates for θ = 60° (β=0.5, oil D80 and potable water).

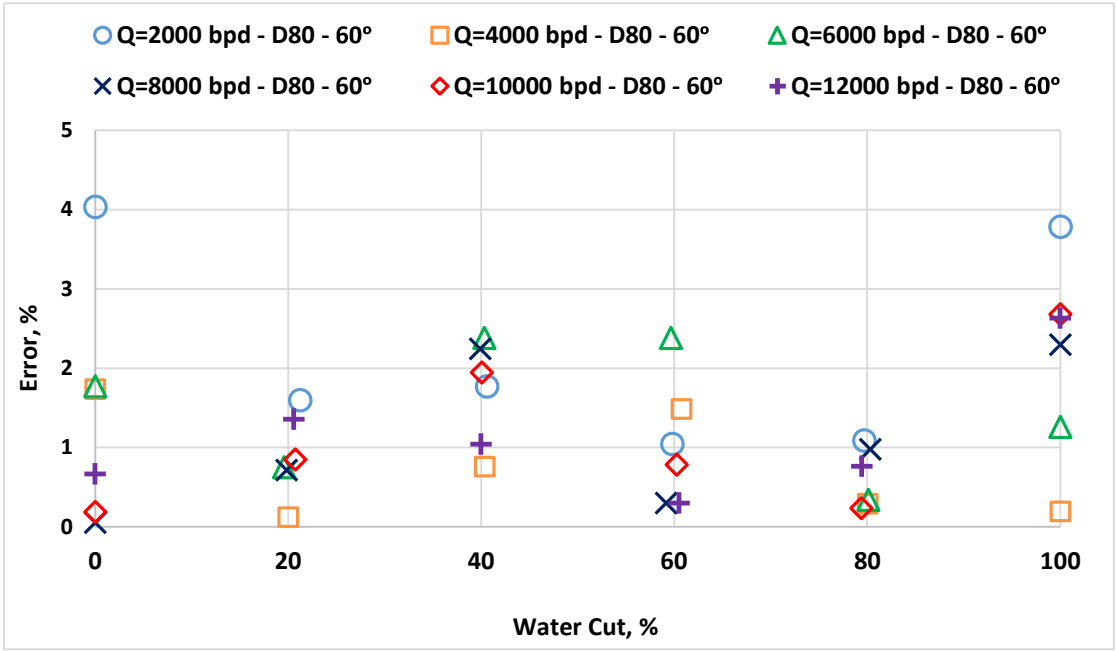

Figure 3.b: Percentage error in the total flow rate using single value of k = 5.93 m².s/h for θ = 60° (β=0.5, oil D80 and potable water).

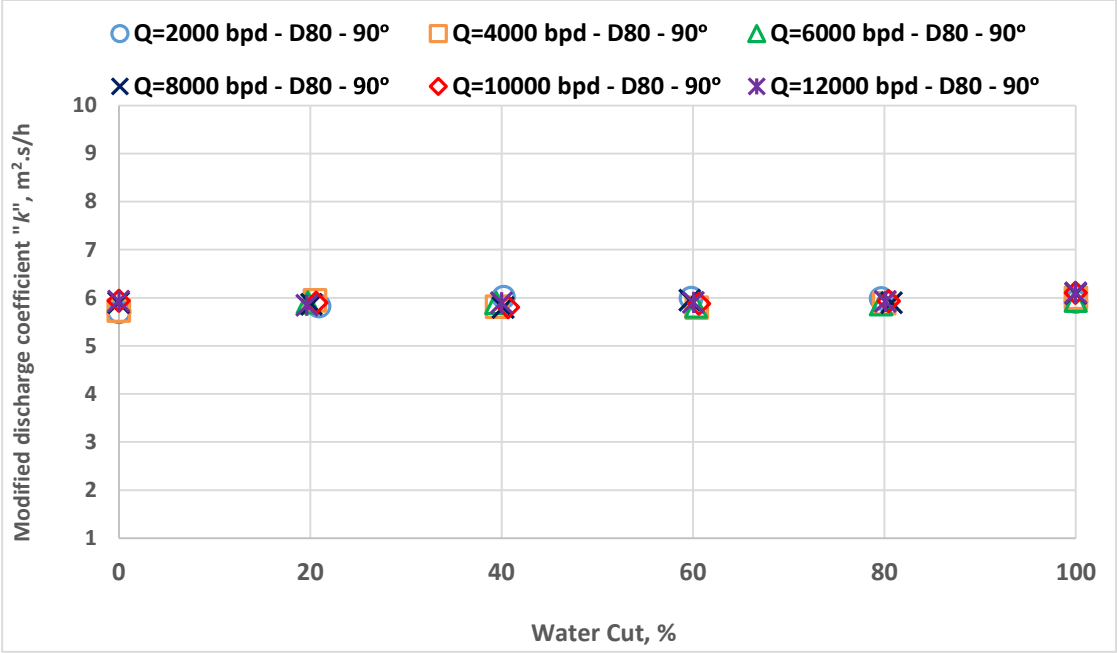

Figure 4.a: Experimental values of k versus water cuts for different fluid mixture flow rates for θ = 90° (β=0.5, oil D80 and potable water).

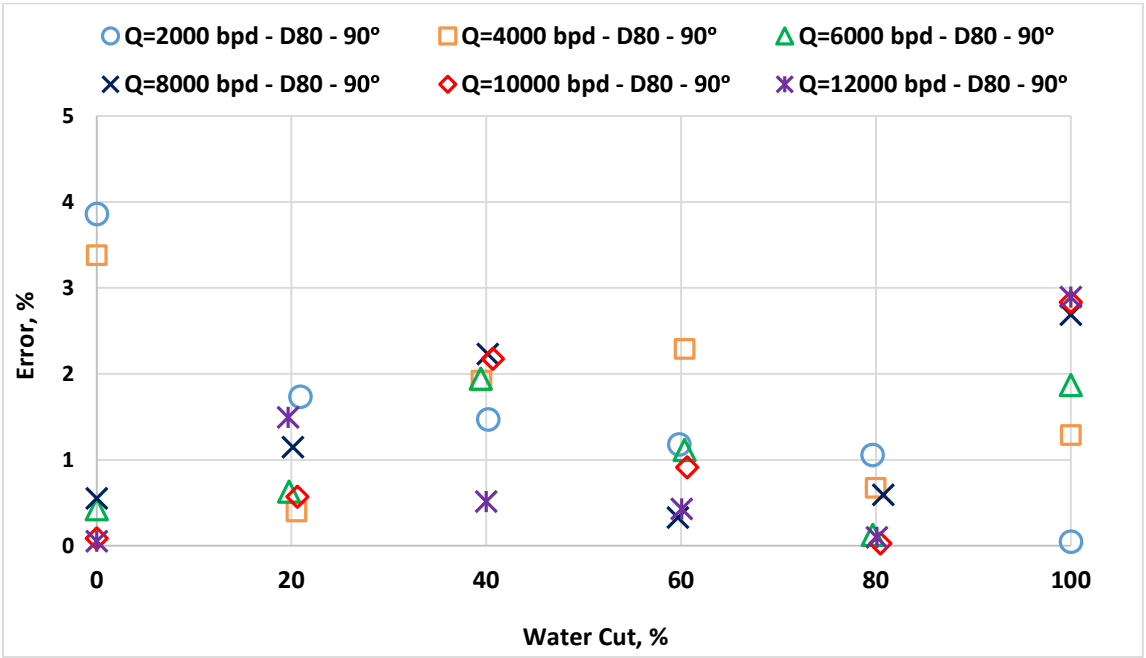

Figure 4.b: Percentage error in the total flow rate using single value of k = 5.93 m^2.s/h for θ = 90° (β=0.5, oil D80 and potable water).

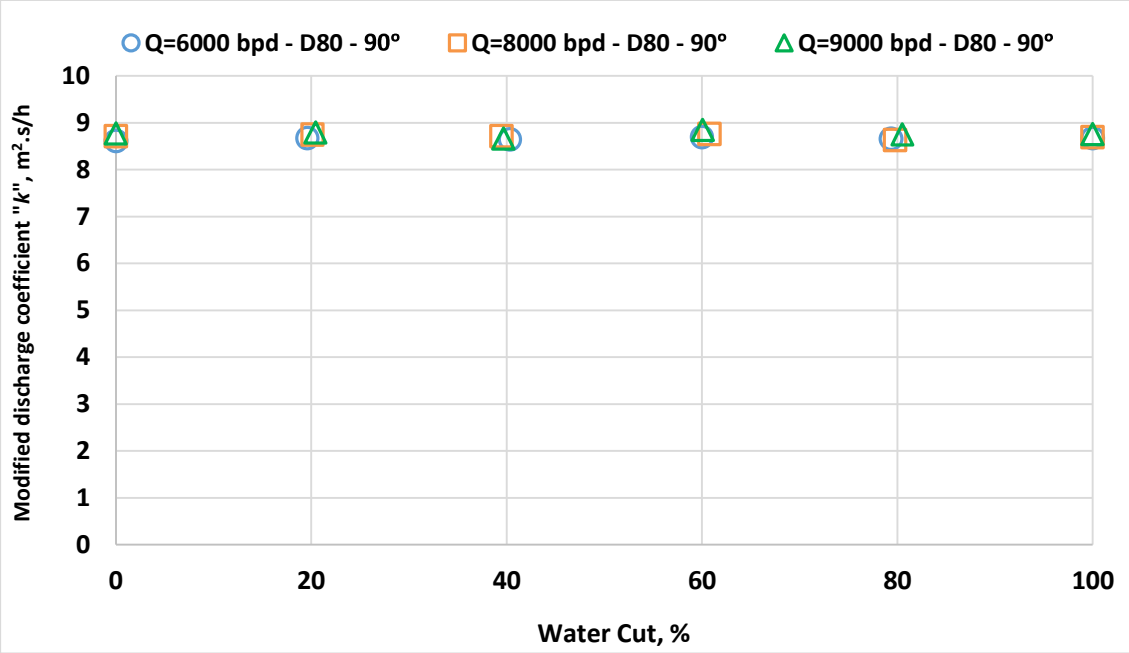

Figure 5.a: Experimental values of k versus water cuts for different fluid mixture flow rates for θ = 90° (β=0.6, oil D80 and potable water).

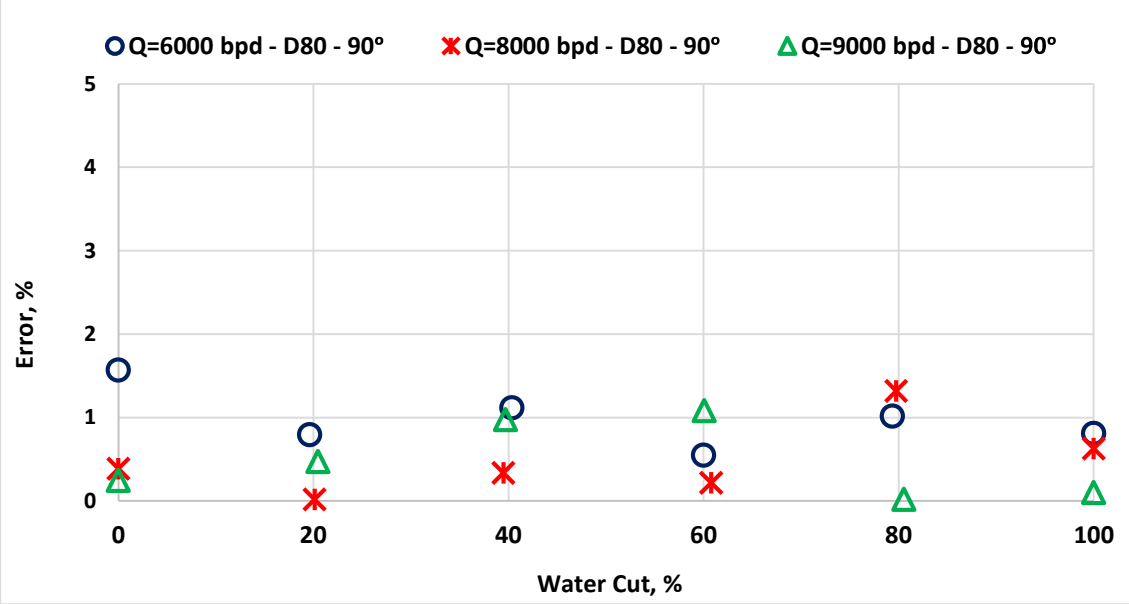

Figure 5.b: Percentage error in the total flow rate using single value of k = 8.75 m^2.s/h for θ = 90° (β=0.6, oil D80 and potable water).

2. Results of the Modified Venturi Discharge Coefficient, k for Oil D130 Data for Vertical Inclination

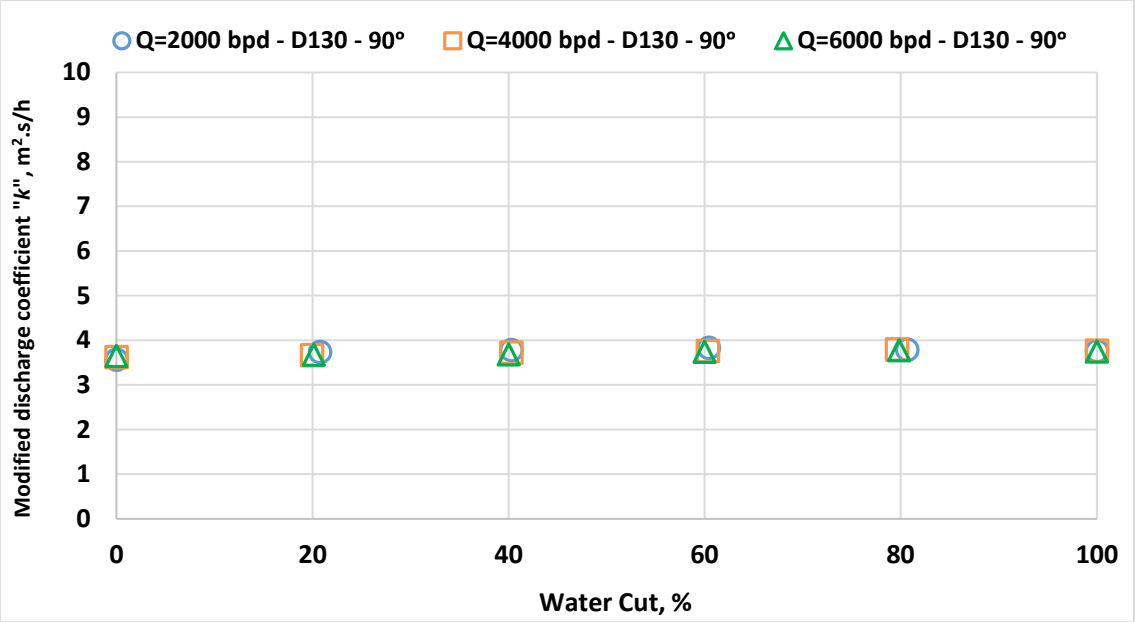

Figure 6.a: Experimental values of k versus water cuts for different fluid mixture flow rates for θ = 90° (β=0.4, oil D130 and potable water).

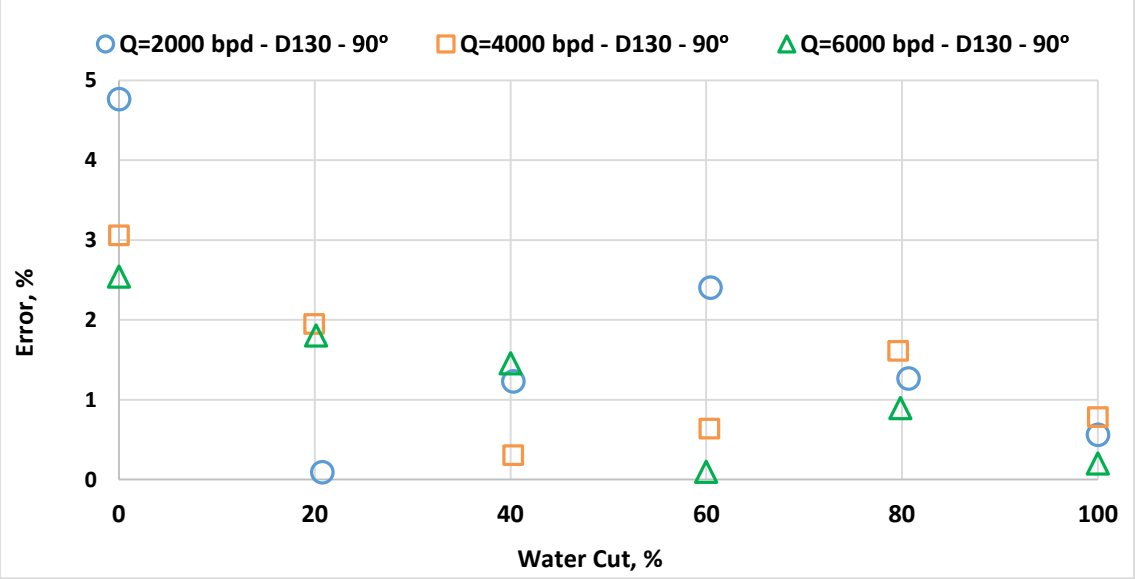

Figure 6.b: Percentage error in the total flow rate using single value of k = 3.73 m^2.s/h for θ = 90° (β=0.4, oil D130 and potable water).

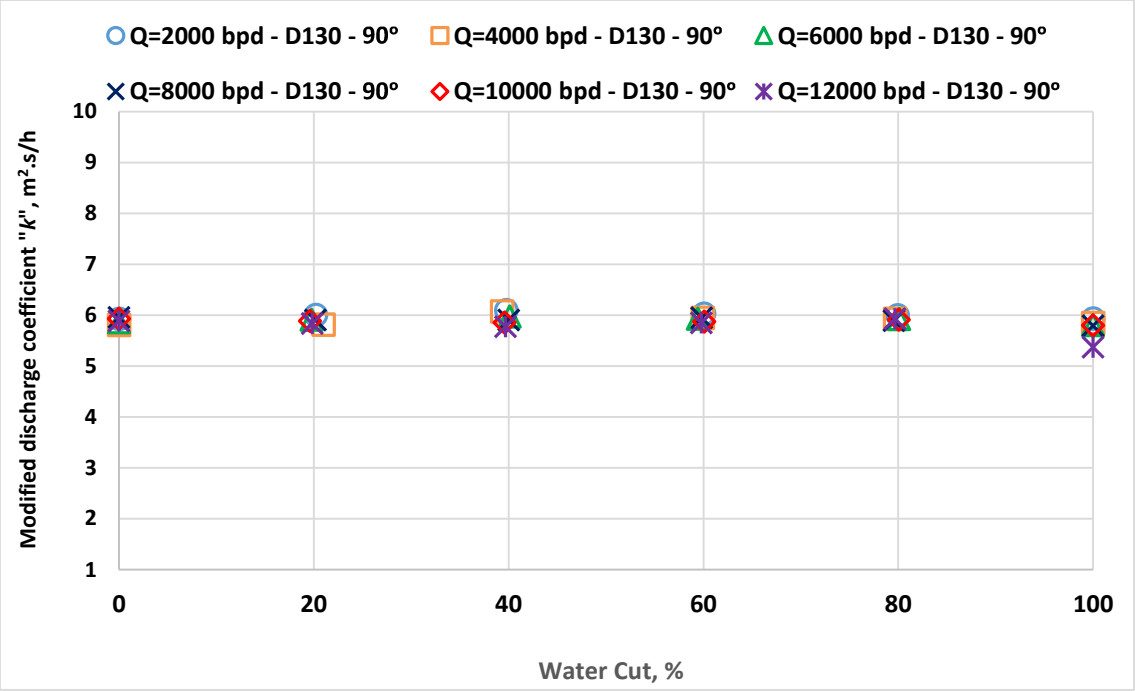

Figure 7.a: Experimental values of k versus water cuts for different fluid mixture flow rates for θ = 90° (β=0.5, oil D130 and potable water).

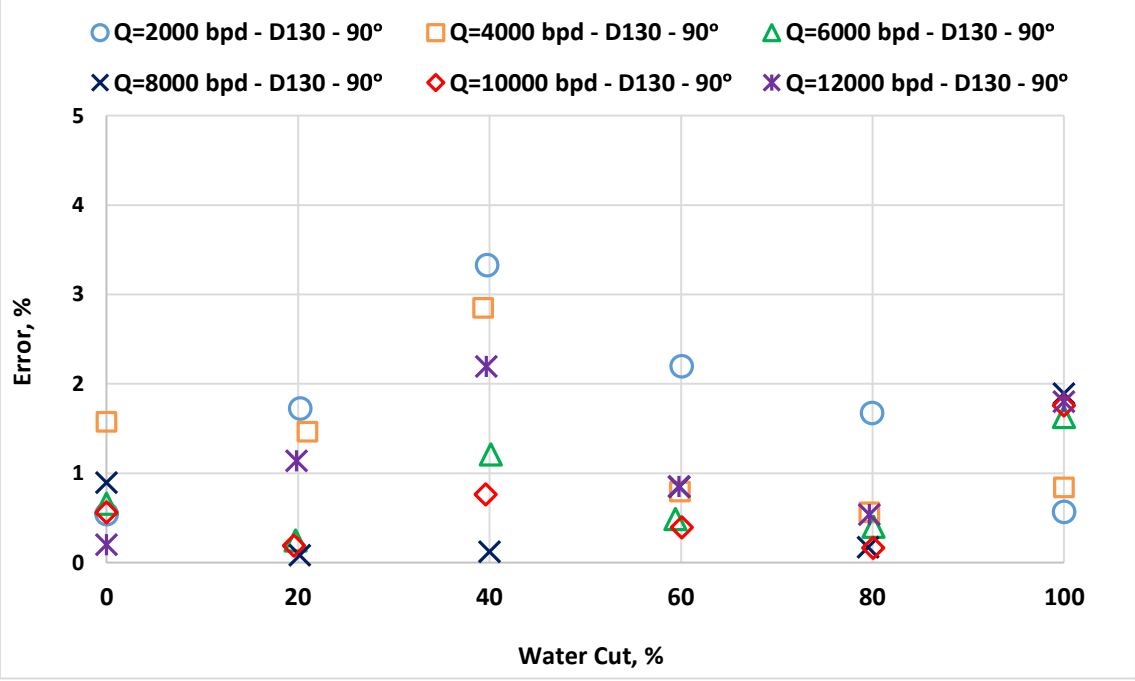

Figure 7.b: Percentage error in the total flow rate using single value of k = 5.93 m^2.s/h for θ = 90° (β=0.5, oil D130 and potable water).

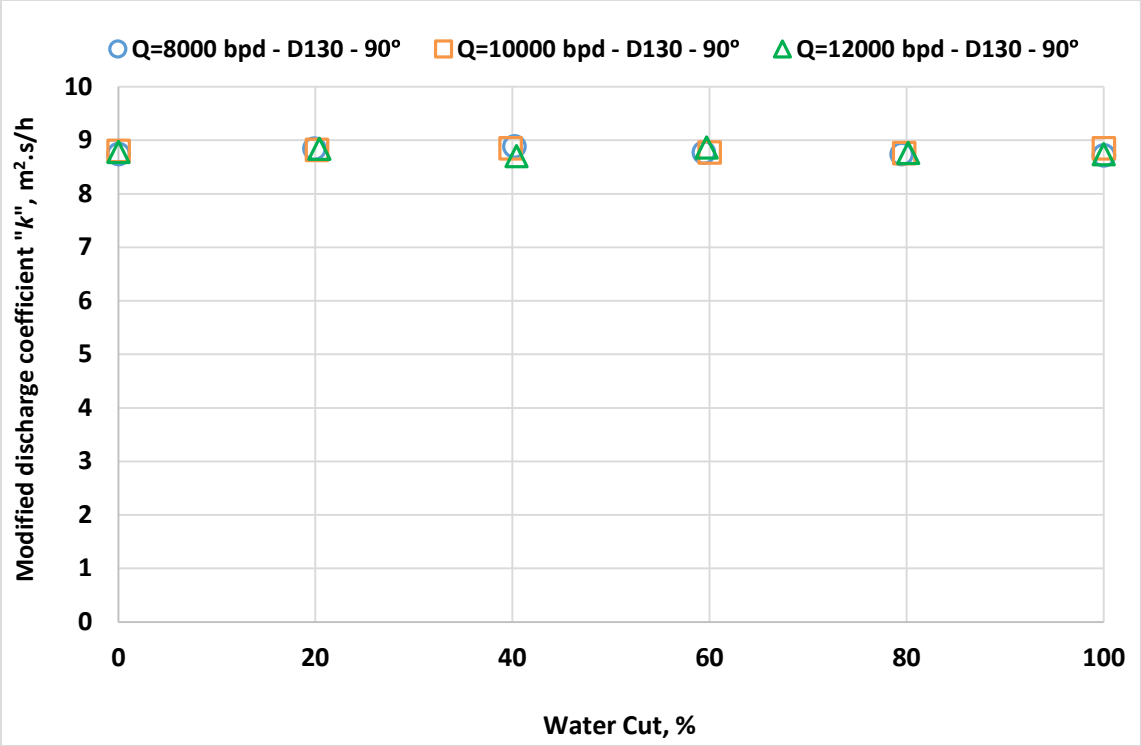

Figure 8.a: Experimental values of k versus water cuts for different fluid mixture flow rates for θ = 90° (β=0.6, oil D130 and potable water).

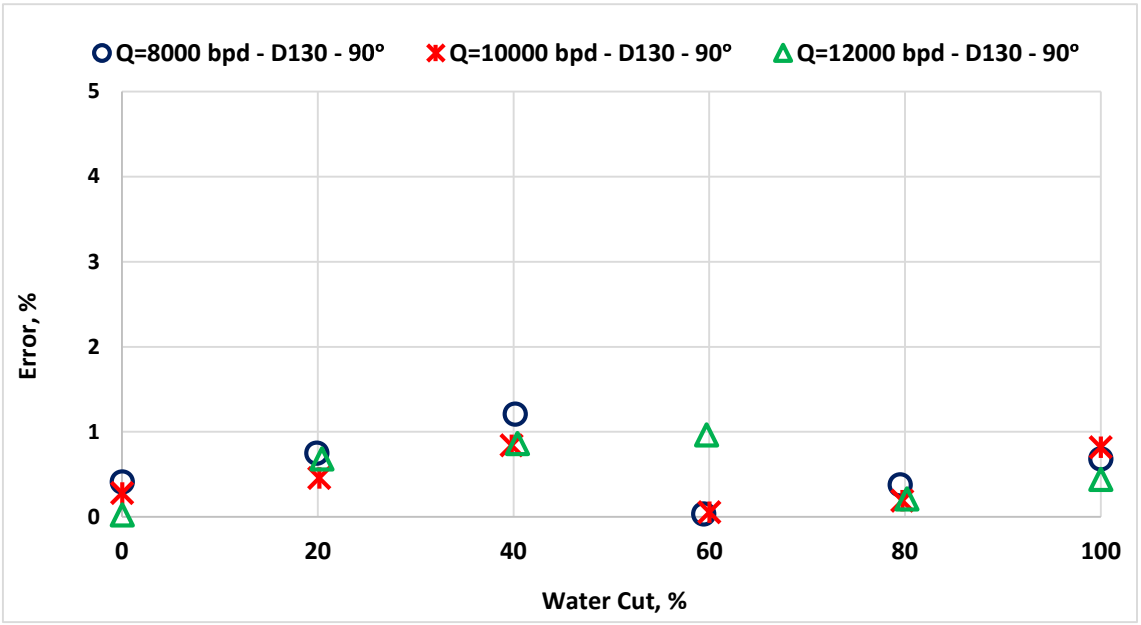

Figure 8.b: Percentage error in the total flow rate using single value of k = 8.75 m^2.s/h for θ = 90° (β=0.6, oil D130 and potable water).

APPENDIX C

RESULTS OF THE VENTURI DISCHARGE COEFFICIENT, C_d

1. Results of Venturi Meter Discharge Coefficient, C_d for Oil D80 Data and for Inclinations (40°, 60° and 90°)

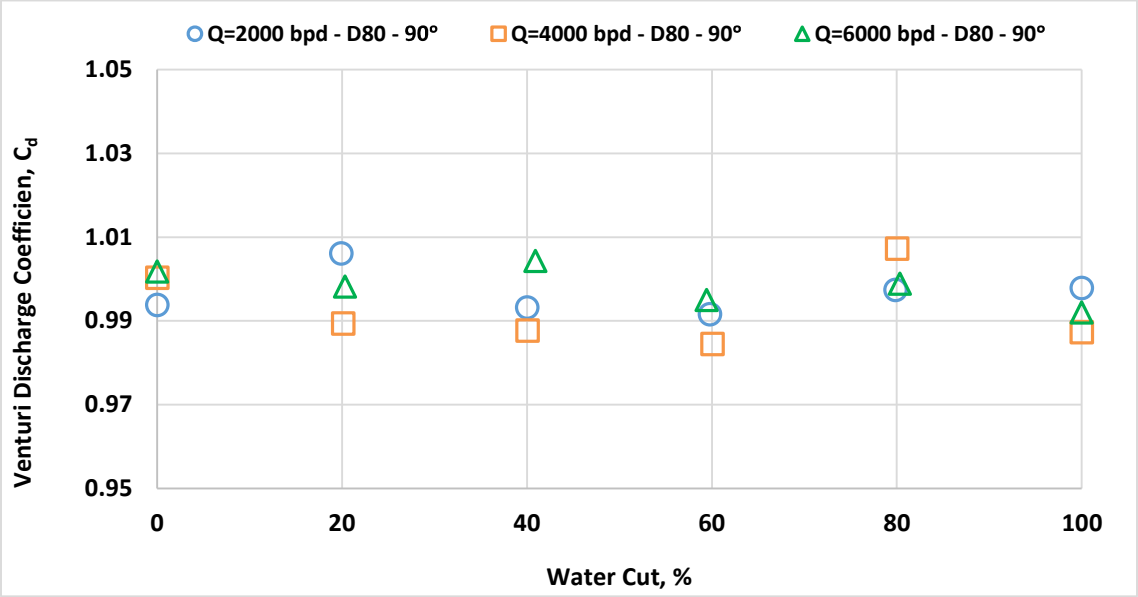

Figure 1: Experimental venturi discharge coefficient, C_d, versus water cut for low fluid mixture flow rates for 90° (β =0.4, oil D80 and potable water).

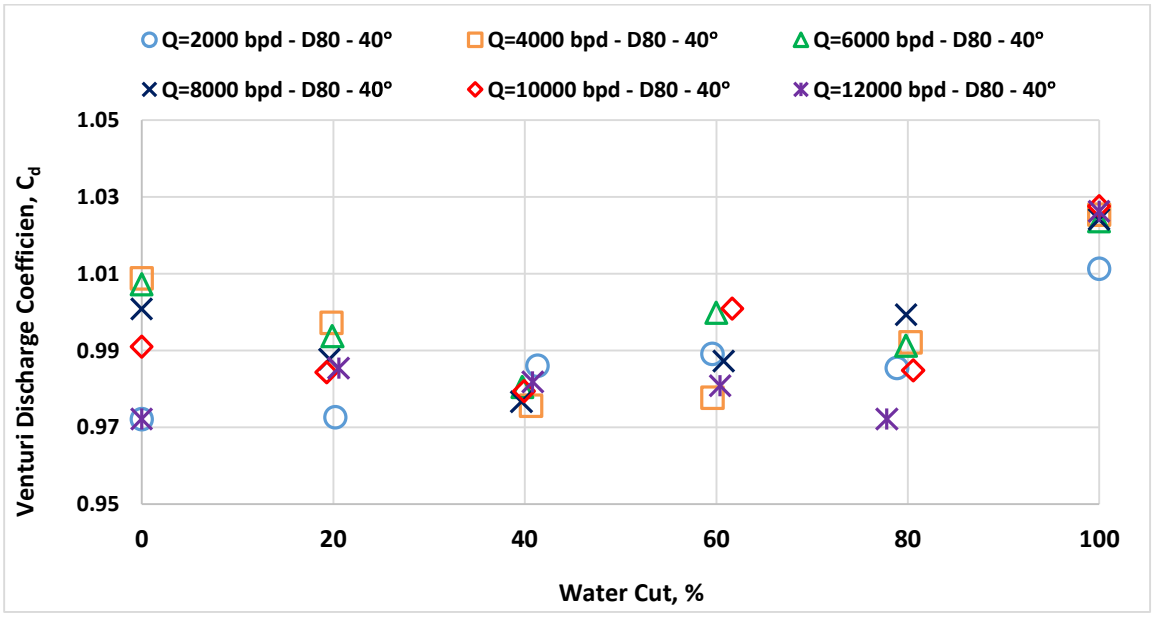

Figure 2: Experimental venturi discharge coefficient, C_d, versus water cut for low fluid mixture flow rates for 40° (β =0.5, oil D80 and potable water).

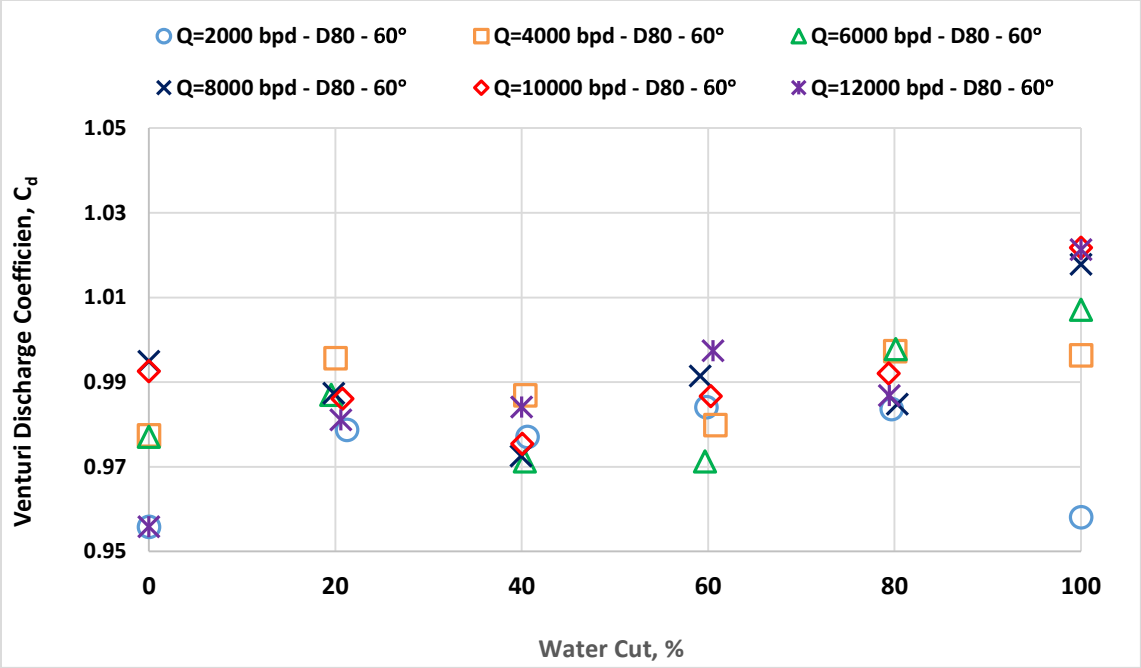

Figure 3: Experimental venturi discharge coefficient, C_d, versus water cut for low fluid mixture flow rates for 60° (β =0.5, oil D80 and potable water).

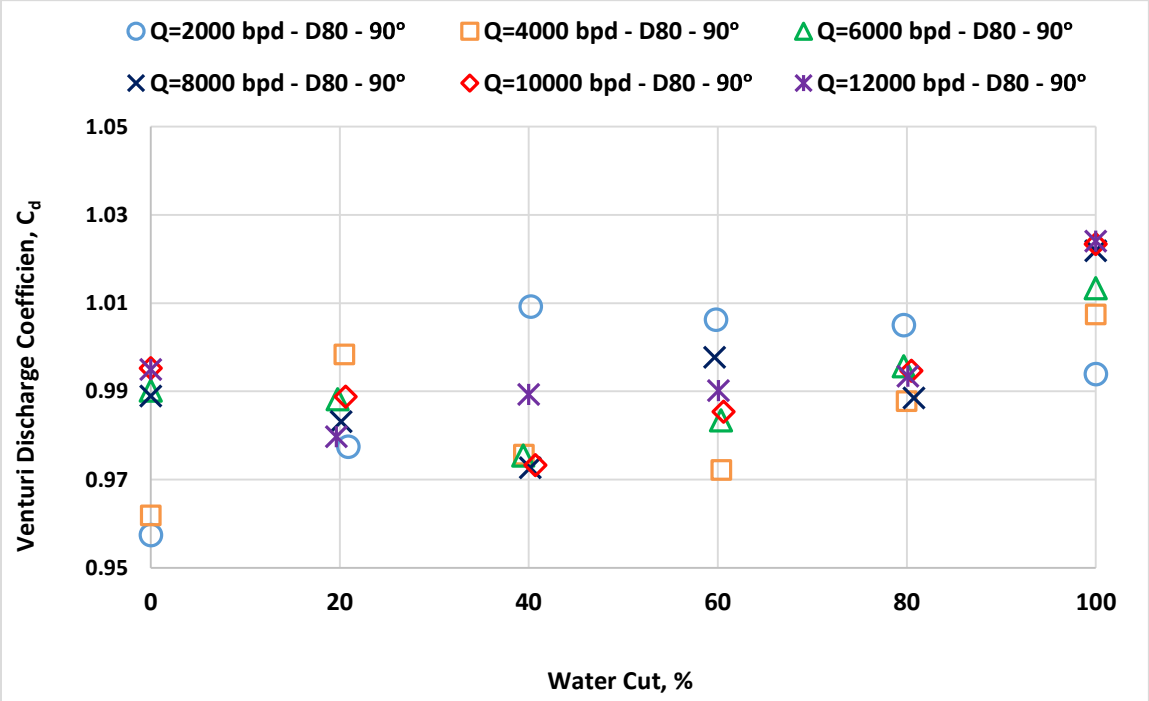

Figure 4: Experimental venturi discharge coefficient, C_d, versus water cut for low fluid mixture flow rates for 90° (β =0.5, oil D80 and potable water).

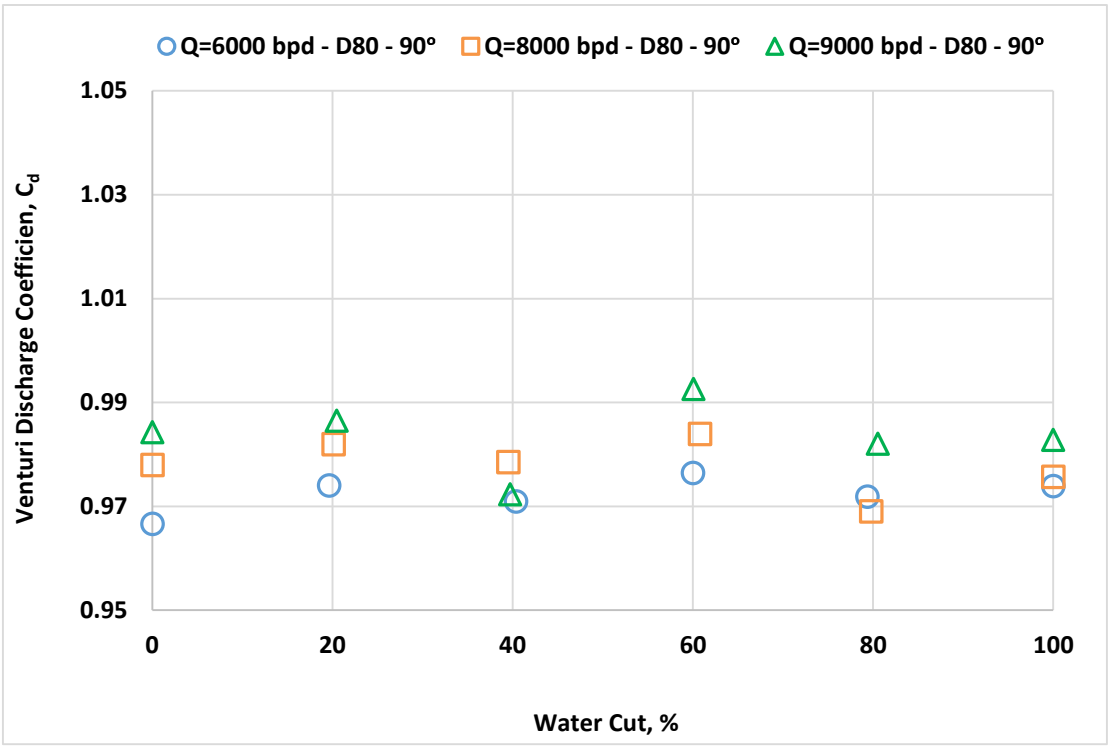

Figure 5: Experimental venturi discharge coefficient, C_d, versus water cut for high fluid mixture flow rates for 90° (β =0.6, oil D80 and potable water).

2. Results of Venturi Meter Discharge Coefficient, C_d for Oil D130 Data and for Vertical Inclination

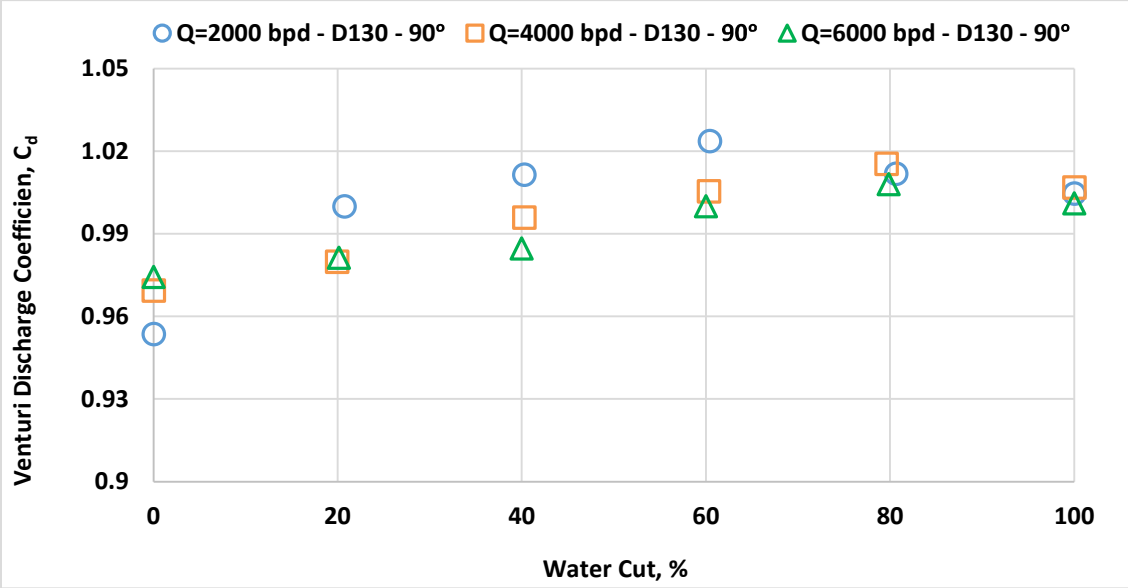

Figure 6: Experimental venturi discharge coefficient, C_d, versus water cut for low fluid mixture flow rates for 90° (β =0.4, oil D130 and potable water).

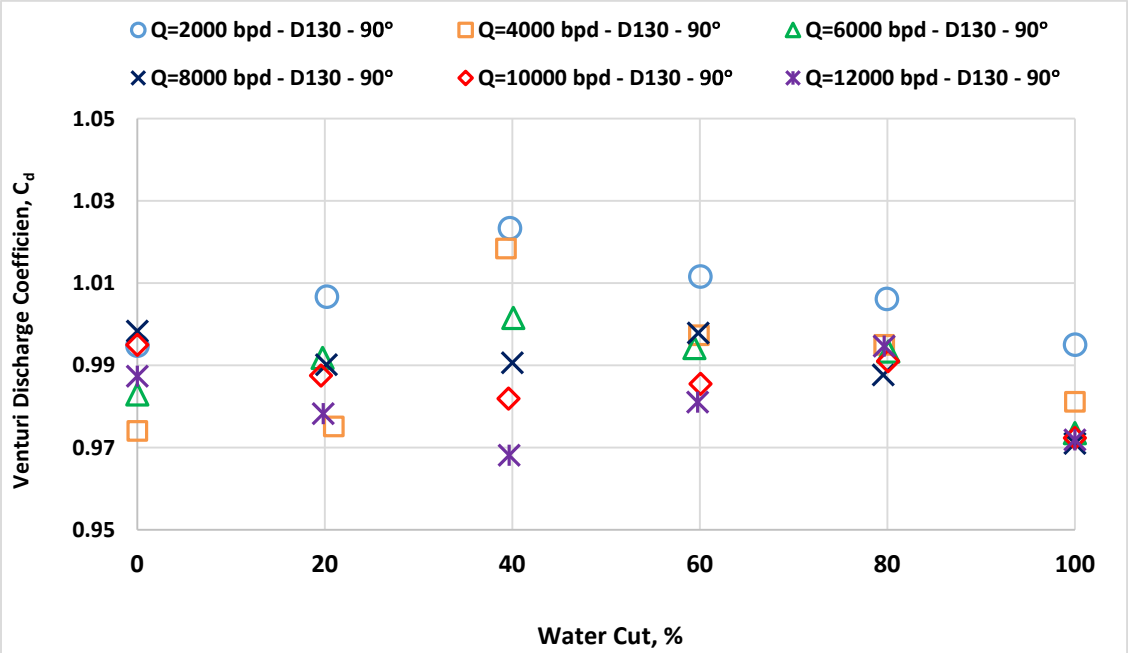

Figure 7: Experimental venturi discharge coefficient, C_d, versus water cut for fluid mixture flow rates for 90° (β =0.5, oil D130 and potable water).

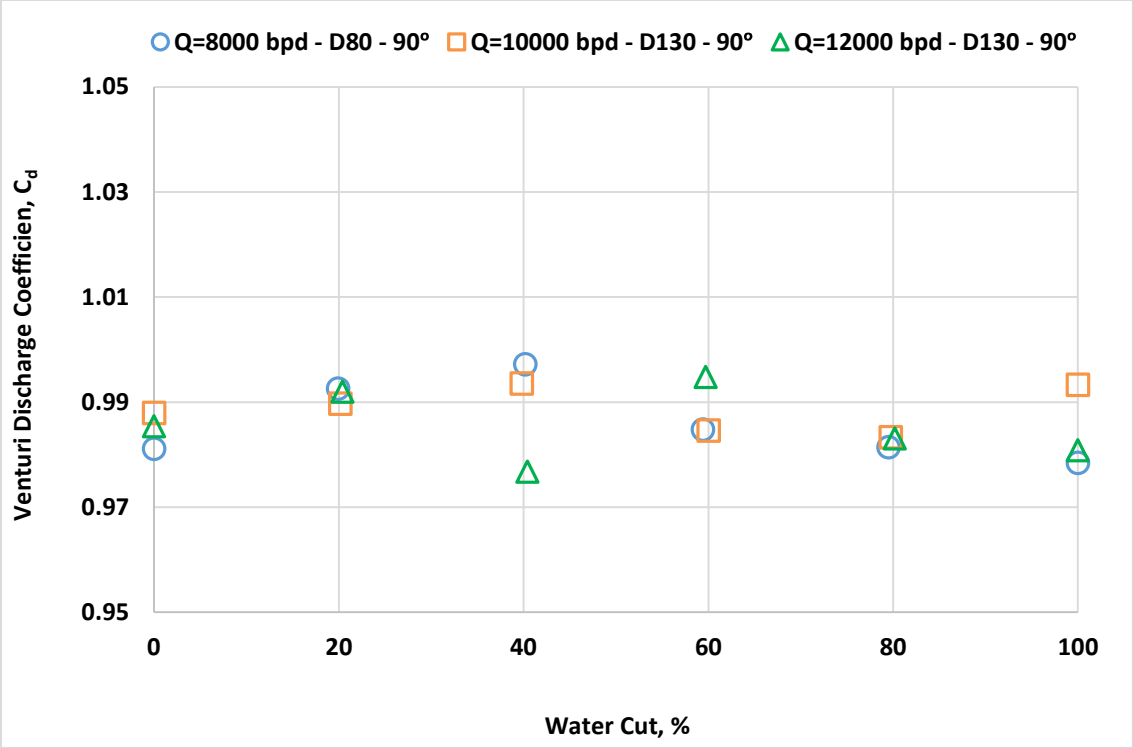

Figure 8: Experimental venturi discharge coefficient, C_d, versus water cut for high fluid mixture flow rates for 90° (β =0.6, oil D130 and potable water).

Vitae

Name	Mujahid Omer Seed Ahmed Elobeid
Nationality	Sudanese
Date of Birth	November 17, 1989
Email	mujahidomer89@gmail.com
Address	P.O. Box 7722, King Fahd University of Petroleum and Minerals, Dhahran 31261, Saudi Arabia

Academic Background

M.Sc. in Mechanical Engineering
(2014 - 2016)
King Fahd University of Petroleum and Minerals, Dhahran, Saudi Arabia
Major: Mechanical Engineering (Thermo-Fluid)

B.Sc. in Mechanical Engineering
(2008 – 2013)
University of Khartoum, Khartoum, Sudan
Major: Mechanical Engineering

Publications

Mujahid O. Elobeid, Luai M. Alhems, Abdelsalam Al-Sarkhi1, Aftab Ahmad, Syed. M. Shaahid Mehaboob Basha, J. J. Xiao, Rafael Lastra and Chidirim E. Ejim. "Effect of Inclination and Water Cut on Venturi Pressure Drop Measurements for Oil-Water Flow Experiments". **Journal of Petroleum Science and Engineering.**
Status: Published.

Mehaboob Basha, Syed. M. Shaahid, Aftab Ahmad, A. M. Al-Sarkhi1, Luai M. Al-Hadhrami, **Mujahid O. Elobeid**, J. J. Xiao, Rafael Lastra and Chidirim E. Ejim. "PRESSURE DROP MEASUREMENTS OF OIL (D80)-WATER FLOW IN 6" HORIZONTAL AND INCLINED ANNULUS PIPE". **Journal of Engineering Research.**
Status: Accepted.

Mujahid O. Elobeid, Aftab Ahmad, Abdelsalam Al-Sarkhi1, Luai M. Alhems, Syed. M. Shaahid Mehaboob Basha, J. J. Xiao, Rafael Lastra and Chidirim E. Ejim. "Pressure Drop Measurements in Venturi Meters of Different Beta Ratio for Oil Water Flow Experiments". **Arabian Journal for Science and Engineering.**
Status: Submitted.

Mujahid O. Elobeid, Aftab Ahmad, Mansoor Alam, Abdelsalam Al-Sarkhi1, Luai M. Alhems, Syed. M. Shaahid Mehaboob Basha, J. J. Xiao, Rafael Lastra and Chidirim E. Ejim. "Effect of Flow Rate, Water Cut and Viscosity on Venturi Pressure Drop Measurements for Oil-Water Flow Experiments".
Status: On progress to be submit within one month to ISI journal.